Mathematical models for respiratory syncytial virus (RSV) transmission

Alexandra B. Hogan

Research School of Population Health

A thesis submitted for the degree of

Doctor of Philosophy

of The Australian National University

June 2017

Declaration

Candidate

I declare that the work contained in this thesis is the result of original research and has not been submitted to any other University or Institution.

This thesis by compilation is based on the following papers to which I made a significant contribution as first author:

1. Hogan, A. B., Mercer, G. N., Glass, K., and Moore, H. C. (2013). Modelling the seasonality of respiratory syncytial virus in young children. In *Proceedings of the 20th International Congress on Modelling and Simulation*, 338–344.
2. Hogan, A. B., Glass, K., Moore, H. C., and Anderssen, R. S. (2015). Age structures in mathematical models for infectious diseases, with a case study of respiratory syncytial virus. In *Proceedings of the Forum of Mathematics for Industry 2014*, 105–116.
3. Hogan, A. B., Glass, K., Moore, H. C., and Anderssen, R. S. (2016). Exploring the dynamics of respiratory syncytial virus (RSV) transmission in children. *Theoretical Population Biology*, 110:78–85.
4. Hogan, A. B., Anderssen, R. S., Davis, S., Moore, H. C., Lim, F. J., Fathima, P., and Glass, K. (2016). Time series analysis of RSV and bronchiolitis seasonality in temperate and tropical Western Australia. *Epidemics* 16:49–55.
5. Hogan, A. B., Glass, K., and Anderssen, R.S. (2017). Complex demodulation: a novel time series analysis method for seasonal infectious diseases. *The ANZIAM Journal* 1–10.

6. Hogan, A. B., Campbell, P. T., Blyth, C. C., Lim, F. J., Fathima, P., Davis, S., Moore, H. C., and Glass, K. (2017). Potential impact of a maternal vaccine for RSV: a mathematical modelling study. Submitted to *Vaccine* (under review).

I also include a paper for which I was the third author. In this paper I assisted with the mathematical modelling and fitting models to data, conducted the sensitivity analysis and contributed to the manuscript:

7. Moore, H. C., Jacoby, P., Hogan, A. B., Blyth, C. C., and Mercer, G. N. (2014). Modelling the seasonal epidemics of respiratory syncytial virus in young children. *PLoS ONE*, 9(6):e100422.

In Appendix B I include an additional paper. While this paper is not related to the research work this thesis, I contributed to the manuscript, and it describes my role in establishing a new international mathematics society during my PhD candidature:

8. Wakayama, M., Hogan, A. B., and Anderssen, R. S. (2015). The formation and launch of the Asia Pacific Consortium of Mathematics for Industry (APCMfI). In *Proceedings of the Forum of Mathematics for Industry 2014*, 143–147.

My specific contribution to each of the six papers for which I was first author is as follows:

1. I took part in planning the research and reviewing the literature. I wrote the MATLAB code for the mathematical model, ran the simulations, and produced the numerical output and figures. I contributed to interpretation of the results. I drafted the manuscript, coordinated co-author input and undertook revisions as requested by the reviewers.
2. I contributed to the research design and surveyed the literature. I wrote the MATLAB and XPP-AUTO code, performed the analysis, and produced the numerical output, figures and tables. I drafted the manuscript, coordinated co-author input and undertook revisions as requested by the reviewer.

3. I contributed to the research design and surveyed the literature. I wrote the MATLAB code for the mathematical model, ran the simulations, and produced the numerical output and figures. I wrote the XPP-AUTO code for the bifurcation analysis, and created the relevant figures. For the sensitivity analysis, I adapted existing sensitivity analysis code for my model, and produced the figures. I drafted the manuscript and coordinated co-author input, including interpretation of the results. I undertook revisions to the manuscript based on the peer review feedback, and managed the submission process.

4. I initiated the research plan and review of the literature. I wrote the MATLAB code for the time series analysis, ran the simulations, and produced the numerical output and figures. All authors interpreted the results. I drafted the manuscript and coordinated co-author input. I undertook revisions as requested by the reviewers.

5. I contributed to the research design and assisted with analysing the existing literature. I wrote the MATLAB code for the time series analysis, ran the simulations, and produced the numerical output and figures. All authors interpreted the results. I drafted the manuscript, coordinated co-author input and managed the submission process.

6. I led the process of planning the model development and analysis. I wrote the MATLAB code for the mathematical models with assistance from PTC, ran the simulations, and produced the numerical output and figures. All authors interpreted the results. I drafted the manuscript, coordinated co-author input and managed the submission process.

The word count for this thesis is approximately 53,000, excluding the front matter, abstract, tables and figures, references, appendices, and numerical code.

Name: Alexandra Barratt Hogan
Date: 12 June 2017

Signature: 

Collaborating authors

I agree that Alexandra Barratt Hogan made the contribution to the authorship and research of paper(s) on which I am a co-author, as stated in the preceding pages.

Name: Kathryn Glass
Date: 6 Oct 2016
Signature: 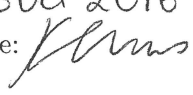

Name: Faye J. Lim
Date: 2 Aug 2016
Signature: 

Name: Hannah C. Moore
Date: 2 Aug 2016
Signature: 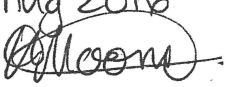

Name: Parveen Fathima
Date: 2 Aug 2016
Signature: 

Name: Stephanie Davis
Date: 18/10/2016
Signature: 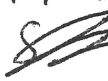

Name: Peter Jacoby
Date: 2/8/16
Signature: 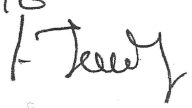

Name: Robert S. Anderssen
Date: 20161007
Signature: 

Name: Christopher C. Blyth
Date: 16/8/16.
Signature: 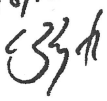

Name: Patricia T. Campbell
Date: 14 October 2016
Signature: 

Acknowledgements

I thoroughly enjoyed my PhD candidature and am very grateful for the wonderful supervision I received. I would first like to thank the chair of my panel, Katie Glass, for her intellectual guidance and mentorship. I really appreciate the time Katie took to meet with me every week, to assist me with both the technical aspects of my research and my writing. Thank you for making my PhD experience such a fulfilling one.

I would also like to acknowledge the contribution made by Geoff Mercer, who sadly passed away in April 2014. Geoff was a wonderful supervisor and mathematician, and a valued member of the academic community. I will always be grateful for how Geoff introduced me to the Australia and New Zealand Industrial and Applied Mathematics (ANZIAM) community. I have since come to know many supportive friends and colleagues in ANZIAM, and attending the society's conference each year has been a highlight of my PhD.

I thank my supervisor Hannah Moore, particularly for her assistance in relation to the data used in this thesis. I am grateful to have had access to a high quality dataset for my PhD research, and thank PathWest Laboratory Medicine, the Linkage and Client Services Teams at the Western Australian Data Linkage Branch, and the custodians of all datasets used in this thesis. I also thank my supervisor Stephanie Davis for her advice, particularly in relation to the clinical aspects of RSV.

I give special thanks to my PhD adviser Bob Anderssen. I learned many things from our robust discussions at the Little Pickle cafe, and greatly value our shared experience in establishing APCMfI. I look forward to more collaborations in the future.

Embarking on a PhD would not be possible without funding support. For this, I thank the ANU, the Research School of Population Health (RSPH) and the National Centre for Epidemiology and Population Health, for my scholarship and additional support. I feel particularly honoured to have received the Peter Baume Travel Grant and the Geoff Mercer Travel Endowment. I also thank the societies from which I have received travel funding, including ANZIAM.

I feel very fortunate to have been part of such a wonderful student group at RSPH. Our morning coffees and afternoon runs provided thesis motivation and created lasting friendships. In particular, I thank Katherine Thurber, Ellie Paige, Cimo Chen, Tanya Muller, Jenny Welsh, Naomi Clarke, Laura Ford, and Angus McLure. I also thank my family, especially Mum, Dad, Micaela, and Dominic, for their encouragement and enthusiasm for my research.

Finally I thank my fiancé, Nick, for his unwavering support. Nick became somewhat of an extra adviser duing my PhD, always keeping on top of where paper submissions were up to, reviewing presentations, and keen to hear about the latest research developments. I'm looking forward to our next journey together.

Abstract

Respiratory syncytial virus (RSV) causes respiratory tract infections in infants and young children. Almost all children experience an RSV infection within the first two years of life, and while mortality due to RSV infection is low in developed countries, the virus presents a significant burden in Australia and internationally. In temperate regions, RSV displays strong seasonal patterns. In Perth, Western Australia, RSV detections show a distinct biennial cycle, and similar patterns have been observed in other temperate locations. While there is no licensed vaccine for RSV, there are several candidates in clinical trials. Understanding the seasonal patterns of RSV, and developing mathematical models that capture key transmission characteristics, can assist with planning the future rollout of an RSV vaccine.

This thesis focusses on three themes: age structure and immunity; seasonality and climate; and vaccination. For the first theme, I present age-structured compartmental mathematical models with waning immunity and seasonal forcing. I fit these models to RSV data for Perth and explore the parameter space and bifurcation structures. The models help explain the different patterns in RSV detections observed globally. In particular, both the seasonality and immunity parameters must exceed certain thresholds for the model to produce biennial patterns, which aligns with observed data. Further, I identify a window of birth rate parameters that produces biennial patterns, showing that RSV seasonality may not be only driven by weather and climatic factors as was previously thought.

The second research theme involves a time series analysis of both RSV and bronchiolitis data, as approximately 70% of bronchiolitis hospitalisations are linked to RSV infection. First, I identify a clear shift in seasonality for both RSV

and bronchiolitis, from the temperate to tropical regions of Western Australia. I then apply a mathematical time series analysis method, complex demodulation, to assess the validity of using bronchiolitis hospitalisations as a proxy for RSV cases. I find bronchiolitis and RSV are similar in terms of timing, but that epidemic magnitudes differ.

To address the third research theme, I adapt the compartmental model to incorporate a finer age structure, contact patterns and naturally-derived maternal immunity, to assess the potential impact of a maternal vaccination strategy for RSV in Perth. I find that the introduction of a maternal vaccine is unlikely to alter the regular biennial RSV pattern, but that the vaccine would be effective in reducing hospitalisations due to RSV in children younger than six months of age.

This thesis adopts both mathematical modelling and data analysis approaches to improve our understanding of RSV dynamics. Developing mathematical models for RSV transmission in the Australian context allows a better understanding of the relative importance of age cohorts, immunity, climatic factors, and demography, in driving different RSV epidemic patterns. Further, data analysis shows the extent to which bronchiolitis hospitalisations are representative of RSV detections, and that different approaches to interventions must be considered in temperate versus tropical Western Australia. These findings will be instrumental in planning an effective vaccine rollout strategy for Western Australia.

Conference presentations and invited talks arising from this thesis

(* presenting author)

1. Hogan, A.B.*, Mercer, G.N., Glass, K., and Moore, H.C. (2013, September). A model for respiratory syncytial virus (RSV) transmission. Poster presentation at the Australian Mathematical Sciences Institute Workshop on Infectious Disease Modelling, Newcastle, Australia. Awarded best poster presentation.
2. Hogan, A.B.*, Mercer, G.N., Glass, K., and Moore, H.C. (2013, November). Modelling the seasonality of respiratory syncytial virus (RSV) in young children. Spoken presentation at the annual NSW/ACT ANZIAM meeting, Sydney, Australia. Awarded prize for best student talk.
3. Hogan, A. B.*, Mercer, G. N., Glass, K., and Moore, H. C. (2013, December). Modelling the seasonality of respiratory syncytial virus in young children. International Congress on Modelling and Simulation, Adelaide, Australia. Awarded prize for student talk.
4. Hogan, A. B.*, Mercer, G. N., Glass, K., and Moore, H. C. (2014, February). A mathematical model for respiratory syncytial virus transmission. Spoken presentation at the annual ANZIAM conference, Rotorua, New Zealand.
5. Hogan, A. B.*, Glass, K., and Moore, H. C. (2014, July). A mathematical model for the transmission of respiratory syncytial virus (RSV). Spoken presentation at the annual Society for Mathematical Biology conference, Osaka, Japan.
6. Hogan, A. B.*, Glass, K., Moore, H. C., and Anderssen, R. S. (2014, October). A model for respiratory syncytial virus transmission. Spoken presentation at the annual Forum Math-for-Industry, Fukuoka, Japan. Extended

abstract published in MI Lecture Note Series Volume 57: Kyushu University, pp 33-34. ISSN 2188-1200.

7. Hogan, A. B.*, Glass, K., Moore, H. C., and Anderssen, R. S. (2014, November). Exploring bifurcations and seasonality in a mathematical model of childhood infectious disease. Spoken presentation at the Melbourne School of Population and Global Heath, The University of Melbourne.

8. Hogan, A. B.*, Glass, K., Moore, H. C., and Anderssen, R. S. (2015, February). Exploring bifurcations and seasonality in a mathematical model of childhood infectious disease. Spoken presentation at the annual ANZIAM conference, Gold Coast, Australia.

9. Hogan, A. B.*, Glass, K., Moore, H. C., and Anderssen, R. S. (2015, February). Mathematical modelling of a childhood respiratory infection. Spoken presentation at the Institute of Mathematics for Industry, Kyushu University, Japan.

10. Hogan, A. B.*, Glass, K., Moore, H. C., and Anderssen, R. S. (2015, April). Exploring the dynamics of a model for a seasonal childhood respiratory infection. Spoken presentation at the inaugural CRE in Infectious Diseases Modelling to Inform Public Health Policy Conference, Melbourne, Australia.

11. Hogan, A. B.*, Glass, K., Moore, H. C., and Anderssen, R. S. (2015, May). Exploring the dynamics of a model for a childhood infection, respiratory syncytial virus (RSV). Spoken presentation at IBM Research, Melbourne, Australia.

12. Hogan, A. B.*, Glass, K., and Anderssen, R. S. (2016, February). The seasonality of RSV and bronchiolitis in the different climatic regions of Western Australia. Spoken presentation at the annual ANZIAM conference, Canberra, Australia.

13. Hogan, A. B.* (2016, May). Mathematical modelling of RSV transmission in Western Australia. Spoken presentation at Telethon Kids Institute, Perth, Australia.

14. Hogan, A. B.*, Moore, H. C., Anderssen, R. S. & Glass, K. (2016, July). Modelling respiratory syncytial virus transmission in Western Australia Spo-

ken presentation at the annual Society for Mathematical Biology conference, Nottingham, England.

15. Hogan, A. B.* (2016, July). Exploring the dynamics of a model for respiratory syncytial virus (RSV) in Western Australia. Spoken presentations at the University of Warwick and the University of Manchester, England.

Contents

1

Introduction

1.1 Background

Respiratory syncytial virus (RSV) causes respiratory tract infections and is a significant cause of hospitalisations in the very young. Globally, RSV is responsible for about 70% of bronchiolitis hospitalisations and 40% of pneumonia hospitalisations in infants less than one year of age (Haynes, 2013; Mansbach et al., 2012), and the burden of RSV surpasses that of influenza in young children (Bourgeois et al., 2009). There is currently no licensed vaccine for RSV, but vaccine development has been gaining momentum over the past decade, with several pharmaceutical companies reporting RSV vaccine candidates in various stages of clinical trials (Broadbent et al., 2015).

In temperate climates, the available data shows seasonal patterns of RSV infection, with peaks of infection incidence in the winter months. Highly regular annual and biennial (two year) dynamics are often observed in temperate regions, although the seasonal behaviour is less defined in the tropics. While various hypotheses have been put forward to explain this seasonality, including higher rainfall and cooler temperatures in the winter months, the observed patterns in the available data have yet to be fully documented and explained.

1.2 Research motivation

The health care and economic burden of RSV is substantial, yet the transmission characteristics of RSV are not well understood, and little is known about the drivers of the seasonal patterns of incidence. The complexities of the transmission dynamics relate to age-dependent susceptibility and force of infection, the role of adults in transmission, the nature of immunity to RSV following an infection, and the particular temporal patterns of the virus.

In epidemiology, mathematical modelling has provided an improved understanding of the behaviour of seasonal infections (Altizer et al., 2006; Grassly and Fraser, 2006; Keeling and Rohani, 2008). Mathematical models are tools that can be used by researchers, health care planners and policy practitioners to help understand the causes of epidemics, and identify the groups in a population who are driving transmission. Models have been used to predict the outcomes of different epidemic intervention strategies, identify the key elements of past outbreaks, and inform future epidemic planning, for diseases such as measles (Roberts and Tobias, 2000) and hepatitis E (Mercer and Siddiqui, 2011). However, because the dynamics of infection are complex, and because RSV has received relatively little attention compared to other infectious diseases such as influenza, there is a paucity of representative transmission models for RSV in the literature. In light of the potential future introduction of an RSV vaccine, such models are needed to determine optimal vaccine rollout strategies for different jurisdictions.

The state of Western Australia is a particuarly suitable region for which to investigate the characteristics of RSV transmission, because of its climatic diversity, and the availability of high quality population-based linked data that is not readily accessible elsewhere. Western Australia spans a range of climatic zones, including temperate and tropical, and is also divided into different administrative health regions. In Western Australia, population-based laboratory data is collected through a state-wide public pathology provider, and data may be linked through the Western Australia Data Linkage System (WADLS). For this research, I accessed data relating to RSV laboratory detections and acute lower respiratory illness hospitalisations, derived from a broader birth cohort data linkage study (Moore et al., 2011). Access to this data enabled me to investigate RSV dynamics for the setting of Western Australia.

In this thesis, mathematical modelling and data analysis techniques were applied to explore the transmission dynamics of RSV, to better understand and document RSV's seasonal patterns, and to investigate the impact of an RSV vaccination strategy, with a particular focus on RSV in Western Australia.

1.3 Research themes

The goal of this thesis is to obtain a better understanding of the transmission dynamics of RSV by developing mathematical models that capture the RSV infection process. Three research topics form the basis for the grouping of chapters:

1. Age structure and immunity;
2. Seasonality and climate; and
3. Vaccination.

Research theme 1: Age structure and immunity
The aim of this research theme was to investigate strategies for incorporating age structures into RSV transmission models, and to identify the key parameters that influence the model outcomes, with a particular focus on immunity and demography. Age-structured compartmental models were fitted to the population-based linked laboratory dataset of RSV positive identifications in metropolitan Western Australia, and this fitting process allowed validation of the model. A preliminary sensitivity analysis indicated plausible ranges for different parameters, and the fitted model provided baseline parameter values for subsequent model analysis.

Research theme 2: Seasonality and climate
The goal for this theme was to explore and document the differences in seasonal patterns for RSV in different climatic zones. This was approached from two perspectives: a bifurcation and parameter space analysis of the dynamic model, and time series analysis of the RSV data. For the modelling component, the fitted model parameters from research theme 1 were used as a baseline for quantitative numerical analysis. I undertook several analyses to determine the ranges of parameter values that produce different qualitative outputs. In the analysis, I focussed on the seasonal forcing function parameters, waning immunity, and the

birth rate, with the objective of determining the relative contribution of these parameters to the seasonal dynamics produced by the model.

The second component centered on an analysis of data for Western Australia from eight different health regions. These health regions cover a range of climatic zones, including temperate and tropical. Mathematical time series analysis methods (Fourier analysis and complex demodulation) were used to investigate the changing patterns of both RSV and bronchiolitis over time.

Research theme 3: Vaccination

The goal for this research theme was to build on the model development and data analysis undertaken for research themes 1 and 2, in order to consider a vaccination strategy for RSV. I extended the compartmental model to incorporate a more detailed age structure and contact patterns between different age groups, and validated the model using hospitalised RSV cases. I then incorporated a maternal vaccine into the model, and varied the vaccine coverage, effectiveness, and duration parameters in order to evaluate the potential impact of a maternal RSV vaccine on the number of RSV-related hospitalisations in Perth.

2

Literature review

2.1 Introduction

Respiratory syncytial virus (RSV) is a major cause of respiratory tract infections in young children, and annual epidemics occur globally in many countries. First identified in chimpanzees in the 1950s, RSV was shortly thereafter found in infants with respiratory illness (Fields et al., 2013; Hall, 1981). The burden of RSV is significant. One recent analysis estimated that in 2005, 33.8 million new episodes of RSV occurred worldwide in children younger than five years of age (Nair et al., 2010).

This literature review is in two parts. In the first part, I discuss the known epidemiology of RSV, the available treatment options, the progress towards vaccine development, and the data on RSV detections in different climatic zones. In the second part, I provide a brief summary of the mathematics of infectious disease modelling, before discussing the mathematical modelling of RSV published in the literature to date.

2.2 The clinical nature and epidemiology of RSV

2.2.1 The virus and the clinical picture

Human RSV belongs to the *Paramyxoviridae* family of viruses, and is more specifically in the *Pneumovirus* subfamily (Domachowske and Rosenberg, 1999; González et al., 2012).

Figure 2.1: Left: coloured transmission electron micrograph of RSV particles (Hall, 2010). Right: schematic diagram of RSV (Smyth and Openshaw, 2006).

RSV is a single-stranded enveloped RNA virus with a genome that encodes 11 proteins, with the F and G proteins the most important surface glycoproteins (Ren et al., 2014) (see Figure 2.1). Isolates of RSV can be divided into two broad serological subgroups: RSV-A and RSV-B. Within these two major serotypes, 11 RSV-A and 23 RSV-B genotypes have been identified (although typing at the genotype level is not discussed further in this thesis) (Esposito et al., 2015).

RSV is spread through direct exposure to droplet secretions from the nose and mouth (from coughing and sneezing), and also through contact with contaminated fomites (Hall and Douglas, 1981; Paes, 2003). Symptoms of RSV are typically those of a cold, such as coughing, wheezing, hoarseness and fever. In its more severe form, it can cause conditions such as bronchiolitis, laryngotracheobronchitis, croup or pneumonia (Hall, 1981; Ismail and Reisner, 2001; Sorce, 2009). Severe disease is most likely to develop in the first few months of life, due to immunological and physiological immaturity (particularly small airway size) (Ruckwardt et al., 2016). Severe RSV infection has also been associated with the development of asthma and recurrent wheeze in later childhood (Borchers et al., 2013; Sigurs et al., 2000; Tregoning and Schwarze, 2010). Some children are at greater risk of

having a severe RSV infection, including children born prematurely, and those with existing lung conditions (such as cystic fibrosis), congenital heart disease or immunosuppression (González et al., 2012; Ismail and Reisner, 2001; Sorce, 2009). Birth during the first half of the RSV season is also reported to place a child at greater risk of developing a severe RSV infection, possibly due to lower maternal antibody levels or allowing a longer period for virus exposure in the early months of life (Simoes, 2003).

The latent period is the time between contracting an infection and becoming infectious. For RSV, this is generally reported as between four and five days (Fields et al., 2013; Hall, 1981; Lessler et al., 2009; Sorce, 2009). In terms of the duration of infectiousness, a study of hospitalised infants by Hall et al. (1976a) found that the mean duration of shedding was 6.7 days with a range of 1 to 21 days. The study also found that infants younger than one month of age shed a greater quantity of virus, and that RSV shedding tended to be greater and more prolonged in infants with a more severe infection, suggesting that the duration and quantity of shedding may be related to both age and severity of illness. A study by Okiro et al. (2010) of 193 children from 151 families, with a median age of 21 months, found that the mean duration of shedding was 4.5 days, and that children with a history of RSV infection had a 40% increased rate of recovery, which may be translated to a reduced period of infectiousness.

While it is widely accepted that immunity to RSV after an infection is short, the duration of immunity is not well understood. In a ten year prospective longitudinal study of children followed in a research day-care program, the attack rates for the first, second and third RSV infections were found to be 98%, 75% and 65%, respectively (Henderson et al., 1979). In a study by Hall et al. (1991), 15 adults with previous RSV infection were challenged with a safety-tested RSV virus of the same strain group, at two, four, eight, 14, 20 and 26 months after the initial natural infection. Reinfection was measured by nasal washes and immunofluorescence testing. The study found that by two months after the first challenge, about half of the subjects had been reinfected, and by eight months, two thirds had become reinfected. Within 26 months, 73% had had two or more RSV infections and 47% had had three or more.

2.2.2 The burden of disease

Mortality due to RSV infection in developed countries is low, occurring in less than 0.1% of cases (Wang and Law, 1998), while little data have been published about RSV morbidity and mortality in developing countries (Weber et al., 1998). However, hospitalisation costs in both developed and developing regions are estimated to be substantial (Haynes, 2013; Leader and Kohlhase, 2003; Tregoning and Schwarze, 2010; Yorita et al., 2007), making RSV a significant economic and health care system burden and a current priority for vaccine development (Broadbent et al., 2015; Cheon et al., 2014; Keener, 2014; Nyiro et al., 2015).

RSV is mainly observed in children younger than two years and studies suggest that almost every child will have contracted RSV by the time they reach this age (Hall, 1981; Sorce, 2009), with an estimated 0.5–2% of infants requiring hospitalisation due to severity of the symptoms (McNamara and Smyth, 2002). Newborn infants are typically protected from RSV infection by maternal antibodies until about six weeks of age (although infection can still occur in this early phase of life) (Cane, 2001; Domachowske and Rosenberg, 1999), and the highest numbers of observed RSV cases occur in children aged six weeks to six months (Brandenburg et al., 1997; Sullender, 2000). It is unclear whether RSV is mainly transmitted by children or adults (Weber et al., 2001), although introduction into a family is thought to often occur through a school-aged child (Hall, 1981; Hall et al., 1976b).

RSV is the leading cause of hospitalisation in young children (González et al., 2012) and an estimated 1% of all primary RSV infections lead to hospital admission for bronchiolitis (Hall, 1981). In a global meta-analysis, Nair and colleagues estimated that in 2005, 3.4 (2.8–3.4) million young children were hospitalised for RSV-related illness, and found that developing countries bear the largest RSV disease burden (Nair et al., 2010). Estimates of the hospitalisation rate for RSV-related illness vary substantially, although it is unclear whether this is due to methodological differences or true geographic differences in the burden of respiratory illness (Borchers et al., 2013; Hall et al., 2013). As RSV is not a notifiable disease, there is a lack of systematic surveillance data, making worldwide comparisons difficult (Ranmuthugala et al., 2011). A recent study in the United States estimated the RSV hospitalisation rate to be 5.2 per 1,000 children under 24 months of age. Research published in Australia estimated hospitalisation rates between 8.7 and 10.6 per 1,000 children under 12 months of age (Ranmuthugala et al., 2011).

While RSV is mainly a disease of young children, it is thought that repeat infections can occur throughout life (Cane, 2001; Henderson et al., 1979), and that RSV presents as a common cold in older children and adults (Hall, 1981; Smyth and Openshaw, 2006). Several studies have reported on outbreaks of RSV in aged care facilities and estimated the mortality caused by RSV in these older age groups (Hardelid et al., 2013; van Asten et al., 2012). One such study found that up to 18% of pneumonia hospitalisations in adults aged above 65 years are due to RSV infection (Han et al., 1999).

The healthcare system cost due to RSV is substantial. An Australian study found that RSV hospitalisations cost AU $9 million per year in New South Wales alone, and that the mean cost per episode in children aged less than five years is AU $6350 (Homaira et al., 2015). Another Australian study estimated the total direct healthcare cost as between AU $24–50 million annually (Ranmuthugala et al., 2011). One study estimated that in the United States, the total hospital charges for RSV-coded primary diagnoses between 1997–2000 exceeded US $2.6 billion (Leader and Kohlhase, 2003) and another study estimated the medical cost associated with children under five years of age to be US $652 million (Paramore et al., 2004). Note that these estimates do not account for indirect costs, such as those associated with carers' time away from work.

2.2.3 Treatments and vaccine development

Treatment for RSV is usually in the form of supportive care. For hospitalised infants, depending on the severity of the infection, treatment may include oxygen therapy, ventilatory support, fever reduction, fluid intake, nutrition and rest (Sorce, 2009). The antiviral drug Ribavirin is approved by some international bodies to treat RSV-associated illness, but is not widely used in Australia. The use of Ribavirin is somewhat controversial due to questions about its efficacy, occupational risks (with it being administered through an aerosol spray), and high cost (Cane, 2001; Ventre and Randolph, 2007).

Many national guidelines recommend passive immunoprophylaxis for high risk children with the humanised monoclonal antibody palivizumab (Resch, 2014). While palivizumab is ineffective as a treatment for established RSV infection (Haynes, 2013), it has been found to be a safe and effective prophylaxis for premature and other high-risk children (The IMpact-RSV Study Group, 1998). High risk children include premature infants,

those with chronic lung disease, and those with congenital heart disease. Prophylaxis does not prevent RSV infection, yet monthly intramuscular injections of palivizumab lessen the severity of symptoms once an individual is infected and reduce hospitalisation rates (Bolisetty et al., 2005). While palivizumab is licensed in Australia to be administered to children at high risk of RSV disease and for the prevention of serious lower respiratory tract disease caused by RSV, there is no formal recommendation regarding palivizumab administration for RSV in Australia (Alexander et al., 2012; Australian Technical Advisory Group on Immunisation, 2013). Additionally, the use of palivizumab for prophylaxis is expensive, costing approximately AUD $7,500 per course (Fitzgerald et al., 2012), and the timing of the RSV season must be understood for effective prophylaxis scheduling (Moore et al., 2009a,b).

There is currently no licensed vaccine for RSV, despite about 50 years of vaccine research. An earlier formalin inactivated RSV vaccine, known as FI-RSV, reached clinical trials in the 1960s, but caused serious adverse reactions in young children upon being infected with RSV (Fields et al., 2013; Haynes, 2013). This disease enhancement, as well as the lack of a suitable animal model and an imcomplete understanding of the RSV immune response mechanism, hampered subsequent efforts to produce an RSV vaccine (Saso and Kampmann, 2016). However, RSV vaccine development has recently gained momentum, and a range of vaccine types – protein-based, gene-based and live-attenuated – are now in preclinical development or being evaluated in clinical trials (Fields et al., 2013; Haynes, 2013; Polack, 2015; Roberts et al., 2016). Several distinct target populations have been identified for RSV vaccine administration: infants under six months of age, who are at the highest risk of severe disease; children over six months of age; pregnant women; and the elderly (Anderson et al., 2013). Different vaccines for each of these target groups are being developed and tested separately (PATH, 2017).

Maternal vaccination, where infants are protected via antibody transfer through the placenta, has been successful for other diseases, such as influenza, pertussis and tetanus in a range of jurisdictions (Saso and Kampmann, 2016). Vaccination of women in their third trimester of pregnancy is now being considered for RSV, and could form a viable strategy (Polack, 2015). Novavax commenced phase 3 trials for a RSV F nanoparticle vaccine for pregnant women in late 2015 (NCT02624947) and other candidates are in the vaccine pipeline (ClinicalTrials.gov, 2016; PATH, 2017). Given the known short duration

of immunity following infection with RSV, protection from a vaccine will be temporary, and for a maternal vaccine, the protection in infants would likely only persist for up to the first six months of life. However, the objective of a maternal vaccination strategy would be to delay the onset of an infant's first RSV infection, so as to reduce the incidence of RSV disease in infants in their first few months of life, at the time when a child is more likely to develop serious symptoms (Hall et al., 1991; Saso and Kampmann, 2016). There is also some evidence that reducing the burden of severe RSV in young children may also reduce the impact of secondary conditions, such as asthma and wheezing in later childhood (Moore et al., 2015; Polack, 2015; Roche et al., 2003).

2.2.4 The seasonal patterns of RSV

In this section of the literature review, I describe the observed seasonal patterns of RSV. I review the available longitudinal datasets for RSV detections at the global level, and examine in more detail six datasets for RSV in countries other than Australia.

The distinct seasonal pattern exhibited by RSV infections in temperate climates is widely acknowledged (Dowell, 2001; Haynes, 2013; Tang and Loh, 2014). Similarly to influenza, most RSV infections occur during the winter months, with very low levels of infection during the summer. Unique, however, is the consistent pattern of infection, in both timing and magnitude of the number of infections, that is not typical of influenza.

RSV activity in temperate climates tends to be associated with the cooler months, whether wet or dry (Weber et al., 1998). Outbreaks of RSV usually occur between early winter and late spring (Sorce, 2009), and persist for between two and five months (Hall, 2001; Kim et al., 1973; Panozzo et al., 2007). RSV infections often exhibit a biennial, or two year, seasonal pattern. This is where a year of high RSV incidence is followed by a year of low RSV activity, with the next year returning to a year of high incidence, and so on. In some such regions, the low incidence RSV epidemic starts later in the year compared to the high incidence epidemic; this pattern may be characterised as a 'delayed biennial' pattern. Simplistic examples of annual, biennial and delayed biennial patterns are shown in Figure 2.2.

RSV in tropical climates exhibits different seasonal patterns, with cases occurring throughout the year and less pronounced seasonal peaks. This is likely because the climates in these regions display less extreme differences in temperature and moisture between the summer and winter months, compared to temperate regions (Chan et al., 2002; Reese and Marchette, 1991). In the tropics, the onset of the RSV season is typically associated with the rainy season (Stensballe et al., 2003; Weber et al., 1998).

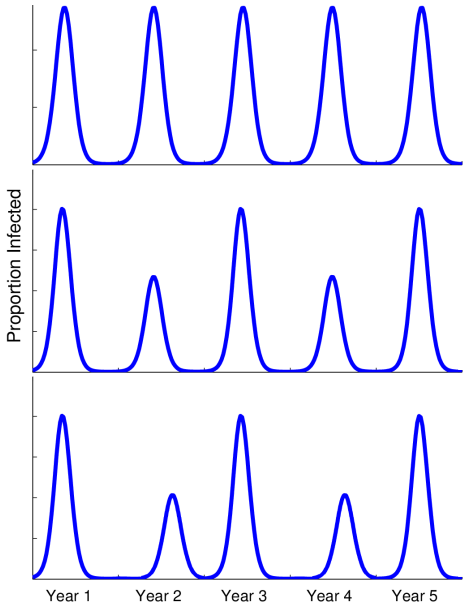

Figure 2.2: Examples of annual (upper panel), biennial (middle panel), and delayed biennial (lower panel) seasonal patterns.

The causes of seasonality in RSV transmission are not well understood. A review of the scientific literature on the causes of infectious disease seasonality identified four groups of mechanisms: (a) survival of pathogen outside host; (b) host behaviour; (c) host immune function; and (d) abundance of vectors and non-human hosts (Grassly and Fraser, 2006). As RSV is not vector-borne, the abundance of vectors and non-human hosts are not a contributing factor. Excluding this last group, all other mechanisms are plausible for RSV and are discussed below.

Survival of pathogen outside host: The ability of a pathogen to survive outside a host organism is affected by changes in environmental conditions such as humidity, temperature and exposure to sunlight, which vary seasonally. Humidity has been shown to affect the survival of RSV in experimental conditions, but it is unknown whether it is important for transmission (Weber et al., 2001). In a Singapore-based study, Chew et al. (1998) found that higher incidence of RSV correlated with low humidity in the tropics, but other studies have shown a correlation between RSV activity and high humidity (Yusuf et al., 2007). Increased RSV activity has been found to correlate with lower temperatures in a number of temperate locations, but this relationship is less consistent in tropical regions (Noyola and Mandeville, 2008; Tang and Loh, 2014; Vandini et al., 2013; Welliver, 2009).

Host behaviour: Social factors, such as indoor crowding during the cold or wet months of the year, have been proposed as potential drivers of seasonal incidence of infectious diseases. A study by Waris (1991) suggested that the timing of the school vacation in Finland contributes to the biennial pattern. However, a study by Acedo et al. (2011) showed that linking the school term with RSV's seasonal fluctuations in Valencia, Spain, is difficult because of the delay of several months between the beginning of the school period and the maximum RSV peak.

Host immune function: Some research suggests a relationship between vitamin D deficiency and RSV infection in childhood, with reduced vitamin D levels thought to impair wintertime host immune function (Belderbos et al., 2011; Yusuf et al., 2007). However, this link remains contested in the literature. A study by Beigelman et al. (2015) examined infants hospitalised with bronchiolitis, who were then tested positive for RSV, and found no link between RSV severity and vitamin D levels.

Another possible reason for RSV's distinct seasonal pattern is the circulation of the two serotypes, RSV-A and RSV-B. There is no firm consensus in the scientific literature about the predominance of one subgroup over the other (Paes, 2003), and no significant difference in the severity of symptoms between the two serotypes has been identified (Hirsh et al., 2014). Studies have shown that the two serotypes generally co-circulate within epidemics (Cane, 2001; Esposito et al., 2015). White et al. (2005) implemented a mathematical modelling approach to investigate RSV transmission, incorporating the two serotypes, and found that strain circulation could help explain patterns observed in England and Wales, and Turku, Finland. However, a study in Zagreb, Croatia, over two calendar years, suggested that the biennial pattern occurs independently of virus subtype (Mlinaric-Galinovic et al., 2009). The latter finding has been supported in other studies. In some regions, one serotype has been found to dominate for two years (Hall et al., 1990; Waris, 1991), and in other regions, the relative proportions of RSV-A and RSV-B vary from year to year (Cane et al., 1994). Zlateva et al. (2007) identified a regular three year cycle of serotype dominance in Belgium, with two years of RSV-A dominance followed by one year of RSV-B dominance. Serotype circulation could be a contributing factor, but is unlikely to be the main driver of biennial patterns of RSV in temperate regions (Pitzer et al., 2015), and due to the nature of the data available for Western Australia, investigating the dynamics of the two strains is beyond the scope of this thesis.

Table 2.1: This table shows selected published data for RSV detections for a range of locations and latitudes. The observed qualitative pattern in the data is described for each location. In cases where the data shows a marked annual or biennial cycle, I have used those terms to describe the pattern. In some instances where the data could not be described as either annual or biennial, I have used the term 'single epidemic peak'. The term 'odd/even years' refers to a northern hemisphere winter that begins at the end of an odd year and continues into the beginning of an even year (and vice versa for the term 'even/odd').

Location	Latitude	Study data	Pattern	Reference
Finland	60.1708° N (Helsinki)	Monthly detections, lab confirmed, for 1981–1990	Markedly delayed biennial, high years peaking in Nov–Dec–Jan odd/even years	Waris (1991)
Oslo, Norway	59.9500° N	Monthly detections, hospitalised cases, lab confirmed, for 1972–1978	Delayed biennial in the first four epidemic years	Ørstavik et al. (1980)
Stockholm, Sweden	59.3294° N	Biweekly detections, hospitalised cases, lab confirmed, 1984–1993	Delayed biennial pattern, high years peaking in Dec–Feb odd/even years	Reyes et al. (1997)
Leuven, Belgium	50.8833° N	Monthly detections, lab confirmed, 1996–2006, A & B subtypes	Annual peak in December each year	Zlateva et al. (2007)
Stuggart, Germany	48.7833° N	Monthly detections, hospitalised cases, lab confirmed, 1996–2004	Biennial (small delay), high years peaking in Jan–Feb of odd years	Terletskaia-Ladwig et al. (2005)
Switzerland	46.8333° N	Monthly detections, lab confirmed, 1988–1999	Biennial (small delay), high years peaking in winter of even/odd years	Duppenthaler et al. (2003)
Bern, Switzerland	46.9500° N	Monthly detections, pediatric hospital cases, lab confirmed, 1997–2001	Biennial (small delay), high years peaking in winter of even/odd years	Duppenthaler et al. (2003)
Zagreb region, Croatia	45.8167° N	Monthly detections, hospitalised cases, lab confirmed, 1994–2005	Delayed biennial, high years peaking in Dec–Jan even/odd years	Mlinaric-Galinovic et al. (2008)
Sapporo, Japan	43.0667° N	Monthly detections, lab confirmed, 82 cases in five epidemic years 1980–1987	Annual January peak in 4 of 5 years	Tsutsumi et al. (1988)
Salt Lake City, Utah, U.S.A.	40.7500° N	Weekly detections, lab confirmed, children ≤ 2, 2001–2008	Single epidemic peak each year in winter months (possibly biennial)	Leecaster et al. (2011)
Valencia, Spain	39.4667° N	Weekly detections, hospitalised cases, children ≤ 2, for 2001–2004	Single epidemic peak each year in the winter months	Corberán-Vallet and Santonja (2014)

Location	Latitude	Study data	Pattern	Reference
Colorado, U.S.A.	39.0000° N	Weekly RSV hospitalisations 1996–2006	Biennial (high peaks in odd winters)	Zachariah and Shah (2009)
Maryland, U.S.A.	39.0000° N	Weekly community, inpatient and intensive care detections, lab confirmed, 2002–2007	Annual winter peaks	Spaeder and Fackler (2012)
Washington D.C., U.S.A.	38.9047° N	Monthly detections, lab confirmed, 1957–1973	Alternating short and long intervals between epidemics	Kim et al. (1973); Parrott et al. (1974)
Fukuoka, Japan	33.5833° N	Weekly cases from 120 medical institutions, not all lab confirmed, 2006–2012	Single epidemic peak each year in the winter months	Onozuka (2015)
Israel	32.0667° N	Monthly detections, hospitalised cases, lab confirmed, 2005–2012, A & B subtypes	Single epidemic peak each year in the winter months	Hirsh et al. (2014)
Taiwan	23.5000° N	Monthly RSV hospitalisations, children ≤ 5, detections based on hospital coding, 2004–2007	Biannual, with peaks each spring and autumn	Chi et al. (2011)
The Gambia	13.4667° N	Monthly detections, lab confirmed, hospitalised cases, 1993–2002	Outbreaks in rainy season in first six years, followed by two irregular outbreaks, then two regular outbreaks	van der Sande et al. (2004)
Singapore	1.3000° N	Monthly detections, lab confirmed, hospitalised cases, 1990–1994	Annual seasonal pattern with May–June peak	Chew et al. (1998)
Santiago, Chile	33.4500° S	Monthly detections, lab confirmed, hospitalised cases, 1989–2000	Biennial, with two high years in 1993 and 1994 and high peaks in even year winters thereafter	Avendaño et al. (2003)
Sydney, Australia	33.8650° S	Monthly detections, lab confirmed, hospitalised cases, 1979–1983	Single epidemic peak each year in the winter months	de Silva and Hanlon (1986)

2.2.5 The global seasonality of RSV infection

I reviewed the available literature to identify the dominant RSV seasonal pattern (particularly whether annual or biennial) in a range of countries and regions. This summary, while not exhaustive, indicates how RSV dynamics vary with latitude, and is shown in Table 2.1. An important caveat is that RSV is not a notifiable disease, and that testing practices vary in different countries. Here, I also present six datasets in greater detail: these are for Santiago, Finland, Stuggart, Switzerland, Croatia and Salt Lake City. These datasets were chosen because they all represent at least six consecutive years, show a clear seasonal pattern, and correspond to a range of different latitudes. It should be noted that for the studies reviewed here, there is no consistent empirical test used to determine whether a dataset displays an annual or biennial pattern; this assessment is typically made by human judgement.

Santiago, Chile

In a surveillance study in Santiago, Chile, over 12 years (January 1989 to December 2000), 4,618 hospitalised infants under two years of age were tested for RSV (Avendaño et al., 2003). The positive detection data (Figure 2.3) indicates a clear biennial epidemic pattern, with the exception of 1993 and 1994, where two consecutive high activity RSV seasons were observed. Interestingly, from 1994 onwards, a pattern of high-early then low-late epidemics became evident. That is, a major RSV epidemic occurred in mid-winter, and was followed by a minor RSV epidemic with a late winter peak the following year. The next major epidemic would again peak at the same time as that two years prior. Avendaño et al. (2003) found that the mean duration of RSV epidemics was 4.5 months, with a range of 3.5 to 6 months, where a detection rate of more than 20% in hospitalised infants tested for RSV was used as the definition for an epidemic.

Finland

A study conducted in Finland between January 1981 and March 1990 collected laboratory-verified positive RSV identifications from 3,285 patients (Waris, 1991). These data (Figure 2.4) show a clear biennial pattern, with high-early and low-late epidemics in alternate years. The high-incidence epidemics began in December or January every second year, and were followed by a minor peak in spring the following year. The delay between major and minor epidemic peaks appears to be longer than for the Chilean dataset in the previous section.

Figure 2.3: RSV data, Santiago, Chile - Acute lower respiratory illness visits (dashed line) and the percentage of those in which RSV was detected (solid line), for hospitalised infants and outpatient visits at the Roberto del Rio Children's Hospital, between 1989 and 2000 inclusive (Avendaño et al., 2003).

Figure 2.4: RSV data, Finland - RSV positive laboratory diagnoses by month in Finland, between January 1991 and March 1990 (Waris, 1991).

Figure 2.5: RSV data, Stuggart, Germany - Absolute number of total RSV investigations and positive results by month, from January 1996 to May 2004 (Terletskaia-Ladwig et al., 2005).

Figure 2.6: RSV data, Switzerland - The main plot shows the number of positive RSV detections per week from 1988 to 1999, where each datapoint is a moving three week average. The inset plot in the top right shows the RSV detections per week at the University Children's Hospital of Bern, between July 1997 and June 2001 (Duppenthaler et al., 2003).

There were very few positive RSV cases between epidemics. The authors suggested that the school vacation, which occurs in Finland from the beginning of June until mid-August, interrupts the epidemic spread after the smaller peak every second year (Waris, 1991).

Stuggart, Germany

A study by Terletskaia-Ladwig et al. (2005) in southern Germany sought to identify the timing of RSV outbreaks. The study found that RSV seasons presented a regular biennial rhythm, where the season with high RSV activity occurred earlier than the subsequent season of low RSV activity. The authors also found that the RSV epidemics in southern Germany oscillated in antiphase with the epidemics in Finland and Sweden. A plot depicting the total number of RSV investigations and number of positive RSV results is shown in Figure 2.5. An earlier study by Weigl et al. (2002) in Kiel, Germany, over a seven year period, did not identify such a clear biennial pattern. However this may be due to the low number of samples tested in that instance.

Figure 2.7: RSV data, Croatia - Monthly RSV cases in Zagreb County, Croatia, between July 1994 and June 2005 (Mlinaric-Galinovic et al., 2008).

Switzerland

A regional study of RSV hospitalisations in Bern, Switzerland, was conducted over a four year period (Duppenthaler et al., 2001), and later complemented by a broader study

Figure 2.8: RSV data, Salt Lake City, Utah, USA – Weekly positive RSV detection data for children under two years of age (Leecaster et al., 2011). The axis titles are edited for visual clarity.

of national laboratory notifications for RSV positive test results over a 12 year period (Duppenthaler et al., 2003). The latter study confirms this biennial periodicity in both the magnitude of seasonal peaks and the timing of RSV epidemics, shown in Figure 2.6. The authors suggest that the increase in the number of RSV detections in the twelve year dataset is likely due to widening availability and use of commercial RSV detection kits, rather than an increase in RSV infections.

Croatia

A biennial cycle of RSV infections was observed in north-west Croatia (Mlinaric-Galinovic et al., 2008), in a study over 11 years of hospitalised children who tested positive for RSV. The study data are shown in Figure 2.7. Again, a two year pattern was observed, with a major RSV epidemic occurring in December or January each year, and a delayed minor RSV epidemic peak occurring up to 16 months later.

Salt Lake City, Utah

In a study in Salt Lake City, Utah (Leecaster et al., 2011), RSV testing data from the Primary Children's Medical Center (the major pediatric health care facility in Utah) were collected for children under two years of age. The authors described a biennial seasonal pattern in the size of the epidemic each year, shown in Figure 2.8, however this biennial pattern is not immediately apparent as the magnitude of the peaks in alternate years is not as regular as observed in other datasets. Another study comprising eight counties in Utah (Lyon et al., 1996) also identified a biennial epidemic pattern, with major RSV epidemic peaks in even-year winters between 1985 and 1992.

2.3 Mathematical modelling of RSV

Mathematical models are important tools for analysing, understanding and predicting outbreaks of infectious diseases (Hethcote, 2007). In this section I first provide some background on mathematical tools used to model infectious disease epidemics, focusing on compartmental ordinary differential equation models. I then present an overview of the mathematical models for RSV in the literature to date.

2.3.1 Background to infectious disease modelling

There are several distinct approaches to the mathematical modelling of epidemics. These approaches may be categorised as deterministic, stochastic, or time series, or some combination of these forms. Within these categories, different types of models include individual-based models, models on networks, compartmental models, household models, and Bayesian models. In this thesis I focus on a type of deterministic, ordinary differential equation (ODE) model using the 'Susceptible-Infectious-Recovered' (SIR) paradigm, and provide a brief introduction to this model. In 1927, Kermack and McKendrick (1927) published the first paper in a series of three articles on the theory of mathematical epidemiology. This paper presented the important Threshold Theorem and is regarded as a classic in the field. The SIR formulation is a special case of the general Kermack-McKendrick model, first described in the 1927 paper, and has since been widely applied in the modelling of infectious disease dynamics. For a more comprehensive explanation of other types of epidemic models,

there are a number of excellent resources that may be consulted, including the widely-referenced book by Anderson and May (1991) and the more recent texts by Keeling and Rohani (2008) and Diekmann et al. (2013).

The approach of the compartmental framework is to divide a population into different compartments that correspond to the stages of an infection. Each compartment corresponds to a proportion of, or number of people in, a defined population. These compartments describe whether individuals are susceptible to infection S, infectious I, or recovered from infection and immune R. Here the SIR framework is discussed further in the context of compartmental ODE models. In this type of SIR model, demography is represented by the inclusion of a birth rate μ, which corresponds to an average life expectancy of $1/\mu$. In the example discussed here, the birth and death rates are equal, therefore the total population N remains constant over time t. Such an assumption is suitable for infectious diseases where the infection life cycle is relatively short compared to the average individual lifespan, and the death rate due to the disease is negligible. The transmission rate is represented by β and the recovery rate is represented by γ, where $1/\gamma$ is the average period of infectiousness. The differential equation model representing this process is

$$\begin{aligned}
\frac{dS}{dt} &= \mu N - \beta S\frac{I}{N} - \mu S && (2.1)\\
\frac{dI}{dt} &= \beta S\frac{I}{N} - \gamma I - \mu I && (2.2)\\
\frac{dR}{dt} &= \gamma I - \mu R && (2.3)\\
N &= S + I + R. && (2.4)
\end{aligned}$$

In this thesis, in Chapters 4–6, where I present an extension of Equations (2.1)–(2.4), I formulate the modelled compartments in terms of proportions. This means that I set $N = 1$ and treat the compartments as proportions of the total population, rather than numbers of individuals. In Chapter 7, where I parametrise the model for a fixed population size, I instead model the number of individuals in each compartment, and N is set as the total population. A schematic diagram for the ordinary differential equation SIR model described by equations (2.1)–(2.4) is presented in Figure 2.9.

A limitation of the ODE model is that its formulation assumes a spatially and socially homo-

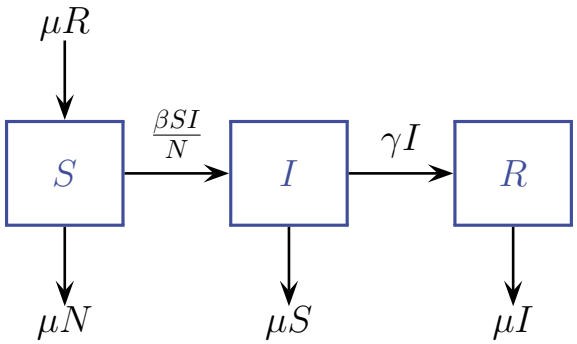

Figure 2.9: Schematic diagram of the SIR model, where μ is the birth and death rate, $1/\gamma$ is the average infectious period and β is the transmission rate.

geneous population, where every susceptible individual has the same risk of being infected by an infectious individual. However, these type of deterministic models have a history of providing useful insights and predictions (Bansal et al., 2007; Burr and Chowell, 2008), and adaptations of the SIR compartmental ODE framework allow some of these heterogeneities (such as age structures) to be included. Several such adaptations are addressed in this thesis. A further consideration is that in employing deterministic models, stochastic events inherent in any population are disregarded. However, deterministic models are more analytically tractable and computationally efficient, and suitable for sufficiently large populations, such as those considered in this thesis. Another drawback of the compartmental ODE approach is that, due to the model formulation, the time spent in each compartment is exponentially distributed (Keeling and Rohani, 2008). However, there are model adaptations that can be used to address this limitation, and the SIR compartmental ODE framework remains widely used (Keeling and Rohani, 2008, pp. 93–102).

Some infectious diseases, including RSV, may be characterised by their seasonality, where the incidence varies at different times of the year. Seasonal dynamics may be incorporated into the model by replacing the parameter β with a time-varying sinusoidal forcing function, such as

$$\beta(t) \quad = \quad b_0[1 + b_1 \sin(2\pi t + \phi)]. \tag{2.5}$$

In Equation (2.5), the parameter b_0 represents the mean transmission rate, b_1 represents the amplitude of seasonal forcing which must be in the range $[0, 1]$, and ϕ is a phase shift

parameter, enabling peak disease incidence to be fitted to data.

2.3.2 Mathematical models for RSV

Despite the significant health and economic burden of RSV, few mathematical models for RSV transmission have been published to date. Here I review several RSV models presented in the literature, categorising papers according to model type: deterministic compartmental models, stochastic models and time series models. I then review the published models for the future rollout of a RSV vaccine. I did not identify any papers using an individual-based approach to model population-level RSV transmission, although this approach has been applied in modelling a RSV vaccine (Poletti et al., 2015).

Deterministic compartmental models

Several compartmental ODE models have been developed for RSV, and some of these have been expanded to include a latent class and age-structuring. Sinusoidal functions are typically used to replicate seasonality in RSV transmission, and Nelder Mead or Markov Chain Monte Carlo methods may be used for parameter estimation.

One of the most comprehensive and widely referenced mathematical modelling papers for RSV published to date is that by Weber et al. (2001). The authors first considered a simple compartmental ODE model for RSV infection. The transmission was modelled by a cosine seasonal forcing function. The authors then developed a more complex model that incorporated a latent period, maternally derived immunity, and gradual reduction in susceptibility to reinfection. In order to incorporate reduced susceptibility, the authors assumed that the reduced risk is 50% after one infection, 35% after two infections and 25% after three infections. Additional S, E (exposed or latent), I and R classes were introduced with a corresponding scaled transmission function for each transmission event. Weber et al. (2001) fitted the models to data from four regions: The Gambia; Florida; Finland; and Singapore. The authors found that both the simple and complex models fit the datasets almost equally well, noting that RSV epidemics can be modelled surprisingly well using relatively simple ODE models. The biennial seasonal pattern was replicated by both models. The authors showed that the fitted values of the relative amplitude (i.e. the magnitude of seasonal forcing) were greater in temperate regions that displayed a biennial pattern, and lower in tropical regions.

Figure 2.10: The schematic diagram of the model described in Leecaster et al. (2011). The diagram illustrates the flow between compartments in the SEIDR model.

Leecaster et al. (2011) developed models to predict the characteristics (such as peak epidemic timing and total size) of future RSV epidemics. The authors presented a Susceptible-Exposed-Infectious-Detected-Recovered (SEIDR) model for RSV detections and fitted this model to a dataset from Salt Lake City, Utah, over seven years (the dataset is discussed in Subsection 2.2.5). The S, E and I classes were split into two compartments: children less than two years of age; and those aged two years and above. Transmission was modelled using a seasonal forcing function, with the seasonality parameter, as described in Equation (2.5), assumed to be $b_1 = 1$. The schematic representation of the model is shown in Figure 2.10. Limitations of this modelling approach include the omission of waning immunity, and the amplitude of seasonal forcing being fixed at the maximum value. It is also unclear whether the extent of variation in the transmission parameters estimated for the model is epidemiologically realistic.

In the Leecaster et al. (2011) study, linear regression modelling was also used to estimate relationships between the final epidemic size, days to epidemic peak, and the length of the epidemic. Leecaster et al. (2011) found that exponential growth was correlated with epidemic characteristics, and that the epidemic start time and the transmission parameter co-varied with the epidemic season. While these results are useful for health policy-makers, further work is required to understand the underlying drivers of variation in epidemic dynamics.

White et al. (2005) presented a differential equation model that accounted for infection with the two main RSV subtypes: RSV-A and RSV-B, in England/Wales and Finland.

The authors noted that the models reproduced the overall pattern in the data, as well as the dominance of the RSV-A subtype, and that the fitted seasonal transmission terms (overall transmission, amplitude and phase) varied between the two locations. As discussed in the paper, further work is required to model RSV vaccination strategies that take account of antigenic diversity (White et al., 2005), but without A/B strain data for different regions, this is difficult.

White et al. (2007) identified the important role of RSV immunity in its transmission dynamics, described nested differential equation models for RSV transmission, and fitted these models to RSV case data for eight different regions. Four different post-infection immunity scenarios were examined: partial susceptibility; altered infection duration; reduced infectiousness; and temporary immunity. For this model, lifelong partial immunity produced the best fit to the data.

Capistrán et al. (2009) outlined a SIRS model with seasonal forcing and proposed a method to estimate the model parameters, which they used to fit the model to data for The Gambia and Finland. The authors found seasonal forcing was necessary in order to reproduce the biennial pattern observed in the Finland data, and concluded that the forced model is more appropriate than the unforced model in terms of comparison to real data.

In a recent analysis, Paynter et al. (2014b) investigated the ecological drivers of RSV seasonality in the Philippines. Their model included a second susceptible class for individuals with reduced susceptibility following an initial RSV infection, and classes for latent and infectious individuals with a subsequent RSV infection. In this work, the authors also experimented with a square wave transmission term that accounted for decreased transmissibility over the summer holidays, as well as a seasonally driven birth rate. Paynter et al. (2014b) found that the cosine transmission function was appropriate for replicating the observed RSV seasonality in the Philippines The authors found no link between temperature, dew point and relative humidity, and the patterns in RSV cases, and suggested that school holidays were also unlikely to play a role. However, seasonal malnutrition and rainfall were identified as possible drivers of RSV seasonality in this setting.

Stochastic modelling approaches

A study by Acedo et al. (2011) explored a different modelling approach, presenting a random

network model for RSV transmission between individuals, using hospitalisation data for Valencia, Spain. In this study, no periodic forcing was used to simulate seasonality. The authors showed that for a range of values of the infection probability and contact parameter, the model produced sustained annual seasonal dynamics. The authors suggested that social and demographic factors could play a more important role in the seasonal dynamics of RSV than the climatic factors usually identified, and pointed out that understanding the relative roles of social contacts and demographic changes, compared to external factors, is important in considering prophylaxis and vaccination policies.

Time series approaches

Several RSV modelling papers have used time series approaches and real weather variables as predictive tools to forecast the dynamics of RSV epidemics and allow for better resource utilisation, particularly in hospitals. One such study by Walton et al. (2010) used Naive Bayes classifier models based on weather data in Salt Lake County, Utah, in order to predict the start week of RSV epidemics. The study showed that temperature and wind speed were good predictors of RSV epidemics, although the authors noted that wind speed had been a poor indicator in previous studies. The authors also suggested that such models could be useful for real time forecasts, although separate models would be needed for high-peak and low-peak years where biennial patterns in RSV detections are observed.

Paynter et al. (2015) used hospitalisation data from Cairns and Townsville, in the north-eastern tropical region of Australia, in a cross-correlation analysis to determine the correlation between selected weather variables and RSV admissions. Based on this study, the authors concluded that the seasonality of RSV infection in two areas of tropical Queensland may be driven by rainfall, but noted that in order to fully assess the link between climatic factors and RSV in the tropics, further research was required (Paynter et al., 2015).

Spaeder and Fackler (2012) developed forecasting models for weekly RSV incidence in three separate settings: the community, the inpatient pediatric hospital and the intensive-care unit. Auto-correlation functions were used to identify base models and maximum likelihood estimation was implemented to calculate the parameter coefficients. While the study was for a single community and institution, the models produced accurate one and two week forecasts.

Modelling vaccination strategies for RSV

The need for mathematical modelling to help determine RSV vaccination strategies has recently been identified (Graham, 2014; Munywoki et al., 2014), yet few modelling papers have explored vaccination for RSV so far.

A newborn vaccination strategy was investigated in Acedo et al. (2010a) for the Spanish region of Valencia, in order to estimate the cost-effectiveness of potential RSV vaccination strategies. The modelling approach moved a fraction of susceptible newborns into a vaccinated class, where they remained until they reached the next age group, at which point they moved to the second susceptible class. This strategy assumed booster doses of the vaccine in the first year of life, such that the immunisation period would be at least equal to the immunity of those who have recovered from RSV infection. In subsequent work, an RSV vaccine cost analysis was conducted based on a stochastic social network model, with children vaccinated at two months, four months and one year of age (Acedo et al., 2010b). In this study, the examined costs were for hospitalisation, vaccination and parental work loss. A three dose vaccination schedule was found to be cost-effective, assuming four lost days of parental work for each infected child.

Bos et al. (2007) developed a health-economic model for RSV vaccination in The Netherlands, where around 3,670 children are hospitalised annually for RSV infection. The model estimated hospitalisation costs using regression analysis, and the results were used as inputs for a cohort model, where infants were followed for 24 months. Several scenarios were considered, including seasonal vaccination, and the study found that an RSV vaccine could prevent between 1,000 and 3,000 hospitalisations annually, depending on vaccine effectiveness and the month of vaccine delivery. Meijboom et al. (2012) conducted a cost-effectiveness analysis of an RSV vaccination scheme for children in The Netherlands. Several different vaccination strategies, including two- or three-dose schemes, seasonal vaccination and year-round vaccination were considered. The authors developed a Markov model for the analysis. The analysis showed that, for some scenarios, a vaccine might be cost-effective, but that better estimates of vaccine efficacy based on clinical trials were needed for more accurate estimates.

A study by Poletti et al. (2015) considered RSV vaccination strategies in Kenya, using an individual-based model. An important factor implemented in this approach was that the

model used household studies to enable characterisation of different forms of transmission, and also accounted for different vaccination effectiveness and duration scenarios. This work identified school-aged children as the main source of transmission in a household. It also proposed alternative vaccination targets to those most at risk of severe infection: expectant mothers and school-aged children. However, this study was particular to the low-income environment and household structure of Kenya, and the results may not be translatable to other settings, prompting the need for such modelling studies to be conducted elsewhere.

Kinyanjui et al. (2015) developed an deterministic age-structured model for a low-income country setting. The population was subdivided into 99 age classes: 24 classes for each month for the first two years of life, and yearly thereafter. The authors used two different contact matrices to reflect different social mixing scenarios, and vaccination of children older than six months was incorporated into the modelling. This study found that RSV vaccination could be effective if administered after the waning of natural maternally-derived immunity, and before the first RSV infection.

Directions for future work

The mathematical modelling of RSV transmission published to date employs several different techniques, including compartmental deterministic models, stochastic models and time series approaches. However, there are far fewer mathematical modelling papers for RSV than for some other infectious diseases, such as influenza and pertussis, and as such there remains scope to improve and analyse RSV models further to improve our understanding of transmission dynamics. Examining these models collectively, simple sinusoidal forcing terms in deterministic models have been shown to adequately capture the known seasonal patterns of RSV in temperate regions. These studies also indicate that waning immunity plays an important role, and is a necessary component of RSV transmission models.

Seasonality is a key feature of RSV transmission and many temperate regions show strong annual or biennial patterns. The seasonality of RSV in the tropics, however, is less well documented. The drivers of these seasonal patterns of RSV remain unknown, with some inconsistencies in the findings concerning potential climate drivers. A range of factors, including climate and weather, social factors, serotype diversity, and demographic factors could play a role, or could be of different relative importance in different locations. There is clearly a need to understand the local epidemiology of RSV in order to accurately model

RSV dynamics in different locations.

Finally, with RSV vaccine candidates in pre-clinical and clinical trials, there is a need for mathematical modelling to help determine optimal vaccination strategies. Despite the high burden of illness attributable to RSV, there is a paucity of data available, and RSV has received less modelling attention than other infectious diseases such as influenza and pertussis. The RSV modelling conducted so far is largely focussed on hospitalisation burden and cost estimates, but is limited in quantity, and requires more data in order to improve the estimates. There is clearly scope to further explore RSV transmission models in this area, as more information about possible RSV vaccines becomes available.

3

Data sources and linkage

3.1 Introduction

The RSV and bronchiolitis data for this thesis were derived from ongoing data linkage research projects that are being conducted under the guidance of my PhD supervisor Hannah Moore, at the Telethon Kids Institute in Western Australia. All data cleaning and coding were conducted by the research team at the Telethon Kids Institute. I was provided a cleaned set of data with the required variables for my project. This chapter contains a brief description of the data linkage process, and an explanation of the variables used for this thesis.

3.2 Data linkage

Data linkage is the process whereby records from different administrative sources or systems are brought together for each person in a cohort, using a best-practice protocol that protects the privacy of individuals (Holman et al., 1999; Kelman et al., 2002). Records are linked by probabilistic matching on identifying details of an individual (such as name and date of birth), where the outcome information (such as medical records) is absent. Each individual is then assigned a unique code. The de-identified outcome data is then linked using the unique codes, and is available for researchers to use, following ethical approval and compliance with strict confidentiality policies (Moore, 2011; Moore et al., 2011).

Western Australia is a world leader in data linkage for health research, due to the breadth of information available for linkage and the data linkage infrastructure. Further, Western Australia is the only jurisdiction in Australia where population-based laboratory data is routinely collected through a centralised public pathology provider, PathWest. This has resulted in a unique set of laboratory-confirmed RSV detections on which this research is based.

In Western Australia, population-based administrative health datasets may be linked through the Western Australian Data Linkage System (WADLS). For this thesis, population-level data from several core administrative datasets were used: the Birth and Death Registrations, the Midwives Notification System (MNS), the Hospital Morbidity Data Collection (HMDC) and the PathWest Laboratory Medicine Database (PathWest). PathWest provides reference pathology services to the single tertiary paediatric hospital and all but three other hospitals in Western Australia that admit children. For RSV, four laboratory testing methods are used: immunofluorescence, polymerase chain reaction (PCR), viral culture, and complement fixation. The HMDC encompasses all public and private hospital admissions in Western Australia, and therefore provides complete coverage of hospital data in the state. From the HMDC, the principle diagnosis codes and an additional 20 codes (from the ICD-10 AM system) were used to identify acute lower respiratory infection (ALRI) admissions.

3.3 Western Australia research projects

Data for this thesis are derived from two separate projects conducted at the Telethon Kids Institute. Brief descriptions of these projects follow, and details of the data coding and cleaning are available elsewhere (Moore et al., 2011).

3.3.1 Dataset 1: 1996–2005

The purpose of the first study was to use total population data to describe the characteristics of respiratory infections, in order to plan for epidemics in Western Australia. These data were derived from a retrospective population-based cohort study of 245,249 singleton births in 1996–2005 in Western Australia. For this thesis, only PathWest data were used with the merged birth cohort from Dataset 1.

3.3.2 Dataset 2: 1996–2012

A second study is aimed at investigating the pathogen-specific burden of respiratory infections (the Triple I Study). The data in this study were derived from a cohort of 469,589 singleton births in 1996–2012 in Western Australia. This is an updated and more complete version of the earlier dataset, as the data extraction protocols, particularly for the laboratory data, were optimised. For this thesis, PathWest and HMDC data were used with the merged birth cohort.

3.3.3 Data used in this thesis

For this thesis, the de-identified linked data were prepared for analysis so as to include only the variables of interest for the present research. The data were presented in the form of line entry records, where one line represents a single RSV test or bronchiolitis hospitalisation.

Western Australia is classified into nine administrative health regions: Kimberley, Pilbara-Gascoyne, Midwest-Murchison, Goldfields-South East, Wheatbelt, Great Southern, South West, North Metropolitan and South Metropolitan. These regions may also be classified as metropolitan, rural or remote. For the first dataset, only data for the combined Metropolitan health regions were analysed. For the second dataset, all health regions were analysed, with the North and South Metropolitan combined into a single region. For the PathWest data, the region was based on the postcode of the mother at the time of the child's birth. For the HMDC data, the region was based on the postcode of residence at the time of hospital admission.

Other information included in the datasets was the hospital admission date (for the HMDC data), test date (for the PathWest data), and date of birth. For the PathWest data, each entry indicated whether the RSV test was positive or negative, and the type of test conducted. For the HMDC data, each entry showed the primary, secondary and subsequent diagnoses.

The first dataset, for 1996–2005, was used for the analyses in Chapters 4 and 5. The second dataset, for 1996–2012, was used for the analysis in Chapters 6 and 7. A diagram representing the data linkage system for Datasest 2, as applicable to the analyses in this thesis, is shown in Figure 3.1.

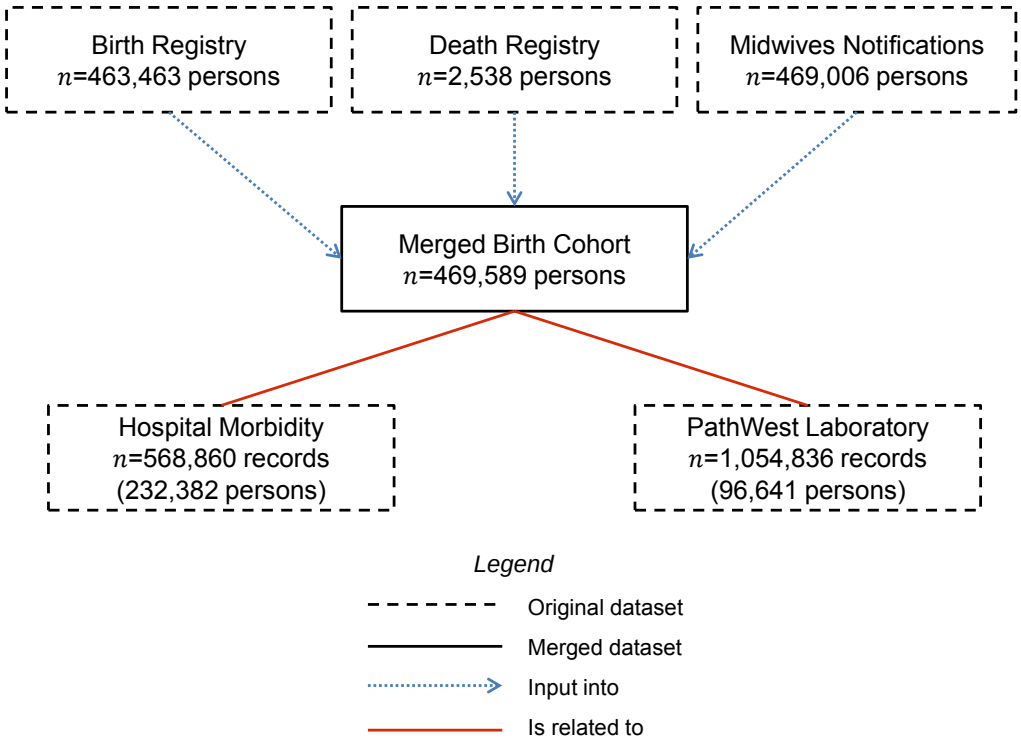

Figure 3.1: Diagram illustrating the data linkage for Dataset 2, as applicable for this thesis.

4

Age-structured models for RSV

4.1 Introduction

This chapter includes two peer-reviewed papers. The first paper is published in the *Proceedings of the 20th International Congress on Modelling and Simulation* (*MODSIM*). In this paper I introduce deterministic, ordinary differential equation models for RSV, with both single and multiple age classes. The models are of the compartmental SIR form described in the Literature Review, and I include a preliminary exploration of the dynamics of these models. The main outcome of this paper is to introduce the age-structured differential equation model for RSV transmission, and show that the model produces both annual (one-year) and biennial (two-year) dynamics for a range of plausible parameter values. While the model can also produce delayed biennial patterns for ranges of different parameter values, these patterns are explored in Chapters 5 and 6 in the context of a broader parameter space analysis.

The second paper is published in *PLoS ONE*, and describes how the multiple age class model was fitted to RSV data for one age class (children younger than 24 months) in Western Australia. As the third author of this paper, my contribution was assisting to develop the model, running simulations, and performing the sensitivity analysis. In the additional material after these two papers, I extend the approach taken in the *PLoS ONE* paper to demonstrate how the compartmental model can be successfully fitted to two childhood age classes simultaneously, by modifying the fitting routine and fit statistic. The resulting

parameters from fitting to two age classes will be the starting point for the parameter space analysis of the model in later chapters.

4.2 Papers

Hogan, A. B., Mercer, G. N., Glass, K., and Moore, H. C. (2013). Modelling the seasonality of respiratory syncytial virus in young children. In *Proceedings of the 20th International Congress on Modelling and Simulation*, 338–344.

Moore, H. C., Jacoby, P., Hogan, A. B., Blyth, C. C., and Mercer, G. N. (2014). Modelling the seasonal epidemics of respiratory syncytial virus in young children. *PLoS ONE*, 9(6):e100422.

20th International Congress on Modelling and Simulation, Adelaide, Australia, 1–6 December 2013
www.mssanz.org.au/modsim2013

Modelling the seasonality of respiratory syncytial virus in young children

A.B. Hogan[a], **G.N. Mercer**[a], **K. Glass**[a], **H.C. Moore**[b]

[a]*National Centre for Epidemiology and Population Health, Australian National University, Canberra, Australia*
[b]*Telethon Institute for Child Health Research, Centre for Child Health Research, University of Western Australia, Perth, Australia*
Email: Alexandra.Hogan@anu.edu.au

Abstract: Respiratory syncytial virus (RSV) is a major cause of acute lower respiratory tract infections in infants and young children. The transmission dynamics of RSV infection among young children are still poorly understood (Hall et al., 2009) and mathematical modelling can be used to better understand the seasonal behaviour of the virus. However, few mathematical models for RSV have been published to date (Moore et al., 2013; Weber et al., 2001; Leecaster et al., 2011) and these are relatively simple, in contrast to studies of other infectious diseases such as measles and influenza.

A simple SEIRS (Susceptible, Exposed, Infectious, Recovered, Susceptible) type deterministic ordinary differential equation model for RSV is constructed and then expanded to capture two separate age classes with different transmission parameters, to reflect the age specific dynamics known to exist for RSV. Parameters in the models are based on the available literature.

In temperate climates, RSV dynamics are highly seasonal with mid-winter peaks and very low levels of activity during summer months. Often there is an observed biennial seasonal pattern in southern Australia with alternating peak sizes in winter months. To model this seasonality the transmission parameter $\beta(t)$ is taken to vary sinusoidally with higher transmission during winter months, such as in models presented in Keeling and Rohani (2008) for infections such as measles and pertussis:

$$\beta(t) = \beta_0[1 + \beta_1 \sin(\frac{2\pi t}{52})]. \quad (1)$$

This seasonal forcing reflects increases in infectivity and susceptibility thought to be due to multiple factors including increased rainfall, variation in humidity, and decreased temperature (Cane, 2001; Weber et al., 1998).

Sinusoidally forced SIR-type models are known to support complex multi-periodic and even chaotic solutions. For realistic parameter values, obtained from the literature, and depending on the values selected for β_0 and β_1, the model predicts either annual peaks of the same magnitude, or the observed biennial pattern that can be explained by the interaction of the forcing frequency and the natural frequency of the system. This behaviour is in keeping with what is observed in different climatic zones.

Keywords: *Mathematical model, infectious disease, respiratory syncytial virus, seasonality*

1 INTRODUCTION

Respiratory syncytial virus (RSV) is a significant health and economic burden in Australia and internationally. Epidemics are strongly seasonal, occurring each winter in temperate climates (Cane, 2001) and during the rainy season in tropical climates (Simoes, 1999), usually lasting between two and five months (Hall, 1981; Kim et al., 1973).

There are only limited RSV data sets published and often these are only over short time spans. Recent data sets that span numerous years for Utah in the U.S.A. (Leecaster et al., 2011), southern Germany (Terletskaia-Ladwig et al., 2005) and Western Australia (Moore et al., 2013), show a distinct biennial seasonal pattern with higher peaks in alternate winter seasons. These regions all have a temperate climate and experience significant seasonal variation in climate. Other data sets, such as for Singapore (Chew et al., 1998) and the Spanish region of Valencia (Acedo et al., 2011) show annual seasonal behaviour, with peaks of the same magnitude each year.

While the mortality rate for previously healthy children is low, RSV causes high rates of hospitalisation for children under two years of age and has also been identified as a cause of mortality in the elderly (Faskey et al., 2005; Simoes, 1999; Hardelid et al., 2013). Clinical symptoms may vary from those of a mild infection to severe bronchiolitis or pneumonia (Hall, 1981).

In the young, infection with RSV does not cause long lasting protective immunity, meaning that individual children may be repeatedly infected. There is currently no licensed vaccine available, nor any antiviral treatments commonly used for RSV infection in Australia.

The aim of this study is to develop RSV models that reproduce the biennial pattern observed in temperate climates. In later work these models will be fitted to available data. Thus we present a SEIRS model for a single age class for RSV infection, where the transmission rate is seasonally forced, such as in models presented in Keeling and Rohani (2008). An investigation into the types of behaviour possible in this model is undertaken. To better reflect the known epidemiology of RSV, we then introduce a second age class into the model with a second transmission rate and investigate how this affects the transmission dynamics.

2 MODEL FOR A SINGLE AGE CLASS

A deterministic ordinary differential equation model is developed for the transmission of RSV for 0-23 month old children. This age group was chosen as the literature indicates that almost all children have been infected by the time they reach this age (Hall, 1981; Sorce, 2009). As it remains unclear to what degree adults carry and shed the virus, thereby infecting children, the adult population was not included in the model.

The population is divided into four compartments, where S represents the proportion of the population that is susceptible to infection; E represents the proportion of the population that is exposed but not yet infected; I represents the proportion that is infected with the virus; and R represents the proportion of the population that is recovered and temporarily immune to reinfection. The SEIRS-type model was selected for two reasons. Firstly, the virus is known to have a latency period between an individual being exposed to the infection and becoming infectious. This period is of the same order of magnitude as the infectious period and hence needs to be included to accurately represent the disease dynamics. Secondly, infection from the virus does not cause long-lasting immunity, hence recovered individuals may return to the susceptible class and be reinfected.

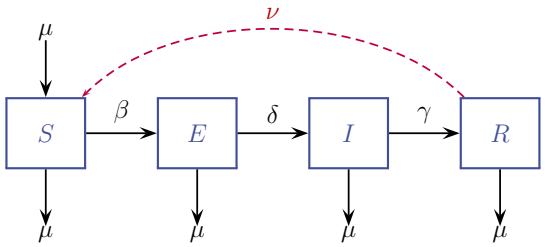

Figure 1. Schematic diagram for single age class SEIRS model for RSV transmission.

A schematic representation of the model is shown in Figure 1. The average recovery period is represented by $\frac{1}{\gamma}$,

the average latency period (the time between contracting the infection and becoming infectious) is represented by $\frac{1}{\delta}$ and the average duration of immunity is represented by $\frac{1}{\nu}$. The rate of entering the model (the birth rate) is equal to the rate at which individuals age out of the model, and is represented by μ. The virus is transmitted between individuals at rate β.

The differential equations, where time in weeks is represented by t, are

$$\frac{dS}{dt} = \mu - \beta SI - \mu S + \nu R \tag{2}$$

$$\frac{dE}{dt} = \beta SI - \delta E - \mu E \tag{3}$$

$$\frac{dI}{dt} = \delta E - \mu I - \gamma I \tag{4}$$

$$\frac{dR}{dt} = \gamma I - \mu R - \nu R. \tag{5}$$

2.1 Parameter values

The birth rate and ageing rate μ is chosen as in Moore et al. (2013) and is based on the average number of births per week in the metropolitan region of Western Australia. This gives an average weekly birth rate of 0.012. Assuming the birth and ageing rates are equal simplifies the calculations as it ensures the population size remains constant. Here this assumption does not change the overall dynamics of the system.

Based on the literature, the average latency period for RSV is assumed to be four days (Weber et al., 2001; Moore et al., 2013). Other models, such as those presented by Leecaster et al. (2011), assume a latency period of five days. A four day latency period equates to δ being 1.754 (or $\frac{1}{0.57}$).

Similarly, the average recovery period is based on estimates in previous models for RSV of 10 days (Weber et al., 2001; Moore et al., 2013; Acedo et al., 2010; Leecaster et al., 2011), and within the range of one to 21 days identified by Hall et al. (1976). This gives γ equal to 0.714 (or $\frac{1}{1.4}$).

The immunity period is the time between recovering from a RSV infection to becoming susceptible to the virus again. Although not currently well understood, there is some evidence that the immunity period is around 200 days which equates to ν being 0.035 (or $\frac{1}{28.57}$). This again is the value used in previous modelling of RSV (Weber et al., 2001; Moore et al., 2013; Acedo et al., 2010).

The transmission rate $\beta(t)$, given at Equation 1, was chosen to reflect the observed annual seasonality of RSV in temperate climates. Similar seasonal forcing has been applied in other models for RSV transmission (Weber et al., 2001; Moore et al., 2013; Acedo et al., 2010; Arenas et al., 2008; Leecaster et al., 2011). The sinusoidal function, with a period of 52 weeks, accounts for the observed higher transmission between children during the winter months. The term β_0 represents the average transmission rate and β_1 represents the amplitude of the seasonal fluctuation (Keeling and Rohani, 2008).

For the purpose of investigating the overall dynamics of this model, a range of values was considered for β_0. For β_1, a value of 0.6 was assumed (noting that $0 < \beta_1 \leq 1$), in order to replicate the conditions in temperate climates where strong seasonality is observed. For some seasonally forced models for RSV, values as high as 1 (Leecaster et al., 2011) have been assumed. Other models assume much lower values for β_1, such as between 0.10 and 0.36 (Arenas et al., 2008). In future work we will estimate these parameters β_0 and β_1 using longitudinal data from Western Australia.

2.2 Numerical solution

The system of differential equations was solved and plotted using MATLAB's ode45 routine. A burn in time of 80 years was used to allow the system to stabilise and thereby remove the dependence on the initial conditions. When there is no seasonality in the transmission rate (when β is constant, β_1=0), the natural oscillations in the system die out and the system reaches a steady state. With seasonality, there is either a distinct biennial pattern, with higher peaks in alternate winter seasons, or peaks of the same magnitude each year, depending on the values selected for β_0 and β_1. Figure 2(a) depicts a plot of a biennial pattern solution for the infected population, with β_0=1.1 and β_1=0.6.

As there are values of β_0 and β_1 where there is no biennial pattern but instead where the seasonal peak reaches the same maximum each year, adjacent seasonal peaks versus the parameter β_0 were plotted in order to better

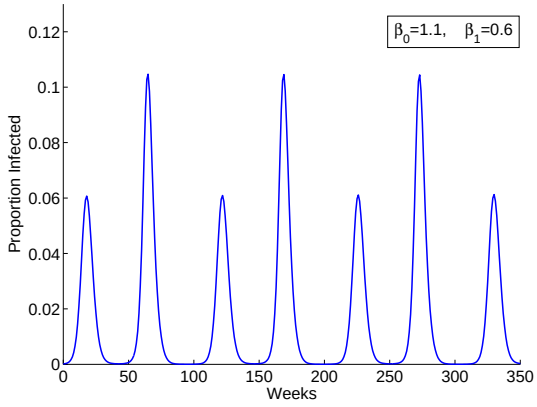

(a) A numerical solution for the infected population of a single age class SEIRS model for RSV transmission with a sinusoidally forced transmission parameter.

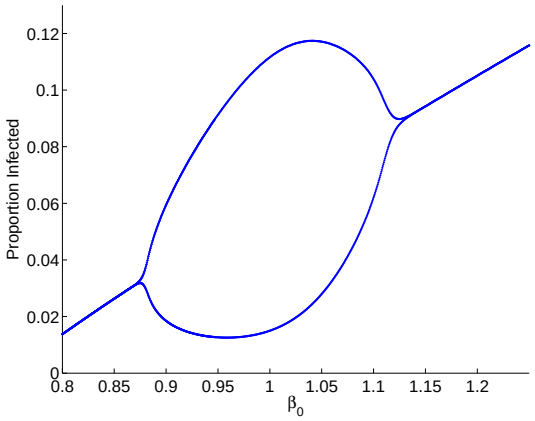

(b) Maximum proportion of infectives at adjacent seasonal peaks versus the bifurcation parameter β_0, for the single age class system. The parameter determining the amplitude of the forcing, β_1, is 0.6

Figure 2.

understand the bifurcation patterns of the system. Figure 2(b) gives an impression of the bifurcation structure of the model, showing seasonal peaks over two adjacent years. Where the seasonal pattern is annual, only a single peak is shown, whereas biennial dynamics gives two distinct peaks. There is a specific range of possible values for β_0 for which the system will feature the biennial seasonal pattern. Outside this range, the system reverts to a regular annual seasonal pattern. These results are in keeping with what is observed in different climatic zones.

3 MODEL FOR TWO AGE CLASSES

Studies show that the transmission dynamics of RSV change as children age. That is, incidence is higher for children aged less than 12 months than those in the 12-23 month age class (Moore et al., 2010). It is still unclear why older children are less affected. Possible reasons are reduced susceptibility, or less severe symptoms (so less infections are reported), as a result of prior infection with the virus; or due to having better developed immune systems than younger children. Thus, we present a second set of differential equations to account for two age classes and two transmission parameters, β_A and β_B.

The second model is the set of differential equations

$$\frac{dS_1}{dt} = \mu - \beta_A S_1(I_1 + I_2) - \eta S_1 + \nu R_1 \tag{6}$$

$$\frac{dE_1}{dt} = \beta_A S_1(I_1 + I_2) - \delta E_1 - \eta E_1 \tag{7}$$

$$\frac{dI_1}{dt} = \delta E_1 - \eta I_1 - \gamma I_1 \tag{8}$$

$$\frac{dR_1}{dt} = \gamma I_1 - \eta R_1 - \nu R_1 \tag{9}$$

$$\frac{dS_2}{dt} = \eta S_1 - \beta_B S_2(I_1 + I_2) - \eta S_2 + \nu R_2 \tag{10}$$

$$\frac{dE_2}{dt} = \eta E_1 + \beta_B S_2(I_1 + I_2) - \delta E_2 - \eta E_2 \tag{11}$$

$$\frac{dI_2}{dt} = \eta I_1 + \delta E_2 - \eta I_2 - \gamma I_2 \tag{12}$$

$$\frac{dR_2}{dt} = \eta R_1 + \gamma I_2 - \eta R_2 - \nu R_2. \tag{13}$$

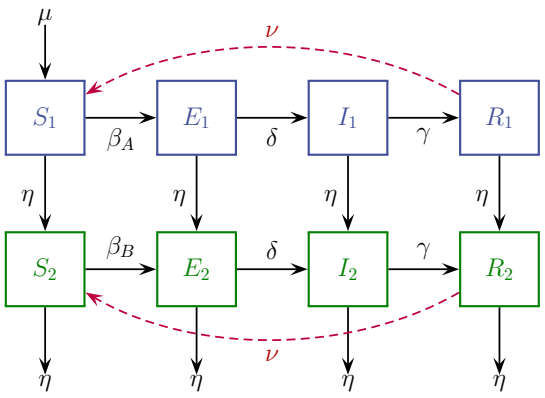

Figure 3. Schematic description of a SEIRS model for RSV transmission that takes into account two separate age classes: children aged <12 months, where the virus is transmitted at rate β_A; and 12-23 month old children, where the virus is transmitted at rate β_B.

The parameters μ, γ, δ and ν are as presented for the single age class model in Equations (2)-(5). An additional parameter η is introduced to reflect the ageing from the <12 month age class into the 12-23 month age class, and also to reflect the ageing out of the 12-23 month class. This rate is assumed to be equal and distributed evenly over time, therefore η is taken to be $\frac{1}{52}$. A schematic diagram of the two age class system is given in Figure 3.

The transmission rates are β_A, for the <12 month age class, and β_B, for the 12-23 month age class. Both are of the sinusoidal form presented for the single age class model at Equation (1). Here the parameter β_0 in β_B was selected to produce a reduced average transmission rate for the 12-23 month old age class, to better reflect the different transmission dynamics for older children. The β_1 parameter is the same for β_A and β_B, to represent the same climatic region.

3.1 Numerical solution

The system of differential equations was solved using MATLAB's inbuilt ode45 routine, with a burn in time of 80 years. The model accurately mimics the expected lower number of infectives in the 12-23 month age class and again produces the biennial pattern for both age classes, as observed in the single age class system. Figure 4(a) shows a solution for the infected population for each age class. Adjacent seasonal peaks for increasing values of β_0 were again examined, showing that, as for the single age class system, there is a specific range of possible values for β_0 that produce the biennial seasonal pattern 4(b).

4 DISCUSSION

By sinusoidally forcing the transmission parameter, both models depict either a distinct biennial seasonality, or annual seasonal peaks of the same magnitude, for realistic parameter values depending on the values selected for β_0 and β_1. These results are in keeping with what is observed in different climatic zones. We showed that a simple single age class model, with demography, is sufficient to achieve these seasonal patterns. Both the single age class model, and the expanded model with two age classes, now provide a base on which to add complexities.

Future work will investigate varying the recovery, latency and immunity parameters for different age classes, as well as a more detailed bifurcation analysis of both systems. There is a possibility of more complex behaviour than the two-cycle pattern observed here being present. We will also investigate whether prior exposure is the reason for reduced susceptibility, through expanding the model and fitting with population-based linked laboratory data for the metropolitan region of Western Australia.

There is currently no licensed vaccine for RSV available in Australia. Vaccine development to date has been problematic due to lack of an ideal animal model for the the disease, and the challenges of immunising infants

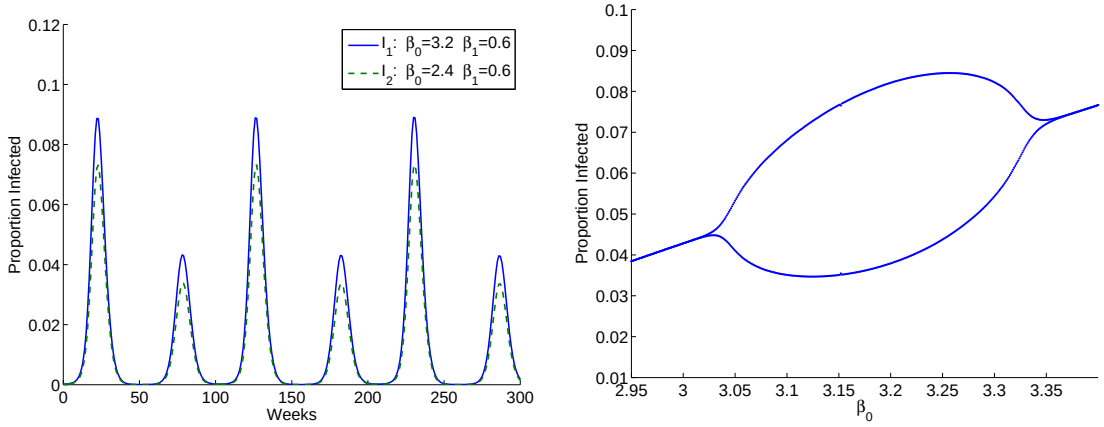

(a) A numerical solution for the infected populations for the <12 month age class and the 12-23 month age class of a SEIRS model for RSV transmission, where the transmission parameter for each age class is sinusoidally forced.

(b) Maximum proportion of infectives at adjacent seasonal peaks versus β_0 (with $\beta_B = 0.75\beta_A$), demonstrating the biennial behaviour over a range of values. In this case, the parameter β_1 is 0.6.

Figure 4.

who are immunologically immature (Crowe Jr, 2002). However, with a new vaccine currently undergoing phase two trials (Anderson et al., 2013), we will also look at the optimal timing in the transmission cycle for the roll out of a vaccination program.

REFERENCES

Acedo, L., J. Moraño, and J. Díez-Domingo (2010). Cost analysis of a vaccination strategy for respiratory syncytial virus (RSV) in a network model. *Mathematical and Computer Modelling 52*(7-8), 1016–1022.

Acedo, L., J. Moraño, R. Villanueva, J. Villanueva-Oller, and J. Díez-Domingo (2011). Using random networks to study the dynamics of respiratory syncytial virus (RSV) in the Spanish region of Valencia. *Mathematical and Computer Modelling 54*(7-8), 1650–1654.

Anderson, L. J., P. R. Dormitzer, D. J. Nokes, R. Rappouli, A. Roca, and B. S. Graham (2013). Strategic priorities for respiratory syncytial virus (RSV) vaccine development. *Vaccine 31S*, B209–B215.

Arenas, A. J., J. A. Moraño, and J. C. Cortés (2008). Non-standard numerical method for a mathematical model of RSV epidemiological transmission. *Computers & Mathematics with Applications 56*(3), 670–678.

Cane, P. A. (2001). Molecular epidemiology of respiratory syncytial virus. *Reviews in medical virology 11*(2), 103–116.

Chew, F. T., S. Doraisingham, A. E. Ling, G. Kumarasinghe, and B. W. Lee (1998). Seasonal trends of viral respiratory tract infections in the tropics. *Epidemiology and Infection 121*(1), 121–128.

Crowe Jr, J. E. (2002). Respiratory syncytial virus vaccine development. *Vaccine 20*, S32–S37.

Faskey, A., P. Hennessey, M. Formica, C. Coz, and E. Walsh (2005). Respiratory Syncytial Virus Infection in Elderly and High-Risk Adults. *New England Journal of Medicine 352*(17), 1749–1760.

Hall, C. B. (1981). Respiratory syncytial virus. In R. D. Feigin and J. D. Cherry (Eds.), *Textbook of Paediatric Infectious Diseases*, pp. 1247–1267. Philadelphia; London: W. B. Saunders Company.

Hall, C. B., R. G. Douglas, and J. M. Geiman (1976). Respiratory syncytial virus infections in infants: quantitation and duration of shedding. *The Journal of Pediatrics 89*(1), 11–15.

Hall, C. B., G. A. Weinberg, M. K. Iwane, A. K. Blumkin, K. M. Edwards, M. A. Staat, P. Auinger, M. R. Griffin, K. A. Poehling, D. Erdman, C. G. Grijalva, Y. Zhu, and P. Szilagyi (2009). The burden of respiratory syncytial virus infection in young children. *The New England Journal of Medicine 360*(6), 588–598.

Hardelid, P., R. Pebody, and N. Andrews (2013). Mortality caused by influenza and respiratory syncytial virus by age group in England and Wales 1999-2010. *Influenza and Other Respiratory Viruses 7*(1), 35–45.

Keeling, M. J. and P. Rohani (2008). *Modeling Infectious Diseases in Humans and Animals*. Princeton University Press.

Kim, H. W. H. A., J. Arrobio, C. D. Brandt, C. Barbara, G. Pyles, J. L. Reid, R. M. Chanock, and R. H. Parrott (1973). Epidemiology of Respiratory Syncytial Virus. *American Journal of Epidemiology 98*, 216–225.

Leecaster, M., P. Gesteland, T. Greene, N. Walton, A. Gundlapalli, R. Rolfs, C. Byington, and M. Samore (2011). Modeling the variations in pediatric respiratory syncytial virus seasonal epidemics. *BMC Infectious Diseases 11*(1), 105.

Moore, H., P. Jacoby, C. Blyth, and G. Mercer (2013). Modelling the seasonal epidemics of Respiratory Syncytial Virus in young children. Submitted to Influenza and Other Respiratory Viruses.

Moore, H. C., N. de Klerk, P. Richmond, and D. Lehmann (2010). A retrospective population-based cohort study identifying target areas for prevention of acute lower respiratory infections in children. *BMC Public Health 10*(1), 757.

Simoes, E. A. (1999). Respiratory syncytial virus infection. *Lancet 354*(9181), 847–852.

Sorce, L. R. (2009). Respiratory syncytial virus: from primary care to critical care. *Journal of pediatric health care: official publication of National Association of Pediatric Nurse Associates & Practitioners 23*(2), 101–108.

Terletskaia-Ladwig, E., G. Enders, G. Schalasta, and M. Enders (2005). Defining the timing of respiratory syncytial virus (RSV) outbreaks: an epidemiological study. *BMC Infectious Diseases 5*, 20.

Weber, A., M. Weber, and P. Milligan (2001). Modeling epidemics caused by respiratory syncytial virus (RSV). *Mathematical Biosciences 172*(2), 95–113.

Weber, M. W., E. K. Mulholland, and B. M. Greenwood (1998). Respiratory syncytial virus infection in tropical and developing countries. *Tropical Medicine & International Health 3*(4), 268–280.

OPEN ACCESS Freely available online

PLOS ONE

Modelling the Seasonal Epidemics of Respiratory Syncytial Virus in Young Children

Hannah C. Moore[1]*, Peter Jacoby[1], Alexandra B. Hogan[2], Christopher C. Blyth[3,4], Geoffry N. Mercer[2]

1 Telethon Kids Institute, University of Western Australia, Perth, Australia, **2** National Centre for Epidemiology and Population Health, Australian National University, Canberra, Australia, **3** School of Paediatrics and Child Health, University of Western Australia, Perth, Australia, **4** Department of Paediatric and Adolescent Medicine, Princess Margaret Hospital for Children, Perth, Australia

Abstract

Background: Respiratory syncytial virus (RSV) is a major cause of paediatric morbidity. Mathematical models can be used to characterise annual RSV seasonal epidemics and are a valuable tool to assess the impact of future vaccines.

Objectives: Construct a mathematical model of seasonal epidemics of RSV and by fitting to a population-level RSV dataset, obtain a better understanding of RSV transmission dynamics.

Methods: We obtained an extensive dataset of weekly RSV testing data in children aged less than 2 years, 2000–2005, for a birth cohort of 245,249 children through linkage of laboratory and birth record datasets. We constructed a seasonally forced compartmental age-structured Susceptible-Exposed-Infectious-Recovered-Susceptible (SEIRS) mathematical model to fit to the seasonal curves of positive RSV detections using the Nelder-Mead method.

Results: From 15,830 specimens, 3,394 were positive for RSV. RSV detections exhibited a distinct biennial seasonal pattern with alternating sized peaks in winter months. Our SEIRS model accurately mimicked the observed data with alternating sized peaks using disease parameter values that remained constant across the 6 years of data. Variations in the duration of immunity and recovery periods were explored. The best fit to the data minimising the residual sum of errors was a model using estimates based on previous models in the literature for the infectious period and a slightly lower estimate for the immunity period.

Conclusions: Our age-structured model based on routinely collected population laboratory data accurately captures the observed seasonal epidemic curves. The compartmental SEIRS model, based on several assumptions, now provides a validated base model. Ranges for the disease parameters in the model that could replicate the patterns in the data were identified. Areas for future model developments include fitting climatic variables to the seasonal parameter, allowing parameters to vary according to age and implementing a newborn vaccination program to predict the effect on RSV incidence.

Citation: Moore HC, Jacoby P, Hogan AB, Blyth CC, Mercer GN (2014) Modelling the Seasonal Epidemics of Respiratory Syncytial Virus in Young Children. PLoS ONE 9(6): e100422. doi:10.1371/journal.pone.0100422

Editor: Richard J. Sugrue, Nanyang Technical University, United States of America

Received December 16, 2013; **Accepted** May 27, 2014; **Published** June 26, 2014

Funding: HCM is funded by National Health and Medical Research Council Fellowship #1034254. The funders had no role in study design, data collection and analysis, decision to publish, or preparation of the manuscript.

Competing Interests: The authors have declared that no competing interests exist.

* Email: hannah.moore@telethonkids.org.au

Introduction

Respiratory syncytial virus (RSV) is the most common cause of acute lower respiratory infections (ALRI) in children, especially those aged less than two years. While RSV is not a notifiable disease, the health and economic burden for young children surpasses that of influenza in Australia, with an estimated incidence ranging from 435–869/1000 infant population [1]. In the United Kingdom RSV mortality rates in those aged less than 15 years have been shown to be on par with those of influenza [2]. RSV follows a distinct seasonality in most geographical areas with peaks during winter months associated with cooler temperatures and increased rainfall, [3–6] however RSV incidence can be highly variable within countries and between regions within a country depending on the level of seasonal forcing [7].

Mathematical models have been used in epidemiology to characterise annual epidemics of respiratory infections and measure the likely impact of intervention programs [8,9]. Models can also determine the optimum timing of interventions and the proportion of the population that need to be vaccinated in order to reach the herd immunity threshold. There is currently no licenced vaccine for RSV, but immunoprophylaxis with RSV-specific monoclonal antibodies is effective in reducing RSV-related severe disease [10]. Furthermore, an attenuated intranasal RSV/parainfluenza virus type 3 vaccine (MEDI-534) and a live attenuated intranasal RSV vaccine (MEDI-559) have recently undergone Phase 1 clinical trials in infants and young children [11,12]. Mathematical models are likely to be useful in assessing the impact of such vaccines. However, to improve the accuracy of these models, real population data are needed to fit the model

parameters. Unlike notifiable diseases where positive detections are reported nationally, RSV models rely on hospitalisations or routinely collected laboratory data. To date, variations of simple compartmental models for RSV have been constructed using hospitalisation data from The Gambia, Singapore, Florida (USA) and Finland [13] and Spain [14]. A further model has since been developed using RSV testing data from a major children's hospital in Utah (USA) [15]. These models have shown that they can reliably mimic the distinctive seasonal characteristics of RSV. However, due to the differences in climate between these regions, which result in different levels of seasonal forcing, RSV models need to be developed and fitted to specific geographical areas.

We have access to total population-based linked data including state-wide routinely collected laboratory data through the Western Australian Data Linkage System (WADLS). Demographic, clinical and laboratory data are linked following a best practice protocol [16] in which personal identifiers are separated from health and laboratory data and linked by a separate linkage team to produce a project-specific child identifier key. De-identified data for each of the datasets are then given to the approved research team for analysis. In this study, we establish a compartmental model of RSV transmission based on positive detections of RSV in metropolitan Western Australian children, obtained through population-based data linkage. Secondly, we explore variations in the model fit with changes in the disease parameters of the latency and infectious periods, and the reduction in the susceptibility and infectiousness for older children and adults due to reinfection and ageing.

Methods

Population and Setting

Western Australia covers approximately 2.5 million square kilometres and has a population of 2.2 million [17]. The Western Australian Department of Health classifies residential postcodes into three major geographical regions: metropolitan (the capital city, Perth, and its surrounds), rural (South West and North Eastern areas outside of the metropolitan region) and remote (the far East and far North Western Australia). The state crosses several climatic zones with a temperate climate in the metropolitan and southern regions and a tropical climate in the northern regions. Approximately three-quarters of Western Australia's population reside in the metropolitan area. There is one dedicated tertiary level paediatric teaching hospital, Princess Margaret Hospital for Children (PMH) located in the state capital, Perth. At PMH, it is standard practice to collect nasopharyngeal aspirates (NPA) for respiratory virus detection on all children admitted to hospital with ALRI [18]. A recommendation for respiratory pathogen testing is in place at other smaller metropolitan and non-metropolitan hospitals across Western Australia.

Population-based data

Previously we have extracted data from WADLS on 245, 249 singleton live births (7.1% of which are Aboriginal) in Western Australia between 1996 and 2005 from the Midwives' Notification System, Birth and Death Register and the Hospital Morbidity Database System. Details of data cleaning are provided elsewhere [19,20]. In brief, our linked dataset contains information on birth details, demographics and hospitalisation episodes for ALRI between 1996 and 2005.

We have also extracted data from the PathWest Laboratory Database concerning routine detections of respiratory viruses and bacteria. PathWest Laboratory Medicine Western Australia (PathWest) is the government-funded public laboratory service and consists of all public pathology laboratories in Western Australia and carries out a full range of diagnostic testing for infectious diseases. Details of the component datasets within the PathWest Laboratory Database are given elsewhere [21]. Laboratory data were available from 2000 to 2005 for all children in the birth cohort for ages 0–9 years. Respiratory samples received at PathWest for viral testing are routinely investigated for RSV, influenza viruses A and B, adenoviruses and parainfluenza virus types 1–3. RSV was detected by either immunofluorescent antigen detection, polymerase chain reaction (PCR) and/or viral culture. Testing methods for RSV did not change between 2000 and 2005.

We used the residential postcode of the mother at the time of her child's birth as recorded on the Midwives' Notification System to classify laboratory detections to either the metropolitan, rural and remote regions of Western Australia. To establish a model of metropolitan RSV transmission in a temperate climate, we restricted our data to RSV testing and positive detections in children born in metropolitan areas. Ethical approval for this study was granted by Princess Margaret Hospital for Children Ethics Committee and the Department of Health Western Australia Human Research Ethics Committee. Access to the population-based data was approved by the Western Australian Data Linkage Branch.

Model structure

We adapted the RSV compartmental transmission models used by others [13,15,22] and constructed a Susceptible (S) – Exposed (E) – Infectious (I) – Recovered (R) – Susceptible (S) model with two age classes. S_1, E_1, I_1 and R_1 represented those individuals aged less than 2 years and S_2, E_2, I_2, and R_2 represented those individuals aged 2 years and over. Our SEIRS model was defined by a series of differential equations:

$$\frac{dS_1}{dt} = \mu - \beta S_1(I_1 + \alpha I_2) - \eta_1 S_1 + \nu R_1$$

$$\frac{dE_1}{dt} = \beta S_1(I_1 + \alpha I_2) - \eta_1 E_1 - \sigma E_1$$

$$\frac{dI_1}{dt} = \sigma E_1 - \eta_1 I_1 - \gamma I_1$$

$$\frac{dR_1}{dt} = \gamma I_1 - \eta_1 R_1 - \nu R_1$$

$$\frac{dS_2}{dt} = \eta_1 S_1 - \delta\beta S_2(I_1 + \alpha I_2) - \eta_2 S_2 + \nu R_2$$

$$\frac{dE_2}{dt} = \eta_1 E_1 + \delta\beta S_2(I_1 + \alpha I_2) - \eta_2 E_2 - \sigma E_2$$

$$\frac{dI_2}{dt} = \eta_1 I_1 + \sigma E_2 - \eta_2 I_2 - \gamma I_2$$

$$\frac{dR_2}{dt} = \eta_1 R_1 + \gamma I_2 - \eta_2 R_2 - \nu R_2$$

where: μ is the birth rate, β is the disease transmission rate, η_1 is the ageing rate from $(SEIR)_1$ to $(SEIR)_2$, η_2 is the ageing rate of leaving $(SEIR)_2$ which is related to birth/death rate, $1/\sigma$ is the average latency period, $1/\gamma$ is the average infectious period and $1/\nu$ is the average duration of immunity. The scaling parameters α and δ represent the reductions in infectivity and susceptibility respectively for the older age group compared to those aged less than 2 years. Each model class represents the proportion of the total population. A schematic representation of the model is shown in Figure 1.

Parameters

The parameters were based either on real data from our previous population-based data linkage studies, estimates from the literature or were estimated during the model fitting process. Data were aggregated at the weekly level so the time period of interest is a week and all rates are quoted as per week for consistency.

Birth rate (μ) and ageing rates (η1 and η2). Age class 1 represented those aged less than 2 years and age class 2 represented those aged 2 years or more. Therefore, the weekly ageing rate was assumed to be 1/(2*52) for moving from $(SEIR)_1$ to $(SEIR)_2$. We assumed an overall stable population with a life expectancy of 80 years and that deaths in those aged less than 2 years are insignificant to the older age group following Keeling and Rohani [22]. Therefore the rate of entering the model, or the birth/death rate, was assumed to be equal to the ageing rate for leaving $(SEIR)_2$ and was calculated as 1/(78*52).

Latency period ($1/\sigma$). The latency period is defined as the time between being infected and becoming infectious. Based on previous literature [13], this was initially assumed to be an average of 4 days (0.57 of a week). Values between 2 and 6 days were later tested to determine the effect on the model fit.

Infectious period ($1/\gamma$). The infectious period estimates the time an individual remains infectious. Previous RSV models have assumed this to be 10 days [13–15]. This estimate has been based on a previous analysis of 23 infants where the average duration of shedding of RSV was 6.7 days with a range from 1–21 days [23]. In order to be consistent with the literature, our initial model assumed an average infectious period of 10 days (1.4 weeks). Values between 7 and 12 days for this parameter were later tested to determine the effect on the model fit.

Duration of immunity ($1/\nu$). The duration of immunity is defined as the time between entering the recovery state to becoming susceptible again for a subsequent RSV infection. In previous literature [13] the duration of immunity has been estimated to be 200 days (25.6 weeks). In a more recent RSV model, the duration of immunity that produced the best fit to the data was a yearly rate of 1.59 which approximately translates to 230 days (32.9 weeks) [14]. Due to the seasonal nature of RSV epidemics the duration of immunity is difficult to measure from observational data as the risk of reinfection depends on the time of year of the first infection. An infection late in an epidemic season has a lower risk of reinfection that season than an earlier infection and is more likely to be reinfected in the following season. This effect greatly biases the calculation of the duration of immunity and probably leads to an overestimate. Due to the great uncertainty in this parameter and its impact on the outcome in the model we elected to make the duration of immunity a variable to be fitted rather than estimated from the literature.

Transmission parameter (β). To account for the distinct seasonality of RSV, the disease transmission parameter was calculated as follows:

$$\beta = \beta_0\left(1+\beta_1\cos\left(\frac{2\pi t}{52}+\phi\right)\right)$$

This is based on harmonic analysis that we have previously shown to accurately model RSV seasonality in metropolitan Western Australia [3]. This seasonality function allowing for varying amplitude over an annual cycle with a horizontal shift is common in modelling seasonal outbreaks and has been used in previous RSV transmission models [13,14,22]. The component parameters β_0, β_1 and φ (phase shift) were estimated through the model fitting process with t representing time in weeks. Here β_0 is the average transmission rate and β_1 is the degree of seasonality which is defined over the range [0,1] with higher values more appropriate for regions with stronger seasonal drivers.

Scaled susceptibility (δ). To account for less reported infections in those aged 2 years or more, we included a scaling parameter to reduce the susceptibility of the older age class being infected by both infectious age classes. Based on reinfection studies [24,25] initially the scaling parameter was set to 0.65 and later a range from 0.5 to 0.8 was considered.

Scaled infectiousness (α). To account for reduced transmission in those aged 2 years or more, we included a scaling parameter to reduce the transmission from the infected population in the older age class, to the susceptible population in both age classes. The literature on the level of transmission from older children and adults to younger children is scarce, thus as a starting point in the model we set the scaled infectiousness to be the same

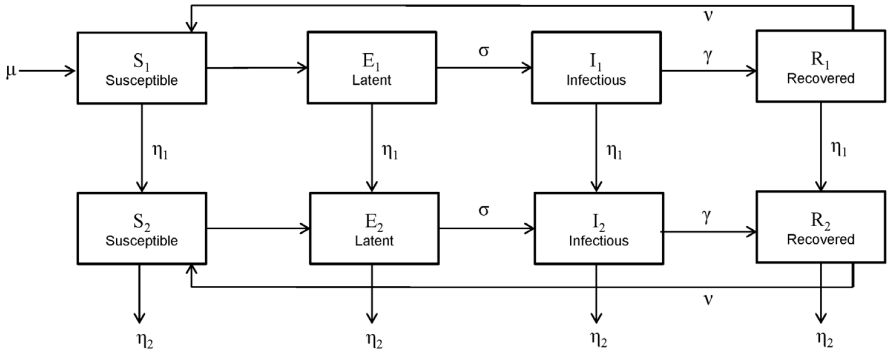

Figure 1. Schematic representation of RSV SEIRS model with two age groups. $(SEIRS)_1$ represents those aged less than 2 years and $(SEIRS)_2$ represents those aged 2 years or more.
doi:10.1371/journal.pone.0100422.g001

as the scaled susceptibility, at 0.65 with a range from 0.5 to 0.8 considered.

Model fitting

The SEIRS model was developed in Cran R statistical package [26], using the *deSolve* function to numerically solve the differential equations and verified in MATLAB. The model was used to fit the components of the seasonal transmission parameter, β_0, β_1 and φ, and the inverse of the immunity period ν. The model was fitted to data regarding positive RSV detections in children aged less than 2 years between 2000 and 2005 in metropolitan Western Australia. Since the model is a population wide model based on proportions in each class and the data are for reported RSV cases from population-based linked data, the model results were scaled to represent this proportion of the total community cases. This scaling was done by ensuring the total number of cases over the 6 years of the study and the model agreed. After using a set of initial conditions for β_0, β_1, φ and ν, we used the Nelder-Mead method in Cran R with the *neldermead* package [27] to fit the model to our actual RSV data. The weekly cumulative number of cases in the first age class (children aged less than 2 years) from the model and the real data was used in the model fitting process. The fit statistic that was minimised during the model fitting process was defined as:

$$F = \sqrt{\sum_{i=1}^{n} (data_i - SEIRS_i)^2}$$

where $data_i$ and $SEIRS_i$ are the weekly number of cases aged less than 2 years in the data and SEIRS model outcome and i is the index for all weeks from the beginning of 2000 until the end of 2005. In contrast to Leecaster and colleagues [15] the fit statistic is not scaled by the model value as this gives a poorer fit due to the long periods over the summer months with very small case numbers.

In addition to fitting the components of the transmission parameter and the immunity parameter, we explored the variation in the fitted value of these four parameters and the model fit statistic by varying the duration of the latency period (2 to 6 days), the recovery period (7 to 12 days), and the scaled infectiousness and susceptibility parameters (0.5 to 0.8). The variations used were based on a literature search and the epidemiology of RSV detections and hospitalisations using our Western Australian data.

Results

RSV detections

There were 15,830 specimens collected in metropolitan children aged less than 2 years between 2000 and 2005 that were tested for RSV with 21% (n = 3394) being positive for RSV by direct immunofluorescence, viral culture or PCR. Of the positive RSV detections, 89.7% were identified from specimens collected from hospitalised children, 9.4% were identified from specimens collected from non-hospital patients, that is patients attending emergency departments or hospital associated out-patient clinics, and the remaining 0.9% were collected in children from private laboratories associated with general practices. There were 4813 specimens in those aged 2–8 years that were tested and from those 11% (n = 534) were positive for RSV. Specimens tested and found positive for RSV followed a clear seasonal pattern with peaks in the winter months of June to August and very few cases during the summer months of December to February (Figure 2). There was also a distinct biennial seasonal pattern in both testing and positive detections with alternating peaks. The average maximum number of weekly detections in the higher peaks for years 2000, 2002 and 2004 was 73 compared with an average of 45 detections per week for years 2001, 2003 and 2005. The proportion of specimens tested that were positive for RSV ranged from 0% in off season months to 74% in the peak periods.

SEIRS model

The SEIRS model was fitted to the 6 years of RSV positive identifications. The transmission parameter values that minimised the fit statistic using the Nelder-Mead method were $\beta_0 = 1.99$, $\beta_1 = 0.65$, $\varphi = 2.43$ and $\nu = 0.044$ (translating to an immunity period of about 23.5 weeks), resulting in a fit statistic of F = 89.575. This best fit of the model to the data displayed alternating peak sizes that accurately mimicked the observed data (Figure 3). In contrast to the models of Leecaster and colleagues [15] the parameter values used here are constant across the entire dataset and do not vary by epidemic year. That is, there is a natural period 2 oscillation in the model with these parameter values giving the alternating peaks observed in the data. Using different parameter values for different years was not required to achieve the biennial cycle. The biennial cycle was found to exist over a range of parameter values and was not restricted to narrow parameter choices. It should be noted that there are other regions of the parameter space that had a poorer fit to the data that did not exhibit this period 2 oscillation but instead had peaks of equal size as has been observed in some other models [13,14].

Parameter variation

We explored differences in the fit statistic and transmission parameter values through the variation of duration of the latency and infectious periods, and the scaling parameters for reduced susceptibility and infectiousness in the older age class. A summary of the results is given in Table 1. We did not investigate the variation in the parameter ϕ because this simply represents the horizontal fitting of the model to the dataset and does not change the dynamics of the system overall.

Based on the available literature, our initial estimate of the latency period was 4 days. To allow for variation around this value, we tested values within the range of 2 days (weekly rate of 1/0.28) and 6 days (weekly rate of 1/0.86) All values within this range produced a good model fit (F = 90.03 to F = 92.32; Table 1), with the best fit agreeing with our initial estimate of 4 days.

Similar to other RSV models, our model initially assumed the infectious period to be 10 days. This original estimate was based on a study reporting the mean duration of shedding of RSV to be 6.7 days with the range of 1–21 days [23]. An additional study found the shedding duration to be between 3.4 and 7.4 days but considerably longer (9 days and potentially longer) for children aged less than 2 years [28]. While we do not have available viral shedding data, we explored hospital length of stay as a proxy for the infectious period. This assumes that infectiousness is linked to symptom presentation which may not be true. In addition, patients may be discharged from hospital whilst still showing symptoms that are not serious enough to warrant continued hospitalisation. It is expected that hospital stay would be an underestimation of infectious period. From linking the RSV laboratory data to hospitalisation data, we identified 2,424 hospitalisations in children aged less than 2 years in metropolitan Western Australia. The median length of hospital stay was 3 days with the range of 0–6 days. To allow for additional time before and after the hospital stay, where a child may still be infectious, we explored models with infectious periods of 7 days (weekly rate of 1/1) to 12 days (weekly rate of 1/1.7). Despite the epidemiology of RSV infections in

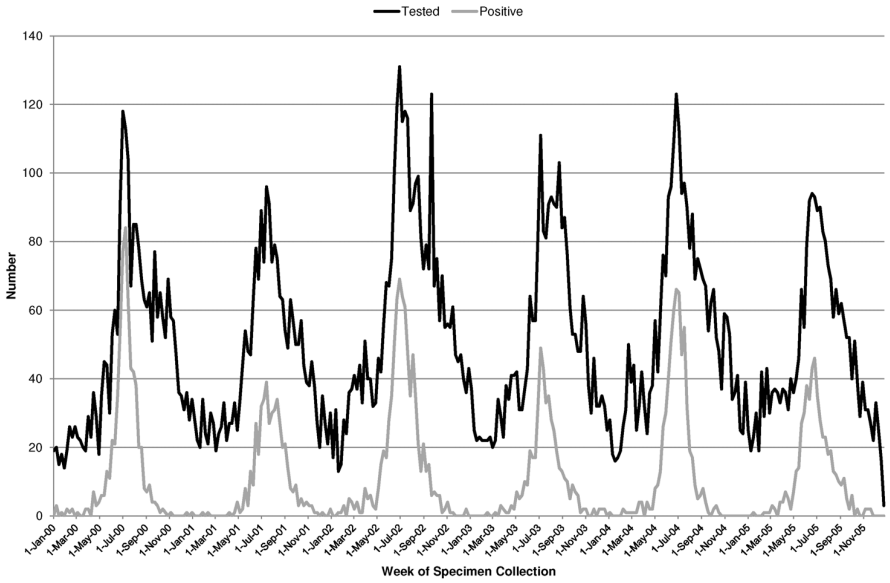

Figure 2. Weekly number of specimens tested and found positive for RSV in metropolitan Western Australian children aged less than 2 years from January 2000 to December 2005.
doi:10.1371/journal.pone.0100422.g002

Western Australia suggesting the optimal estimate for the infectious period in the vicinity of 5–12 days, only periods in the range of 8–11 days were successful in producing a model with the biennial seasonal pattern; outside this range the model gave an annual pattern which does not concord with the data.

Very few studies have been undertaken to ascertain to what level RSV is transmitted from adults to children, with RSV in

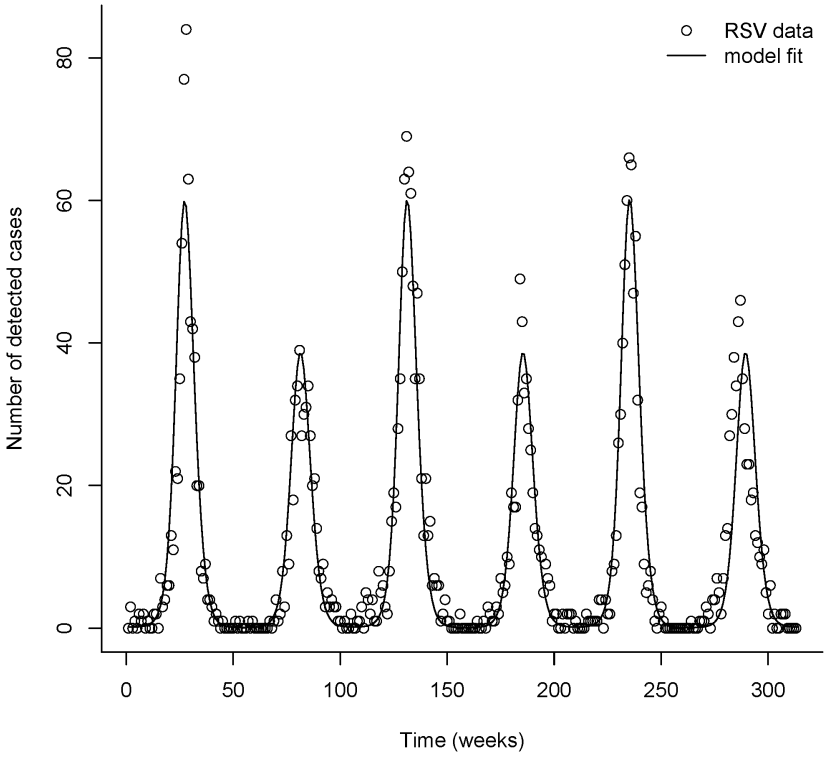

Figure 3. Observed RSV identifications in those aged less than 2 years and the fitted SEIRS model. The parameters used in the model are $\alpha = 0.65$; $\delta = 0.65$; $\gamma = 1/1.4$; and $\sigma = 1/0.57$, producing a fit statistic of $F = 89.5751$.
doi:10.1371/journal.pone.0100422.g003

Table 1. Sensitivity analysis of the fit statistic and fitted transmission parameters for varying duration of immunity and infectious period.

Test conducted	Parameter variation		Fitting parameters			Fit statistic (F)
	Parameter	Value tested	β_0	β_1	ν	
Parameters for best fit: $\alpha = 0.65$; $\delta = 0.65$; $\gamma = 1/1.4$; $\sigma = 1/0.57$	-	-	1.9896	0.6495	0.0438	89.5751
Reduction in infectiousness for adults	α	0.5	2.5639	0.6775	0.0454	90.3653
	α	0.8	1.6300	0.6262	0.0436	89.6733
Reduction in susceptibility for adults	δ	0.5	2.5534	0.6279	0.0445	90.1470
	δ	0.8	1.6488	0.6667	0.0468	90.2240
Variation to latency period	$1/\sigma$	1/0.28	1.9113	0.5879	0.0474	90.0338
	$1/\sigma$	1/0.86	2.1255	0.6618	0.0457	92.3239
Variation to infectious period	$1/\gamma$	1/1.14	2.3617	0.6478	0.0464	91.6664
	$1/\gamma$	1/1.57	1.8289	0.6599	0.0428	90.2565

The assumed values of the parameters are $\alpha = 0.65$; $\delta = 0.65$; $\gamma = 1/1.4$; and $\sigma = 1/0.57$ unless otherwise varied, as indicated in the table.
doi:10.1371/journal.pone.0100422.t001

adults most often presenting as the "common cold" [24]. One study by Henderson et al (1979) found that the attack rate for first RSV infection was 98%, 75% for second infections and 65% for third infections [25]. As such, values between 0.5 and 0.8 were tested for the scaling parameters α and δ. Suitable model fits, close to the optimal fit, were found for all tests in this range, with the best fits for values between 0.6 and 0.7.

For the parameter ranges tested, the fitted duration of immunity had little variation with typical values around 160 days ($\nu = 0.0438$) and a range from 148 to 164 days. As expected, the most sensitive fit parameter was the average transmission parameter β_0. Reducing either the susceptibility or infectiousness for the older age class required an increase in the transmission rate for the model to fit the data. Increasing the infectious period reduced the required level of transmission. Varying the latency period did not have a significant impact on the transmission parameter. The fitted value of the seasonality parameter, β_1, was consistent across the sensitivity analysis with a value typically around 0.65 and a range from 0.59 to 0.68. The only other model that has been fitted to biennial pattern RSV data assumed an overly large seasonal forcing parameter of $\beta_1 = 1$ and required other parameters to vary season by season to obtain a good fit to the data [15].

The best fitting transmission estimates and the corresponding fit statistic for the different combinations of the duration of immunity and recovery period are shown in Table 1. The fit statistic for realistic parameter choices ranged from $F = 89.575$ (the best fit) to 92.324. A number of parameter choices produced seasonal epidemics curves of alternating peak sizes, consistent with the RSV data. However, the model that minimised the residual sum of errors assumed a latency period of 4 days and infectious period of 10 days, in keeping with earlier estimates in the literature.

Discussion

RSV is the most commonly detected pathogen in children with ALRI and both RSV testing and positive detections in Western Australia exhibit distinct seasonality with alternating peaks in winter months. Using positive RSV detections obtained through population-based data linkage, we have constructed a simple mathematical model to mimic these seasonal patterns of detections in the metropolitan population of Western Australia. Our age-structured model accurately captures the biennial seasonal epidemic curves that were observed in children aged less than 2 years between 2000 and 2005. The compartmental SEIRS model, based on several assumptions, now provides a base model on which to expand and increase complexity.

All models are based on assumptions of epidemiological parameters of the disease in question. There is a paucity in the literature of the characteristics of RSV infection including duration of shedding and infectiousness. Previous models have used the infectious period of 10 days based on a study of 23 infants [23]. In another Kenyan community study of 193 children, the mean duration of shedding was 4.5 days and varied between severity of infection and recent history of infection [29]. While we investigated models with infectious periods ranging from 7 to 12 days, we could only replicate the biennial seasonal peaks of RSV with infectious periods between 8 and 11 days; outside this range a suitable fit could not be found with only annual patterns produced by the model.

Our initial estimate for the duration of immunity was 200 days (~6.6 months), based on previous RSV models in the literature [13]. We investigated this estimate using data regarding RSV reinfections. From our linked laboratory data, there were 4,920 RSV positive identifications between 2000 and 2005 throughout Western Australia in those aged less than 2 years. Of these, 92.6% were single infections and 363 (7.4%) were reinfections (6.3% were second time infections, 0.7% third time infections and 0.2% fourth time infections). Excluding those reinfections with positive RSV identifications from specimens collected less than 14 days apart (most likely to be indicative of the same infection), there were 99 reinfections where the time between positive RSV identification was >14 days. Of these 99 reinfections, 80 were identified in children from metropolitan Western Australia. The mean time between subsequent RSV infections from reinfections in metropolitan children was 250 days (8.21 months) and the range was 15–592 days. However, the duration of immunity that the produced the best fit for the model was 160 days. It is possible that immunity wanes several months before the onset of a subsequent RSV season, but that there are not enough infected individuals in the population at that time for the infection to gain momentum and hence our estimate of the immunity period from the data is an overestimate.

We have identified several improvements that can be made to the model which will become the focus of future work. First, we will improve the age structure of the model to allow the

transmission parameters to vary between the different age groups as opposed to our current model where we assume the same transmission rate for each age group with a fixed scaling parameter. The incidence of RSV is greater in infants aged less than 12 months than those in the second year of life, as we have previously shown with hospitalisation rates for bronchiolitis for which RSV is mostly associated [19]. Therefore a natural next step is to further refine the age classes into those aged less than 12 months, 12–23 months and 2 years and over. This will result in a higher number of parameters to fit to the data and therefore will increase the complexity of the model. The advantage is that age-specific interventions, such as vaccination, are easily incorporated in the modelling framework.

Second, we will introduce non-metropolitan data on RSV detections and investigate the changes in the parameters. Parts of rural and remote Western Australia experience tropical climate and therefore, are very likely to experience a different seasonal pattern in terms of peak height and duration. Our total population-based data allows us to investigate seasonality based on geographical location. To achieve this accurately, we will investigate whether the transmission parameters can be modelled as functions of climatic variables of each geographical region such as average weekly temperatures, rainfall and humidity. A study in Utah correlated climatic variables to hospitalisation data coded for RSV and RSV-bronchiolitis and concluded that temperature and wind speed were the best fitting climatic variables [30]. Due to the differing geographical regions, the effect of corresponding climatic variables on RSV detections may be different in Australia. Indeed, other RSV transmissions with an annual pattern have had lower estimates for the seasonal forcing parameter β_1, depending on the climatic region. In models from tropical regions, β_1 has been typically small (e.g. Gambia: 0.16–0.20; Florida: 0.10–0.13 and Singapore: 0.14–0.20); whereas models from temperate climate regions with more distinct seasonality have a larger β_1 (e.g. Finland: 0.16–0.39) [13].

Third, to measure the likely impact of future interventions, we will model the introduction of a newborn vaccination program and predict the effect on RSV incidence. Such analyses have been previously attempted by modelling [14] and economic models using Monte Carlo simulation methods [31]. However, until such time as accurate vaccine efficacy estimates can be derived from vaccine trial data, these models will continue to be based on multiple assumptions. The benefit of this modelling approach is that different scenarios around age of vaccination, efficacy and waning period of the vaccine can be investigated to inform future vaccination policy.

We also did not investigate RSV transmission by Aboriginality or other risk groups for RSV. Our previous analysis of metropolitan RSV identifications showed no difference in seasonality of RSV in metropolitan Aboriginal and non-Aboriginal children [3]. However, as we extend our model to include non-metropolitan data, disaggregating according to Aboriginality will be important due to the higher burden of illness in Aboriginal children from rural and remote areas [32,33].

Conclusions

We have successfully developed a model to mimic the biennial seasonal epidemic curves of RSV identifications in metropolitan Western Australia. A strength of our model is the quality of data that it is based on, gathered from individual-level linked total population-based data sources. Not all RSV positive detections are associated with hospitalisations so it is important to not limit data sources to the severe end of the clinical spectrum. RSV continues to be a major pathogen in children and until such time that positive identifications of RSV become mandatory, future studies will need to rely on routinely collected laboratory data.

Acknowledgments

The authors would like to acknowledge David W Smith, Anthony D Keil, Brett Cawley, Simon Williams, Rodney Bowman and Peter Cosgrove who assisted with acquisition, coding and interpreting laboratory data, Matt Cooper who assisted with R code, the Western Australian Data Linkage Branch for their assistance in our application to extract data from the Western Australian Data Linkage System, Deborah Lehmann who assisted with the original study design and Kathryn Glass for helpful discussions on aspects of the modelling. HCM, PJ, ABH and CCB gratefully acknowledge the significant contribution of the late Prof. Geoffry Mercer to this paper who passed away suddenly on the 12th April 2014.

Author Contributions

Conceived and designed the experiments: HCM GNM. Performed the experiments: HCM PJ ABH GNM. Analyzed the data: HCM PJ ABH GNM. Contributed reagents/materials/analysis tools: HCM PJ CCB ABH GNM. Wrote the paper: HCM PJ CCB ABH GNM. Provided clinical interpretation of the data: CCB.

References

1. Ranmuthugala G, Brown L, Lidbury BA (2011) Respiratory syncytial virus–the unrecognised cause of health and economic burden among young children in Australia. Commun Dis Intell 35: 177–184.
2. Hardelid P, Pebody R, Andrews N (2012) Mortality caused by influenza and respiratory syncytial virus by age group in England and Wales 1999–2010. Influenza Other Respi Viruses doi:10.1111/j.1750-2659.2012.00345.x.
3. Moore HC, De Klerk N, Richmond P, Keil AD, Lindsay K, et al. (2009) Seasonality of respiratory viral identification varies with age and Aboriginality in metropolitan Western Australia. Pediatr Infect Dis J 28: 598–603.
4. Stensballe LGM, Devasundaram JKMM, Simoes EAFMD, Piedra PAM (2003) Respiratory syncytial virus epidemics: the ups and downs of a seasonal virus. Pediatr Infect Dis J 22: S21–S32.
5. Vicente D, Montes M, Cilla G, Perez-Yarza EG, Perez-Trallero E (2003) Hospitalization for respiratory syncytial virus in the paediatric population in Spain. Epidemiol Infect 131: 867–872.
6. Viegas M, Barrero PR, Maffey AF, Mistchenko AS (2004) Respiratory viruses seasonality in children under five years of age in Buenos Aires, Argentina: a five-year analysis. J Infect 49: 222–228.
7. Nair H, Nokes DJ, Gessner BD, Dherani M, Madhi SA, et al. (2010) Global burden of acute lower respiratory infections due to respiratory syncytial virus in young children: a systematic review and meta-analysis. Lancet 375: 1545–1555.
8. Milne GJ, Kelso JK, Kelly HA, Huband ST, McVernon J (2008) A small community model for the transmission of infectious diseases: comparison of school closure as an intervention in individual-based models of an influenza pandemic. PLoS One 3: e4005.
9. Fraser C, Donnelly CA, Cauchemez S, Hanage WP, Van Kerkhove MD, et al. (2009) Pandemic potential of a strain of influenza A (H1N1): early findings. Science 324: 1557–1561.
10. Bolisetty S, Wheaton G, Chang AB (2005) Respiratory syncytial virus infection and immunoprophylaxis for selected high-risk children in Central Australia. Aust J Rural Health 13: 265–270.
11. Yang C-F, Wang CK, Malkin E, Schickli JH, Shambaugh C, et al. (2013) Implication of respiratory syncytial virus (RSV) F transgene sequence heterogeneity observed in Phase 1 evaluation of MEDI-534, a live attenuated parainfluenza type 3 vectored RSV vaccine. Vaccine 31: 2822–2827.
12. Malkin E, Yogev R, Abughali N, Sliman J, Eickhoff M, et al. (2013) Safety, shedding and immunogenicity of a live attenuated intranasal RSV vaccine in RSV-seronegative children; 19–22 November; Capetown, South Africa.
13. Weber A, Weber M, Milligan P (2001) Modeling epidemics caused by respiratory syncytial virus (RSV). Math Biosci 172: 95–113.
14. Acedo L, Diez-Domingo J, Morano JA, Villanueva RJ (2010) Mathematical modelling of respiratory syncytial virus (RSV): vaccination strategies and budget applications. Epidemiol Infect 138: 853–860.
15. Leecaster M, Gesteland P, Greene T, Walton N, Gundlapalli A, et al. (2011) Modeling the variations in pediatric respiratory syncytial virus seasonal epidemics. BMC Infect Dis 11.

16. Kelman CW, Bass AJ, Holman CD (2002) Research use of linked health data–a best practice protocol. Aust N Z J Public Health 26: 251–255.
17. Australian Bureau of Statistics (2011) 3101.0 Australian Demographic Statistics. Canberra: Australian Bureau of Statistics.
18. Bradley JS, Byington CL, Shah SS, Alverson B, Carter ER, et al. (2011) The management of community-acquired pneumonia in infants and children older than 3 months of age: clinical practice guidelines by the Pediatric Infectious Diseases Society and the Infectious Diseases Society of America. Clin Infect Dis 53: E25–E76.
19. Moore HC, De Klerk N, Richmond P, Lehmann D (2010) A retrospective population-based cohort study identifying target areas for prevention of acute lower respiratory infections in children. BMC Public Health 10: 757.
20. Moore HC, Lehmann D, De Klerk N, Jacoby P, Richmond P (2012) Reduction in disparity for pneumonia hospitalisations between Australian Indigenous and non-Indigenous children. J Epidemiol Community Health 66: 489–494.
21. Moore HC, De Klerk N, Keil AD, Smith DW, Blyth CC, et al. (2012) Use of data linkage to investigate the aetiology of acute lower respiratory infection hospitalisations in children. J Paediatr Child Health 48: 520–528.
22. Keeling MJ, Rohani P (2007) Modeling Infectious Diseaes in Humans and Animals. Princeton: Princeton University Press.
23. Hall CB, Douglas RGJ, Geiman JM (1976) Respiratory syncytial virus infections in infants: quantitation and duration of shedding. J Pediatr 89: 11–15.
24. Hall CB (1981) Respiratory syncytial virus. In: Feigin RD, Cherry JD, editors. Text of Pediatric Infectious Diseases. Philadephia: WB Saunders Company. 1247–1267.
25. Henderson FW, Collier AM, Clyde WAJ, Denney FW (1979) Respiratory-syncytial-virus infections, reinfections and immunity. A prospective, longitudinal study in young children. N Engl J Med 300: 530–534.
26. R Development Core Team (2012) R: A language and environment for statistical computing. Vienna, Austria: R Foundation for Statistical Computing.
27. Bihorel S, Baudin M (2012) Neldermead: R port of the Scilab neldermead module. R package version 1.0–7 ed.
28. Hall CB, Geiman JM, Biggar R, Kotok DI, Hogan PM, et al. (1976) Respiratory syncytial virus infections within families. N Engl J Med 294: 414–419.
29. Okiro EA, White LJ, Ngama M, Cane PA, Medley GF, et al. (2010) Duration of shedding of respiratory syncytial virus in a community study of Kenyan children. BMC Infect Dis 10.
30. Walton NA, Poynton MR, Gesteland PH, Maloney C, Staes C, et al. (2010) Predicting the start week of respiratory syncytial virus outbreaks using real time weather variables. BMC Med Inform Decis Mak 10: 68.
31. Meijboom MJ, Rozenbaum MH, Benedictus A, Luytjes W, Kneyber MCJ, et al. (2012) Cost-effectiveness of potential infant vaccination against respiratory syncytial virus infection in The Netherlands. Vaccine 30: 4691–7000.
32. Carville K, Lehmann D, Hall G, Moore H, Richmond P, et al. (2007) Infection is the major component of the disease burden in Aboriginal and non-Aboriginal Australian children: a population-based study. Pediatr Infect Dis J 26: 210–216.
33. Moore H, Burgner D, Carville K, Jacoby P, Richmond P, et al. (2007) Diverging trends for lower respiratory infections in non-Aboriginal and Aboriginal children. J Paediatr Child Health 43: 451–457.

4.3 Additional material

As an extension of the modelling work in the *PLoS ONE* paper (Moore et al., 2014), I adapted the fitting routine for the 0–24 month age class, and applied it to the differential equation model presented in the *MODSIM* paper (Hogan et al., 2013). The age-structured model in the *MODSIM* paper reflects the transmission dynamics for two childhood age classes: children less than 12 months of age, and children between 12 and 23 months of age. I simultaneously fitted the two infectious classes in the model, I_1 and I_2, to the corresponding data, using the modified least squares fit statistic

$$F = \sqrt{\sum_{i=1}^{n}(\text{data}_{1_i} - \text{model}_{1_i})^2 + \sum_{i=1}^{n}(\text{data}_{2_i} - \text{model}_{2_i})^2},$$

where data_{1_i} and data_{2_i} are the weekly numbers of cases in the data for the two age groups, model_{1_i} and model_{2_i} are the model outputs of new cases each week, and i is the weekly index. Note that the RSV cases in this dataset account for the severe end of the illness spectrum, as not all RSV episodes are associated with a laboratory test. However, there is an implicit assumption that the number of detected cases over time is proportional to all cases in that age group, as it is expected that observed patterns in the detected cases are representative of community infection dynamics.

The transmission function $\beta(t)$ was given by

$$\beta(t) = \beta_0[1 + \beta_1 \sin(2\pi t/52 + \phi)].$$

Table 4.1: Table of parameter values for the two age class model fitted to RSV data for children 0–11 months and 12–23 months. The rates are in weeks.

Parameter	Description	Value	Fixed/fitted
β_0	Overall transmission	61.650	Fitted
β_1	Amplitude of seasonal forcing	0.522	Fitted
α	Reduced susceptibility in older children	0.228	Fitted
ϕ	Phase shift	-0.449	Fitted
$1/\nu$	Duration of immunity (weeks)	32.895	Fitted
$1/\delta$	Duration of latent period (weeks)	0.570	Fixed
$1/\gamma$	Duration of infectious period (weeks)	1.300	Fixed
μ	Birth rate	431/1658992	Fixed
η	Ageing rate	1/52	Fixed

The model was successfully fitted to data for two age classes simultaneously, with a fit statistic of $F = 84.64$ (Figure 4.1). The fitted model captures the biennial dynamics for both age groups, and reflects the higher incidence of RSV infection in 0–11 month old children in the dataset. The data are remarkably regular, with RSV epidemics occurring at almost the same time each year, allowing for the phase shift parameter to be held constant in the model fitting routine. However, the plotted results show that in the final year in the dataset (2005), the epidemic peak took place slightly earlier than in other years, resulting in a poorer fit to the data for that year. Further, the model does not fit the data well at the epidemic peaks in the high-incidence years. This limitation arises due to the nature of the sinusoidal forcing function used to represent seasonality in the model, which does not sufficiently capture the sharp peaks at the height of each epidemic in the data. It would be possible to consider other types of seasonal forcing mechanisms that more accurately reflect this behaviour, however, sine and cosine forcing functions are well accepted in the literature, straightforward to implement, and I found that overall, the fitted model captured the timing and relative sizes of epidemics well. The fixed and fitted model parameters are in Table 4.1.

The duration of immunity is one of the least well understood aspects of RSV infection. In the *PLoS ONE* paper, the fitted immunity rate corresponded to a duration of 160 days, compared to estimates of 200 days in the existing literature (Weber et al., 2001). In the present model, the fitted rate corresponded to an immunity period of 230 days. In terms of the transmission function, the fitted overall transmission rate was $\beta_0 = 61.65$, compared to values between 1.630 and 2.564 in the *PLoS ONE* paper, reflecting the different model structure, as the present model does not have an adult age class contributing to RSV transmission. The fitted amplitude of seasonal forcing was $\beta_1 = 0.522$, similar to the fitted values between 0.588 and 0.678 in the *PLoS ONE* paper.

The outcome of this fitting exercise, together with the modelling work presented in the two papers in this chapter, validates using the present model for two childhood age classes for future work. It provides a foundation for model development and expansion, which will be explored further in this thesis. It also identifies plausible ranges for parameters, with an indication of the sensitivity of the parameters to the model structure, which provides a starting point for the parameter space investigation of the model in Chapter 5.

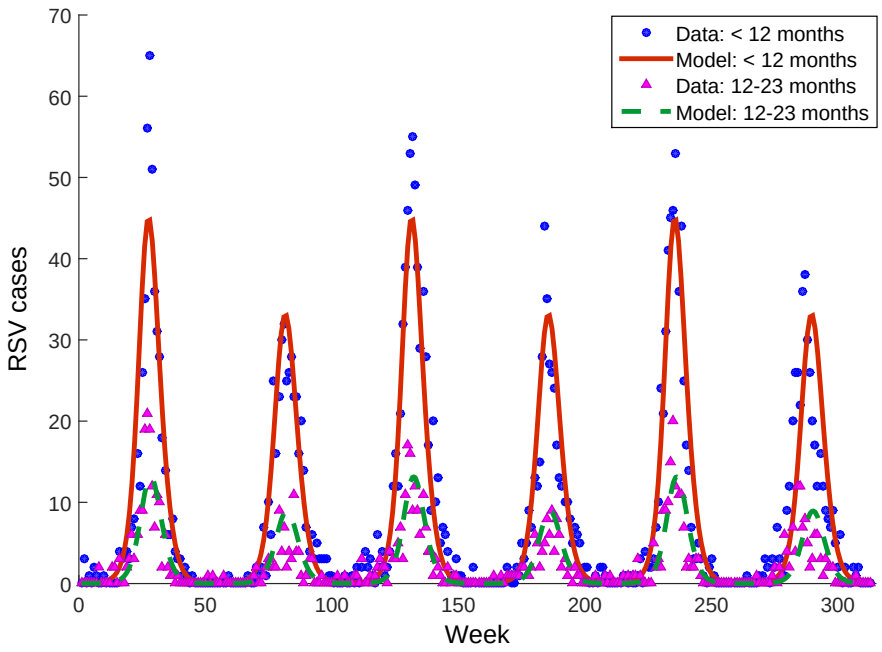

Figure 4.1: Observed RSV identifications in the Metropolitan region of Western Australia for children aged less than 12 months (dots), and children aged between 12 and 23 months (triangles), together with the fitted SEIRS model (solid and dashed lines).

5

Analysis of the seasonally forced, age structured model

5.1 Introduction

This chapter includes two publications. The first paper is published as a peer-reviewed conference proceeding in the Springer series *Maths for Industry*. In this paper I explore different age structures in the compartmental ordinary differential equation model, and show that for the RSV transmission model, the inclusion of an age structure with continuous ageing does not change the overall qualitative dynamics produced by the model. This finding validates using a model with only two age classes for the subsequent numerical analyses.

The second paper is published in *Theoretical Population Biology*. In this paper I present sensitivity, parameter space and bifurcation analyses of the two age class model for RSV transmission. The main outcome of this paper is to explore the ranges of parameters that produce different types of solution dynamics – annual, biennial, delayed biennial and tropical – and to quantify the sensitivity of variation in the model output to the parameters. The results in this paper help to explain the different patterns in RSV detections observed globally. In particular, both the immunity and seasonality parameters must exceed certain thresholds for the model to produce biennial and delayed biennial patterns, which aligns with immunity estimates from clinical studies, and RSV epidemic patterns observed at

different latitudes. Further, a central region of birth rate parameters produces biennial patterns, outside which regular annual patterns occur. This shows that RSV seasonality may not be only driven by weather and climatic factors, but that demography seems to also play a key role. Finally, the supplementary material to this paper outlines the calculation of the basic reproduction number R_0 in the absence of seasonality, which has implications for RSV control measures.

5.2 Papers

Hogan, A. B., Glass, K., Moore, H. C., and Anderssen, R. S. (2015). Age structures in mathematical models for infectious diseases , with a case study of respiratory syncytial virus. In *Proceedings of the Forum of Mathematics for Industry 2014*, Springer, 105–116.

Hogan, A. B., Glass, K., Moore, H. C., and Anderssen, R. S.(2016). Exploring the dynamics of respiratory syncytial virus (RSV) transmission in children. *Theoretical Population Biology*, 110:78–85.

Age Structures in Mathematical Models for Infectious Diseases, with a Case Study of Respiratory Syncytial Virus

Alexandra B. Hogan, Kathryn Glass, Hannah C. Moore and Robert S. Anderssen

Abstract Mathematical modelling plays an important role in understanding the dynamics of transmissible infections, as information about the drivers of infectious disease outbreaks can help inform health care planning and interventions. This paper provides some background about the mathematics of infectious disease modelling. Using a common childhood infection as a case study, age structures in compartmental differential equation models are explored. The qualitative characteristics of the numerical results for different models are discussed, and the benefits of incorporating age structures in these models are examined. This research demonstrates that, for the SIR-type model considered, the inclusion of age structures does not change the overall qualitative dynamics predicted by that model. Focussing on only a single age class then simplifies model analysis. However, age differentiation remains useful for simulating age-dependent intervention strategies such as vaccination.

Keywords Respiratory syncytial virus · Infectious disease · Mathematical modelling · Bifurcation analysis · Seasonality

---

The original version of this chapter was revised: The erratum to this chapter is available at DOI 10.1007/978-4-431-55342-7_23.

A.B. Hogan ( ) · K. Glass
The Australian National University, Canberra, Australia
e-mail: alexandra.hogan@anu.edu.au

K. Glass
e-mail: kathryn.glass@anu.edu.au

H.C. Moore
The University of Western Australia, Perth, Australia
e-mail: hannah.moore@telethonkids.org.au

R.S. Anderssen
The Commonwealth Scientific and Industrial Research Organisation (CSIRO), Acton, Australia
e-mail: bob.anderssen@csiro.au

R.S. Anderssen et al. (eds.), *Applications + Practical Conceptualization + Mathematics = fruitful Innovation*, Mathematics for Industry 11,
DOI 10.1007/978-4-431-55342-7_9

1 The Purpose and Applications of Infectious Disease models

In epidemiology, mathematical modelling is used to understand the dynamics of transmissible infections. This knowledge has important implications for health care planning and disease interventions. Mathematical models are tools that can help predict the impact of various control strategies on patterns of infection; can assist with understanding the groups of a population that are driving the transmission; and can allow control strategies to be tested and subsequently implemented effectively. For example, mathematical modelling techniques have been widely used in influenza pandemic planning [15, 16], in helping identify the drivers of seasonality in pre-vaccination measles epidemics [17, 18] and in understanding the dynamics of pertussis (whooping cough) outbreaks in young children [31].

This paper provides an overview of the mathematics of infectious disease modelling in the context of a common childhood respiratory infection. In particular, this work examines the extent to which age structures should be incorporated into the modelling, and shows how seasonality and waning immunity can be implemented in relatively simple compartmental models.

2 Introduction to the Mathematics of Infectious Disease Models

Mathematical models applied to infectious disease dynamics typically use deterministic, stochastic, or time series approaches. This paper will focus on a specific type of deterministic, ordinary differential equation model, employing the Susceptible-Infectious-Recovered (SIR) model approach. This model was first introduced by Kermack and McKendrick in 1927 [26] and has since been widely applied to model infectious disease dynamics.

The approach of the SIR framework is to divide a specified population into different compartments that correspond to the states of an infection. These compartments describe whether individuals are susceptible to an infection, infectious, or recovered. The basic SIR model is presented at Eqs. 1–4. Assuming a homogeneous, well-mixed population, S represents the number of individuals in a defined population who are susceptible, while I represents the number of individuals who are infectious and able to infect susceptible individuals. The class R represents the number of individuals who are 'removed' (recovered and immune to reinfection).

Demography is represented by the inclusion of a birth rate μ, which corresponds to an average life expectancy of $1/\mu$ years. In this example, the birth rate is assumed

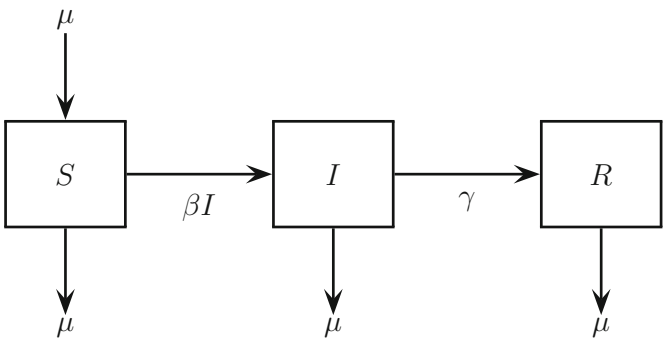

Fig. 1 Schematic diagram for the SIR deterministic ordinary differential equation model

to equal the death rate, such that the total population, represented by N, remains constant over time t. Such an assumption is suitable for infectious diseases where the infection life cycle is relatively short compared to the average individual lifespan and the death rate due to the disease is negligible. The recovery rate is represented by γ, where $1/\gamma$ is the average duration of infection in years. A schematic representation of this structure is shown in Fig. 1. The differential equation model corresponding to such dynamics is given by

$$\frac{dS}{dt} = \mu N - \beta S\frac{I}{N} - \mu S \tag{1}$$

$$\frac{dI}{dt} = \beta S\frac{I}{N} - \gamma I - \mu I \tag{2}$$

$$\frac{dR}{dt} = \gamma I - \mu R \tag{3}$$

$$N = S + I + R. \tag{4}$$

Though the SIR model is one of the simplest forms of a suite of compartmental models, it encapsulates the essence of many infectious disease situations with sufficient accuracy to be able to make useful predictions. Additional states may be included (such as a temporarily immune class) and complexities added (such as age structures). The SIR model and its variations are described extensively elsewhere [4, 11, 23, 25].

3 Respiratory Syncytial Virus

Respiratory syncytial virus (RSV) causes respiratory tract infections in young children. It is the most common pathogen found in children aged less than two years hospitalised with respiratory symptoms and studies indicate that almost all children will have been infected by the time they reach two years [19, 28, 32]. Because of the significant health care and economic burden of RSV (discussed for example in [12, 20, 38]), an improved understanding of its transmission dynamics is required

to assist with health care planning. However, because the dynamics of RSV infection are poorly understood, there remains a need for representative models that are validated by the available data.

RSV dynamics have a clear age structure. RSV incidence is higher for children under 12 months than those between 12 and 24 months [29]. Peak incidence is observed in children between two and four months [32]. Newborn infants are typically protected from RSV infection by maternal antibodies until about six weeks of age (although infection can still occur in this early phase of life) [9, 13]. RSV infection data is usually collected from hospitalised cases, hence the cases observed are for severe infection only. However, the dynamics observed at the severe end of the disease spectrum may be representative of the dynamics in the broader community.

Few studies have been undertaken to examine the transmission of RSV among adults, but it is thought that repeated infection can occur throughout life [9, 22], and that in older children and adults, RSV symptoms present as those of a common cold [19]. Several studies have reported on outbreaks of RSV in aged care facilities and estimated the mortality caused by RSV in these older age groups [21, 35].

An important feature of RSV, in terms of understanding its transmission patterns and burden, is its seasonal behaviour. In temperate climates, RSV typically displays annual seasonal patterns, with high numbers of infections in winter and relatively low numbers in the summer months. In some temperate regions, biennial patterns of RSV infection have been detected. Such dynamics have been observed in Switzerland [14], Finland [36], Chile [7] and Australia [29].

Finally, immunity to RSV following recovery from infection is thought to be short-lived, averaging around 200 days [37]. Consequently, children can be infected in consecutive years.

Mathematical models of RSV must therefore take account of different patterns of severe illness with age, of seasonality in disease transmission, and must allow for the waning of disease immunity following recovery from infection.

4 An Age Structured Modelling Approach to RSV

Several models for RSV that implement the SIR approach have been published [10, 30, 37, 39, 40]. A time series approach has been examined by Spaeder et al. [33], and a network approach by Acedo et al. [2, 3]. Stochastic methods have been investigated by Arenas et al. [5].

In the work of Leecaster et al., an age-structured compartmental approach is used to distinguish between children less than two years old, and adults, with an additional 'Detected' class [27]. Acedo et al. divide the population into children under one year of age, and the remaining population, in order to model a vaccination strategy for RSV [1]. In recent work by Moore et al. [29], age structuring is used to fit a compartmental model to RSV detection data for children up to two years of age in Perth, Western Australia. The present paper builds upon the work presented published by Moore et al. [29], using parameters relevant to RSV dynamics in Western Australia.

In the following sections, compartmental models for RSV are presented. These models take into account the known clinical characteristics and epidemiological features of RSV, such as waning immunity, a latent period, and seasonal changes in the degree of transmission. The age-structured modelling approach is implemented for one, two and three age groups, in order to capture the transmission and susceptibility characteristics of different age groups. Numerical solutions are found and the resulting qualitative characteristics of the dynamics are discussed.

4.1 A Single Age Class Model for RSV

The simplest model for RSV transmission is that of a single age class. In this situation the age group was chosen to be the combined child and adult population, with no differentiation between age groups, and with the birth rate equal to the death rate. A latent disease class, represented by E, is included to reflect the state where an individual is infected with RSV, but not yet infectious. The disease states are presented as proportions of a population, such that $S + E + I + R = N = 1$. This model was first presented in [24] and the relevant equations are reproduced here as Eqs. 5–9.

$$\frac{dS}{dt} = \mu - \beta SI + \nu R - \mu S \tag{5}$$

$$\frac{dE}{dt} = \beta SI - \delta E - \mu E \tag{6}$$

$$\frac{dI}{dt} = \delta E - \gamma I - \mu I \tag{7}$$

$$\frac{dR}{dt} = \gamma I - \nu R - \mu R \tag{8}$$

$$\beta = b[1 + a\sin(2\pi t)] \tag{9}$$

To incorporate the effect of seasonal fluctuations in the number of infected cases, the transmission parameter β is replaced with a sinusoidal forcing function, shown at Eq. 9. The birth rate μ was chosen based on birth and population data from Western Australia [6] and corresponds to a life expectancy of 74 years. The infectious rate δ is based on previous studies and corresponds to a latent period of four days [37]. Similarly, the recovery rate γ is based on previous studies in the literature and corresponds to an infectious period of nine days [2, 27, 37].

The waning immunity parameter ν is less well understood and is therefore chosen by fitting models to data from Western Australia, as demonstrated in [29], and corresponds to an immunity period of 230 days. The amplitude of seasonal forcing a was selected based on the same fitting routine, and the parameter b was allowed to vary. Parameter definitions and values are summarised at Table 1.

Table 1 Parameter values for the compartmental models are estimated from the literature, from population data, and from fitting the two age class model to weekly detection data for metropolitan Western Australia as demonstrated in [29]

Parameter	Description	Value	References
μ	Birth rate for Perth, Western Australia	0.0135	[6]
b	Overall transmission		
a	Amplitude of seasonal forcing	0.522	Fitted value, as in [29]
δ	Infectious rate	91.479	[37]
γ	Recovery rate	40.110	[2, 27, 37]
ν	Waning immunity rate	1.585	Fitted value, as in [29]
η_i	Ageing rate	$\eta_1 = \eta_2 = 1$, $\eta_3 = 0.0139$	
σ_i	Transmission scaling factor	$\sigma_2 = 1$, $\sigma_3 = 0.6$	
α_i	Susceptibility scaling factor	$\alpha_2 = 0.228$, $\alpha_3 = 0.6$	Fitted value, as in [29]

The rates are given in years

4.2 Multiple Age Class Models for RSV

There are two main approaches employed in the literature to simulate the ageing process in models for disease transmission. One is the continuous approach, where each compartment in the model is assumed to be a function of both age and time (see [25] for a concise explanation of this method), and the model can be represented as a system of partial differential equations. While realistic, this approach is complicated and the equations are more difficult to solve numerically.

A simpler approach is to treat age groups as compartments in the model, replicating the susceptible, infectious and removed states for each age class. While increasing the number of ordinary differential equations, the system remains straightforward to solve numerically. In this paper, we concentrate only on this second approach to age structures. Detailed examples of where the continuous approach has been used can be found elsewhere [8, 34, 41], although not for RSV.

The multiple age class compartmental model for three age classes is shown in Eqs. 10–17. The age classes are children up to 12 months of age; children aged between 12 and 24 months; and the remaining population. The model may also be adjusted for two age classes only. The seasonal forcing term for each age class is shown in Eqs. 18–19. In the following model, the youngest age class (denoted '1') includes the birth term, with additional classes (denoted 'i') representing older age groups.

$$\frac{dS_1}{dt} = \mu - \beta_1 S_1 (I_1 + \sum_{i=2}^{3} \sigma_i I_i) + \nu R_1 - \eta_1 S_1 \tag{10}$$

$$\frac{dE_1}{dt} = \beta_1 S_1 (I_1 + \sum_{i=2}^{3} \sigma_i I_i) - \delta E_1 - \eta_1 E_1 \tag{11}$$

$$\frac{dI_1}{dt} = \delta E_1 - \gamma I_1 - \eta_1 I_1 \tag{12}$$

$$\frac{dR_1}{dt} = \gamma I_1 - \nu R_1 - \eta_1 R_1 \tag{13}$$

$$\frac{dS_i}{dt} = \eta_{i-1} S_{i-1} - \beta_i S_i (I_1 + \sum_{i=2}^{3} \sigma I_i) + \nu R_i - \eta_i S_i \tag{14}$$

$$\frac{dE_i}{dt} = \eta_{i-1} E_{i-1} + \beta_i S_i (I_1 + \sum_{i=2}^{3} \sigma I_i) - \delta E_i - \eta_i E_i \tag{15}$$

$$\frac{dI_i}{dt} = \eta_{i-1} I_{i-1} + \delta E_i - \gamma I_i - \eta_i I_i \tag{16}$$

$$\frac{dR_i}{dt} = \eta_{i-1} R_{i-1} + \gamma I_i - \nu R_i - \eta_i R_i \tag{17}$$

$$\beta_1 = b[1 + a \sin(2\pi t)] \tag{18}$$

$$\beta_i = \alpha_i \beta_{i-1} \tag{19}$$

$$i = 2, 3$$

In comparison to the single age class model of Eqs. 5–9, the additional parameters in the model with multiple age classes are σ_i, which represents the reduced transmissability for age class i, and α_i which represents the reduced susceptibility in age group i. The extent to which transmission is reduced for older age classes is not well understood. Hence, transmission was not scaled for the 12–24 month old age class, but was selected as 0.6 for the older age group as in [29]. Similarly for the susceptibility scaling parameter α, the value for reduced susceptibility was selected for the second age group based on Western Australian data, and chosen to be 0.6 for the older age group. The parameter η_i represents the rate of ageing out of age group i, where $1/\eta_i$ is the time spent in age group i. Infection-specific parameters are the same as those for the single age class model. The parameter values for the chosen age structure are presented at Table 1.

4.3 Numerical Solutions

The compartmental ordinary differential equation systems for one, two and three age classes, shown in Eqs. 5–19, were solved numerically using MATLAB's inbuilt *ode45* integrator. The values of the fixed parameters are given in Table 1.

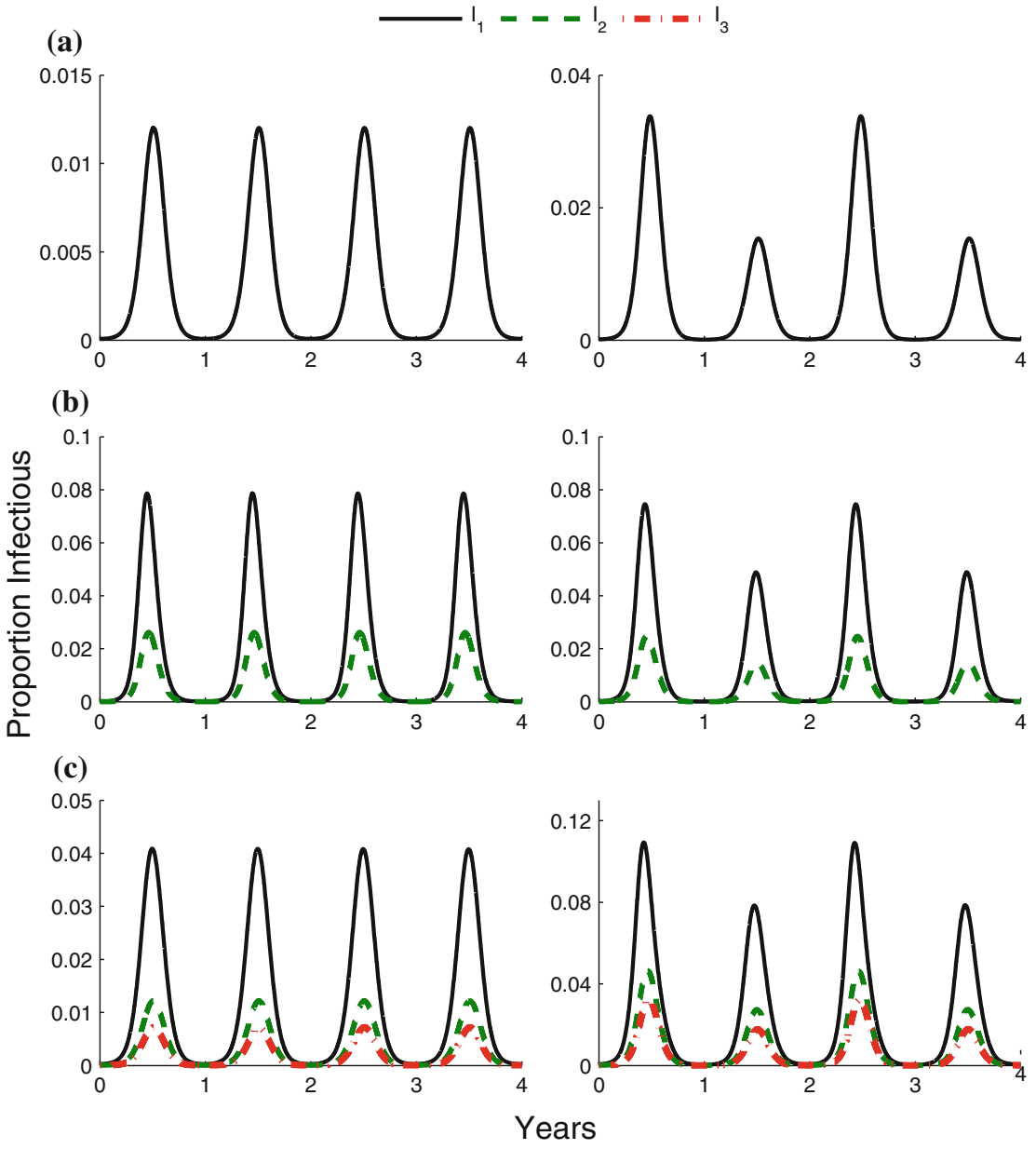

Fig. 2 This figure shows two numerical solutions for compartmental RSV models, for each of **a** one, **b** two and **c** three age classes. For each model, the numerical output demonstrates that either an annual or biennial pattern may be produced, depending on the value of the transmission parameter b. The values of b are as follows: **a** 45, 49; **b** 3400, 3200; **c** 460, 530. Other parameter values are provided in Table 1

The transmission parameter b was chosen to vary, in order to demonstrate different numerical solutions. The range of possible b values that produced plausible numerical solutions varied depending on the model age structure. This is a consequence of how the models were formulated. The model compartments (S, E, I, R), were assumed to be proportions of the chosen population, rather than numbers of individuals. For each age class, the compartments in that age classes summed to 1 at $t = 0$, and the total population did not remain constant as the birth rate and the 'ageing out' or death

rate were not equal for all model structures; this changed the degree of transmission required to sustain annual epidemics. In practice, exact values of the transmission parameter b will vary according to the data the model is fitted to.

Depending on the value of b chosen, and holding other parameters constant, the model solutions produced either annual or biennial patterns. Examples of solutions for different values of the transmission parameter b are shown in Fig. 2. In this figure, the values of b were selected to be within a range that produced plausible solutions and so as to demonstrate markedly different dynamics.

In order to more clearly show the range of b values that produce either annual or biennial patterns of infection, a numerical bifurcation analysis was undertaken using XPP-AUT software. The analysis was conducted for each of the compartmental models, for one, two and three age classes, with bifurcation parameter b. The output is shown in Fig. 3. For each plot, the y-axis is the proportion of infectious individuals I at the seasonal peak, for the youngest age class. We can observe how the infectious peak changes as the value of transmission parameter increases, and whether the model dynamics are annual or biennial.

Figure 3 shows that for each model, there exists a region of solutions with biennial dynamics contained by two period doubling bifurcations. Either side of this region the solutions revert to annual seasonal dynamics. This analysis demonstrates the similar qualitative dynamics for the one, two and three age class models for RSV. A more

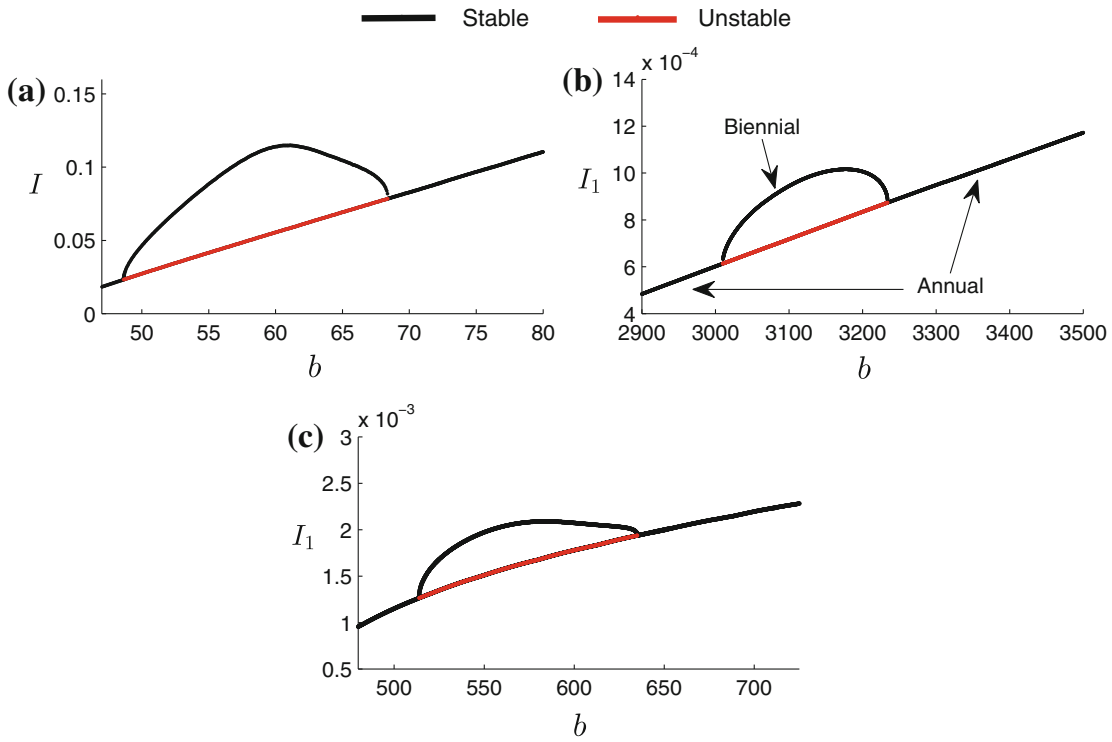

Fig. 3 This figure shows a bifurcation diagram for each of the compartmental RSV models, for **a** one, **b** two and **c** three age classes. The bifurcation parameter is the overall transmission b. For each model, the qualitative behaviour is similar, where there is a region of values of b that produces period two (biennial) solutions, and a region either side that produces period one (annual) solutions

detailed bifurcation analysis (for example, exploring other bifurcation parameters) is outside the scope of the present paper, but will be explored in a forthcoming publication.

5 Discussion

Mathematical modelling is an important tool for understanding the patterns of infectious disease transmission, and one use of these models is for simulation of disease-specific intervention strategies. Infectious disease interventions are often targeted for different age groups, particularly for children. The ability to implement age-structured modelling approaches is useful for studying the theoretical outcome of a vaccination strategy that is concentrated on specific age groups.

The purpose of this paper is to provide an overview of infectious disease modelling, with a focus on a common childhood respiratory infection. A series of ordinary differential equation models for RSV are presented, incorporating the known clinical characteristics of the infection. Age structures for one, two and three age classes are implemented using the compartmental approach, in order to examine the dynamics of the numerical solutions.

It is found that for the models considered, the qualitative dynamics of the numerical solutions are either annual or biennial, depending on the degree of transmission. Further, the dynamics of the solutions are qualitatively similar for the one, two and three age class systems. Despite adding the complexities of additional age classes, the overall patterns of disease transmission were the same, with a higher transmission rate in younger age groups producing a higher proportion of infectious cases.

This finding has useful implications for studying the dynamics of infectious disease models. It suggests that where the overall behaviour of a model is being investigated, and different possible patterns of disease transmission being considered, the age structuring may be ignored and the simplest single age class model considered. As the number of differential equations is reduced, numerical analyses (such as phase plane and bifurcation) are much simpler and often more readily interpreted. Age structures may of course be included at a later stage of model development, but considering only the single age class (here the younger population only) greatly simplifies analytical and numerical testing in situations where interventions are not being studied.

References

1. Acedo, L., Díez-Domingo, J., Moraño, J.-A., Villanueva, R.-J.: Mathematical modelling of respiratory syncytial virus (RSV): vaccination strategies and budget applications. Epidemiol. Infect. **138**(6), 853–60 (2010)
2. Acedo, L., Moraño, J.-A., Díez-Domingo, J.: Cost analysis of a vaccination strategy for respiratory syncytial virus (RSV) in a network model. Math. Comp. Model. **52**(7–8), 1016–1022 (2010)

3. Acedo, L., Moraño, J.-A., Villanueva, R.-J., Villanueva-Oller, J., Díez-Domingo, J.: Using random networks to study the dynamics of respiratory syncytial virus (RSV) in the Spanish region of Valencia. Math. Comp. Model **54**(7–8), 1650–1654 (2011)
4. Anderson, R.M., May, R.M.: Infectious Diseases of Humans: Dynamics and Control. Oxford University Press, Oxford (1991)
5. Arenas, A.J., González-Parra, G., Moraño, J.-A.: Stochastic modeling of the transmission of respiratory syncytial virus (RSV) in the region of Valencia, Spain. BioSystems **96**(3), 206–212 (2009)
6. Australian Bureau of Statistics.: Births, Australia, 2009, Table 2 Births, Summary, Statistical Divisions 2004 to 2009, time series spreadsheet, cat. no. 3301.0, viewed 20 September 2014. http://www.abs.gov.au/AUSSTATS/abs
7. Avendaño, L.F., Palomino, M.A., Larrañaga, C.: Surveillance for respiratory syncytial virus in infants hospitalized for acute lower respiratory infection in Chile (1989 to 2000). J. Clin. Microbiol. **41**(10), 4879–4882 (2003)
8. Busenberg, S., Cooke, K., Iannelli, M.: Endemic thresholds and stability in a class of age-structured epidemics. SIAM J. Appl. Math. **48**(6), 1379–1395 (1988)
9. Cane, P.A.: Molecular epidemiology of respiratory syncytial virus. Rev. Med. Virol. **11**(2), 103–16 (2001)
10. Capistrán, M., Moreles, M., Lara, B.: Parameter estimation of some epidemic models. The case of recurrent epidemics caused by respiratory syncytial virus. Bull. Math. Biol. **71**, 1890–1901 (2009)
11. Diekmann, O., Heesterbeek, H., Britton, T.: Mathematical Tools for Understanding Infectious Disease Dynamics. Princeton University Press, Princeton (2013)
12. Díez-Domingo, J., Pérez-Yarza, E.G., Melero, J.A., Sánchez-Luna, M., Aguilar, M.D., Blasco, A.J., Alfaro, N., Lázaro, P.: Social, economic, and health impact of the respiratory syncytial virus: a systematic search. BMC Infect. Dis. **14**(1), 544 (2014)
13. Domachowske, J.B., Rosenberg, H.F.: Respiratory syncytial virus infection: immune response, immunopathogenesis, and treatment. Clin. Microbiol. Rev. **12**(2), 298–309 (1999)
14. Duppenthaler, A., Gorgievski-Hrisoho, M., Frey, U., Aebi, C.: Two-year periodicity of respiratory syncytial virus epidemics in Switzerland. Infection **31**(11–12), 75–80 (2003)
15. Ferguson, N.M., Cummings, D.A.T., Cauchemez, S., Fraser, C., Riley, S., Meeyai, A., Iamsirithaworn, S., Burke, D.S.: Strategies for containing an emerging influenza pandemic in Southeast Asia. Nature **437**(7056), 209–214 (2005)
16. Germann, T.C., Kadau, K., Longini, I.M., Macken, C.A.: Mitigation strategies for pandemic influenza in the United States. Proc. Natl. Acad. Sci. USA **103**(15), 5935–5940 (2006)
17. Grenfell, B.T., Bjørnstad, O.N., Kappey, J.: Travelling waves and spatial hierarchies in measles epidemics. J. Nat. **414**, 716–723 (2001)
18. Grenfell, B.T., Bolker, B.M.: Population dynamics of measles. In: Scott, M.E., Smith, G. (eds.) Parasitic and Infectious Diseases: Epidemiology and Control, pp. 219–234. Academic Press, Orlando (1994)
19. Hall, C.B.: Respiratory syncytial virus. In: Feigin, R.D., Cherry, J.D. (eds.) Textbook of Paediatric Infectious Diseases, vol. II, pp. 1247–1267. W.B. Saunders Company, Philadelphia (1981)
20. Hall, C.B., Weinberg, G.A., Iwane, M.K., Blumkin, A.K., Edwards, K.M., Staat, M.A., Auinger, P., Griffin, M.R., Poehling, K.A., Erdman, D., Grijalva, C.G., Zhu, Y., Szilagyi, P.: The burden of respiratory syncytial virus infection in young children. N. Engl. J. Med. **360**(6), 588–598 (2009)
21. Hardelid, P., Pebody, R., Andrews, N.: Mortality caused by influenza and respiratory syncytial virus by age group in England and Wales 1999–2010. Influenza Other Respir. Viruses **7**(1), 35–45 (2013)
22. Henderson, F.W., Collier, A.M., Clyde Jr, W.A., Denny, F.W.: Respiratory-syncytial-virus infections, reinfection and immunity: a prospective, longitudinal study in young children. N. Engl. J. Med. **300**(10), 530–534 (1979)
23. Hethcote, H.W.: The mathematics of infectious diseases. SIAM Rev. **42**(4), 599–653 (2007)

24. Hogan, A.B., Mercer, G.N., Glass, K., Moore, H.C.: Modelling the seasonality of respiratory syncytial virus in young children. In: 20th International Congress on Modelling and Simulation, vol. 9, pp. 338–344. Adelaide, Australia (2013)
25. Keeling, M.J., Rohani, P.: Modeling Infectious Diseases in Humans and Animals. Princeton University Press, Princeton (2008)
26. Kermack, W.O., McKendrick, A.G.: A contribution to the mathematical theory of epidemics. Proc. R. Soc. Lond. A. **115**, 700–721 (1927)
27. Leecaster, M., Gesteland, P., Greene, T., Walton, N., Gundlapalli, A., Rolfs, R., Byington, C., Samore, M.: Modeling the variations in pediatric respiratory syncytial virus seasonal epidemics. BMC Infect. Dis. **11**(1), 105 (2011)
28. Moore, H.C., de Klerk, N., Keil, A.D., Smith, D.W., Blyth, C.C., Richmond, P., Lehmann, D.: Use of data linkage to investigate the aetiology of acute lower respiratory infection hospitalisations in children. J. Paediatr. Child Health **48**(6), 520–528 (2012)
29. Moore, H.C., Jacoby, P., Hogan, A.B., Blyth, C.C., Mercer, G.N: Modelling the seasonal epidemics of respiratory syncytial virus in young children. PLoS ONE **9**(6), e100422 (2014)
30. Paynter, S., Yakob, L., Simões, E.A.F., Lucero, M.G., Tallo, V., Nohynek, H., Ware, R.S., Weinstein, P., Williams, G., Sly, P.D.: Using mathematical transmission modelling to investigate drivers of respiratory syncytial virus seasonality in children in the Philippines. PLoS ONE **9**(2), e90094 (2014)
31. Rohani, P., Zhong, X., King, A.A.: Contact network structure explains the changing epidemiology of pertussis. Science **330**, 982–985 (2010)
32. Sorce, L.R.: Respiratory syncytial virus: from primary care to critical care. J. Pediatr. Health Care **23**(2), 101–108 (2009)
33. Spaeder, M.C., Fackler, J.C.: A multi-tiered time-series modelling approach to forecasting respiratory syncytial virus incidence at the local level. Epidemiol. Infect. **140**(4), 602–607 (2012)
34. Tudor, D.: An age-dependent epidemic model with application to measles. Math. Biosci. **147**, 131–147 (1985)
35. van Asten, L., van den Wijngaard, C., van Pelt, W., van de Kassteele, J., Meijer, A., van der Hoek, W., Kretzschmar, M., Koopmans, M.: Mortality attributable to 9 common infections: significant effect of influenza A, respiratory syncytial virus, influenza B, norovirus, and parainfluenza in elderly persons. J. Infect. Dis. **206**(5), 628–639 (2012)
36. Waris, M.: Pattern of respiratory syncytial virus epidemics in Finland: two-year cycles with alternating prevalence of groups A and B. J. Infect. Dis. **163**(3), 464–469 (1991)
37. Weber, A., Weber, M., Milligan, P.: Modeling epidemics caused by respiratory syncytial virus (RSV). Math. Biosci. **172**(2), 95–113 (2001)
38. Welliver, R.C.: Review of epidemiology and clinical risk factors for severe respiratory syncytial virus (RSV) infection. J. Pediatr. **143**(5 Suppl), S112–S117 (2003)
39. White, L.J., Mandl, J.N., Gomes, M.G.M., Bodley-Tickell, A.T., Cane, P.A., Perez-Brena, P., Aguilar, J.C., Siqueira, M.M., Portes, S.A., Straliotto, S.M., Waris, M., Nokes, D.J., Medley, G.F.: Understanding the transmission dynamics of respiratory syncytial virus using multiple time series and nested models. Math. Biosci. **209**(1), 222–239 (2007)
40. White, L.J., Waris, M., Cane, P.A., Nokes, D.J., Medley, G.F.: The transmission dynamics of groups A and B human respiratory syncytial virus (hRSV) in England & Wales and Finland: seasonality and cross-protection. Epidemiol. Infect. **133**(2), 279–289 (2005)
41. Zhu, G.: Threshold and stability results for an age-structured epidemic model. Comput. Math. Appl. **42**, 883–907 (2001)

Theoretical Population Biology 110 (2016) 78–85

Contents lists available at ScienceDirect

Theoretical Population Biology

journal homepage: www.elsevier.com/locate/tpb

Exploring the dynamics of respiratory syncytial virus (RSV) transmission in children

Alexandra B. Hogan [a,*], Kathryn Glass [a], Hannah C. Moore [b], Robert S. Anderssen [c]

[a] National Centre for Epidemiology and Population Health, Building 62, Corner Mills and Eggleston Roads, The Australian National University, Canberra ACT 2601, Australia

[b] Wesfarmers Centre of Vaccines and Infectious Diseases, Telethon Kids Institute, The University of Western Australia, Western Australia, Australia

[c] CSIRO Data61; Mathematical Sciences Institute, The Australian National University; Mathematics and Statistics, La Trobe University, Australia

HIGHLIGHTS

- Our RSV model successfully replicates seasonal patterns in different regions.
- Seasonal forcing must exceed a threshold to produce the biennial dynamics of temperate zones.
- Births and waning immunity may drive the 'delayed biennial' cycles seen in some countries.

ARTICLE INFO

Article history:
Received 28 July 2015
Available online 4 May 2016

Keywords:
Respiratory syncytial virus
Infectious disease
Mathematical modelling
Bifurcation analysis
Seasonality

ABSTRACT

Respiratory syncytial virus (RSV) is the main cause of lower respiratory tract infections in children. Whilst highly seasonal, RSV dynamics can have either one-year (annual) or two-year (biennial) cycles. Furthermore, some countries show a 'delayed biennial' pattern, where the epidemic peak in low incidence years is delayed. We develop a compartmental model for RSV infection, driven by a seasonal forcing function, and conduct parameter space and bifurcation analyses to document parameter ranges that give rise to these different seasonal patterns. The model is sensitive to the birth rate, transmission rate, and seasonality parameters, and can replicate RSV dynamics observed in different countries. The seasonality parameter must exceed a threshold for the model to produce biennial cycles. Intermediate values of the birth rate produce the greatest delay in these biennial cycles, while the model reverts to annual cycles if the duration of immunity is too short. Finally, the existence of period doubling and period halving bifurcations suggests robust model dynamics, in agreement with the known regularity of RSV outbreaks. These findings help explain observed RSV data, such as regular biennial dynamics in Western Australia, and delayed biennial dynamics in Finland. From a public health perspective, our findings provide insight into the drivers of RSV transmission, and a foundation for exploring RSV interventions.

1. Introduction

Respiratory syncytial virus (RSV) is one of the predominant causes of respiratory tract infections in young children and seasonal epidemics are observed globally. RSV detections are known to be age-dependent, with an estimated 60% of children infected with RSV in their first year of life (Glezen et al., 1986) and almost all children infected by the time they turn two years of age (Hall, 1981; Sorce, 2009). Fewer infections are detected in older children and adults. Immunity to RSV following recovery from infection is partial and limited in duration, and reinfection throughout early childhood is common (Hall et al., 1991; Meng et al., 2014). However, the specific mechanisms of the immune response to RSV following recovery from an infection are not well documented (Hall et al., 1991; Lambert et al., 2014) and the average duration of immunity is not accurately known.

Winter RSV epidemics occur in many temperate countries, with few infections in the summer months (Duppenthaler et al., 2003; Gilchrist et al., 1994; Hirsh et al., 2014; Terletskaia-Ladwig et al., 2005). However, the underlying drivers of these seasonal patterns are not well understood. Weather-related factors such as lower temperatures, higher rainfall and reduced sunlight, as well as social factors such as indoor crowding in the colder and wetter months,

* Corresponding author.
E-mail address: alexandra.hogan@anu.edu.au (A.B. Hogan).

http://dx.doi.org/10.1016/j.tpb.2016.04.003
0040-5809/

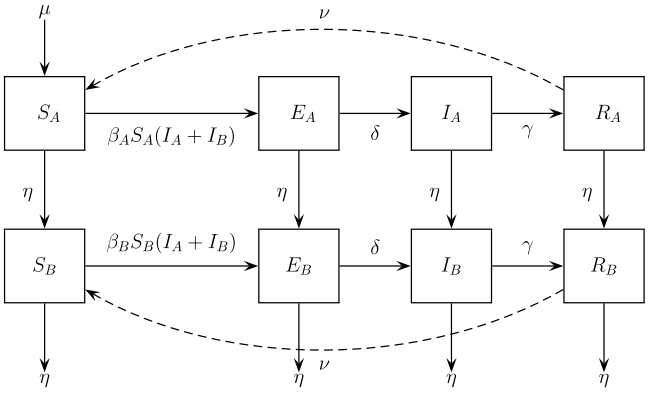

Fig. 1. The schematic diagram for the SEIRS model for two age classes, where A refers to children under 12 months of age, and B refers to children between 12 and 24 months. The boxes represent disease states, and the arrows illustrate the progression of states of infection. The line representing the flow from recovered to susceptible individuals is dashed for visual clarity. Further details of the model formulation and terminology can be found in Hogan et al. (2015).

are all possible causes (Chan et al., 2002; Reese and Marchette, 1991).

Observed seasonality in the incidence of infectious diseases has implications for interventions. For RSV, prophylaxis with the monoclonal antibody palivizumab has been found to be safe and effective for high-risk children (The IMpact-RSV Study Group, 1998), although it is expensive and the timing of the RSV season must be understood for effective implementation. There is currently no licenced vaccine for RSV, although several vaccines are being evaluated (PATH, 2015). Phase two clinical trials of an RSV vaccine have been commenced by GlaxoSmithKline in healthy women (NCT02360475) (ClinicalTrials.gov, 2015). Phase three clinical trials of RSV F nanoparticle vaccines for pregnant women (NCT02624947) and for the elderly (NCT02608502) have been commenced by Novavax (ClinicalTrials.gov, 2015, 2016). Rollout of a future vaccination strategy will need to be based on a comprehensive understanding of seasonality in order to optimise the timing of delivery.

Mathematical models play a key role in identifying the drivers of observed patterns of infectious diseases, as well as informing the planning of potential health interventions (Keeling and Rohani, 2008). Previous models of RSV have concentrated on modelling the data from specific geographic regions (Weber et al., 2001; Leecaster et al., 2011; Moore et al., 2014), with several studies suggesting that climatic factors drive seasonal transmission (Weber et al., 2001; Paynter et al., 2014; Walton et al., 2010). The current literature, however, does not explain why seasonal dynamics differ between temperate locations. Recent work has identified that the interaction between demography and imperfect immunity can affect the dynamics of infectious diseases (Dafilis et al., 2014; Morris et al., 2015). Here, using a SEIRS model, we explore how the birth rate, waning immunity and seasonality might interact to yield different dynamics of RSV. We classify the numerical solutions produced by this model and identify the main parameters that contribute to different qualitative outputs. Finally, we link these findings to RSV data from different countries.

2. Model and parameter values

A deterministic, ordinary differential equation SEIRS model for RSV transmission is shown in Eq. (1). A schematic diagram identifying the progression between disease states is provided in Fig. 1, where S, E, I and R represent, respectively, the susceptible, exposed, infectious and recovered proportions of each age group. In order to capture the known epidemiology of RSV with respect to age, the model is compartmentalised for two age classes: children under 12 months of age are denoted by A, and those between 12 and 24 months of age are denoted by B. This model was first presented in Hogan et al. (2013).

$$\begin{aligned}
\frac{dS_A}{dt} &= \mu - \beta_A S_A(I_A + I_B) + \nu R_A - \eta S_A \\
\frac{dE_A}{dt} &= \beta_A S_A(I_A + I_B) - \delta E_A - \eta E_A \\
\frac{dI_A}{dt} &= \delta E_A - \gamma I_A - \eta I_A \\
\frac{dR_A}{dt} &= \gamma I_A - \nu R_A - \eta R_A \\
\frac{dS_B}{dt} &= \eta S_A - \beta_B S_B(I_A + I_B) + \nu R_B - \eta S_B \\
\frac{dE_B}{dt} &= \eta E_A + \beta_B S_B(I_A + I_B) - \delta E_B - \eta E_B \\
\frac{dI_B}{dt} &= \eta I_A + \delta E_B - \gamma I_B - \eta I_B \\
\frac{dR_B}{dt} &= \eta R_A + \gamma I_B - \nu R_B - \eta R_B.
\end{aligned} \tag{1}$$

This age structure was chosen as severe RSV infections are typically detected in children under 24 months of age and the majority of children hospitalised with RSV are under 12 months of age (Weber et al., 1998). Although RSV has more recently been identified as an important pathogen in adults (Hall, 2001), the transmission mechanism between different age groups is not well understood. Furthermore, it is thought that RSV is typically introduced into a households by a school-aged child (Munywoki et al., 2014), suggesting that adults are not the main drivers of transmission. In recent work, we showed that this model produces qualitatively similar dynamics regardless of whether adults were incorporated (Hogan et al., 2015), hence adults were not included in the present model.

The seasonal nature of the transmission dynamics is modelled using a sinusoidal forcing function (such as in Keeling and Rohani, 2008; Weber et al., 2001; Arenas et al., 2008) given in Eq. (2). For the older age class (the 12–24 month old children), reduced susceptibility to infection is modelled by scaling the seasonal forcing function by a factor α.

$$\begin{aligned}
\beta_A(t) &= b_0[1 + b_1 \sin(2\pi t + \phi)] \\
\beta_B(t) &= \alpha \beta_A(t).
\end{aligned} \tag{2}$$

The default parameter values, listed in Table 1, have been chosen from the literature or have been obtained by fitting the model to RSV data from Perth in Western Australia. To fit these parameters, the model was solved numerically using the `MATLAB` `ode45` routine, and the parameters ν, b_0, b_1, α and ϕ were varied, while the other parameters remained fixed. We used the `MATLAB` `fminsearch` function to perform the fitting with a modified least squares statistic to fit the model to the two infectious age classes simultaneously, such as in Moore et al. (2014). Note that our estimate of the immunity period ($1/\nu$) is slightly longer than the 200 days assumed by other models (Weber et al., 2001; Leecaster et al., 2011; Moore et al., 2014). The phase shift parameter ϕ allows the model to be fitted to data from different regions, where RSV epidemics peak at different times. Our present analysis is not directly linked to data from one region, and hence the parameter ϕ was set to zero. A summary of default parameter values and analysis ranges are listed at Table 1.

For the sensitivity and bifurcation analyses, biologically realistic ranges were chosen for the parameters that were allowed to vary. The birth rate μ was allowed to vary in the range

Table 1
Table of default parameter values, where rates are given in years. Fitted values were obtained by fitting the model to laboratory confirmed RSV cases from Perth, Western Australia (Moore et al., 2014).

Parameter	Definition	Value	Range	Reference
μ	Birth rate for Perth in 2009	$\frac{22,394}{1,658,992} = 0.0135$	$0.01 \leq \mu \leq 0.02$	Australian Bureau of Statistics (2009)
η	Ageing rate	1		
b_0	Overall transmission rate	3,215	$2,900 \leq b_0 \leq 3,500$	Fitted value
b_1	Amplitude of seasonal forcing	0.522	$0 \leq b_1 \leq 1$	Fitted value
α	Scaling factor for reduced susceptibility in older children	0.228	$0 \leq \alpha \leq 1$	Fitted value
$1/\delta$	Latent period	4 days		Weber et al. (2001)
$1/\gamma$	Infectious period	9 days		Weber et al. (2001), Leecaster et al. (2011), Acedo et al. (2010)
$1/\nu$	Immunity period	230 days	182 to 304 days	Fitted value
ϕ	Phase shift	0		

[0.01, 0.02], which corresponds to a life expectancy of between 50 and 100 years, such as in Dafilis et al. (2014). The rate of waning immunity ν was allowed to vary in the range [1.2, 2], which corresponds to an immunity period of between 182 and 304 days. The value for the transmission rate b_0 varied in the range 2900–3500 and the amplitude of seasonal forcing varied in the range [0, 1].

The basic reproduction number $\mathcal{R}_0$ was calculated using the Next Generation Matrix method (Brauer and Castillo-Chavez, 2012). Seasonal forcing was not included, but rather the average transmission rate was used, which provides a basic reproduction number in the absence of seasonal fluctuations in transmission (see Supplementary Material, Appendix A). Substituting the default parameter values from Table 1, we found that $\mathcal{R}_0 = 1.32$. This is in the range [1.2, 2.1] suggested by Weber et al. (2001) for another compartmental RSV transmission model, although we acknowledge it does not fully capture seasonality in the reproduction number (Grassly and Fraser, 2006).

3. Sensitivity analysis

A sensitivity analysis was used to identify which parameters contribute most to variation in model output. For the RSV model, the key parameters explored were the immunity parameter ν, the birth rate μ, the scaling parameter α, the transmission parameter b_0 and the seasonality parameter b_1. In the case of the immunity parameter, there is relatively little epidemiological evidence to quantify the duration of immunity following infection. A similar situation holds for the scaling parameter α that accounts for reduced susceptibility in older children, which is reported but not generally quantified in the literature. Finally, parameter values for the birth rate, transmission rate, and strength of seasonal forcing are likely to vary with population, and no one fixed value is appropriate for all populations.

The sensitivity analysis was performed using the method of Partial Rank Correlation Coefficient (PRCC), using Latin Hypercube Sampling (LHS) to efficiently sample the parameter space. The PRCC gives a value for each parameter between -1 and $+1$, with an absolute value close to 1 indicating that the parameter strongly influences the model outcome. The outcome chosen for our sensitivity analysis was the cumulative number of infectious individuals for both age classes over time. We found that, after allowing for a burn in period, the correlation coefficient remained constant over time. As such, the outcome is shown for a single time point in Fig. 2.

The parameters most strongly correlated with the cumulative number of infectious individuals were the recovery rate γ, the birth rate μ and the transmission rate b_0. The PRCC for the recovery rate γ (the inverse of the duration of infectiousness) was close to -1, indicating that increasing the rate of recovery (or decreasing the duration of infectiousness) contributes to a lower number of infectious individuals. The PRCC for the birth rate μ was close to $+1$, indicating that increasing the inflow of susceptibles substantially contributes to a higher cumulative number of infective individuals. Similarly, increasing the transmission parameter b_0 greatly contributed to the number of infectives over time.

Based on this analysis, several parameters were selected to be explored in more detail. While the recovery rate γ was highly inversely correlated with RSV infections, the duration of infectiousness has been well documented compared to the other parameters. The birth rate μ was further examined, as demographic factors vary between countries. The waning immunity parameter ν was also explored, given that less is known about the duration of immunity for RSV compared to other clinical factors. Finally, the parameters b_0 and b_1 in the seasonal forcing functions β_A and β_B were investigated. Although b_1 was not highly correlated with the outcome, differences in RSV dynamics for different countries and climates are well documented, and we expect the seasonality parameter to play an important role in capturing climatic factors.

4. Parameter space analysis

In earlier work (Hogan et al., 2013; Moore et al., 2014; Hogan et al., 2015), we described the basic dynamics of the numerical solutions to the model. We characterise the solutions as either 'annual' (period one) solutions or 'biennial' (period two) solutions, shown at (i) and (ii), respectively, in Fig. 3. Biennial patterns in RSV disease levels have been observed a number of regions including Chile (Avendaño et al., 2003), Germany (Terletskaia-Ladwig et al., 2005), Switzerland (Duppenthaler et al., 2003) and northern U.S.A. states such as Wyoming and South Dakota (Pitzer et al., 2015). We can further classify the biennial dynamics to describe where the timing of the minor peak (the year of fewer infections in a biennial cycle) occurs markedly later than the major peak, shown in Fig. 3(iii). We refer to this type of pattern as 'delayed biennial'. Such dynamics have been observed in Finland (Waris, 1991) and Croatia (Mlinaric-Galinovic et al., 2008). Finally, reducing the amplitude of seasonal forcing b_1 such as in Fig. 3(iv) replicates the RSV dynamics typically observed in tropical climates, with less pronounced annual peaks (Chan et al., 2002) and disease occurring at a low level throughout the year. Setting the amplitude of seasonality to $b_1 = 0$ (so that no seasonal forcing occurs) results in damped oscillations, with no long-term seasonality in disease incidence, thus the periodicity seen here is a result of seasonal forcing.

We examined the dynamics of the numerical solutions with respect to the birth rate μ and the rate of waning immunity ν by solving the equations for a range of parameter values and then identifying the amplitude and location of the annual peaks (Fig. 4). In each case, we compared the timing of the epidemic peak in a given year with the timing of the peak in the following year. Annual or regular biennial cycles showed no difference in timing, whereas delayed biennial dynamics showed a difference

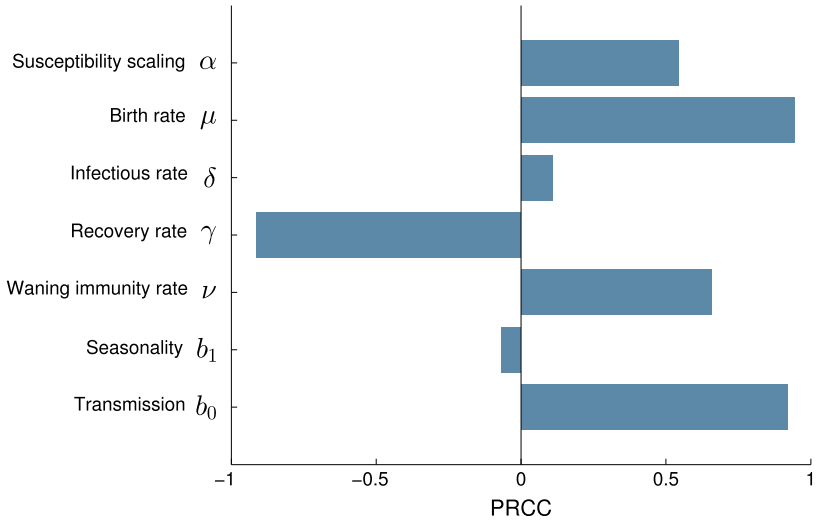

Fig. 2. Output of the Partial Rank Correlation Coefficient (PRCC) sensitivity analysis, where Latin Hypercube Sampling (LHS) was used to sample the parameter space. PRCC values indicate the strength of association between model parameters and the cumulative number of infective individuals. As the correlation for each parameter remained constant over time, the output is shown at a single time point.

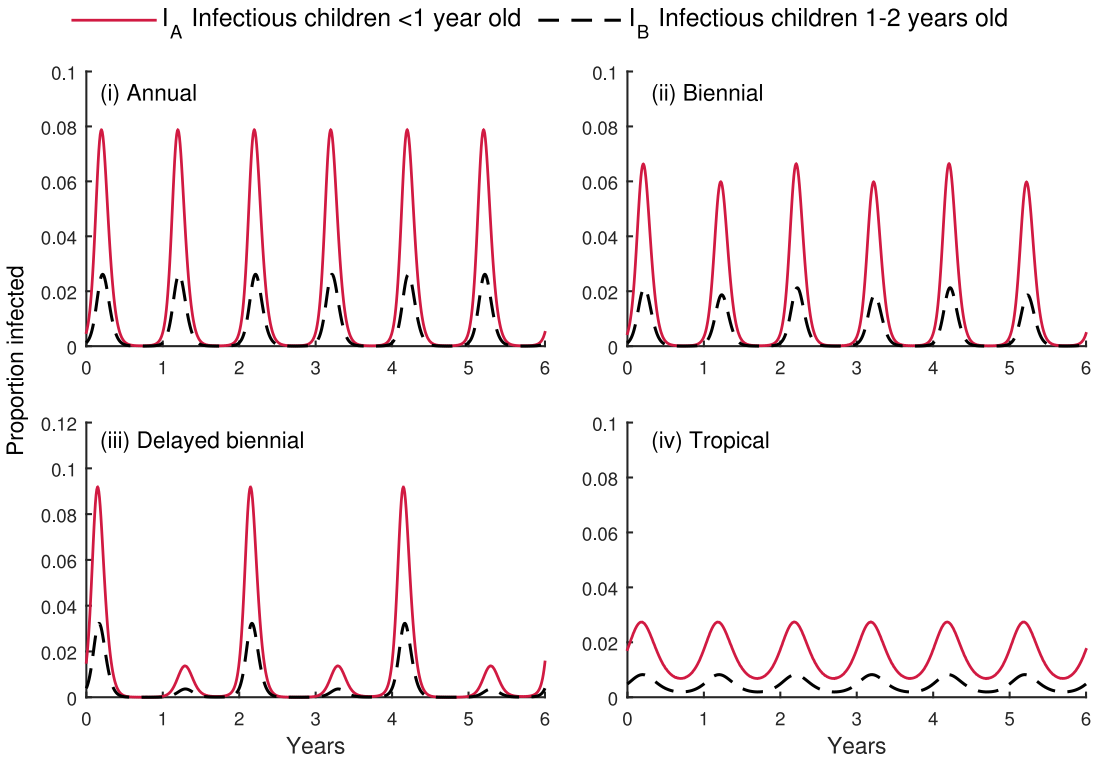

Fig. 3. Four plots demonstrating the qualitative types of model output: annual, biennial, delayed biennial and tropical. Plot (ii) shows the model output with the parameters fixed at the baseline values listed in Table 1. For the other plots, one parameter was varied while the others were fixed at the baseline values, in order to produce different dynamics: (i) $b_0 = 3401$, (iii) $\nu = 1.15$, and (iv) $b_1 = 0.1$. They illustrate the key role played by the forcing function in determining the observed differences in the dynamics.

(the 'delay') of up to 50 days. Varying the birth rate μ showed a region of delayed biennial dynamics, outside of which regular annual dynamics were present. Varying the immunity parameter ν showed that, for shorter durations of immunity, the model produces annual solutions only, whereas increasing this parameter within a biologically plausible range produces biennial patterns. Fig. 4(i) and (ii) show separately the results of the parameter space analysis for μ and ν. Fig. 4(iii) shows a two parameter map demonstrating the regions of annual and biennial output, and the extent of the minor peak delay in days.

5. Bifurcation analysis

The sinusoidal forcing term in Eq. (2) reflects changes in transmission caused by climatic variation throughout the year, and drives the seasonal dynamics produced by the model. A bifurcation analysis allows us to quantify the different types of dynamics produced by the model, for different values of these two parameters, within plausible ranges. We are interested in examining the stable periodic solutions of our model and how the dynamics of these solutions change for different parameter choices.

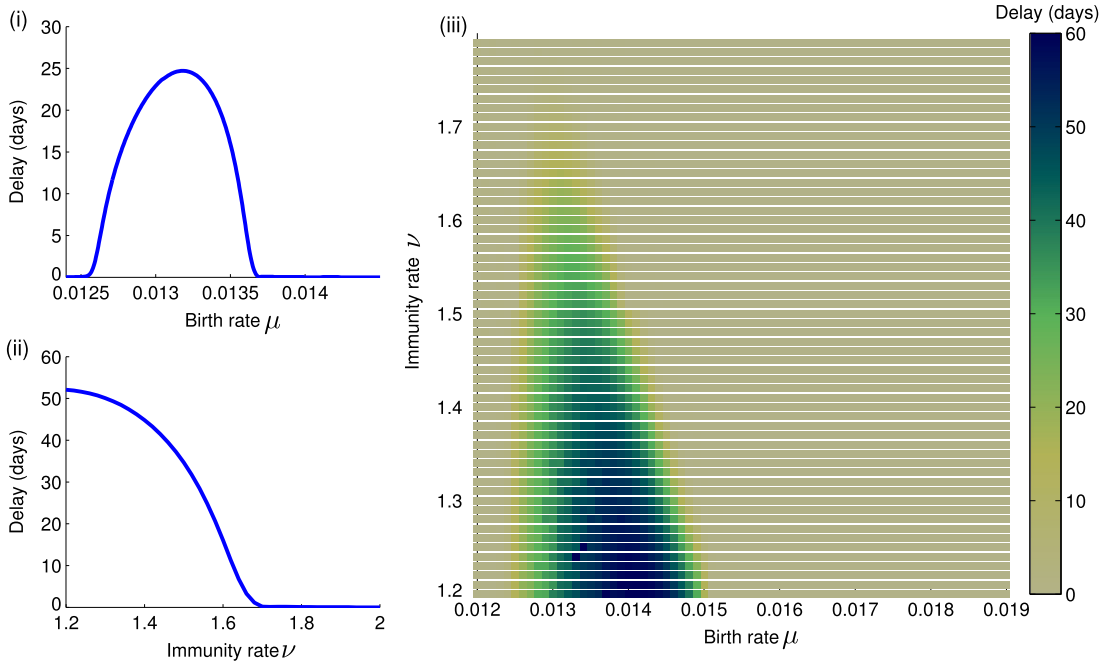

Fig. 4. Variations in the timing of seasonal peaks as a function of the birth rate μ and the immunity rate ν. Figures (i) and (ii) show the delay in days of the 'minor' peak for a range of μ and ν values respectively, with all other parameters fixed. Figure (iii) shows the timing delays on a colour scale as a function of both μ and ν. Figures (i) and (ii) were created using a log-transformed version of the model for improved numerical accuracy. Parameters not stated have the values listed in Table 1.

For this part of the analysis, the differential equations were solved and the bifurcation analysis was performed using the continuation package AUTO within XPPAUT (Ermentrout, 2002). AUTO tracks the bifurcation curves of periodic systems by linearising about fixed points and finding the eigenvalues of the resulting system matrix (Ermentrout, 2001; Doedel, 1981). Plots were produced using MATLAB. XPPAUT requires the system of differential equations to be autonomous. Consequently, we transformed our non-autonomous periodic forcing term using the Hopf oscillator, as in Aguiar et al. (2011), McLennan-Smith and Mercer (2014) and Dafilis et al. (2014). This oscillator is driven by the following coupled system

$$\frac{du}{dt} = u(1 - u^2 - v^2) - 2\pi v,$$
$$\frac{dv}{dt} = v(1 - u^2 - v^2) + 2\pi u,$$

and has the solution

$$u(t) = \cos(2\pi t), \qquad v(t) = \sin(2\pi t).$$

The differential equations were first integrated for 400 years to allow the system to stabilise. The final solution point was then used as initial conditions to integrate the model for one period (one year) in order to perform the bifurcation analysis in AUTO. The bifurcation analysis was conducted for the transmission parameter b_0 and the amplitude of seasonal forcing b_1. The outputs of the bifurcation analysis are shown at (i) and (ii) in Fig. 5. For each figure, the y-axis shows the peak number of infectives. For the region of period-doubling solutions, the stable solution (the green line) is depicted as the maximum proportion of infectious individuals in the year with the higher number of cases. The blue line is used to highlight the unstable solution. The younger age class is used to show the bifurcation dynamics, however, the older age class produces similar results.

The bifurcation diagrams for b_0 and b_1 show similar qualitative characteristics. Both feature a central region of biennial dynamics, contained within a single period doubling bifurcation and a single period halving bifurcation. Parameter values outside this central region therefore produce regular annual dynamics. A range of initial conditions were sampled for the bifurcation analysis in order to identify other potential basins of attraction, however the annual and biennial cycles seem to be a robust feature of this model.

It is of interest to observe the system dynamics when the two key parameters are varied simultaneously, as the bifurcation analysis of b_0 may depend on that of b_1. The bifurcation analysis for b_0 was carried out using a range of different values for the seasonal forcing parameter b_1. The period doubling and halving bifurcations were recorded, and the results of this analysis are shown in Fig. 5(iii). This plot shows the region of parameter combinations of b_0 and b_1 that will produce biennial dynamics (within the region captured by the two curves) and annual dynamics (outside the region). Panel (iv) shows the delay on a colour map for the same two parameters, in a similar fashion to Fig. 4(iii).

6. Discussion

In this study, we showed that our age structured mathematical model for RSV transmission (1) was able to produce four qualitatively distinct types of dynamics: annual, biennial, delayed biennial and tropical. We identified the key parameters in the model (birth rate, rate of waning immunity, transmission rate, and seasonality) that explain these different dynamics, and documented the parameter ranges for which these dynamics occur.

Our parameter space analysis allowed us to examine the ranges of the birth and immunity rates that produced annual, biennial and delayed biennial dynamics. Both the immunity rate and the birth rate effectively moderate the flow of susceptibles into the population. However, the parameter space analysis showed that there is an intermediate range of birth rates that correspond to delayed biennial dynamics, outside of which the dynamics revert to regular annual. This output is consistent with the birth rate analysis in Rohani et al. (2003). In addition, the work by Pitzer et al. indicates that the transition from biennial to annual RSV dynamics in California between the 1990s and 2000s may be due to changes in the birth rate (Pitzer et al., 2015).

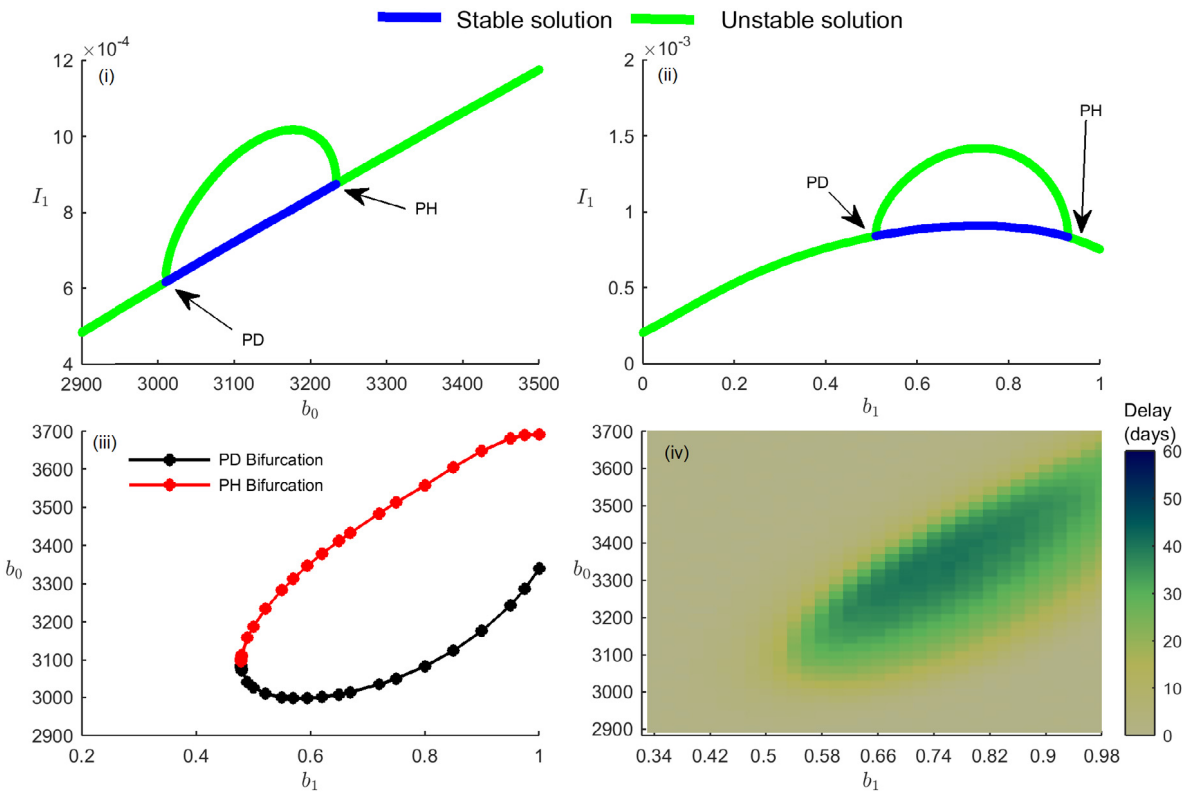

Fig. 5. The bifurcation structure of the model. The first two plots show (i) a bifurcation diagram for the transmission parameter b_0 and (ii) a bifurcation diagram for the amplitude of seasonal forcing b_1. For the b_0 bifurcation, all other parameters are fixed, with $b_1 = 0.522$. For the b_1 bifurcation, all other parameters are fixed, with $b_0 = 3,215$. Both diagrams show similar qualitative dynamics, with a central region of period two dynamics contained within a single period doubling (PD) and single period halving (PH) bifurcation. Plots (iii) and (iv) show, respectively, a two-parameter bifurcation diagram and the timing delay on a colour scale for b_0 and b_1.

The analysis of the immunity parameter alone produced a different picture from that of other parameters, with a one-way transition from regular annual to delayed biennial dynamics as the duration of immunity increases. Although birth rates vary between countries, we expect that the typical duration of immunity would be consistent across different regions, being a clinical feature of RSV. As RSV immunity is not well understood, this analysis adds insight into values that might be reasonable. The two parameter analysis in Fig. 4 suggests that the duration of immunity must be at least 220 days for annual, biennial and delayed biennial dynamics to occur for different birth rates, although we acknowledge that this value may change with different demographic model structures. In a similar model where one 0–24 month age class was fitted to data, the fitted duration of immunity was 160 days (Moore et al., 2014). These results complement the existing literature on the contribution of birth rate and waning immunity to infectious disease dynamics (Dafilis et al., 2014; Morris et al., 2015; Earn et al., 2000).

Model findings show good agreement with data from around the world. Times series data for RSV in Finland shows a markedly delayed biennial pattern (Waris, 1991). The average birth rate for Finland between 1981 and 1990 (the time period of the data) (Statistics Finland, 2015) corresponded with the rates that produced a delayed pattern in our analysis. RSV detections for Switzerland between 1988 and 1999 show a regular biennial pattern (Duppenthaler et al., 2003), and the birth rate of up to 0.0127 during this time period (Swiss Federal Statistical Office, 2015) corresponds with the non-delayed dynamics indicated by our analysis. Another interesting comparison is Colorado and Maryland, U.S.A. Both states have a similar latitude, and hence similar expected seasonal fluctuations. However, biennial dynamics have been observed in Colorado (Zachariah and Shah, 2009) and annual dynamics in Maryland (Spaeder and Fackler, 2012), where the birth rate has historically been lower.

There are two distinct serotypes of RSV: RSV-A and RSV-B. This model does not model the dynamics of the two different RSV strains, due to limited data. Strain diversity has been suggested as a possible driver of biennial dynamics (White et al., 2005), however other studies have shown that the biennial dynamics cannot be explained only by circulation of the two subtypes (Mlinaric-Galinovic et al., 2009; Zlateva et al., 2007; Pitzer et al., 2015).

We established the existence of period doubling and period halving bifurcations when the transmission and seasonality parameters were changed. Stone (1993) showed that such patterns are an alternative to the period-doubling route to chaos that is often present in these types of population models. The existence of period doubling and period halving bifurcations suggests robust dynamics, which is consistent with the known regularity of RSV outbreaks worldwide. Our bifurcation analysis also indicated that the seasonality parameter must exceed a threshold in order for the model to produce biennial dynamics. This corresponds to the known epidemiology of RSV, where biennial patterns are typically observed in temperate regions only, where there is a marked difference in climate between the summer and winter months. In tropical regions, where the climate may be more consistent year-round, winter peaks of RSV are less pronounced.

The sinusoidal forcing function applied in this paper is commonly used in models for seasonal epidemics. A drawback of this approach is that this function is a proxy for any number of seasonal (such as climatic, weather-related or social) variables. There is scope to include a more realistic transmission function that incorporates such factors and this will be considered in future work.

The model simulates RSV infection in two child age groups and does not include adults. RSV infections are mainly observed in young children, however it is not clear whether the low numbers of infections recorded in adults are due to fewer infections in

older age groups, or less severe symptoms that result in fewer detections. In recent work (Hogan et al., 2015), we showed that our model produces qualitatively similar dynamics irrespective of whether or not adults are included, and so only two age groups were modelled for this study. In future work, we will consider a more extensive age-structured model that incorporates both adult and child age structures, as well as an appropriate contact matrix. Furthermore, a drawback of the compartmental approach to age structuring, rather than continuous ageing, is that the time spent in each age class is exponentially distributed (Keeling and Rohani, 2008). However, the compartmental ageing approach is more mathematically tractable than a continuous approach and is widely used in the literature.

Knowledge of the seasonal trends of RSV infections, and a better understanding of what is driving these seasonal patterns in different parts of the world, provides many benefits, including health system preparedness (Chew et al., 1998). The sensitivity and parameter space analysis in our study shows that demography plays an important role in RSV dynamics. While RSV epidemics are remarkably consistent in many regions, a shift in the birth rate could have implications for the timing and magnitude of RSV, which may necessitate a change in prophylaxis administration for high risk children. Prophlyaxis for RSV is costly and as such schedules need to based around times that produce the maximum effectiveness during the peak of the RSV season. An understanding of the drivers of RSV seasonality and predicting peak activity would aid in planning the most cost effective RSV prophylaxis programs. Furthermore, RSV vaccine development is proceeding rapidly. Our analysis provides insight into the most important parameters to consider when developing models for vaccine administration, such as immunity and transmission, and the differences that might be expected in these parameters in different regions. In future work, we will consider how to adapt this model to help plan for the rollout of a RSV vaccine.

Acknowledgements

The authors wish to thank the Linkage and Client Services Teams at the Western Australian Data Linkage Branch, in particular Brett Cawley from the PathWest Laboratory Database. HCM is supported by National Health and Medical Research Council Fellowship APP1034254.

Appendix A. Supplementary material

Supplementary material related to this article can be found online at http://dx.doi.org/10.1016/j.tpb.2016.04.003.

References

Acedo, L., Moraño, J.-A., Díez-Domingo, J., 2010. Cost analysis of a vaccination strategy for respiratory syncytial virus (RSV) in a network model. Math. Comput. Modelling 52 (7–8), 1016–1022. http://dx.doi.org/10.1016/j.mcm.2010.02.041.

Aguiar, M., Ballesteros, S., Kooi, B.W., Stollenwerk, N., 2011. The role of seasonality and import in a minimalistic multi-strain dengue model capturing differences between primary and secondary infections: complex dynamics and its implications for data analysis. J. Theoret. Biol. 289, 181–196. http://dx.doi.org/10.1016/j.jtbi.2011.08.043.

Arenas, A.J., González, G., Jódar, L., 2008. Existence of periodic solutions in a model of respiratory syncytial virus RSV. J. Math. Anal. Appl. 344, 969–980. http://dx.doi.org/10.1016/j.jmaa.2008.03.049.

Australian Bureau of Statistics, 2009. Australia, Table 2 Births, Summary, Statistical Divisions – 2004 to 2009 time series, cat. no. 3301.0. URL www.abs.gov.au.

Avendaño, L.F., Palomino, M.A., Larrañaga, C., 2003. Surveillance for respiratory syncytial virus in infants hospitalized for acute lower respiratory infection in Chile (1989 to 2000). J. Clin. Microbiol. 41 (10), 4879–4882. http://dx.doi.org/10.1128/JCM.41.10.4879.

Brauer, F., Castillo-Chavez, C. (Eds.), 2012. 9.10 The next generation matrix. In: Mathematical Models in Population Biology and Epidemiology, second ed.. Springer, pp. 393–402. http://dx.doi.org/10.1007/978-1-4614-1686-9.

Chan, P.W.K., Chew, F.T., Tan, T.N., Chua, K.B., Hooi, P.S., 2002. Seasonal variation in respiratory syncytial virus chest infection in the tropics. Pediatr. Pulmonol. 34 (1), 47–51. http://dx.doi.org/10.1002/ppul.10095.

Chew, F.T., Doraisingham, S., Ling, A.E., Kumarasinghe, G., Lee, B.W., 1998. Seasonal trends of viral respiratory tract infections in the tropics. Epidemiol. Infect. 121 (1), 121–128.

ClinicalTrials.gov, 2015. Safety, reactogenicity and immunogenicity study of different formulations of GlaxoSmithKline (GSK) Biologicals' investigational RSV vaccine (GSK3003891A), in Healthy Women. URL https://clinicaltrials.gov/ct2/show/NCT02360475.

ClinicalTrials.gov. 2015. A study to evaluate the efficacy of an RSV F vaccine in older adults. URL https://clinicaltrials.gov/ct2/show/NCT02608502.

ClinicalTrials.gov, 2016. A study to determine the safety and efficacy of the RSV F vaccine to protect infants via maternal immunization. URL https://clinicaltrials.gov/ct2/show/NCT02624947.

Dafilis, M.P., Frascoli, F., McVernon, J., Heffernan, J.M., McCaw, J.M., 2014. The dynamical consequences of seasonal forcing, immune boosting and demographic change in a model of disease transmission. J. Theoret. Biol. 361, 124–132. http://dx.doi.org/10.1016/j.jtbi.2014.07.028.

Doedel, E.J., 1981. AUTO: A program for the automatic bifurcation analysis of autonomous systems. Congr. Numer. 30, 265–284.

Duppenthaler, A., Gorgievski-Hrisoho, M., Frey, U., Aebi, C., 2003. Two-year periodicity of respiratory syncytial virus epidemics in Switzerland. Infection 31 (2), 75–80. http://dx.doi.org/10.1007/s15010-002-3124-8.

Earn, D.J.D., Rohani, P., Bolker, B.M., Grenfell, B.T., 2000. A simple model for complex dynamical transitions in epidemics. Science 287, 667–670. http://dx.doi.org/10.1126/science.287.5453.667.

Ermentrout, B., 2001. XPPAUT5.0 – the differential equations tool.

Ermentrout, B., 2002. Simulating, Analyzing, and Animating Dynamical Systems: A Guide to XPPAUT for Researchers and Students. SIAM.

Gilchrist, S., Török, T.J., Gary, H.E., Alexander, J.P., Anderson, L.J., 1994. National surveillance for respiratory syncytial virus, United States, 1985–1990. J. Infect. Dis. 170 (4), 986–990. http://dx.doi.org/10.1093/infdis/170.4.986.

Glezen, W.P., Taber, L.H., Frank, A.L., Kasel, J.A., 1986. Risk of primary infection and reinfection with respiratory syncytial virus. Am. J. Dis. Child. 140 (6), 543–546.

Grassly, N.C., Fraser, C., 2006. Seasonal infectious disease epidemiology. Proc. R. Soc. B Biol. Sci, 273 (1600), 2541–2550. http://dx.doi.org/10.1098/rspb.2006.3604.

Hall, C.B., 1981. Respiratory syncytial virus. In: Feigin, R.D., Cherry, J.D. (Eds.), Textbook of Paediatric Infectious Diseases, Vol. II, first ed.. W. B. Saunders Company, Philadelphia; London, pp. 1247–1267.

Hall, C.B., 2001. Respiratory syncytial virus and parainfluenza virus. N. Engl. J. Med. 344 (25), 1917–1928. http://dx.doi.org/10.1056/NEJM200106213442507.

Hall, C.B., Walsh, E.E., Long, C.E., Schnabel, K.C., 1991. Immunity to and frequency of reinfection with respiratory syncytial virus. J. Infect. Dis. 163 (4), 693–698. http://dx.doi.org/10.1093/infdis/163.4.693.

Hirsh, S., Hindiyeh, M., Kolet, L., Regev, L., Sherbany, H., Yaary, K., Mendelson, E., Mandelboim, M., 2014. Epidemiological changes of respiratory syncytial virus (RSV) infections in Israel. PLoS One 9 (3), e90515. http://dx.doi.org/10.1371/journal.pone.0090515.

Hogan, A.B., Glass, K., Moore, H.C., Anderssen, R.S., 2015. Age structures in mathematical models for infectious diseases, with a case study of respiratory syncytial virus. In: Applications + Practical Conceptualization +Mathematics = Fruitful Innovation – Proceedings of the Forum of Mathematics for Industry. Springer, pp. 105–116.

Hogan, A.B., Mercer, G.N., Glass, K., Moore, H.C., 2013. Modelling the seasonality of respiratory syncytial virus in young children. In: 20th International Congress on Modelling and Simulation, Adelaide, Australia, Vol. 9. pp. 338–344. http://dx.doi.org/10.1371/journal.pone.0100422.

Keeling, M.J., Rohani, P., 2008. Modeling Infectious Diseases in Humans and Animals. Princeton University Press.

Lambert, L., Sagfors, A.M., Openshaw, P.J.M., Culley, F.J., 2014. Immunity to RSV in early-life. Front. Immunol. 5, 1–14. http://dx.doi.org/10.3389/fimmu.2014.00466.

Leecaster, M., Gesteland, P., Greene, T., Walton, N., Gundlapalli, A., Rolfs, R., Byington, C., Samore, M., 2011. Modeling the variations in pediatric respiratory syncytial virus seasonal epidemics. BMC Infect. Dis. 11 (1), 105. http://dx.doi.org/10.1186/1471-2334-11-105.

McLennan-Smith, T.A., Mercer, G.N., 2014. Complex behaviour in a dengue model with a seasonally varying vector population. Math. Biosci. 248, 22–30. http://dx.doi.org/10.1016/j.mbs.2013.11.003.

Meng, J., Stobart, C.C., Hotard, A.L., Moore, M.L., 2014. An overview of respiratory syncytial virus. PLoS Pathog. 10 (4), e1004016. http://dx.doi.org/10.1371/journal.ppat.1004016.

Mlinaric-Galinovic, G., Vojnovic, G., Cepin-Bogovic, J., Bace, A., Bozikov, J., Welliver, R.C., Wahn, U., Cebalo, L., 2009. Does the viral subtype influence the biennial cycle of respiratory syncytial virus? Virol. J. 6, 133. http://dx.doi.org/10.1186/1743-422X-6-133.

Mlinaric-Galinovic, G., Welliver, R.C., Vilibic-Cavlek, T., Ljubin-Sternak, S., Drazenovic, V., Galinovic, I., Tomic, V., 2008. The biennial cycle of respiratory syncytial virus outbreaks in Croatia. Virol. J. 5 (18), http://dx.doi.org/10.1186/1743-422X-5-18.

Moore, H.C., Jacoby, P., Hogan, A.B., Blyth, C.C., Mercer, G.N., 2014. Modelling the seasonal epidemics of respiratory syncytial virus in young children. PLoS One 9 (6), e100422. http://dx.doi.org/10.1371/journal.pone.0100422.

Morris, S., Pitzer, V., Viboud, C., Metcalf, C.J.E., Bjørnstad, O.N., Grenfell, B.T., 2015. Demographic buffering: titrating the effects of birth rate and imperfect immunity on epidemic dynamics. J. Roy. Soc. Interface 12 (104), 20141245. http://dx.doi.org/10.1098/rsif.2014.1245.

Munywoki, P.K., Koech, D.C., Agoti, C.N., Lewa, C., Cane, P.a., Medley, G.F., Nokes, D.J., 2014. The source of respiratory syncytial virus infection in infants: a household cohort study in rural Kenya. J. Infect. Dis. 209, 1685–1692. http://dx.doi.org/10.1093/infdis/jit828.

PATH, 2015. RSV Vaccine Snapshot. URL http://sites.path.org/vaccinedevelopment/files/2015/12/RSV-snapshot-Dec2015v5.pdf.

Paynter, S., Yakob, L., Simões, E.A.F., Lucero, M.G., Tallo, V., Nohynek, H., Ware, R.S., Weinstein, P., Williams, G., Sly, P.D., 2014. Using mathematical transmission modelling to investigate drivers of respiratory syncytial virus seasonality in children in the Philippines. PLoS One 9 (2), e90094. http://dx.doi.org/10.1371/journal.pone.0090094.

Pitzer, V.E., Viboud, C., Alonso, W.J., Wilcox, T., Metcalf, C.J., Steiner, C.A., Haynes, A.K., Grenfell, B.T., 2015. Environmental drivers of the spatiotemporal dynamics of respiratory syncytial virus in the United States. PLoS Pathog. 11 (1), e1004591. http://dx.doi.org/10.1371/journal.ppat.1004591.

Reese, P.E., Marchette, N.J., 1991. Respiratory syncytial virus infection and prevalence of subgroups A and B in Hawaii. J. Clin. Microbiol. 29 (11), 2614–2615.

Rohani, P., Green, C.J., Mantilla-Beniers, N.B., Grenfell, B.T., 2003. Ecological interference between fatal diseases. Nature 422 (6934), 885–888. http://dx.doi.org/10.1038/nature01542.

Sorce, L.R., 2009. Respiratory syncytial virus: from primary care to critical care. J. Pediatr. Health Care 23 (2), 101–108. http://dx.doi.org/10.1016/j.pedhc.2007.11.004.

Spaeder, M.C., Fackler, J.C., 2012. A multi-tiered time-series modelling approach to forecasting respiratory syncytial virus incidence at the local level. Epidemiol. Infect. 140 (4), 602–607. http://dx.doi.org/10.1017/S0950268811001026.

Statistics Finland, Accessed 28 July 2015. Official Statistics of Finland (OSF): Births [e-publication], ISSN=1798-2413. URL www.stat.fi/til/synt/tau_en.html.

Stone, L., 1993. Period-doubling reversals and chaos in simple ecological models. Nature 365 (6447), 617. http://dx.doi.org/10.1038/365617a0.

Swiss Federal Statistical Office, Accessed 28 July 2015. Population. URL www.bfs.admin.ch/bfs/portal/en/index/themen/01.html.

Terletskaia-Ladwig, E., Enders, G., Schalasta, G., Enders, M., 2005. Defining the timing of respiratory syncytial virus (RSV) outbreaks: an epidemiological study. BMC Infect. Dis. 5 (20), http://dx.doi.org/10.1186/1471-2334-5-20.

The IMpact-RSV Study Group 1998. Palivizumab, a humanized respiratory syncytial virus monoclonal antibody, reduces hospitalization from respiratory syncytial virus infection in high-risk infants. Pediatrics 102 (3), 531–537. http://dx.doi.org/10.1542/peds.102.3.531.

Walton, N.A., Poynton, M.R., Gesteland, P.H., Maloney, C., Staes, C., Facelli, J.C., 2010. Predicting the start week of respiratory syncytial virus outbreaks using real time weather variables. BMC Med. Inform. Decis. Mak. 10 (1), 68. http://dx.doi.org/10.1186/1472-6947-10-68.

Waris, M., 1991. Pattern of respiratory syncytial virus epidemics in Finland: two-year cycles with alternating prevalence of groups A and B. J. Infect. Dis. 163 (3), 464–469. http://dx.doi.org/10.1093/infdis/163.3.464.

Weber, M.W., Mulholland, E.K., Greenwood, B.M., 1998. Respiratory syncytial virus infection in tropical and developing countries. Trop. Med. Int. Health 3 (4), 268–280. http://dx.doi.org/10.1046/j.1365-3156.1998.00213.x.

Weber, A., Weber, M., Milligan, P., 2001. Modeling epidemics caused by respiratory syncytial virus (RSV). Math. Biosci. 172 (2), 95–113. http://dx.doi.org/10.1016/S0025-5564(01)00066-9.

White, L.J., Waris, M., Cane, P.A., Nokes, D.J., Medley, G.F., 2005. The transmission dynamics of groups A and B human respiratory syncytial virus (hRSV) in England & Wales and Finland: seasonality and cross-protection. Epidemiol. Infect. 133 (2), 279–289.

Zachariah, P., Shah, S., 2009. Predictors of the duration of the respiratory syncytial virus season. Pediatr. Infect. Dis. J. 28, 772–776.

Zlateva, K.T., Vijgen, L., Dekeersmaeker, N., Naranjo, C., Van Ranst, M., 2007. Subgroup prevalence and genotype circulation patterns of human respiratory syncytial virus in Belgium during ten successive epidemic seasons. J. Clin. Microbiol. 45 (9), 3022–3030. http://dx.doi.org/10.1128/JCM.00339-07.

Supplementary material: Exploring the dynamics of respiratory syncytial virus (RSV) transmission in children

Alexandra B Hogan[a], Kathryn Glass[a], Hannah C Moore[b], Robert S Anderssen[c]

[a] *National Centre for Epidemiology and Population Health, Building 62, Corner Mills and Eggleston Roads, The Australian National University, Canberra ACT 2601 Australia, alexandra.hogan@anu.edu.au (corresponding author)*
[b] *Wesfarmers Centre of Vaccines and Infectious Diseases, Telethon Kids Institute, The University of Western Australia, Western Australia*
[c] *The Commonwealth Scientific and Industrial Research Organisation, Australia*

Keywords: respiratory syncytial virus, infectious disease, mathematical modelling, bifurcation analysis, seasonality

S1. Calculation of R_0

The two age class transmission model is

$$\begin{aligned}
\frac{dS_A}{dt} &= \mu - \beta_A S_A(I_A + I_B) + \nu R_A - \eta S_A \\
\frac{dE_A}{dt} &= \beta_A S_A(I_A + I_B) - \delta E_A - \eta E_A \\
\frac{dI_A}{dt} &= \delta E_A - \gamma I_A - \eta I_A \\
\frac{dR_A}{dt} &= \gamma I_A - \nu R_A - \eta R_A \\
\frac{dS_B}{dt} &= \eta S_A - \beta_B S_B(I_A + I_B) + \nu R_B - \eta S_B \\
\frac{dE_B}{dt} &= \eta E_A + \beta_B S_B(I_A + I_B) - \delta E_B - \eta E_B \\
\frac{dI_B}{dt} &= \eta I_A + \delta E_B - \gamma I_B - \eta I_B \\
\frac{dR_B}{dt} &= \eta R_A + \gamma I_B - \nu R_B - \eta R_B
\end{aligned} \tag{1}$$

We used the Next Generation Matrix method to calculate the basic reproduction number $\mathcal{R}_0$ [1]. The disease free steady state is $x_0 = (\frac{\mu}{\eta}, 0, 0, 0, \frac{\mu}{\eta}, 0, 0, 0)$. The disease states in the model are E_A, I_A, E_B, and I_B. Following the notation of [1], we have:

$$\mathcal{F} = \begin{pmatrix} \beta_A S_A (I_A + I_B) \\ 0 \\ \beta_B S_B (I_A + I_B) \\ 0 \end{pmatrix}$$

$$\mathcal{V} = \begin{pmatrix} \delta E_A + \eta E_A \\ -\delta E_A + \gamma I_A + \eta I_A \\ -\eta E_A + \delta E_B + \eta E_B \\ -\eta I_A - \delta E_B + \gamma I_B + \eta I_B \end{pmatrix}$$

The Jacobian of $\mathcal{F}$ is

$$F = \begin{pmatrix} 0 & \beta_A S_A & 0 & \beta_A S_A \\ 0 & 0 & 0 & 0 \\ 0 & \beta_B S_B & 0 & \beta_B S_B \\ 0 & 0 & 0 & 0 \end{pmatrix}$$

and evaluated at the steady state is

$$F(x_0) = \begin{pmatrix} 0 & \frac{\beta_A \mu}{\eta} & 0 & \frac{\beta_A \mu}{\eta} \\ 0 & 0 & 0 & 0 \\ 0 & \frac{\beta_B \mu}{\eta} & 0 & \frac{\beta_B \mu}{\eta} \\ 0 & 0 & 0 & 0 \end{pmatrix}$$

The Jacobian of $\mathcal{V}$ is

$$V = \begin{pmatrix} \delta + \eta & 0 & 0 & 0 \\ -\delta & \eta + \gamma & 0 & 0 \\ -\eta & 0 & \delta + \eta & 0 \\ 0 & -\eta & -\delta & \eta + \gamma \end{pmatrix}$$

The inverse of V is

$$V^{-1} = \begin{pmatrix} \frac{1}{\eta+\delta} & 0 & 0 & 0 \\ \frac{\delta}{(\eta+\delta)(\eta+\gamma)} & \frac{1}{\eta+\gamma} & 0 & 0 \\ \frac{\eta}{(\eta+\delta)^2} & 0 & \frac{1}{\eta+\delta} & 0 \\ \frac{2\eta^2\delta + \eta\delta^2 + \gamma\eta\delta}{(\eta+\delta)^2(\eta+\gamma)^2} & \frac{\eta}{(\eta+\gamma)^2} & \frac{\delta}{(\eta+\delta)(\eta+\gamma)} & \frac{1}{\eta+\gamma} \end{pmatrix}$$

The largest eigenvalue of FV^{-1} is

$$R_0 = \frac{\delta\mu}{\eta(\eta+\delta)(\eta+\gamma)}[\beta_A + \beta_B + \frac{\beta_A(2\eta^2+\eta\delta+\eta\gamma)}{(\eta+\delta)(\eta+\gamma)}]$$

Evaluated at $\beta_A = 3215$, $\beta_B = 732$, $\eta = 1$, $\delta = 91.48$, $\gamma = 40.11$ and $\mu = 0.0135$, and rounded to two decimal places, $R_0 = 1.32$.

Given that $\eta = 1 \ll \delta, \gamma$, we can also approximate $\mathcal{R}_0$ as:
$\mathcal{R}_0 \approx \frac{\mu}{\gamma}[\beta_A + \beta_B] = 1.33$

S2. Supplementary parameter space exploration

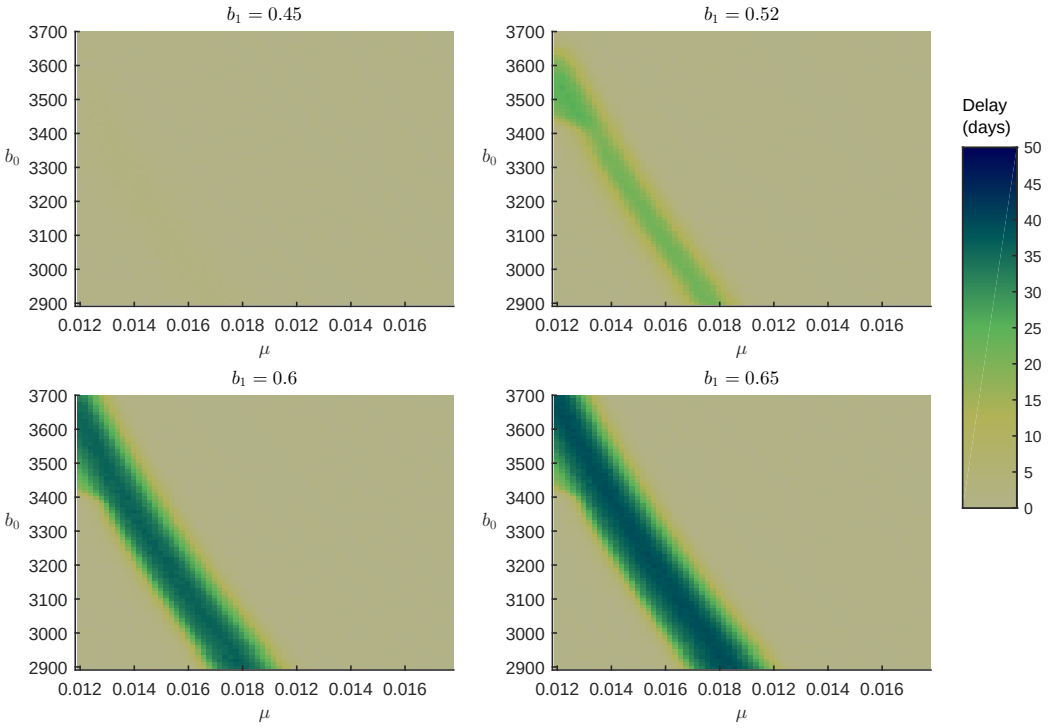

Supplementary Material, Figure S1: Variations in the timing of seasonal peaks as a function of the birth rate μ and the transmission parameter b_0, for different values of the seasonal forcing parameter b_1. The plots show a band of values that produces delayed biennial dynamics, with a longer delay for higher values of b_1. Parameters not stated have the values listed in Table 1 in the main manuscript.

[1] 9.10 The Next Generation Matrix, in: F. Brauer, C. Castillo-Chavez (Eds.), Mathematical Models in Population Biology and Epidemiology, 2nd Edition, Springer, 2012, pp. 393–402. doi:10.1007/978-1-4614-1686-9.

5.3 Additional material

This section describes the technical details of the bifurcation analysis presented in the two papers in this chapter. This part of the analysis was performed using the software XPPAUT and the built in interface to the numerical continuation package AUTO (Doedel, 1981). The analysis was guided by the explanatory guide to XPPAUT by Ermentrout (2002), the Supplementary Material 'Bifurcation of the seasonally forced SIR model using XPPAUT' to Krylova and Earn (2013), and Timothy McLennan-Smith's thesis (McLennan-Smith, 2012). Further information about using XPPAUT and AUTO, including to analyse seasonally forced systems, is also available on the XPPAUT website (Ermentrout, 2016).

XPPAUT is a numerical tool for analysing dynamical systems (Ermentrout, 2002). Importantly, AUTO allows us to track periodic solutions to a set of differential equations as a particular parameter is changed. The stability of each solution is also computed automatically (Ermentrout, 2002). The set of ordinary differential equations analysed in XPPAUT is that presented in the second paper in this chapter, in Equation (1).

5.3.1 XPPAUT input file and process

To solve and analyse a system of differential equations in XPPAUT, the equations must be specified in a `.ode` file, along with initial conditions and parameter values. The input file was created using Microsoft Notepad. An example of the code is provided below. As described in the second paper in this chapter, XPPAUT requires the differential equation system to be autonomous, therefore the periodic forcing terms β_A and β_B were transformed using the Hopf oscillator. A brief outline of the steps required to run the simulation, and identify the bifurcation points, is as follows:

1. Load the `.ode` file into XPPAUT.

2. Integrate the system over the chosen time period, then plot the solution to check it has converged to a stable periodic solution. Here, we integrated the system over a time period of 400 years.

3. Change the total integration time to 1, and integrate the system again, using the final solution from the previous integration as the set of initial conditions. To execute this step, open the 'Initial conditions' menu and choose 'Last'.

4. Open the 'File' menu and select 'AUTO'.
5. Open the 'Parameters' menu and ensure that the first parameter listed is the desired bifurcation parameter.
6. Open the 'Axes' menu and select the variable for the y-axis (in this case, I_A or I_1).
7. Open the 'Run' menu and select 'Periodic'. This will compute the period one solutions for the system, and plot the stable branch of solutions in bright green. The unstable branch of solutions will be plotted in blue.
8. When the computation is complete, select 'Grab' and press Tab until the point of interest is selected (in this case, a period doubling point). Press Enter. Select 'Run' and 'Period doubling' to compute the branch of period two solutions.
9. To continue solutions along a branch in the opposite direction, open the 'Numerics' menu and change the sign of Ds.
10. Open the 'File' menu and select 'Write points' to write the output to a `.dat` file for plotting in `MATLAB`.

An example of the code used for solving the system of ordinary differential equations, and performing a bifurcation analysis with bifurcation parameter b_0, is shown below.

```
## ODES
S1'=mu-b0*(1+b1*u)*S1*(I1+I2)+nu*R1-eta*S1
E1'=b0*(1+b1*u)*S1*(I1+I2)-delta*E1-eta*E1
I1'=delta*E1-gamma*I1-eta*I1
R1'=gamma*I1-nu*R1-eta*R1
S2'=eta*S1-alpha*b0*(1+b1*u)*S2*(I1+I2)-eta*S2+nu*R2
E2'=eta*E1+alpha*b0*(1+b1*u)*S2*(I1+I2)-E2*(delta+eta)
I2'=eta*I1+delta*E2-I2*(eta+gamma)
R2'=eta*R1+gamma*I2-R2*(eta+nu)

## SEASONAL FORCING FUNCTION
u'=u*(1-u^2-v^2)-w*v
v'=v*(1-u^2-v^2)+w*u

## INITIAL CONDITIONS
init u=0.9, v=0.1, S1=0.0121, E1=0.0001, I1=0.0001, R1=0.0012,
init S2=0.0122, E2=0, I2=0.001, R2=0.0013

## PARAMETERS
par b0=2900, b1=0.5216, mu=0.0135, gamma=40.1099, delta=91.4787
par eta=1, , nu=1.5851, w=6.28318530718, alpha=0.2276
```

```
## PLOT OPTIONS
@ yp=I1
@ xlo=0, xhi=30, ylo=0, yhi=1

## NUMERICS AND INTEGRATION TIME
@ total=400
@ trans=399
@ dt=0.001

## AUTO OPTIONS
@ ds=0.0001
@ dsmax=.05
@ parmin=2800,parmax=3500
@ Nmax=20000, Npr=2000, epsl=1e-6, epsu=1e-6, spss=1e-4

## AUTO PLOTTING OPTIONS
@ autoxmax=3500,autoxmin=2800, autoymin=0, autoymax=0.01

## STORAGE AND DATA SAVING
@ maxstor=2000000
@ output=SEIRoutputdata_2ages_b0test.dat

done
```

6

Seasonality in the different climatic zones of Western Australia

6.1 Introduction

This chapter includes two publications. The first paper is published in *The ANZIAM Journal*, and introduces the application of a time series analysis method called complex demodulation to seasonal infectious disease data. This paper outlines the mathematics of complex demodulation, and shows the utility of using synthetic data to inform the interpretation of complex demodulation applied to real data. Complex demodulation is also illustrated in the context of national influenza notifications.

The second paper is published in *Epidemics*, and investigates the seasonal patterns of RSV and bronchiolitis in the different climatic regions of Western Australia, to show the difference in seasonality between the temperate and tropical regions. I apply complex demodulation to RSV and bronchiolitis data for the Metropolitan region to investigate how the size of the seasonal peak and epidemic timing change over time, and compare these outputs for RSV and bronchiolitis.

6.2 Papers

Hogan, A. B., Glass, K., and Anderssen, R. S. (2017). Complex demodulation: a novel time series analysis method for seasonal infectious diseases. *The ANZIAM Journal* 1–10.

Hogan, A. B., Anderssen, R. S., Davis, S., Moore, H. C., Lim, F. J., Fathima, P., and Glass, K. (2016). Time series analysis of RSV and bronchiolitis seasonality in temperate and tropical Western Australia. *Epidemics*, 16:49–55.

ANZIAM J. (First published online 2017), page 1 of 10*
doi:10.1017/S1446181116000377
*Provisional—final page numbers to be inserted when paper edition is published

COMPLEX DEMODULATION: A NOVEL TIME SERIES METHOD FOR ANALYSING SEASONAL INFECTIOUS DISEASES

A. B. HOGAN[✉1], K. GLASS[1] and R. S. ANDERSSEN[2]

(Received 18 May, 2016; accepted 26 October, 2016)

Abstract

Understanding how seasonal patterns change from year to year is important for the management of infectious disease epidemics. Here, we present a mathematical formalization of the application of complex demodulation, which has previously only been applied in an exploratory manner in the context of infectious diseases. This method extracts the changing amplitude and phase from seasonal data, allowing comparisons between the size and timing of yearly epidemics. We first validate the method using synthetic data that displays the key features of epidemic data. In particular, we analyse both annual and biennial synthetic data, and explore the effect of delayed epidemics on the extracted amplitude and phase. We then demonstrate the usefulness of complex demodulation using national notification data for influenza in Australia. This method clearly highlights the higher number of notifications and the early peak of the influenza pandemic in 2009. We also identify that epidemics that peaked later than usual generally followed larger epidemics and involved fewer overall notifications. Our analysis establishes a role for complex demodulation in the study of seasonal epidemiological events.

2010 *Mathematics subject classification*: primary 65T99; secondary 62-07.

Keywords and phrases: seasonality, periodicity, infectious disease, epidemic, influenza, time series analysis.

1. Introduction

Many infectious diseases display annual seasonal patterns, and it is of interest to quantify how these seasonal patterns vary over time. Here, we use complex demodulation to recover the changing amplitude and phase from seasonal infectious disease data, relative to the underlying dominant frequency. Understanding changes in amplitude and phase helps to characterize and describe differences in seasonal patterns.

[1]Research School of Population Health, The Australian National University, Canberra, Australia; e-mail: alexandra.hogan@anu.edu.au, kathryn.glass@anu.edu.au.
[2]CSIRO Data61, Canberra, Australia; e-mail: bob.anderssen@data61.csiro.au.

Motivation for this approach is the success with which complex demodulation has led to an improved understanding of seasonal processes in a variety of health and other situations [9, 12, 14, 17, 20]. In the analysis of the seasonality of suicide time series data [14], applying complex demodulation avoided arbitrary splitting of the data, and led to the conclusion that the strength of suicide seasonality was associated with the absolute number of suicides. Kingan et al. [11] applied complex demodulation to geomagnetic data from a number of observatories in order to improve the analysis of geomagnetic storms. Through the use of complex demodulation, it was established for the first time that the phase of the daily solar geomagnetic variation changed during a geomagnetic storm.

In an earlier work, we explored the use of complex demodulation to analyse time series data for respiratory syncytial virus (RSV) and bronchiolitis in Western Australia [10], and found a very high correlation between the timing of RSV and bronchiolitis epidemics, but weaker correlation between the magnitude of these epidemics. The aim of the present research is to formalize the application of complex demodulation to seasonal epidemic data and to show more broadly how complex demodulation can be used to enhance current understanding of the dynamics of infectious diseases. We first apply the method to synthetic data sets that display key features of epidemic time series data, and use this to understand how the underlying structure in the time series data can be depicted by the amplitude and phase of the demodulated data. We then apply the method to national influenza notification data for Australia, in order to investigate changes in epidemic size and timing.

2. Complex demodulation methodology

The purpose of complex demodulation is to extract and compare information from cyclical time series data. Specifically, it is used to extract the slowly varying amplitude and phase within the time series, relative to the period of the cyclical event.

2.1. Mathematical details In this section, we introduce the mathematical details of complex demodulation, inspired by the excellent introduction to complex demodulation within the framework of Fourier analysis given by Bloomfield [2]. Some of these mathematical details were previously presented in summary form in the supplementary material of Hogan et al. [10].

Let x_t represent a time series of data points with dominant frequency f_0 that may be identified using Fourier analysis. Given that the time series exhibits this strong frequency, it follows that it has a periodic-like signal $x(t)$ with added noise z_t, which can be modelled as

$$x_t = x(t) + z_t, \quad x(t) = R_t \cos(2\pi(f_0 t + \phi_t)), \tag{2.1}$$

where R_t is the instantaneous amplitude, and ϕ_t is the instantaneous phase.

2.1.1 *Model justification.* The motivation for choosing the model in this form, as explained by Hao et al. [8] and Thomas [18], relates to the analytic modelling of

signals in communication theory. If the signal $x(t)$ is a narrow-band signal about a central frequency f_0, which is larger than the bandwidth of its spectrum $X(f)$, then the inverse Fourier transform $x_+(t)$ of the positive part $X_+(f)$ of $X(f)$ becomes the analytic signal associated with $x(t)$. If $x_+(t)$ is written in polar coordinates as $A(t)\exp(ig(t))$, it follows that the corresponding x_t takes the form

$$x_t = A(t)\cos(g(t)), \tag{2.2}$$

where $A(t)$ and $g(t)$ are, respectively, the envelope and phase function of $x(t)$. To generate expressions for $A(t)$ and $g(t)$, we use the above assumption that $x(t)$ is a narrow-band signal, and work with the spectrum

$$W(f) = X_+(f + f_0),$$

which has shifted $X_+(f)$ by the frequency f_0.

On writing the inverse Fourier transform of $W(t)$ in polar coordinates as $|w(t)|\exp(ih(t))$, it algebraically follows that the magnitude $|w(t)|$ corresponds to the envelope function $A(t)$, while the phase function $g(t)$ takes the form

$$g(t) = f_0 t + h(t). \tag{2.3}$$

Combining equations (2.2) and (2.3), and including a noise component z_t, thereby justifies the structure of equation (2.1).

2.1.2 *Implementation of complex demodulation.* Equation (2.1) can be rewritten in terms of exponential functions, giving

$$x_t = \tfrac{1}{2}R_t(e^{2\pi i(f_0 t+\phi_t)} + e^{-2\pi i(f_0 t+\phi_t)}) + z_t. \tag{2.4}$$

There are three key steps that comprise the complex demodulation procedure. The first step is to demodulate the time series, the second is to apply a filter, and the third is to extract the amplitude and phase. Therefore, the time series is first demodulated by multiplying equation (2.4) by $e^{-2\pi i f_0 t}$, where $e^{-2\pi i f_0 t}$ is referred to as the *demodulator*. After rearranging, the new expression $y_t = x_t e^{-2\pi i f_0 t}$ takes the form

$$y_t = \tfrac{1}{2}R_t e^{2\pi i\phi_t} + \tfrac{1}{2}R_t e^{-2\pi i(2f_0 t+\phi_t)} + z_t e^{-2\pi i f_0 t}. \tag{2.5}$$

The objective is then to retain only the first term in equation (2.5), so as to allow the extraction of R_t and ϕ_t. Applying a filter of length at least $1/f_0$ will achieve this by removing the second and third terms. For the present situation, a simple moving average filter with window of length $1/f_0$ is selected, but other possible filters were discussed by Bloomfield [2]. As the second term in the expression oscillates at frequency $-2f_0$, it will be eliminated. We assume that the final term, the noise component, is not smooth, and therefore will also be eliminated by an appropriate filter [2]. The application of a filter meeting the above requirements may be expressed as

$$Y_t = \Gamma[y_t] = \tfrac{1}{2}R_t e^{2\pi i\phi_t},$$

where Y_t is the demodulated, filtered data. The final step is to extract the instantaneous amplitude R_t and the instantaneous phase ϕ_t from Y_t. Then the amplitude and phase are, respectively,

$$R_t = 2|Y_t|,$$
$$\phi_t = \mathrm{Im}\,\frac{\log(Y_t)}{2\pi}.$$

The `angle` and `unwrap` functions in `MATLAB` may be used to compute the phase.

2.2. Application to synthetic data The motivation for using synthetic data is that the changing pattern in the time series is known explicitly, and can thereby be used to identify how this pattern is reflected in the structure of the complex demodulation amplitude and phase. Several synthetic data sets were created using the function

$$x(t) = \{1 + a\cos(2\theta t)\}\{\cos^2(2\theta t + b\cos(2\theta t))\}, \tag{2.6}$$

which, with various choices for a, b and θ, displays key features that are often observed in epidemic time series data. The parameter a can be varied to allow either for peaks of the same size in each period ($a = 0$), or for alternating peak sizes ($0 < a \leq 1$). The parameter b can be varied to allow for either equally spaced peaks ($b = 0$), or a pattern where the peak is delayed every second period ($0 < b \leq 1$). In the subsequent analysis, the terms "annual" and "biennial" are used, respectively, to describe peaks of the same and alternating sizes. The term "regular" is used to describe data where peaks occur at the same point in each period, and the term "delayed" is used to describe data where the peak is delayed every second period.

The results of the complex demodulation process applied to the synthetic data sets are shown in Figures 1 and 2. For each of these data sets, the period is $1/f_0 = 0.25$. In Figures 1 and 2, the data sets are plotted in the top panels (together with a moving average of the data with a window length of 0.25), the amplitudes are shown in the third panel and the phases are depicted in the fourth panel.

Figure 1 shows annual (solid red line) and biennial (dashed black line) synthetic data sets, where the spacing between peaks is the same for each period. For the annual data set, as expected, the filtered amplitude and phase are both uniform. For the biennial data set, the amplitude captures the alternating peak size, whereas, for the phase, small deviations are present. These deviations arise due to the presence of other frequencies in the data (in this case, a frequency of $f_0 = 2$, giving rise to the biennial pattern) that are not removed by the selected annual moving average filter (panel (ii)). If a demodulator with a frequency of $f_0 = 2$ and a corresponding filter are applied to the biennial synthetic data set, the filtered amplitude and phase are instead uniform. We also ran the complex demodulation routine with additional synthetic data, where the relative differences in the heights of the small and large peaks are increased, and found that the deviations are more pronounced (data not shown).

Figure 2 shows two biennial synthetic data sets: panel (i) has a delay before every second (smaller) peak, while panel (ii) has equally spaced peaks. The filtered

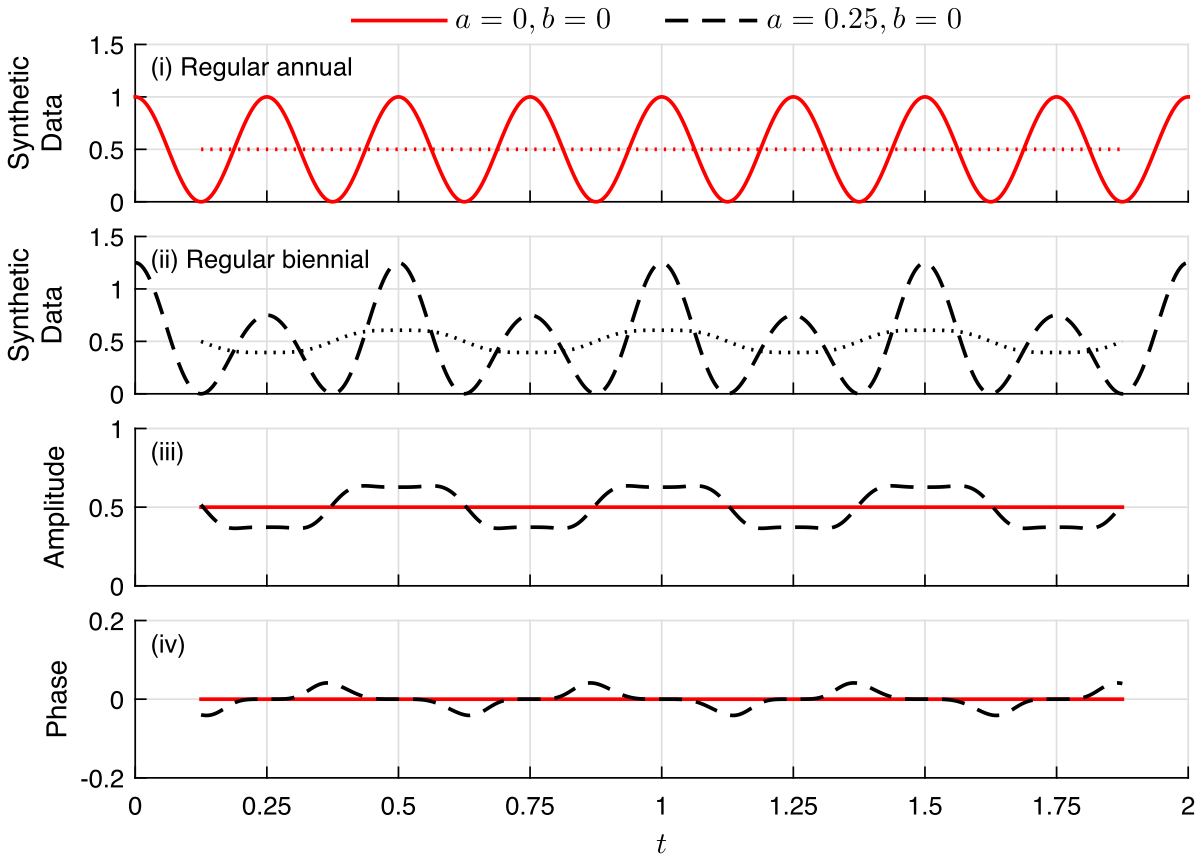

FIGURE 1. Complex demodulation applied to two synthetic data sets: a regular annual pattern (solid red line) and a regular biennial pattern (dashed black line), with $\theta = 2\pi$. Panels (i) and (ii) show the annual and biennial simulated data, along with a centred moving average (the dotted line in each panel). Panels (iii) and (iv) show the demodulated and filtered amplitude and phase, respectively. The synthetic data sets were created using equation (2.6) with parameters listed in the legend above (colour available online).

amplitudes (panel (iii)) are closely aligned, and the phase (panel (iv)) captures the steady epidemic timing for the regular biennial data set (dashed black line) and the alternating between-peak intervals for the delayed biennial data set (solid red line).

Comparing the features of the regular biennial pattern and the corresponding features of the delayed biennial pattern in Figure 2, we can identify how the changing structure of $x(t)$ is reflected in the amplitude and phase. First, the centred moving average in panel (i) rises and falls more rapidly than its counterpart in panel (ii). It rises (falls) because the next peak is arriving earlier (later) than that of the demodulator. Secondly, in panel (iv), the phase for the delayed biennial data shows a stronger difference when compared to that for its regular biennial counterpart, relative to the demodulator. This is expected, as it is the phase that captures the nature of the alternating peak spacing pattern. In particular, it increases sharply in a short inter-peak interval, and drops gradually in a long inter-peak interval. These relationships are of interest, because they can be used to show how patterns in the amplitude and phase can be used as indicators of structure in real data, such as when timing differences between peaks are not immediately apparent. They also illustrate how a centred

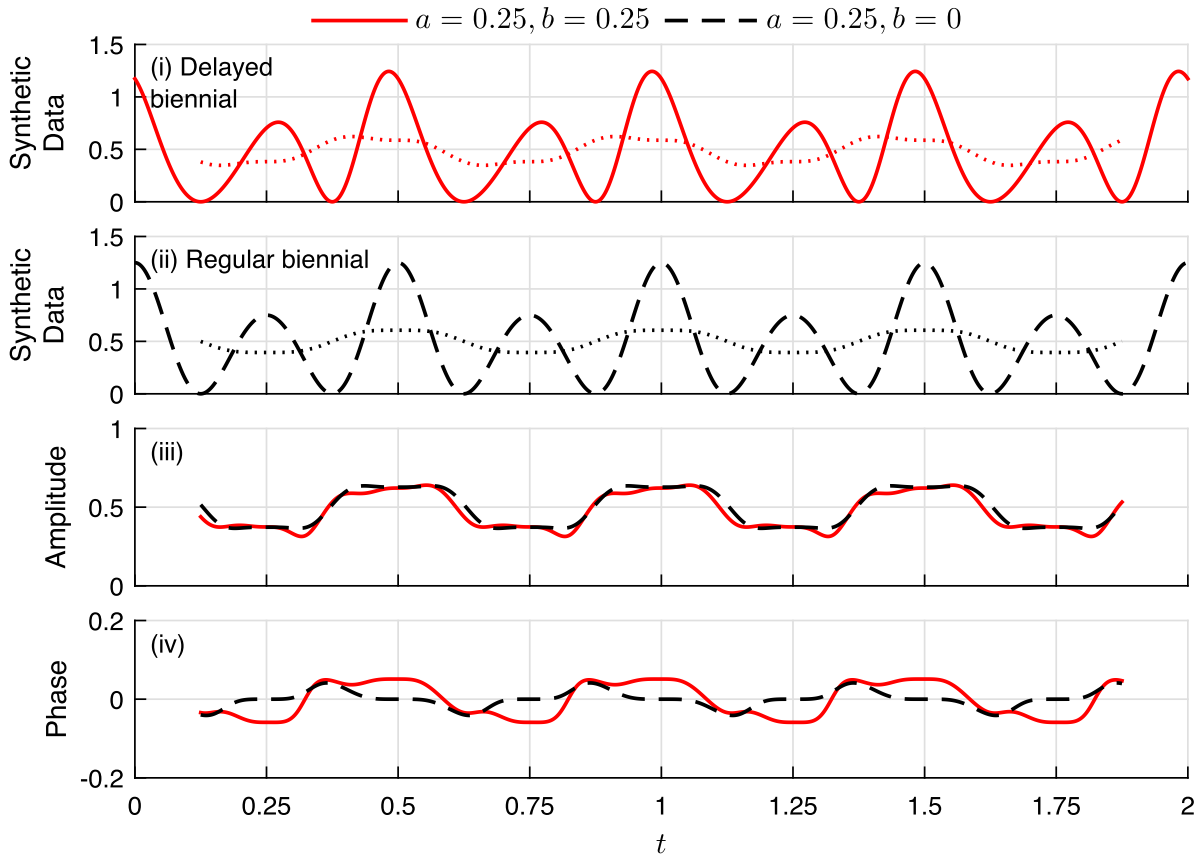

FIGURE 2. Complex demodulation applied to two synthetic data sets: a regular biennial pattern (dashed black line) and a delayed biennial pattern (solid red line), with $\theta = 2\pi$. Panels (i) and (ii) show the data, with a centred moving average (the dotted line in each panel). Panels (iii) and (iv) show the demodulated and filtered amplitude and phase, respectively. The synthetic data sets were created using equation (2.6) with parameters listed in the legend above (colour available online).

moving average contains information about both the timing and size of the peaks, whereas the amplitude and phase depict these components separately.

2.3. Application to influenza data Influenza presents a substantial global health burden, with yearly epidemics in the winter months in many temperate countries, and less defined seasonality in tropical regions [19]. There are several theories concerning the drivers of influenza seasonality, including viral evolution, host immune response and social and environmental factors, but none of these factors conclusively explain influenza dynamics. Influenza seasonality seems likely to be caused by interaction of many different factors [13]. While identifying the drivers of influenza seasonality has proved challenging, complex demodulation allows us to visualize changes in this seasonality over time.

In this paper, we examine influenza data as a representative example of seasonal infectious disease time series data, to investigate how the characteristics of influenza epidemics have shifted over the last ten years in Australia. Complex demodulation highlights these differences quantitatively, allowing identification of features that are not easily identified from visual inspection of the data. For this analysis, we

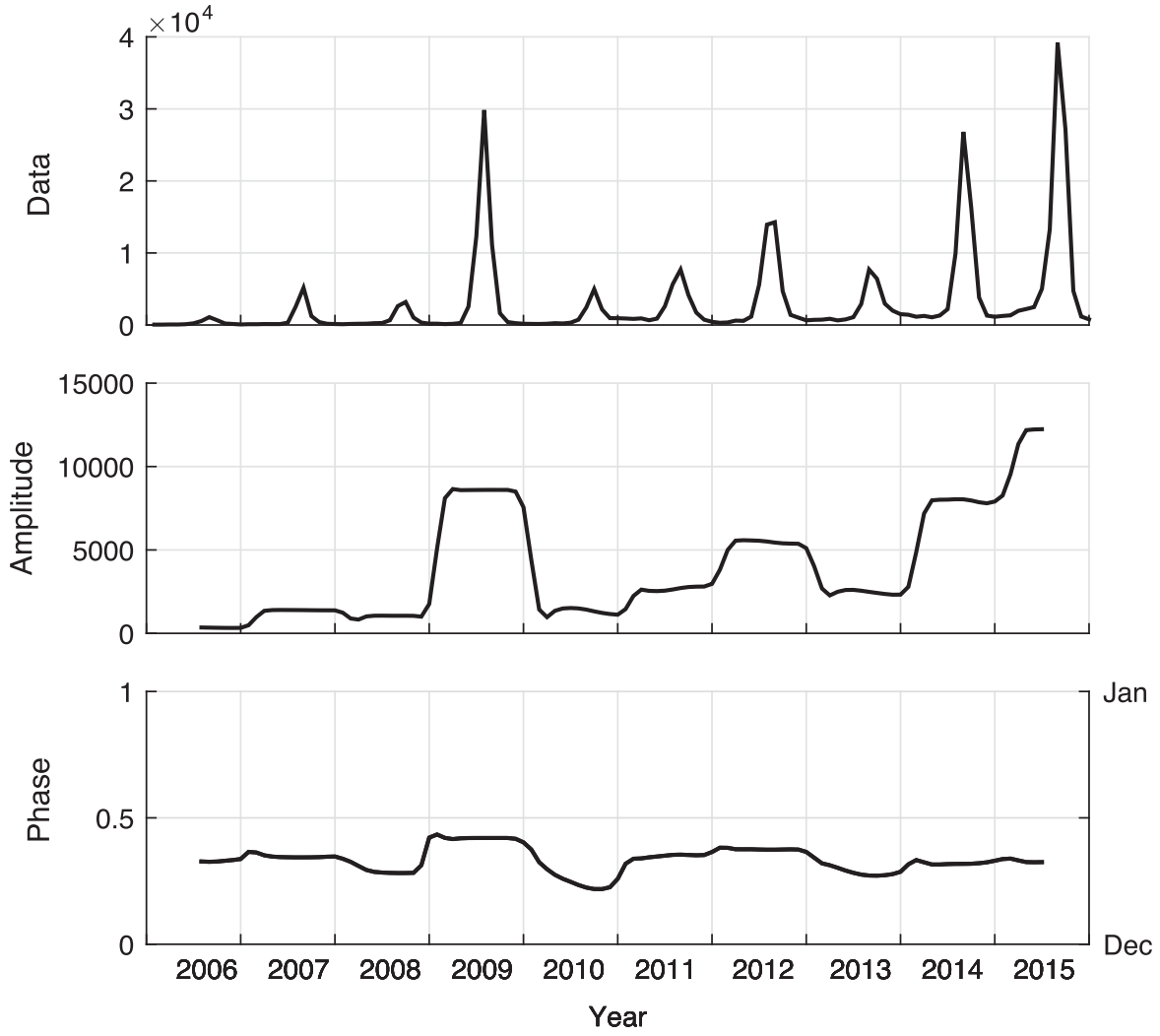

FIGURE 3. National Australian influenza notification data, and the filtered complex demodulation amplitude and phase. The data were obtained from the Australian Government Department of Health [1].

used publicly available data for laboratory-confirmed influenza notifications from the Australian National Notifiable Diseases Surveillance System (NNDSS) [1]. We extracted the number of monthly notifications from 2006 to 2015 inclusive.

The complex demodulation results for the national influenza data are shown in Figure 3. The upper panel presents the monthly data for January 2006 to December 2015. The middle panel depicts the filtered amplitude of the demodulated data and the lower panel represents the filtered phase. The phase is presented in the interval [0, 1], which corresponds to a monthly range of December to January.

The results show several interesting features. In particular, the method extracts both the size and timing components of the pandemic in 2009. While the magnitude of the pandemic is clearly apparent in the time series data and reflected in the amplitude plot, the phase shows that this outbreak took place earlier than in previous years, with the initial onset occurring quite rapidly. The amplitude panel also clearly reflects the trend of increasing numbers of notifications over time. Finally, the phase identifies where

influenza epidemics occurred later in the year, such as in 2008, 2010 and 2013, and the corresponding amplitude indicates that these years typically involved fewer cases than the previous year.

3. Discussion

The analysis presented in this paper provides motivation for the use of complex demodulation in the analysis of periodic infectious disease data. Complex demodulation extracts key seasonal components of interest, the amplitude and phase, in order to quantify and visualize patterns in the data. It can also be used as a tool to compare data for different regions or different diseases.

Complex demodulation complements other time series analysis methods, such as Fourier analysis and wavelet analysis. Fourier analysis is an important method for detecting the different underlying frequencies in a data set, and is used for determining the demodulator in the complex demodulation method [2]. Wavelet analysis has been successfully applied in a variety of contexts, including data for measles epidemics in England [7] and dengue hemorrhagic fever in Thailand [3]. Wavelet analysis is appropriate when the data are non-stationary, that is, when the dominant frequency changes over time, and when the location of some isolated event needs to be identified [16]. In cases where the data are stationary, such as for the present influenza data, complex demodulation offers distinct advantages in that it is suitable for extracting and visualizing variations in the amplitude and phase with respect to those of the underlying dominant frequency over time.

In this paper, we examined synthetic data with annual and biennial patterns (Figures 1 and 2) that are typical of many infectious diseases. For example, while influenza typically displays an annual pattern, diseases such as pre-vaccination measles [4] and RSV [15] often display biennial patterns in temperate regions. The results for these synthetic data sets inform the interpretation of complex demodulation applied to real data. Using synthetic data in the manner outlined above allows features in the complex demodulation amplitude and phase to be related to the known structure in the synthetic data. These features then become indicators of the structure in real data, as explained for the influenza data.

The application to national influenza notification data for Australia demonstrates how complex demodulation can be used to analyse infectious disease dynamics (Figure 3). The amplitude output clearly identifies the earlier outbreak and high number of notifications associated with the pandemic influenza strain of 2009. The increase in amplitude from 2010 onwards reflects an increase in testing practices following the pandemic in 2009. It is interesting to observe that the high-amplitude years (2009 and 2012) are followed by a dip in both the amplitude and the phase the following year, with fewer notified cases and a later epidemic. A possible driver of this behaviour is increased levels of immunity resulting from high incidence in the previous year, although we cannot rule out differences in the distribution of subtypes from year to year that may influence the timing and size of the peak in notifications.

A key consideration in complex demodulation analysis is the interpretation of the amplitude. For each of the Figures 1 and 2, the moving average of the original data set is plotted in panels (i) and (ii), to allow direct comparison with the amplitude. The complex demodulation amplitude is not the amplitude of either the data or the moving average of the data, but reflects the data relative to the demodulator.

In our analysis, we found that small irregularities in the amplitude and phase occur, when a demodulator and filter corresponding to an annual frequency are applied to data with a strong biennial frequency. We also found that increasing the difference between the heights of the small and large peaks produced more pronounced deviations in the phase output. These deviations can be removed by use of a wider moving average window; however, this will remove some desired components of the analysis, as well as more values from the beginning and end of the data set [2].

The drivers of seasonality for diseases such as influenza and RSV remain a much-studied question. While individual climate and demographic drivers have been identified in various settings [5, 6], there is likely no single driver, and a combination of multiple factors leads to higher disease incidence during winter months in temperate regions. Nevertheless, methods such as complex demodulation allow us to better identify yearly variability in these underlying seasonal patterns. In future work, we plan to apply this method to explore the timing of influenza epidemics in different regions of Australia, and investigate the potential of this method to analyse data for two respiratory infections at the same time.

References

[1] Australian Government Department of Health, "Number of notifications of Influenza (laboratory confirmed), Australia, 2016", http://www9.health.gov.au/cda/source/cda-index.cfm.

[2] P. Bloomfield, *Fourier analysis of time series: An introduction* (Wiley, New York, 2000).

[3] B. Cazelles, K. Cazelles and M. Chavez, "Wavelet analysis in ecology and epidemiology: impact of statistical tests", *J. R. Soc. Interface* **11** (2014) 1–10; doi:10.1098/rsif.2013.0585.

[4] B. Finkenstädt and B. Grenfell, "Empirical determinants of measles metapopulation dynamics in England and Wales", *Proc. R. Soc. Lond. B* **265** (1998) 211–220; doi:10.1098/rspb.1998.0284.

[5] D. N. Fisman, "Seasonality of infectious diseases", *Ann. Rev. Pub. Health* **28** (2007) 127–143; doi:10.1146/annurev.publhealth.28.021406.14412.

[6] N. C. Grassly and C. Fraser, "Seasonal infectious disease epidemiology", *Proc. R. Soc. B* **273** (2006) 2541–2550; doi:10.1098/rspb.2006.3604.

[7] B. T. Grenfell, O. N. Bjørnstad and J. Kappey, "Travelling waves and spatial hierarchies in measles epidemics", *Nature* **414** (2001) 716–723; doi:10.1038/414716a.

[8] Y.-L. Hao, Y. Ueda and N. Ishii, "Improved procedure of complex demodulation and an application to frequency analysis of sleep spindles in EEG", *Med. Biol. Eng. Comput.* **30** (1992) 406–412; doi:10.1007/BF02446168.

[9] J. Hayano, J. A. Taylor, A. Yamada, S. Mukai, R. Hori, T. Asakawa, K. Yokoyama, Y. Watanabe, K. Takata and T. Fujinami, "Continuous assessment of hemodynamic control by complex demodulation of cardiovascular variability", *Am. J. Physiol.* **264** (1993) H1229–H1238; http://ajpheart.physiology.org/content/264/4/H1229.long.

[10] A. B. Hogan, R. S. Anderssen, S. Davis, H. C. Moore, F. J. Lim, P. Fathima and K. Glass, "Time series analysis of RSV and bronchiolitis seasonality in temperate and tropical Western Australia", *Epidemics* **16** (2016) 49–55; doi.10.1016/j.epidem.2016.05.001.

[11] P. A. Kingan, P. Bloomfield and R. S. Anderssen, "Phase drift and coherence in geomagnetic data during a magnetic storm (Dst)", *J. Geomagn. Geoelectr.* **32** (1980) 57–65; doi:10.5636/jgg.32.57.

[12] H. Kondo, M. Ozone, N. Ohki, Y. Sagawa, K. Yamamichi, M. Fukuju, T. Yoshida, C. Nishi, A. Kawasaki, K. Mori, T. Kanbayashi, M. Izumi, Y. Hishikawa, S. Nishino and T. Shimizu, "Association between heart rate variability, blood pressure and autonomic activity in cyclic alternating pattern during sleep", *Sleep* **37** (2014) 187–194; doi:10.5665/sleep.3334.

[13] E. Lofgren, N. H. Fefferman, Y. N. Naumov, J. Gorski and E. N. Naumova, "Influenza seasonality: underlying causes and modeling theories", *J. Virol.* **81** (2007); doi:10.1128/JVI.01680-06.

[14] I. W. Nader, J. Pietschnig, T. Niederkrotenthaler, N. D. Kapusta, G. Sonneck and M. Voracek, "Suicide seasonality: complex demodulation as a novel approach in epidemiologic analysis", *PLoS ONE* **6** (2011) e17413; doi:10.1371/journal.pone.0017413.

[15] V. E. Pitzer, C. Viboud, W. J. Alonso, T. Wilcox, C. J. Metcalf, C. A. Steiner, A. K. Haynes and B. T. Grenfell, "Environmental drivers of the spatiotemporal dynamics of respiratory syncytial virus in the United States", *PLoS Pathog.* **11** (2015) e1004591; doi:10.1371/journal.ppat.1004591.

[16] M. B. Priestley, "Wavelets and time-dependent spectral analysis", *J. Time Series Anal.* **17** (1996) 85–103; doi:10.1111/j.1467-9892.1996.tb00266.x.

[17] T. Sasai, M. Matsuura and Y. Inoue, "Change in heart rate variability precedes the occurrence of periodic leg movements during sleep: an observational study", *BMC Neurol.* **13** (2013); doi:10.1186/1471-2377-13-139.

[18] J. B. Thomas, *An introduction to statistical communication theory* (Wiley, New York, 1969).

[19] C. Viboud, W. J. Alonso and L. Simonsen, "Influenza in tropical regions", *PLoS Med.* **3** (2006) 468–471; doi:10.1371/journal.pmed.0030089.

[20] F. Yasuma and J. Hayano, "Respiratory sinus arrhythmia: why does the heartbeat synchronize with respiratory rhythm?", *Chest* **125** (2004) 683–690; doi:10.1378/chest.125.2.683.

Epidemics 16 (2016) 49–55

Contents lists available at ScienceDirect

Epidemics

journal homepage: www.elsevier.com/locate/epidemics

Time series analysis of RSV and bronchiolitis seasonality in temperate and tropical Western Australia

Alexandra B. Hogan[a,*], Robert S. Anderssen[b], Stephanie Davis[a], Hannah C. Moore[c], Faye J. Lim[c], Parveen Fathima[c], Kathryn Glass[a]

[a] National Centre for Epidemiology and Population Health, Research School of Population Health, The Australian National University, Australia
[b] CSIRO Data61; Mathematical Sciences Institute, The Australian National University; Mathematics and Statistics, La Trobe University, Australia
[c] Wesfarmers Centre of Vaccines and Infectious Diseases, Telethon Kids Institute, The University of Western Australia, Australia

ARTICLE INFO

Article history:
Received 3 February 2016
Received in revised form 8 May 2016
Accepted 9 May 2016
Available online 25 May 2016

Keywords:
Respiratory syncytial virus
Bronchiolitis
Complex demodulation
Seasonality
Fourier analysis

ABSTRACT

Respiratory syncytial virus (RSV) causes respiratory illness in young children and is most commonly associated with bronchiolitis. RSV typically occurs as annual or biennial winter epidemics in temperate regions, with less pronounced seasonality in the tropics. We sought to characterise and compare the seasonality of RSV and bronchiolitis in temperate and tropical Western Australia. We examined over 13 years of RSV laboratory identifications and bronchiolitis hospitalisations in children, using an extensive linked dataset from Western Australia. We applied mathematical time series analyses to identify the dominant seasonal cycle, and changes in epidemic size and timing over this period. Both the RSV and bronchiolitis data showed clear winter epidemic peaks in July or August in the southern Western Australia regions, but less identifiable seasonality in the northern regions. Use of complex demodulation proved very effective at comparing disease epidemics. The timing of RSV and bronchiolitis epidemics coincided well, but the size of the epidemics differed, with more consistent peak sizes for bronchiolitis than for RSV. Our results show that bronchiolitis hospitalisations are a reasonable proxy for the timing of RSV detections, but may not fully capture the magnitude of RSV epidemics.

1. Introduction

Respiratory syncytial virus (RSV) is the most common cause of severe respiratory illness in young children. RSV is associated with bronchiolitis and pneumonia, with up to 70% of bronchiolitis hospital admissions attributable to RSV infection (Mansbach et al., 2012). Like influenza (Thai et al., 2015; Alonso et al., 2015), RSV fluctuates with season (Pitzer et al., 2015), potentially due to climatic drivers. In temperate regions, RSV is highly seasonal, with annual or biennial (two-yearly) epidemics, while the epidemiology of RSV in the tropics is less well understood (Weber et al., 1998; Paynter et al., 2014).

To plan for RSV epidemics, two measures are of interest: the number of cases at the epidemic peak, and the timing of this peak. In this paper, we use complex demodulation, a time series approach that allows us to visualise both the timing and size of RSV epidemics, and to detect shifts in epidemic behaviour over time. Complex demodulation has previously been applied to the analysis of geomagnetic data (Kingan et al., 1980) and individual-level health data such as cardiovascular rhythms (Hayano et al., 1993; Shin et al., 1989; Kondo et al., 2014; Sasai et al., 2013), but to our knowledge has not yet been applied to population-level epidemiological data, except in the analysis of suicide data (Nader et al., 2011).

Laboratory testing for RSV is not routinely conducted in all jurisdictions and thus some studies have relied on hospitalisation coding for bronchiolitis to indicate the timing, severity and hospital burden of RSV epidemics (Walton et al., 2010; Murray et al., 2014; Polkinghorne et al., 2011). As other pathogens, such as adenoviruses and influenza viruses, also contribute to the burden of bronchiolitis, it is of interest to investigate the extent to which bronchiolitis hospitalisations are representative of RSV detections.

In this study, we examined over a decade of RSV detections and bronchiolitis hospitalisations in children aged up to 17 years from an extensive linked dataset from Western Australia. Geographic information on individuals in this dataset allowed us to compare seasonal patterns of illness across eight geographic regions spanning temperate, sub-tropical and tropical climate zones. We used a time series approach to identify seasonal patterns in RSV and bronchiolitis epidemics, and to detect changes in the timing and severity

* Corresponding author.
E-mail address: alexandra.hogan@anu.edu.au (A.B. Hogan).

http://dx.doi.org/10.1016/j.epidem.2016.05.001

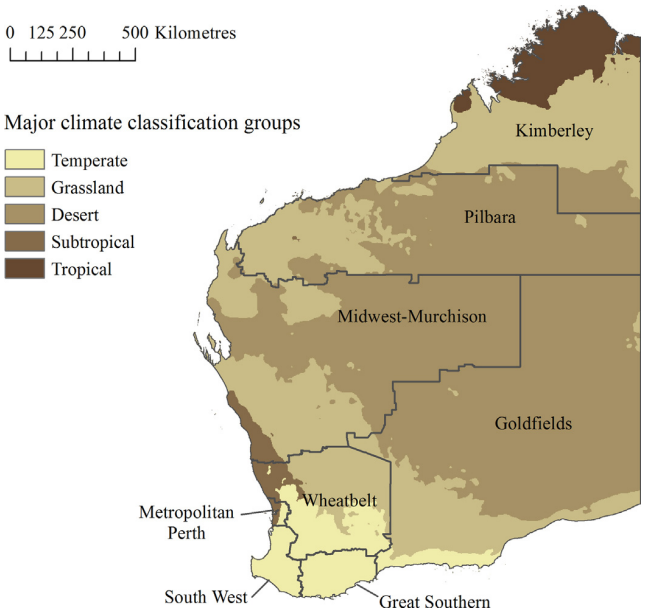

Fig. 1. Geographical map showing the eight administrative health regions in Western Australia and the major climatic zones, based on the Köppen classification system. The data for the climatic zones were sourced from the Australian Government Bureau of Meteorology (2016), and that for the administrative regions from the Australian Bureau of Statistics (2011), using the 2006 Statistical Divisions as a close proxy for the health administrative regions.

of these epidemics over time. By comparing RSV and bronchiolitis data, we assessed the extent to which the characteristics of these outbreaks coincided, and thus the value of bronchiolitis data as a proxy for RSV.

2. Methods

2.1. Setting

Western Australia is Australia's largest state by land area, spanning approximately 2.6 million square kilometres. Approximately 80% of the population resides in the Metropolitan region surrounding and including Perth, in the state's south-west. Western Australia is characterised by a range of climatic zones, including tropical, sub-tropical, grasslands and temperate. The state is classified into different health administrative regions: Kimberley, Pilbara, Goldfields, Midwest-Murchison, Wheatbelt, Great Southern, South West and Metropolitan. Fig. 1 shows a map of the state created using ArcMap 10.3.1, with administrative health regions and the main climatic zones based on the Köppen classification system. As of June 2014, Western Australia had a population of approximately 2.57 million people, 3.6% of whom identify as Aboriginal and Torres Strait Islander (hereafter referred to as Aboriginal) (Australian Bureau of Statistics, 2013). Demographic characteristics vary across the state, with the Pilbara and Kimberley regions (in the north of the state) having a much higher proportion of Aboriginal children and a lower population density than the Metropolitan region (Australian Bureau of Statistics, 2007).

2.2. Linked data

This study forms a part of a larger program of work which aims to investigate the pathogen-specific epidemiology of acute lower respiratory infections in children. For the parent study, using the total population-based Western Australian Data Linkage System (WADLS), data relating to a birth cohort of 469,589 children born in Western Australia from 1996 to 2012 were extracted from the following datasets: Midwives Notification System (MNS), Birth and Death Registry, Hospital Morbidity Data Collection (HMDC), Emergency Department Data Collection (EDDC), PathWest Laboratory Medicine Database (PathWest) and the Western Australian Notifiable Infectious Diseases Database (WANIDD). For this study, we used information for all live births from the MNS, Birth and Death Registry and their associated hospital (from HMDC) and laboratory data (from PathWest).

PathWest covers approximately 80% of all pathology samples in Western Australia and is the reference virology laboratory for the state. PathWest data for RSV testing for the children in our cohort were extracted for January 2000–December 2013. RSV testing was conducted using immunofluorescence, polymerase chain reaction (PCR), viral culture, or complement fixation protocols. For one part of the analysis, these data were combined with hospitalisation data to calculate the number of hospital admissions for which an RSV test was recorded, but elsewhere all PathWest laboratory confirmed RSV data were used, regardless of whether it was associated with a hospital admission. An RSV test was considered to be associated with a hospital admission if the date of specimen collection was within a four day period of hospital admission (48 h before until 48 h after). Repeat tests recorded for the same child within 14 days after the first test were considered as being from the same infection episode and were combined. The geographical region was determined based on the postcode recorded for the mother at the time of the child's birth. The residential postcode at the time of specimen collection was not recorded.

For the bronchiolitis cases, we extracted only hospital admissions where acute bronchiolitis was the primary diagnosis (ICD-10-AM code J21/ICD-9-CM code 466.1) for January 1996–June 2013. These comprised 92% of all admissions with any diagnosis of bronchiolitis. Admissions that occurred within 14 days of each other with the same principal diagnosis were assumed to be due to the same bronchiolitis episode. The geographical region was determined based on the residential postcode of the child at the time of hospital admission.

Ethical approval for this research was granted by the Department of Health Western Australia Human Research Ethics Committee (Projects 2011/78 and 2012/56) and The Australian National University Human Research Ethics Committee (Protocol 2015/177).

2.3. Data analysis

We performed a descriptive analysis of the seasonal pattern of RSV detections by plotting the total number of cases for each month between January 2000 and December 2013 for each health region.

Fourier analysis was applied to the RSV and bronchiolitis data for each of the Metropolitan, Pilbara and Kimberley regions. This method identifies dominant seasonal patterns in data, with a strong signal at 12 months indicating an annual epidemic peak. For the Metropolitan region, the analysis was carried out using weekly data, whereas for the other regions, monthly data were used due to smaller numbers. Linear trends in each dataset were removed using linear regression. The de-trended data were padded with zeros in order to increase the frequency resolution and produce smoothed plots (Bloomfield, 2000). Fourier analysis was performed on the resulting time series data to identify the dominant periodicities (the length of the seasonal cycle), using MATLAB's periodogram analysis algorithm (Bloomfield, 2000).

Complex demodulation was applied to weekly RSV and bronchiolitis data (separately) for January 2000–June 2013 for the Metropolitan region using MATLAB. There were insufficient data to perform complex demodulation for the other regions. An introduction to complex demodulation is provided in the Supplementary

Table 1
The total number of RSV and bronchiolitis cases for each region. The RSV data are for January 2000–December 2013, whereas the bronchiolitis data are for January 1996–June 2013.

Region	Number of RSV cases	% under 2 years	Number of bronchiolitis cases	% under 2 years
Kimberley	348	80.5%	1,852	95.8%
Pilbara	306	82.0%	1,140	95.7%
Midwest-Murchison	381	81.4%	1,164	94.9%
Goldfields	663	82.5%	1,217	96.0%
Wheatbelt	362	77.1%	929	92.0%
Metropolitan	8,969	81.8%	14,681	98.0%
Great Southern	313	72.8%	920	91.3%
South West	498	81.3%	1,338	94.0%

material. Briefly, with respect to an underlying annual seasonality, complex demodulation extracts the size of the epidemics (the 'amplitude') and the timing of the epidemics (the 'phase').

The method is as follows. Using the notation of Bloomfield (2000), we constructed the demodulated series y_t from the given time series data x_t, as:

$$y_t = x_t e^{-2\pi i f_0 t} = R_t e^{2\pi i \phi_t},$$

where the amplitude is represented by R_t, the phase is represented by ϕ_t, and we assumed a 52 week period ($f_0 = 1/52$). A 52-week moving average filter was then applied to smooth the demodulated time series, and we then extracted the amplitude R_t, and the phase ϕ_t, from the smoothed data (see Supplementary material for more detail).

As an addition to a visual representation of the complex demodulation results, we calculated correlation coefficients for the complex demodulation amplitudes and phases for the RSV and bronchiolitis data. This provided a statistical measure of the alignment between the RSV and bronchiolitis data.

In order to perform a preliminary investigation of the relationships between weather variables and RSV and bronchiolitis epidemics, we obtained daily records of minimum and maximum temperatures, and monthly records of total precipitation, from the Australian Government Bureau of Meteorology (2016). We applied complex demodulation to each of these time series, and extracted the filtered amplitudes and phases.

2.4. Sensitivity analysis

While the majority of RSV infections are detected in children less than two years of age, older children may still be diagnosed (Borchers et al., 2013). In the hospital setting, bronchiolitis is generally diagnosed only in children less than two years old. Further, as our analysis was conducted on birth cohort data, not all ages are represented at the start and end of the time windows. To test for any bias resulting from these factors, we repeated the analysis for hospitalisation data for children less than two years of age. There were insufficient data to analyse children two years and older. We also repeated the Fourier analysis of the bronchiolitis data for 2000–2013 in order to perform a direct comparison with the Fourier analysis of the RSV data for the same time period.

3. Results

The descriptive analysis showed that nearly all bronchiolitis hospitalisations were in children less than two years of age, while 73–83% of RSV diagnoses were in children aged less than two years. Table 1 summarises the number of RSV and bronchiolitis cases for each health region. Between 2000 and 2012, of 18,710 hospitalisations with a principal diagnosis of bronchiolitis, 54.6% (n = 10,219) were tested for RSV within 48 h of presenting to hospital. Of these, 58.3% (n = 5966) were found positive for RSV.

Most regions of Western Australia had a seasonal peak in RSV detections in July or August (Fig. 2). However, in the Pilbara region the seasonal peak was less well defined, and no pronounced seasonal peak was visible for the Kimberley region. A corresponding figure for the bronchiolitis data is provided in the Supplementary material (Fig. S2). The subsequent analysis focuses only on the three regions with distinctly different seasonal patterns: the Metropolitan, Pilbara and Kimberley regions.

Both RSV and bronchiolitis exhibited strongly annual seasonal epidemics in the Metropolitan region. This became less pronounced in the Pilbara region, and there was no clear seasonal cycle evident from analysis of the Kimberley data. Figs. 3 and 4 demonstrate this using a Fourier analysis of the RSV and bronchiolitis data. Each graph shows the different seasonal cycles on the horizontal axis, with the strength of this cycle on the vertical axis. A comparison of Figs. 3 and 4 indicates that the periodicities of RSV and bronchiolitis are very similar in all three regions. Results were similar when this analysis was repeated with the dataset restricted to children less than two years of age (see Supplementary Figs. S6 and S7), and when the bronchiolitis dataset was restricted to 2000–2013 (see Supplementary Fig. S5), although in both cases the signal was weaker.

The complex demodulation results are plotted in Fig. 5. The weekly RSV and bronchiolitis cases for Metropolitan Western Australia between January 2000 and June 2013 show a clear seasonal pattern, although there is greater variability in peak heights in the RSV data (Fig. 5, top two panels). With the exception of 2010–2011, there is visible evidence of an alternating pattern of bigger and smaller annual peaks (a biennial pattern) in the RSV data that is less apparent in the bronchiolitis data. The average weekly RSV cases are noticeably higher in even years while there is less change in average weekly bronchiolitis cases. The third 'amplitude' panel also captures the change in the RSV pattern in the years 2010–2012, where the cycle appears to shift from biennial to annual.

In terms of the complex demodulation phase, the peak RSV and bronchiolitis cases are observed in mid-July through to early August throughout 2000–2006 (Fig. 5, fourth panel). Apart from 2007, the timing of the epidemic peaks of RSV and bronchiolitis are very similar, with later epidemic peaks typically coinciding with smaller outbreaks. The correlation coefficient for the complex demodulation phases is $\rho = 0.963$, compared to the amplitude correlation coefficient of $\rho = 0.667$. In 2007 however, there is a clear 'dip' in the phase that indicates a shift in epidemic peak timing in that year, with RSV peaking in September and bronchiolitis peaking in August. We repeated the complex demodulation analysis for children less than two years of age, and found similar results, with correlation coefficients of $\rho = 0.757$ and $\rho = 0.964$ for the complex demodulation amplitudes and phases, respectively (see Supplementary Fig. S8). The complex demodulation results for weather variables in Perth, Western Australia, are shown in Supplementary Figs. S9–S11.

4. Discussion

Our study enabled us to characterise the seasonal patterns of RSV and bronchiolitis in the different climatic zones of Western Australia. The data analysis (Figs. 2–4) showed that both RSV detections and bronchiolitis hospitalisations exhibit clearly defined epidemic peaks in July or August in the southern Western Australia regions. There is a less identifiable seasonal pattern in the Pilbara region in the state's north, and no seasonal peak evident in the Kimberley region. We used complex demodulation (Fig. 5) to show that the timing of RSV and bronchiolitis epidemics over 13 years

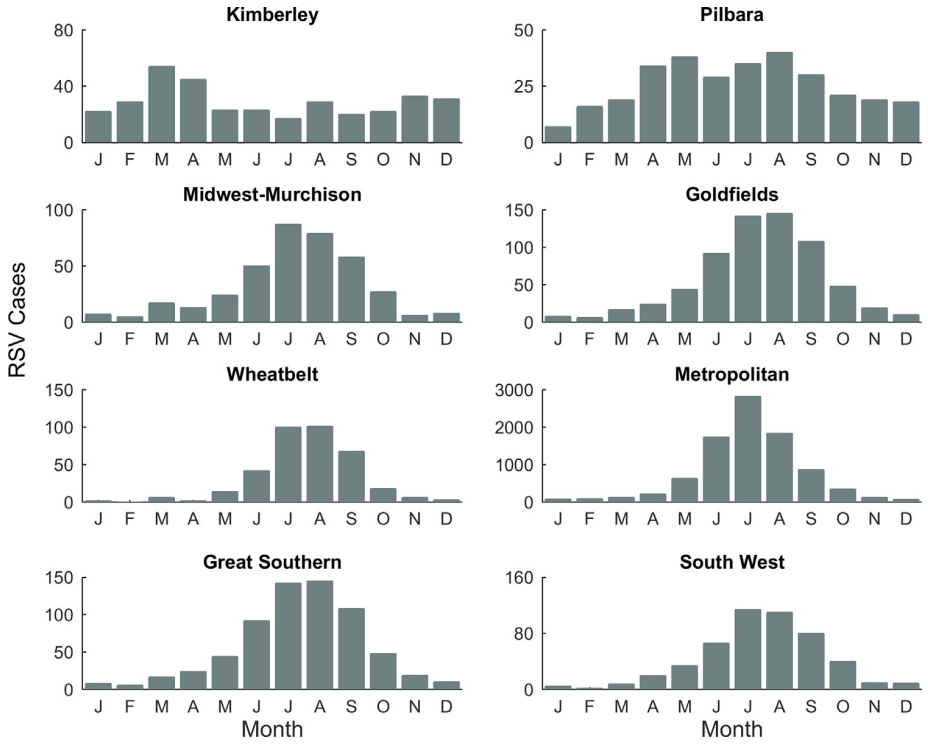

Fig. 2. Total number of positive RSV detections by month between 2000 and 2013 inclusive for each health region in Western Australia. Note that the vertical axis differs by region. See Fig. 1 for a map of these eight regions.

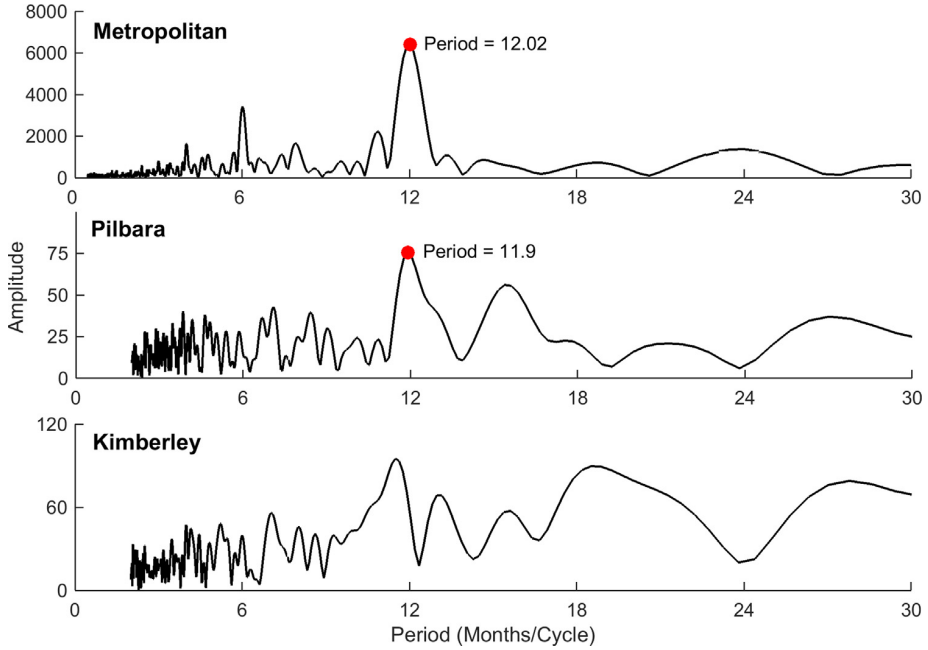

Fig. 3. Monthly periodicity of RSV detections in three health regions in Western Australia: Metropolitan, Pilbara and Kimberley, generated using Fourier analysis. Where a clear dominant period is present (as it is for the Pilbara and Metropolitan regions), the period is marked, but as the periodicity is not clear for the Kimberley, it is not marked.

generally coincided. However, the sizes of the epidemics differed, with a more marked change in the size of RSV epidemics from year to year.

Our findings indicate that there is a clear shift in the seasonality of both RSV and bronchiolitis from temperate to subtropical climatic zones in Western Australia. In the Metropolitan region, there is a dominant annual seasonal pattern that is stronger for RSV than for bronchiolitis, even though there were more bronchiolitis cases in our dataset. This may be because bronchiolitis can be caused by other pathogens (such as rhinovirus and influenza), which have different, or less regular, seasonal patterns. Also in the Metropolitan region, there was a change in dynamics within the time window

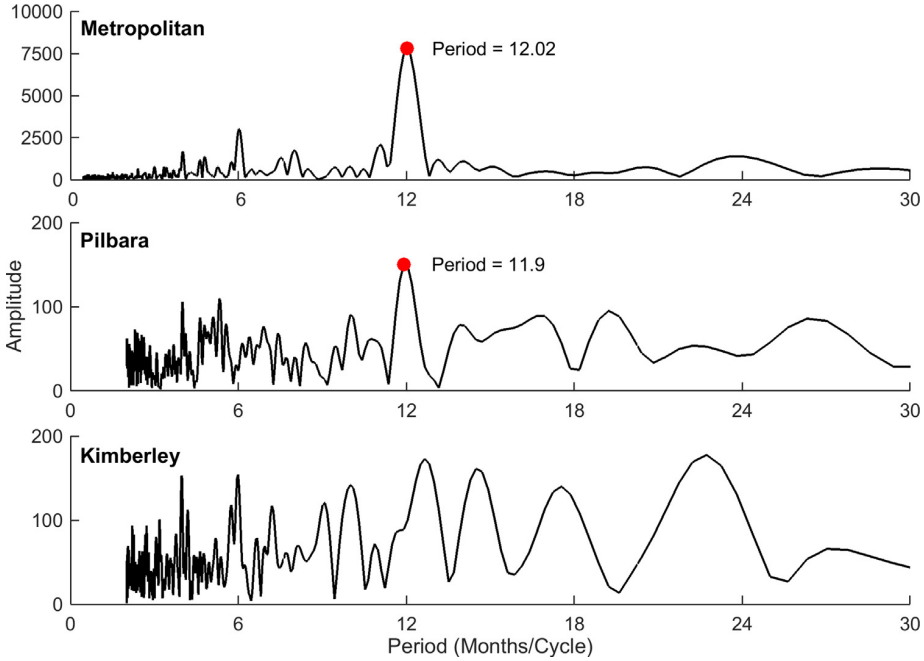

Fig. 4. Monthly periodicity of bronchiolitis hospital admissions in three health regions in Western Australia: Metropolitan, Pilbara and Kimberley generated using Fourier analysis. Where a clear dominant period is present (as it is for the Pilbara and Metropolitan regions), the period is marked, but as the periodicity is not clear for the Kimberley, it is not marked. Here the data analysed was for March 1996–June 2013.

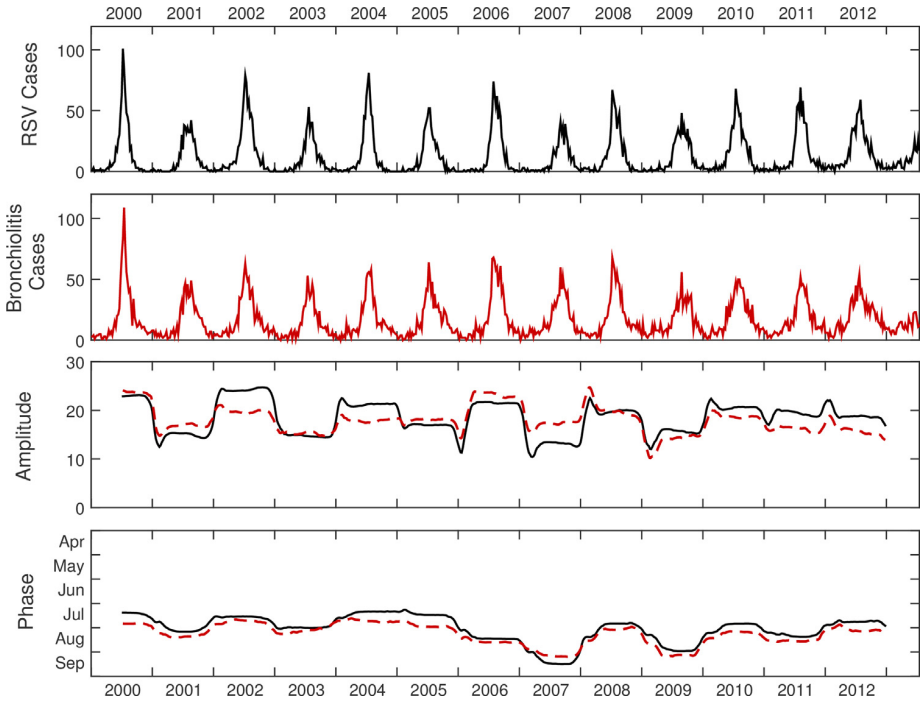

Fig. 5. Results of the complex demodulation analysis applied to RSV and bronchiolitis time series data for Metropolitan Western Australia, for all age groups. The top two panels show weekly RSV and bronchiolitis cases for January 2000–June 2013, while the lower two panels show the amplitude (the yearly moving average of weekly cases for the underlying seasonal pattern), and phase (the timing of the epidemic peak) for RSV (black) and bronchiolitis (red dashed). (For interpretation of the references to colour in this figure legend, the reader is referred to the web version of this article.)

of our dataset, with the RSV dynamics shifting from a biennial pattern to an annual pattern, something that has also been observed in California (Pitzer et al., 2015).

The complex demodulation analysis showed a change in epidemic timing for both RSV and bronchiolitis cases in 2007, where the epidemic peak occurred later than in other years. In another study, we considered factors including demography that could be driving the change in the timing of epidemic peaks in consecutive years (Hogan et al., 2016). As such, we looked at the annual birth rate for Western Australia, but there was no marked change

in either 2006 or 2007 to indicate any demographic shift (Australian Bureau of Statistics, 2009).

Weather has been suggested as a driver of change in RSV's seasonal patterns, and has been investigated in a number of settings (Noyola and Mandeville, 2008; Haynes et al., 2013; Pitzer et al., 2015; Vandini et al., 2013). However, no single driver has yet been identified, and it is likely that a range of factors contribute to the observed seasonal patterns of RSV. Applying complex demodulation to weather records from the Bureau of Meteorology (Supplementary Figs. S9–S11) showed no obvious link between RSV and bronchiolitis dynamics and weather patterns in Western Australia's Metropolitan region, in terms of monthly precipitation and daily maximum temperature. The complex demodulation results for the daily minimum temperature showed dips in amplitude in 2007 and 2009, which corresponded with the dips in phase for RSV and bronchiolitis in the same years. However, further statistical analysis would be required to confirm a link between smaller fluctuations in minimum temperature and delayed RSV epidemics. Another possibility is pathogen interference, such as the circulation of the H3N2 influenza strain in 2007, which resulted in above average influenza circulation (Kelly et al., 2011) and may have competed with RSV.

While RSV outbreaks in temperate climates typically occur in the winter months, seasonal patterns in tropical regions have not been widely studied (Weber et al., 1998). Paynter et al. (2015) investigated the seasonality of RSV in Cairns and Townsville in tropical eastern Australia, and showed that the peak of RSV infections occurs in March in Cairns, and March/April in Townsville. The study indicated that RSV epidemics may be driven by seasonal rainfall in the tropics. Chew et al. (1998) identified a clear seasonal trend in RSV infections in Singapore, with epidemics occurring between March and August, while Chan et al. (2002) documented seasonal variations in RSV infections in Malaysia, with epidemics occurring between November and January. Our data analysis (Figs. 2–4) demonstrated a weak seasonal peak in the Pilbara region, and no clear seasonal pattern in the Kimberley region in Western Australia's north, adding to the existing evidence that RSV dynamics shift between temperate and tropical regions.

Wavelet analysis is another time series method that has been successfully applied to the analysis of epidemiological data (Cazelles et al., 2014, 2007), as well as in other contexts. Wavelet analysis is useful for analysing localised variations in the underlying pattern in the time series data over time. Therefore, wavelet analysis is appropriate when the data is non-stationary (that is, when the dominant frequency changes over time), particularly when the location of some isolated event needs to be identified (Priestley, 1996). In cases where the data is stationary, such as for the present bronchiolitis and RSV data, complex demodulation offers distinct advantages in that is allows us to extract and visualise variations in the data from the underlying dominant seasonal pattern, and it is especially useful for comparing the variation in epidemic size and timing for different datasets. There is potential to apply complex demodulation to other epidemiological datasets, and it could be used to investigate the potential interference patterns between RSV and other respiratory pathogens such as influenza.

A key strength of our study is the breadth of our dataset. Population-based linked epidemiological data for Western Australia provides a valuable opportunity to explore RSV and bronchiolitis dynamics in different climatic regions. While Western Australia spans several climatic zones, data collecting methodologies and health systems are consistent across the state. It should be noted that the dataset is limited to children hospitalised for bronchiolitis or tested for RSV, and not all children with respiratory illness would be hospitalised or tested. However, laboratory testing to detect possible pathogens from respiratory infection-related hospitalisations is routine practice across Western Australia. As our data is likely only accounting for the severe end of the respiratory illness spectrum, we know little about RSV infection in the community. However, we expect patterns observed in the severe cases to be representative of community patterns.

A limitation is that the postcodes in the health regions in northern Western Australia cover large geographic regions, but in practice, spatial distributions of the resident populations in these areas are uneven. In addition, the case numbers for both RSV and bronchiolitis are small in the northern regions, making seasonal patterns in the data more difficult to detect. Furthermore, there was a shift away from viral culture towards more sensitive PCR testing for RSV from 2008 onwards (data not shown) that was not accounted for in the present analysis, but is unlikely to affect seasonal patterns.

Our findings have public health implications for RSV in terms of health care system planning. Immunoprophylaxis with the monoclonal antibody, palivizumab, has been found to be effective in reducing the severity of RSV-related disease, but requires an understanding of the RSV epidemic timing for implementation (The IMpact-RSV Study Group, 1998). Moore et al. (2009), in a study using bronchiolitis hospitalisations as a proxy for RSV-related illness, recommended that immunoprophylaxis schedules to be broadened in non-metropolitan areas in Western Australia. While there is no licensed vaccine for RSV, there are several candidates undergoing clinical trials (Broadbent et al., 2015). Understanding the dynamics of RSV epidemics in different regions will be important for planning optimal vaccine allocation.

Researchers often use bronchiolitis data for analysis of respiratory viruses in young children, as it is more readily available than laboratory data (Murray et al., 2014). While the connection between RSV and bronchiolitis is widely accepted, with the majority of bronchiolitis cases caused by RSV infection, there is a lack of understanding about how this link varies both within and between RSV seasons. Our findings help to justify the value in using bronchiolitis hospitalisation data as a proxy for RSV cases where testing data is less available, particularly in rural and remote areas.

Acknowledgements

The authors acknowledge and thank the Linkage and Client Services Teams at the Western Australian Data Linkage Branch, in particular Alexandra Godfrey, as well as the custodians of all datasets used. We would also like to thank Charmaine Tonkin and Brett Cawley, from PathWest Laboratory Medicine, particularly for their assistance and support in collating the data. This work was supported by National Health and Medical Research Council Project Grant APP1045668. HC Moore is supported by the National Health and Medical Research Council Early Career Fellowship APP1034254. FJ Lim is supported by a University Postgraduate Award from the University of Western Australia.

Appendix A. Supplementary data

Supplementary data associated with this article can be found, in the online version, at http://dx.doi.org/10.1016/j.epidem.2016.05.001.

References

Alonso, Wladimir Jimenez, Guillebaud, Julia, Viboud, Cecile, Razanajatovo, Norosoa Harline, Orelle, Arnaud, Zhou, Steven Zhixiang, Randrianasolo, Laurence, Heraud, Jean Michel, 2015. Influenza seasonality in Madagascar: the mysterious African free-runner. Influenza Other Respir. Viruses 9 (3), 101–109, http://dx.doi.org/10.1111/irv.12308.

Australian Bureau of Statistics, 2007. 4705.0—Population Distribution, Aboriginal and Torres Strait Islander Australians, 2006. Australian Bureau of Statistics (accessed 30.10.15.) http://www.abs.gov.au/ausstats//mf/4705.0.

Australian Bureau of Statistics, 2009. Births, Australia, 2009, Table 2 Births, Summary, Statistical Divisions—2004–2009, Time Series Spreadsheet, Cat. No. 3301.0. Australian Bureau of Statistics, http://www.abs.gov.au/AUSSTATS/abs@.nsf/Lookup/3301.0Main+Features12009?OpenDocument (accessed 20.09.14.).

Australian Bureau of Statistics, 2011. Statistical Division Digital Boundaries (ASGC 2006) Cat. No. 1259.0.30.002. Australian Bureau of Statistics, http://www.abs.gov.au/AUSSTATS/abs@.nsf/Lookup/1259.0.30.002Main+Features12006?OpenDocument (accessed 20.09.14.).

Australian Bureau of Statistics, 2013. 3238.0.55.001—Estimates of Aboriginal and Torres Strait Islander Australians, June 2011. Australian Bureau of Statistics, http://www.abs.gov.au/ausstats/abs@.nsf/mf/3238.0.55.001 (accessed 30.10.15.).

Australian Government Bureau of Meteorology, 2016. Climate Data Online. Australian Government Bureau of Meteorology http://www.bom.gov.au/climate/data/.

Bloomfield, Peter, 2000. Fourier Analysis of Time Series: An Introduction, 2nd ed. Wiley, New York.

Borchers, Andrea T., Chang, Christopher, Gershwin, M. Eric, Gershwin, Laurel J., 2013. Respiratory syncytial virus—a comprehensive review. Clin. Rev. Allergy Immunol. 45, 331–379, http://dx.doi.org/10.1007/s12016-013-8368-9.

Broadbent, Lindsay, Groves, Helen, Shields, Michael D., Power, Ultan F., 2015. RSV, an on-going medical dilemma: an expert commentary on RSV prophylactic and therapeutic pharmaceuticals currently in clinical trials. Influenza Other Respir. Viruses 9 (4), 169–178, http://dx.doi.org/10.1111/irv.12313.

Cazelles, B., Chavez, M., Magny, G.C., Guégan, J.-F., Hales, S., 2007. Time-dependent spectral analysis of epidemiological time-series with wavelets. J. R. Soc. Interface 4 (15), 625–636, http://dx.doi.org/10.1098/rsif.2007.0212.

Cazelles, B., Cazelles, K., Chavez, M., 2014. Wavelet analysis in ecology and epidemiology: impact of statistical tests. J. R. Soc. Interface 11 (91), http://dx.doi.org/10.1098/rsif.2013.0585.

Chan, P.W., Chew, F.T., Tan, T.N., Chua, K.B., Hooi, P.S., 2002. Seasonal variation in respiratory syncytial virus chest infection in the tropics. Pediatr. Pulmonol. 34 (1), 47–51, http://dx.doi.org/10.1002/ppul.10095.

Chew, F.T., Doraisingham, S., Ling, A.E., Kumarasinghe, G., Lee, B.W., 1998. Seasonal trends of viral respiratory tract infections in the tropics. Epidemiol. Infect. 121 (1), 121–128.

Hayano, J., Taylor, J.A., Yamada, A., Mukai, S., Hori, R., Asakawa, T., Yokoyama, K., Watanabe, Y., Takata, K., Fujinami, T., 1993. Continuous assessment of hemodynamic control by complex demodulation of cardiovascular variability. Am. J. Physiol. 264 (4 Pt 2), H1229–38.

Haynes, Amber K., Manangan, Arie P., Iwane, Marika K., Sturm-Ramirez, Katharine, Homaira, Nusrat, Brooks, W. Abdullah, Luby, Stephen, et al., 2013. Respiratory syncytial virus circulation in seven countries with Global Disease Detection Regional Centers. J. Infect. Dis. 208 (3), S246–S254, http://dx.doi.org/10.1093/infdis/jit515.

Hogan, Alexandra B., Glass, Kathryn, Moore, Hannah C., Anderssen, R.S., 2016. Exploring the dynamics of respiratory syncytial virus (RSV) transmission in children. Theor. Popul. Biol. http://dx.doi.org/10.1016/j.tpb.2016.04.003.

Kelly, Heath, Jacoby, Peter, Dixon, Gabriela A., Carcione, Dale, Williams, Simon, Moore, Hannah C., Smith, David W., Keil, Anthony D., Van Buynder, Paul, Richmond, Peter C., 2011. Vaccine effectiveness against laboratory-confirmed influenza in healthy young children: a case-control study. Pediatr. Infect. Dis. J. 30 (2), 107–111, http://dx.doi.org/10.1097/INF.0b013e318201811c.

Kingan, P.A., Bloomfield, P., Anderssen, R.S., 1980. Phase drift and coherence in geomagnetic data during a magnetic storm (D_{st}). J. Geomagn. Geoelec. 32 (1), 57–65, http://dx.doi.org/10.5636/jgg.32.57.

Kondo, Hideaki, Ozone, Motohiro, Ohki, Noboru, Sagawa, Yohei, Yamamichi, Keiichirou, Fukuju, Mitsuki, Yoshida, Takeshi, et al., 2014. Association between heart rate variability, blood pressure and autonomic activity in cyclic alternating pattern during sleep. Sleep 37 (1), 187–194, http://dx.doi.org/10.5665/sleep.3334.

Mansbach, Jonathan M., Piedra, Pedro A., Teach, Stephen J., Sullivan, Ashley F., Forgey, Tate, Clark, Sunday, Espinola, Janice A., Camargo, Carlos A., 2012. Prospective multicenter study of viral etiology and hospital length of stay in children with severe bronchiolitis. Arch. Pediatr. Adolesc. Med. 166 (8), 700–706, http://dx.doi.org/10.1001/archpediatrics.2011.1669.

Moore, Hannah C., Keil, Anthony D., Richmond, Peter C., Lehmann, Deborah, 2009. Timing of bronchiolitis hospitalisations and respiratory syncytial virus immunoprophylaxis in non-metropolitan Western Australia. Med. J. Aust. 191 (10), 574.

Murray, Joanna, Bottle, Alex, Sharland, Mike, Modi, Neena, Aylin, Paul, Majeed, Azeem, Saxena, Sonia, 2014. Risk factors for hospital admission with RSV bronchiolitis in England: a population-based birth cohort study. PLoS One 9 (2), e89186, http://dx.doi.org/10.1371/journal.pone.0089186.

Nader, Ingo W., Pietschnig, Jakob, Niederkrotenthaler, Thomas, Kapusta, Nestor D., Sonneck, Gernot, Voracek, Martin, 2011. Suicide seasonality: complex demodulation as a novel approach in epidemiologic analysis. PLoS One 6 (2), http://dx.doi.org/10.1371/journal.pone.0017413.

Noyola, D.E., Mandeville, P.B., 2008. Effect of climatological factors on respiratory syncytial virus epidemics. Epidemiol. Infect. 136 (10), 1328–1332, http://dx.doi.org/10.1017/S0950268807000143.

Paynter, Stuart, Yakob, Laith, Simões, Erica F., Lucero, Marilla G., Tallo, Veronica, Nohynek, Hanna, Ware, Robert S., Weinstein, Philip, Williams, Gail, Sly, Peter D., 2014. Using mathematical transmission modelling to investigate drivers of respiratory syncytial virus seasonality in children in the Philippines. PLoS One 9 (2), e90094, http://dx.doi.org/10.1371/journal.pone.0090094.

Paynter, Stuart, Ware, Robert S., Sly, Peter D., Weinstein, Philip, Williams, Gail, 2015. Respiratory syncytial virus seasonality in tropical Australia. Aust. N. Z. J. Public Health 39 (1), 8–10, http://dx.doi.org/10.1111/1753-6405.12347.

Pitzer, Virginia E., Viboud, Cécile, Alonso, Wladimir J., Wilcox, Tanya, Metcalf, C. Jessica, Steiner, Claudia A., Haynes, Amber K., Grenfell, Bryan T., 2015. Environmental drivers of the spatiotemporal dynamics of respiratory syncytial virus in the United States. PLoS Pathog. 11 (1), e1004591, http://dx.doi.org/10.1371/journal.ppat.1004591.

Polkinghorne, Benjamin G., Muscatello, David J., Macintyre, C. Raina, Lawrence, Glenda L., Middleton, Paul M., Torvaldsen, Siranda, 2011. Relationship between the population incidence of febrile convulsions in young children in Sydney, Australia and seasonal epidemics of influenza and respiratory syncytial virus, 2003–2010: a time series analysis. BMC Infect. Dis. 11 (1), 291, http://dx.doi.org/10.1186/1471-2334-11-291, BioMed Central Ltd.

Priestley, M.B., 1996. Wavelets and time-dependent spectral analysis. J. Time Ser. Anal. 17 (1), 85–103.

Sasai, Taeko, Matsuura, Masato, Inoue, Yuichi, 2013. Change in heart rate variability precedes the occurrence of periodic leg movements during sleep: an observational study. BMC Neurol. 13 (1), 139, http://dx.doi.org/10.1186/1471-2377-13-139.

Shin, S.J., Tapp, W.N., Reisman, S.S., Natelson, B.H., 1989. Assessment of autonomic regulation of heart rate variability by the method of complex demodulation. IEEE Trans. Biomed. Eng. 36 (2), 274–283.

Thai, Pham Quang, Choisy, Marc, Duong, Tran Nhu, Thiem, Vu Dinh, Yen, Nguyen Thu, Hien, Nguyen Tran, Weiss, Daniel J., Boni, Maciej F., Horby, Peter, 2015. Seasonality of absolute humidity explains seasonality of influenza-like illness in Vietnam. Epidemics 13, 65–73, http://dx.doi.org/10.1016/j.epidem.2015.06.002.

The IMpact-RSV Study Group, 1998. Palivizumab, a humanized respiratory syncytial virus monoclonal antibody, reduces hospitalization from respiratory syncytial virus infection in high-risk infants. Pediatrics 102 (3), 531–537, http://dx.doi.org/10.1542/peds.102.3.531.

Vandini, Silvia, Corvaglia, Luigi, Alessandroni, Rosina, Aquilano, Giulia, Marsico, Concetta, Spinelli, Marica, Lanari, Marcello, Faldella, Giacomo, 2013. Respiratory syncytial virus infection in infants and correlation with meteorological factors and air pollutants. Ital. J. Pediatr. 39 (1), 1, http://dx.doi.org/10.1186/1824-7288-39-1.

Walton, Nephi A., Poynton, Mollie R., Gesteland, Per H., Maloney, Chris, Staes, Catherine, Facelli, Julio C., 2010. Predicting the start week of respiratory syncytial virus outbreaks using real time weather variables. BMC Med. Inform. Decis. Mak. 10 (1), 68, http://dx.doi.org/10.1186/1472-6947-10-68, BioMed Central Ltd.

Weber, M.W., Mulholland, E.K., Greenwood, B.M., 1998. Respiratory syncytial virus infection in tropical and developing countries. Trop. Med. Int. Health 3 (4), 268–280.

Time series analysis of RSV and bronchiolitis seasonality in temperate and tropical Western Australia: Supplementary Material

Total RSV and bronchiolitis cases per year

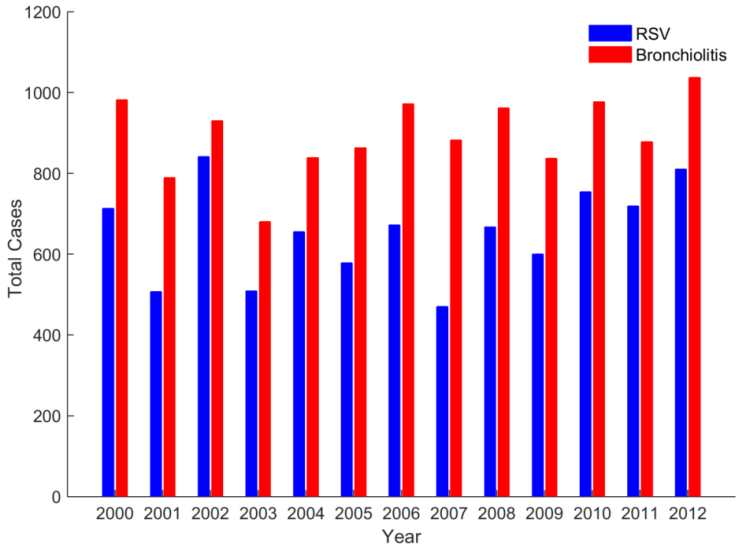

Figure S1 Total number of RSV and bronchiolitis cases per year, for all ages, between 2000 and 2012.

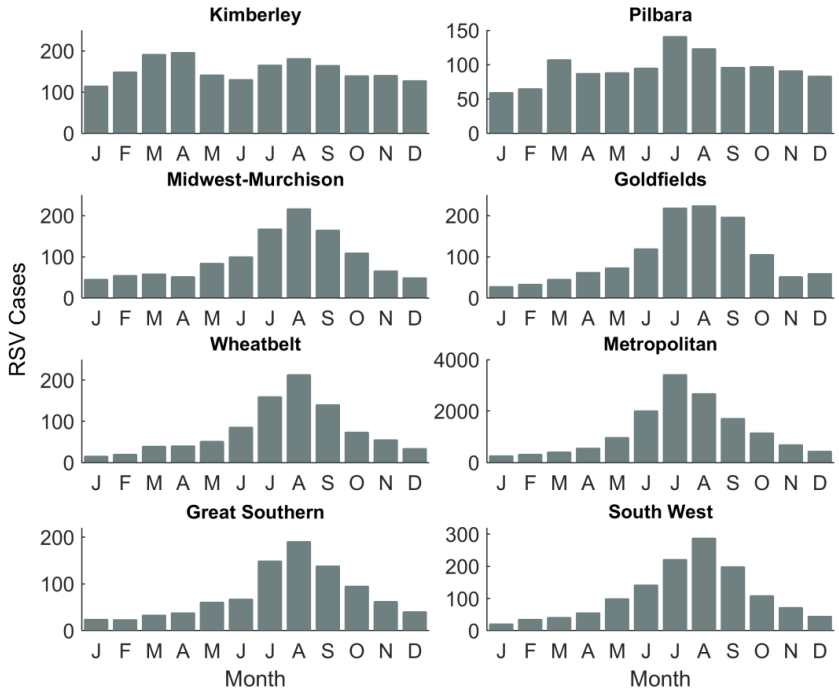

Figure S2 Total number of bronchiolitis hospitalisations by month between January 1996 and December 2012 inclusive for each health region in Western Australia. Note that the vertical axis differs by region.

Introduction to complex demodulation

This brief introduction to complex demodulation is based on the detailed description in Bloomfield (2000), contextualised to the analysis of infectious disease data.

Complex demodulation is a time series analysis method that is useful for visualising and comparing changes in a given time series with respect to a sinusoidal function representing seasonality. In the present example, we apply this method to weekly RSV and bronchiolitis data. We therefore use a unit of time of one week for this analysis.

We describe the seasonal patterns in these data using three terms: amplitude, phase and frequency. The term 'amplitude', denoted by R_t, is related to the number of disease cases at a point in time, whereas the term 'phase', denoted ϕ_t, is related to the timing of the epidemic peak. The 'frequency', denoted f_0, is the number of seasonal cycles in the data per week. Another important term is the 'period', which is the inverse of the frequency. The period is the number of weeks associated with each seasonal cycle.

Background to the method

Let x_t denote the time series of weekly counts of infectious disease cases. From the Fourier analysis, a strong 52 week (one year) cycle has already been identified in the data. Hence, the frequency f_0 may be set to 1/52.

Because we know that our time series exhibits a strong frequency, we can think of the time series as being the sum of the underlying periodic signal, and some noise. That is,

$$x_t = R_t \cos(2\pi(f_0 t + \phi_t)) + z_t.$$

This can be rewritten as

$$x_t = \frac{1}{2} R_t \left(e^{2\pi i(f_0 t + \phi_t)} + e^{-2\pi i(f_0 t + \phi_t)}\right) + z_t.$$

The data series x_t is then demodulated, by multiplying it by $e^{-2\pi i f_0 t}$. The complex demodulated series y_t then takes the form

$$\begin{aligned} y_t &= x_t e^{-2\pi i f_0 t} \\ &= \frac{1}{2}\mathrm{R_t e^{2\pi i \phi_t}} + \frac{1}{2}\mathrm{R_t e^{-2\pi i(2f_0 t + \phi_t)}} + \mathrm{z_t e^{2\pi i f_0 t}}. \end{aligned}$$

To eliminate the second and third terms from the above expression, and retain only the first term, a simple 52-week moving average filter is applied to the demodulated series. The instantaneous amplitude R_t and phase ϕ_t can then be extracted from the first term in the expression.

Implementing the method

To reframe the method described above in practical terms, there are three key steps to implement complex demodulation.

1. Demodulate the data series.
$$y_t = x_t e^{-2\pi i f_0 t}$$
2. Apply a filter (in this case a moving average) to the demodulated data series.
$$z_t = \Gamma[y_t]$$
3. Extract the amplitude and phase from the filtered data series.
$$R_t = 2\,|z_t|$$
$$\phi_t = Im(\log(z))/2\pi$$

In practice, the phase may be calculated in MATLAB using the `angle` and `unwrap` functions:

```
phase = unwrap(angle(z))/(2*pi)
```

Output

Figures S3 and S4 show the output of the complex demodulation analysis applied to synthetic annual and biennial data created using a mathematical model of RSV (Hogan et al. 2015). In each figure, the top panel shows the synthetic data plotted as a time series. The middle and lower panels show the amplitude and phase respectively. The amplitude may be interpreted as the yearly moving average of weekly cases, with respect to the underlying seasonal pattern. The phase may be interpreted as the difference between the starting point of the period and the epidemic peak, as a proportion of the length of the period. In the main text, we have rescaled this to indicate the month of the year in which the epidemic peak occurs.

In Figure S3, where regular annual synthetic data was used, the amplitude is fixed, as the moving average of weekly cases is unchanging from year to year. Similarly, the plot depicting the phase shows that the peaks are occurring at the same time each year.

In Figure S4, where biennial synthetic data was used, the amplitude fluctuates each year to show the transition between big and small peak years. Another feature of the biennial synthetic data is a delay in the small-peak years, with the epidemic peak occurring slightly later than in the big-peak years. This causes the phase to oscillate between two values. The amplitude 'blips' visible in the complex demodulation output are a result of the 52-week moving average filter applied to a delayed biennial dataset.

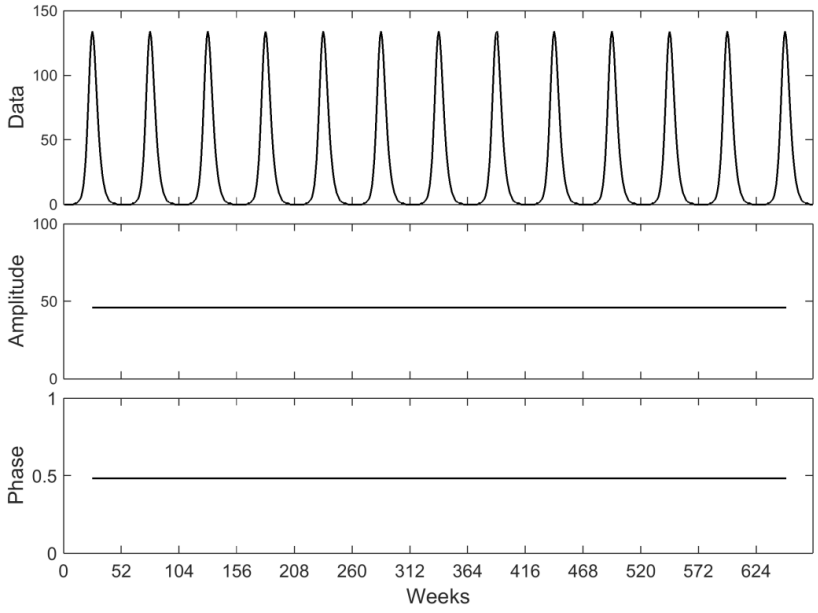

Figure S3 Complex demodulation applied to synthetic annual seasonal data. The amplitude may be interpreted as the yearly moving average of weekly cases in the underlying seasonal pattern, while the phase indicates the timing of the epidemic peak.

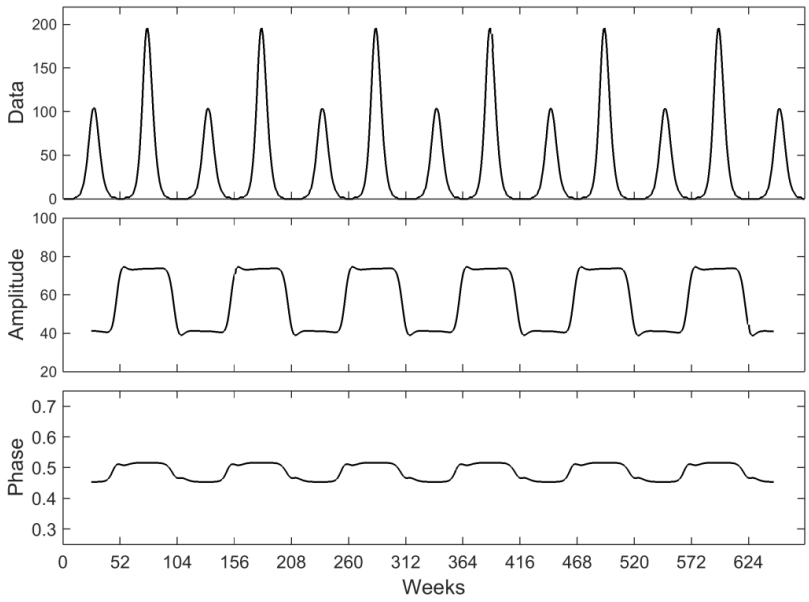

Figure S4 Complex demodulation applied to synthetic biennial data with a slight delay in the small peak years.

Fourier analysis for bronchiolitis data, 2000-2013

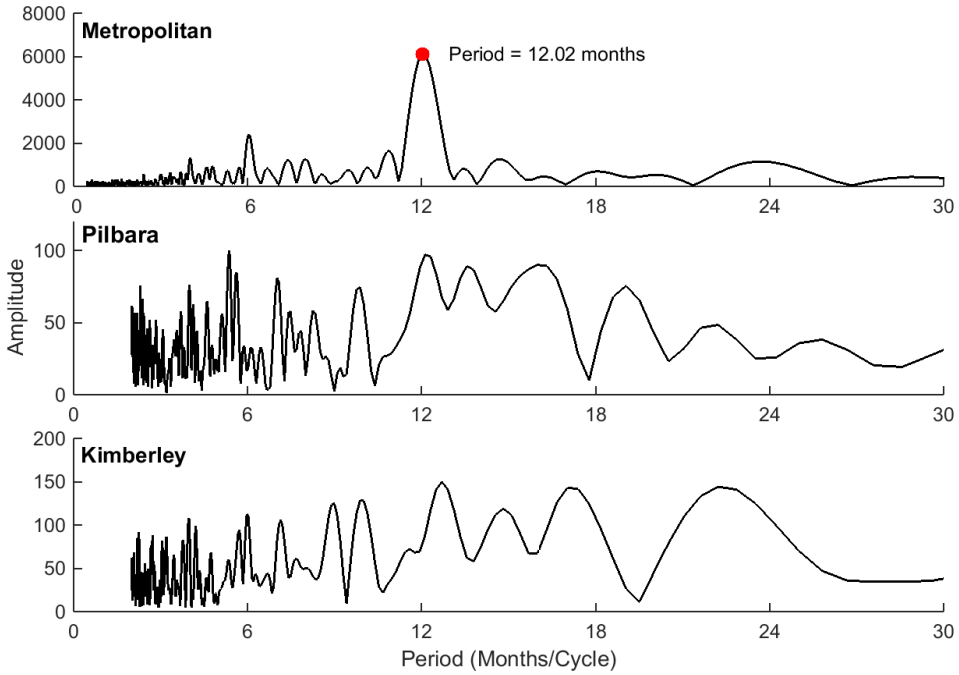

Figure S5 Monthly periodicity of bronchiolitis hospital admissions in three health regions in Western Australia: Metropolitan, Pilbara and Kimberley generated using Fourier analysis. Where a clear dominant period is present (as it is for the Metropolitan region), the period is marked, but as the periodicity is not clear for the Pilbara or the Kimberley, it is not marked. Here the data analysed was for January 2000 to June 2013.

Sensitivity analysis for children less than two years, 2000-2013

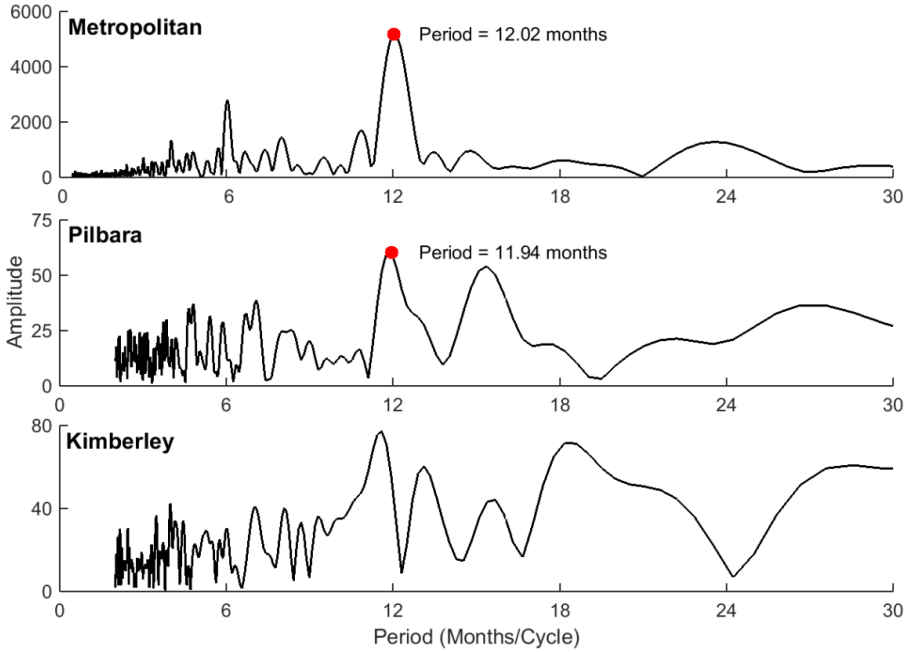

Figure S6 Monthly periodicity of RSV detections in three health regions in Western Australia: Metropolitan, Pilbara and Kimberley generated using Fourier analysis. The data analysed here is for children under two years old only. Where a clear dominant period is present (as it is for the Pilbara and Metropolitan regions), the period is marked, but as the periodicity is not clear for the Kimberley, it is not marked.

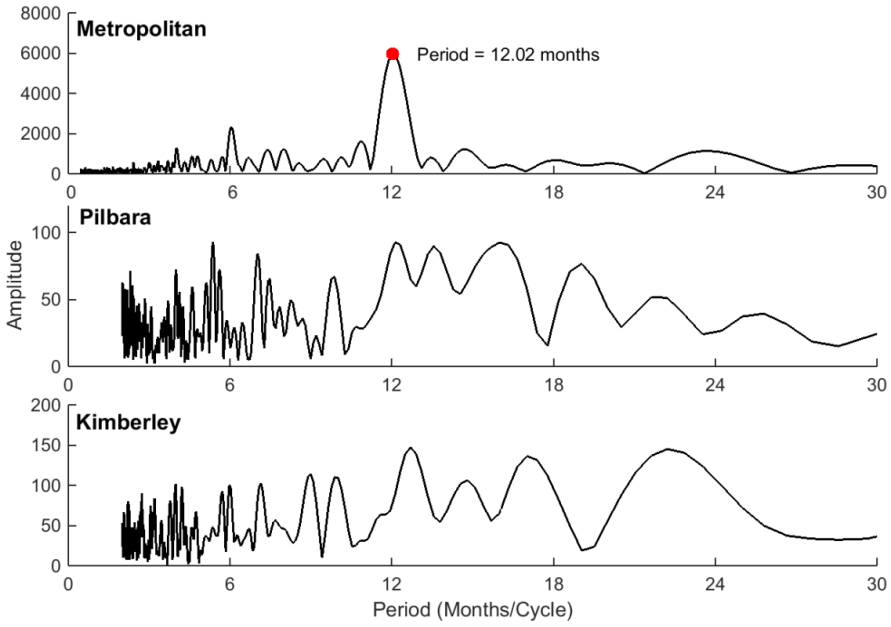

Figure S7 Monthly periodicity of bronchiolitis detections in three health regions in Western Australia: Metropolitan, Pilbara and Kimberley generated using Fourier analysis. The data analysed here is for children under two years old only. Where a clear dominant period is present (as it is for the Metropolitan region), the period is marked, but as the periodicity is not clear for the Pilbara or the Kimberley, it is not marked.

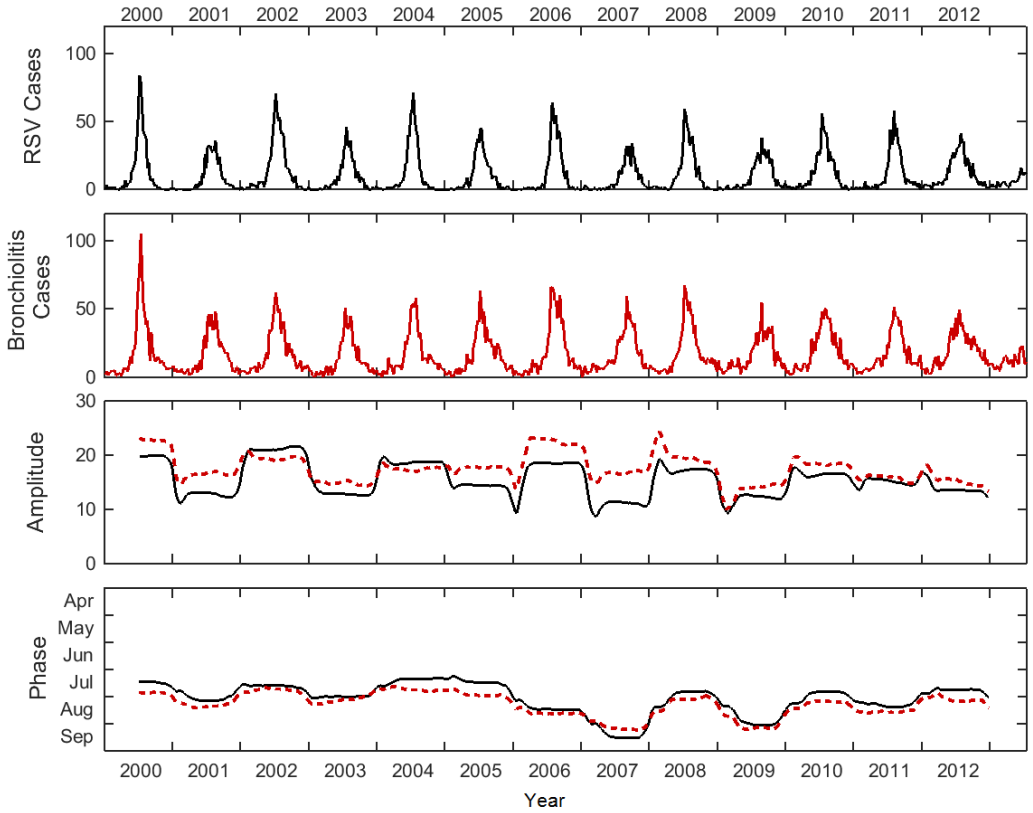

Figure S8 Results of the complex demodulation analysis applied to RSV and bronchiolitis time series data for Metropolitan Western Australia, for children younger than two years of age. The top two panels show weekly RSV and bronchiolitis cases for the January 2000 to June 2013, while the lower two panels show the amplitude (the yearly moving average of weekly cases for the underlying seasonal pattern), and phase (the timing of the epidemic peak) for RSV (black) and bronchiolitis (red dashed).

Exploration of link with weather variables

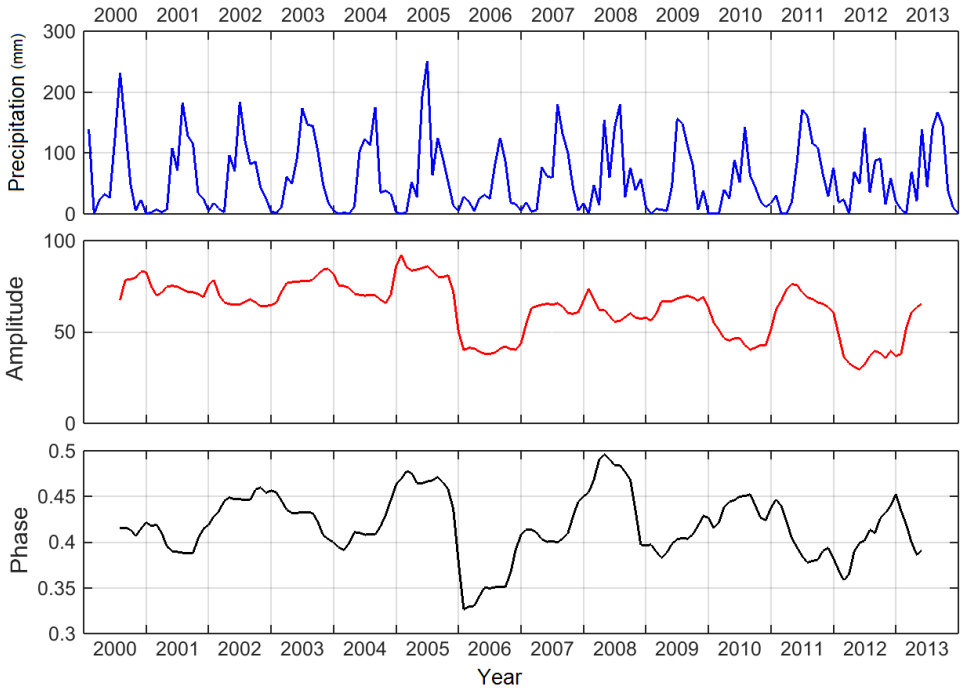

Figure S9 Results of the complex demodulation analysis applied to total monthly precipitation data for the Perth Metro weather station, Western Australia (Australian Government Bureau of Meteorology 2016).

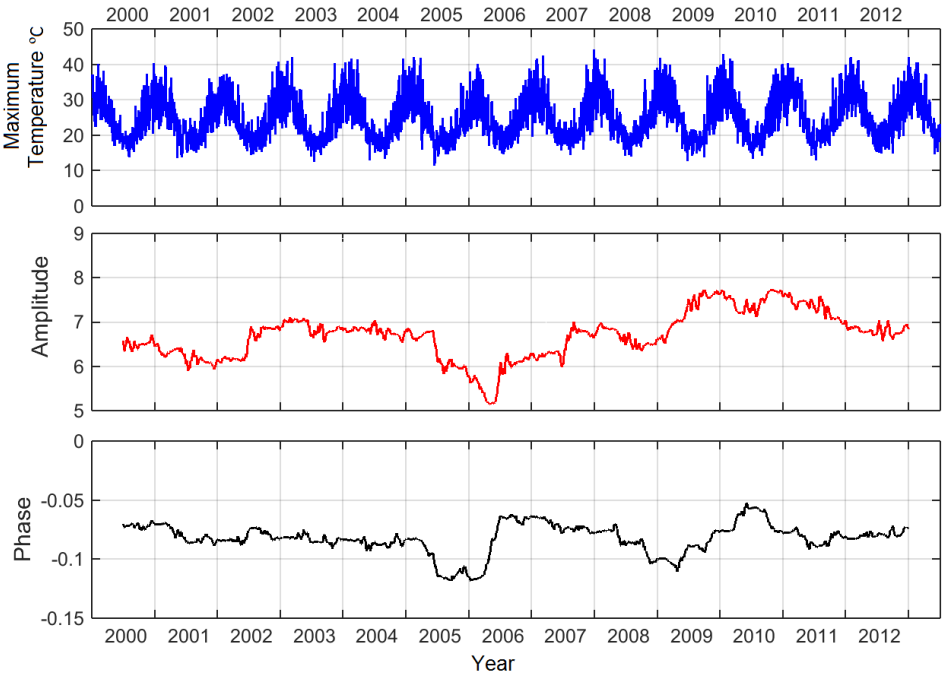

Figure S10 Results of the complex demodulation analysis applied to daily maximum temperature data for the Perth Metro weather station, Western Australia (Australian Government Bureau of Meteorology 2016).

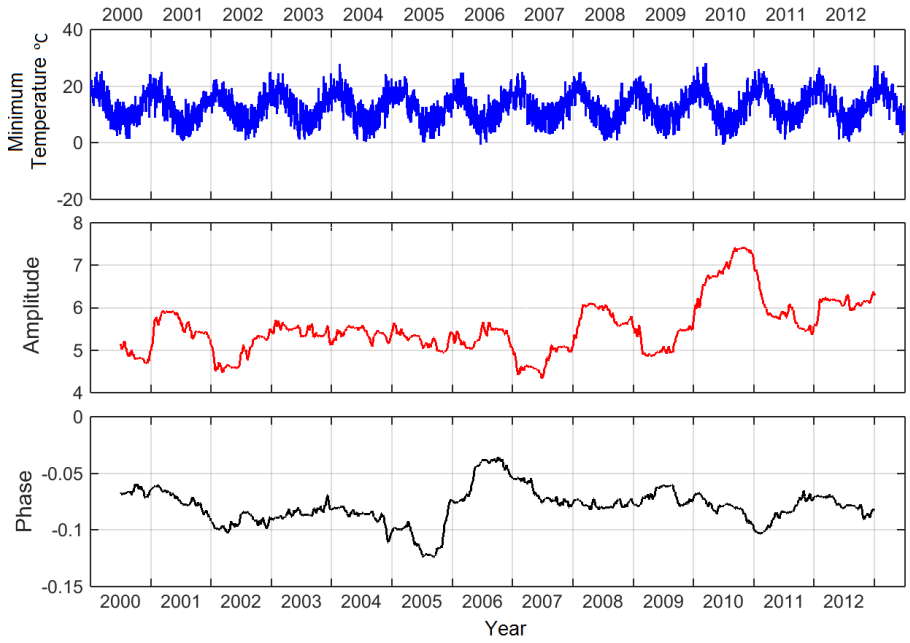

Figure S11 Results of the complex demodulation analysis applied to daily minimum temperature data for the Perth Metro weather station, Western Australia (Australian Government Bureau of Meteorology 2016).

Bibliography

Australian Government Bureau of Meteorology. 2016. "Climate Data Online, Viewed 30 March 2016."

Bloomfield, Peter. 2000. *Fourier Analysis of Time Series: An Introduction*. 2nd ed. New York: Wiley.

Hogan, Alexandra B, Kathryn Glass, Hannah C Moore, and Robert S Anderssen. 2015. "Age Structures in Mathematical Models for Infectious Diseases , with a Case Study of Respiratory Syncytial Virus." In *Applications + Practical Conceptualization + Mathematics = Fruitful Innovation - Proceedings of the Forum of Mathematics for Industry 2014*, 105–16. Springer.

6.3 Additional material

6.3.1 Complex demodulation MATLAB code

An example of the script used for the complex demodulation routine is shown below.

```
% Load data
load RSV_weekly_cases.csv
x=RSV_weekly_cases';

% Demodulate series
N=length(x);
t = (1:N);
f0=1/52;                    %frequency  of the demodulator
s=exp((-2)*pi*1i*f0*t);     %demodulator
Y=x.*s;                     %this is the demodulated series

% Apply centred moving average filter with 52 week window
p=52;
q=(p/2);
z=zeros(1:N);
for i=0+q+1:N-1-q
z(i)=1/p*(0.5*Y(i-q)+0.5*Y(i+q)+sum(Y(i-q+1:i+q-1)));
end

% Extract amplitude and phase
amp=2*abs(z);
phase=unwrap(angle(z))/(2*pi);
```

7

Interventions for RSV outbreaks

7.1 Introduction

This chapter includes one manuscript, which is currently being reviewed by *Vaccine*. In this paper, I extend the compartmental, ordinary differential equation models presented in the earlier chapters to include a more realistic age structure. I then incorporate a maternal vaccine for RSV into the model, as well as a mechanism for naturally-derived protective maternal antibodies. I consider a range of vaccine coverage, effectiveness and duration scenarios to evaluate the likely public health benefit of a maternal RSV vaccine in Western Australia. An example of the MATLAB code used to implement the vaccination model is provided in Appendix B.

7.2 Paper

Hogan, A. B., Campbell, P. T., Blyth, C. C., Lim, F. J., Fathima, P., Davis, S., Moore, H. C., and Glass, K. (2017). Potential impact of a maternal vaccine for RSV: a mathematical modelling study. Submitted to *Vaccine* (under review).

Potential impact of a maternal vaccine for RSV: a mathematical modelling study

Alexandra B Hogan*, Patricia T Campbell, Christopher C Blyth, Faye J Lim, Parveen Fathima, Stephanie Davis, Hannah C Moore†, Kathryn Glass†

*Corresponding author, †Joint senior authors

ABSTRACT

Respiratory syncytial virus (RSV) is a major cause of respiratory morbidity and one of the main causes of hospitalisation in young children. While there is currently no licensed vaccine for RSV, a vaccine candidate for pregnant women is undergoing phase 3 trials. We developed a compartmental age-structured model for RSV transmission, validated using linked laboratory-confirmed RSV hospitalisation records for metropolitan Western Australia. We adapted the model to incorporate a maternal RSV vaccine, and estimated the expected reduction in RSV hospitalisations arising from such a program. The introduction of a vaccine was estimated to reduce RSV hospitalisations in Western Australia by 6–37% for 0–2 month old children, and 30–46% for 3–5 month old children, for a range of vaccine effectiveness levels. Our model shows that, provided a vaccine is demonstrated to extend protection against RSV disease beyond the first three months of life, a policy using a maternal RSV vaccine could be effective in reducing RSV hospitalisations in children up to six months of age, meeting the objective of a maternal vaccine in delaying an infant's first RSV infection to an age at which severe disease is less likely.

KEYWORDS

respiratory syncytial virus; RSV; mathematical model; vaccine model; maternal vaccine

INTRODUCTION

Respiratory syncytial virus (RSV) causes respiratory illness in young children and presents a significant global health burden. In 2005, at least 33·8 million episodes of RSV occurred worldwide in children younger than five years [1]. Almost all children experience an RSV infection by the age of two years, and the highest burden is in children between six weeks and six months of age [2].

There is currently no licensed vaccine for RSV, however it is widely recognised that such a vaccine would have a considerable impact on global public health [3]. Distinct target populations have been identified – pregnant women, infants and young children, and the elderly – and several vaccine candidates for each of these groups are undergoing either clinical trials or preclinical development [3–5]. A potential strategy to protect newborn infants against RSV is to vaccinate pregnant women in the third trimester of pregnancy, and a RSV F nanoparticle vaccine for pregnant women is undergoing phase 3 trials (Novavax, NCT02624947) [6,7].

The potential introduction of a novel RSV vaccine prompts the need for mathematical modelling to inform rollout strategies for target population groups. However, few mathematical modelling studies of RSV vaccination have been published to date, and these have largely focused on infant or childhood vaccines [8–14]. A study modelling the use of a maternal RSV vaccine in Kenya found that such a vaccine would likely reduce RSV incidence in very young children, even with sub-optimal coverage [15]. Here, we model the reduction in RSV hospital admissions due to a maternal RSV vaccination in a high-income setting, under varying levels of coverage and efficacy, using a mathematical model fitted to linked population-based RSV data from Western Australia (WA).

METHODS

Setting and population-based data

Data for this study were sourced from a population-based birth cohort data linkage study on the pathogen-specific burden of acute lower respiratory infections (ALRI). The birth cohort comprised all children born in WA between 1996 and 2012, identified from the Midwives' Notification System and the Birth Registry [16]. Hospital admission records and laboratory records were extracted from the Hospital Morbidity Data Collection and the PathWest Laboratory Database and probabilistically linked through the Western Australian Data Linkage System [17]. PathWest is the sole public pathology service in WA and services all but three hospitals that admit pediatric patients. Only hospital records with both admission and separation dates during the study period (January 1996 to December 2012) were included in these analyses. These are henceforth referred to as hospital admissions. We identified all ALRI hospital admission records from children in the birth cohort through a selection of International Classification of Diseases version 10 Australian modification (ICD-10 AM) diagnosis codes as described in previous work [18]. ALRI was defined as pneumonia (J12-J18), acute bronchiolitis (J21), influenza (J09-J10), whooping cough (A37), bronchitis (J20, J40) and unspecified ALRI (J22). Using linked laboratory data, we further restricted these ALRI admissions to those where RSV was detected within 48 hours of the hospital admission. Further details of the linkage of laboratory and hospital admission records can be found elsewhere [19]. The residential postcode at the time of the hospital admission was used to restrict analyses to cases in the metropolitan region of WA, which consists of the capital city Perth and its surrounds, with a population of 2 million [20]. The resultant dataset included 5,898 laboratory-confirmed RSV-associated ALRI hospital admissions, herein referred to as RSV hospitalisations.

Model without vaccination

We developed a deterministic compartmental mathematical model for RSV transmission, using the Susceptible–Exposed–Infectious–Recovered–Susceptible form as in prior work [21,22]. We included 75 age classes: 60 one-month classes for individuals younger than five years, and five-year age groups thereafter. We set a constant total population size with a uniform age distribution across ages 0–79, and assumed that deaths only take place in the oldest age class, as we were estimating the vaccine impact in infants and young children in a setting where child mortality is very low. To simulate monthly ageing between classes we used cohort ageing.

Cohort ageing is a method where, instead of including continuous ageing rates in the ordinary differential equations (ODEs) to simulate movements between age classes, individuals from each compartment are shifted instantaneously at fixed time points [23–25]. The seasonal nature of RSV transmission was simulated using a cosine forcing function, in line with earlier work [21]. Further details of the model equations are in the Supplementary Material (S1).

Parameters

In line with empirical and modelling studies, we assumed a latent period of four days [26,27], an infectious period of nine days [9,27,28], and that immunity following natural infection persisted for 230 days [21]. It is known that there is trans-placental transfer of protective RSV-specific antibodies from a pregnant woman to her unborn child, however the level of protection is uncertain [29]. Considering studies from Spain, Brazil, Kenya and Turkey, we assumed that unvaccinated infants have some protection from maternally-derived RSV-specific antibodies for the first three months of life [12,30–33]. Based on the seropositive proportion reported in the Brazilian study, we reduced susceptibility to infection by 92% in the first month of life and 55% in the second and third months.

Studies indicate that adults are less infectious than young children, and that RSV is often introduced into a household by an older sibling [34–36]. We therefore introduced a scaling parameter ω that reduced infectiousness in individuals aged ten years and older.

Mixing between age groups was based on the POLYMOD study, using all reported contacts (physical and non-physical) for Great Britain [37]. The contact matrix was first made symmetric using the method described by Brisson et al [24]. Then, since the age classes in the POLYMOD matrices are in groups of five years, we adapted the contact matrix to match the age structure in our model, and the daily values were converted to monthly (Supplementary Material S1). We also tested the sensitivity of the model outcome to a more realistic contact structure in children younger than five years [38].

Model fitting

In the first instance, we attempted to fit the model by varying the reduced infectiousness parameter ω and the transmission function parameters b_0 (the overall transmission), b_1 (the amplitude of seasonal forcing) and ϕ (the phase shift) simultaneously, using a numerical fitting routine. However, we found that the model would fit the data well for a range of starting values for ω. Therefore, we instead adopted a two-fold approach to determine values for these four parameters.

We estimated the three transmission function parameters b_0, b_1 and ϕ by fitting the model to monthly RSV hospitalisations for four key age groups (0–2 months, 3–5 months, 6–11 months and 12–23 months) simultaneously. We fitted the model in MATLAB using maximum likelihood estimation with the inbuilt Nelder Mead algorithm function *fminsearch*, and solved the ODEs using the inbuilt differential equation solver *ode45* [39]. In the fitting routine, we included four parameters ($h_{0-2}, h_{3-5,}$ h_{6-11} and h_{12-23}) to scale the modelled incidence to the RSV hospitalisations data for each of the four key age groups.

We ran the fitting routine for a range of starting values for the reduced infectiousness parameter ω. We then extracted from the model the proportion of 0–23 month old children who were infected by an individual 2–14 years of age. In a study of subcohort data extracted from the same birth cohort from which our RSV hospitalisations data were derived, it was estimated that 45% of the RSV detections in that subcohort were attributable to infection from an older sibling [40]. We therefore selected the fitted parameter set that best reflected this estimate of the proportion of infections in young children caused by an older sibling. Details of all parameter values are in Table 1. The fitting method is further described in the Supplementary Material (S2).

Maternal vaccination model

Maternal vaccination was modelled by incorporating an additional compartment V_i that represented infants in age class i with reduced susceptibility to infection derived from their mother's vaccination (Figure 1). This means that rather than explicitly modelling the vaccination of pregnant women, we modelled infants as being born either with or without maternally-derived vaccine protection. The proportion of infants born into the V_i class (the 'vaccine coverage parameter') encompassed both vaccine uptake by pregnant women, and the proportion of women that develop protective levels of antibodies. The default value for the vaccine coverage parameter κ was set to 50%, and we tested values between 30% and 70%, informed by recent uptake estimates of 70% and 56% for the maternal pertussis and influenza vaccines in WA, and accounting for assumed imperfect development of protective antibodies in vaccinated pregnant women [41].

We assumed that the maternal vaccine would extend the length of natural maternal protection, so that the maximum duration of vaccine-induced protection in infants was six months [42]. This duration is approximately equivalent to the estimated duration of protection afforded to an RSV-infected person following recovery, and similar to estimates in other studies, but we also tested values of three and four months [8,15]. Infants in class V_i had susceptibility to infection scaled by a factor $1-\rho_i$, where ρ_i is a proxy for vaccine effectiveness relative to a completely native individual, without naturally-derived maternal antibody protection. Considering the stated minimal criteria for an RSV maternal vaccine efficacy of 60% [43], we tested values between 60% and 90% for vaccine effectiveness, and used a value of 80% for our default scenario. We also considered the scenario where the effectiveness parameter changed over the period of six months to simulate waning effectiveness, with $\rho_1=\rho_2=\rho_3=0.8, \rho_4=0.6, \rho_5=0.4$ and $\rho_6=0.2$. The vaccination model equations are provided in the Supplementary Material (S1).

Model outcomes and sensitivity analysis

We compared the output of the base model to that of the maternal vaccination model for both the number of infections and number of hospitalisations. Outputs were compared for the equilibrium model solutions after a burn in time of 400 years. We estimated the avoided RSV hospitalisations in children younger than 24 months for a range of vaccine coverage, effectiveness and duration scenarios.

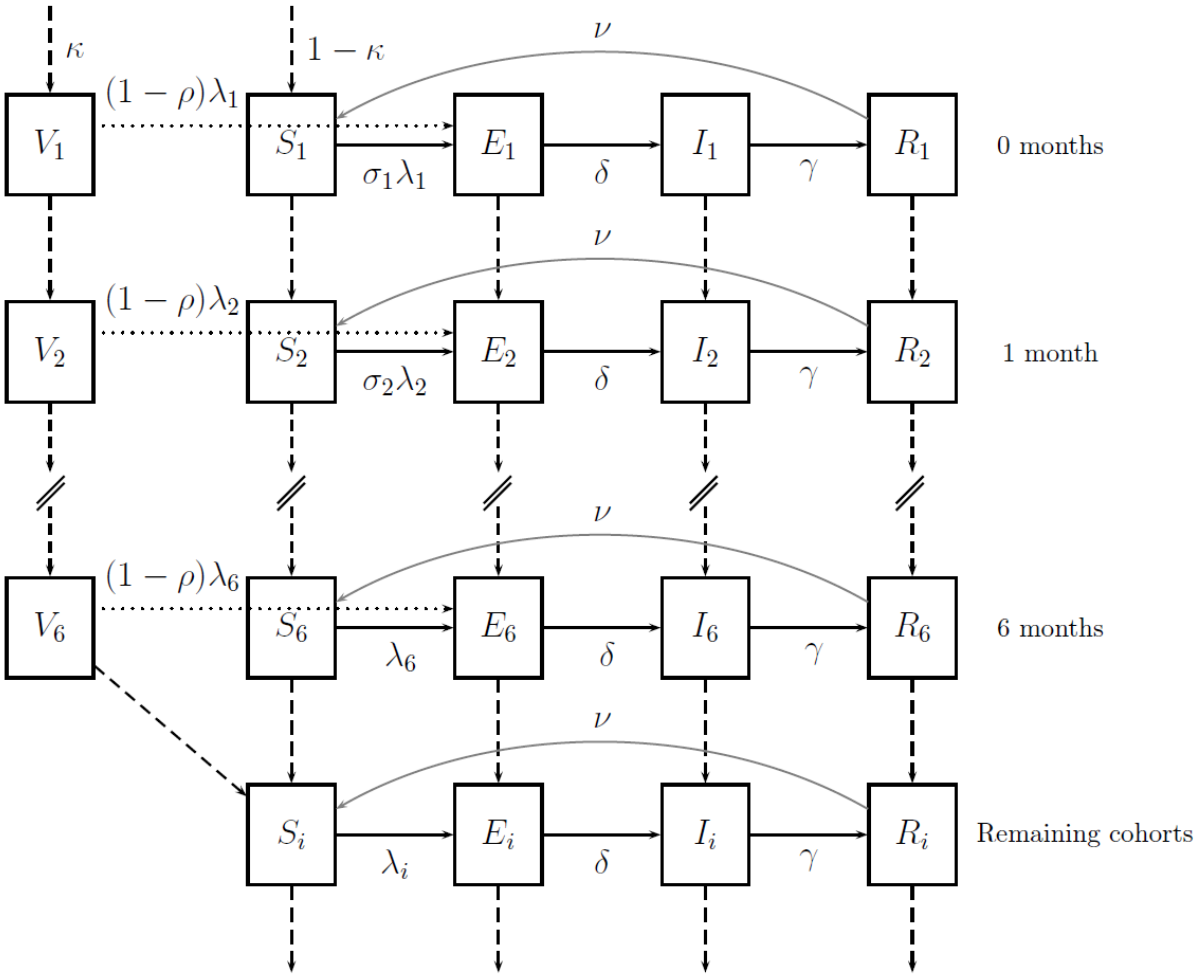

Figure 1. Schematic diagram for the maternal vaccination model, with vaccine-induced immunity assumed to last no longer than six months. The compartments S_i, E_i, I_i, R_i, and V_i represent, respectively, the susceptible, exposed, infectious, recovered, and vaccinated populations, for each age cohort i. The parameters λ_i, δ_i, γ, and ν represent, respectively, the transmission, latent, recovery and immunity rates. Reduced susceptibility due to natural maternally-derived immunity is represented by σ_i. The parameter ρ_i represents vaccine effectiveness and κ represents coverage. Dashed lines represent cohort ageing processes.

The relationship between the RSV-specific antibody titre in infants and protection from RSV disease has not been fully elucidated [44]. We therefore analysed scenarios with lower levels of existing maternal protection by varying the parameters relating to reduced susceptibility in the first three months of life. We considered a scenario with lower natural protection by reducing susceptibility to infection by 75% in the first month of life and 35% in the second and third months. We compared this to a scenario with no natural maternal protection by incorporating no reduced susceptibility in the first three months of life.

We assessed the sensitivity of the model output to variation in model parameters influencing the age-specific force of infection. We varied the level of reduced infectiousness in older age classes by running our analysis for a range of values of ω between 0.4 and 0.8. We also considered the contact data for children younger than 10 years. A limitation of using the POLYMOD data in this study is that the POLYMOD age groups are in five-year cohorts [37]. We investigated whether more finely stratified contact data for children younger than five years would change the model results. We used United Kingdom data from a study that estimated

Table 1. Model parameters for the default scenario where the reduced infectiousness parameter $\boldsymbol{\omega = 0.6}$. Fitted parameter sets for other values of $\boldsymbol{\omega}$ are in Table S1.

Parameter	Definition	Fixed/Fitted	Value	Reference
$1/\delta$	Latent period (days)	Fixed	4	[26,27]
$1/\gamma$	Infectious period (days)	Fixed	9	[9,27,28]
$1/\nu$	Immunity period (days)	Fixed	230	[21]
σ_1	Reduced susceptibility in first age cohort due to naturally-derived maternal immunity (0 months of age)	Fixed	0.08	[30]
σ_2, σ_3	Reduced susceptibility in age cohorts 2 and 3 due to naturally-derived maternal immunity (1 and 2 months of age)	Fixed	0.45	[30]
N	Total population of Greater Perth for ages 0-79 years	Fixed	1,861,923	[20]
ω	Reduced infectiousness in children 10 years and older	Fixed	0.6	
κ	Vaccine coverage	Fixed	0.5	[41]
$1-\rho_i$	Reduced susceptibility due to vaccine, relative to naïve individual, in month i	Fixed	$0.2, i \leq p_{vacc}$ $1, i > p_{vacc}$	[41]
p_{vacc}	Maximum duration of vaccine-induced protection in months	Fixed	6	[8,15]
b_0	Transmission rate	Fitted	0.015	
b_1	Amplitude of seasonal forcing	Fitted	0.397	
ϕ	Phase of seasonal forcing function	Fitted	0.985	
h_{0-2}	Proportion of modelled infections leading to hospitalisation in the 0–2 month age group		0·424	
h_{3-5}	Proportion of modelled infections leading to hospitalisation in the 3–5 month age group		0·088	
h_{6-11}	Proportion of modelled infections leading to hospitalisation in the 6–11 month age group		0·047	
h_{12-23}	Proportion of modelled infections leading to hospitalisation in the 12–23 month age group		0·020	

Table 2. Avoided hospitalisations over a 24 month period for a range of scenarios, represented as the number of avoided hospitalisations per 1000 children in that age group (the risk difference), and as a percentage risk reduction (1 – RR, where RR is the relative risk). The default parameter set has vaccine coverage of 50%, vaccine effectiveness of 80%, and maximum duration of vaccine-induced immunity of six months. Note that the measure of vaccine effectiveness described here is relative to a completely naïve individual, without natural maternal antibody protection. All other parameter values are reported in Table S1.

Scenario	**0–2 month age group per 1000 (percentage reduction)**	**3–5 month age group per 1000 (percentage reduction)**
Default		
50% coverage, 80% effectiveness, 6 months duration	13 (26%)	12 (40%)
Coverage		
30% coverage	8 (16%)	7 (24%)
70% coverage	18 (37%)	17 (56%)
Effectiveness		
60% effectiveness	3 (6%)	9 (30%)
70% effectiveness	8 (16%)	10 (35%)
90% effectiveness	18 (37%)	14 (46%)
Waning effectiveness	6 (13%)	5 (18%)
Duration		
3 months vaccine-induced immunity	12 (25%)	0 (0%)
4 months vaccine-induced immunity	13 (26%)	4 (13%)
Higher effectiveness and coverage		
90% effectiveness, 70% coverage	25 (51%)	19 (63%)
Lower effectiveness and coverage		
70% effectiveness, 30% coverage	5 (10%)	6 (21%)

contact frequencies in individuals in one-year age groups to stratify the contact matrix parameters for our age cohorts under five years of age [38], but retained the POLYMOD parameters for the contact rates between individuals older than five years. Finally, we considered the impact of the uniform age distribution in our model. We ran the models for the default parameter set using a non-uniform age distribution, based on age distribution data for Greater Perth in 2014 [20].

Ethical approvals for this study were received from the Department of Health WA Human Research Ethics Committee (#2012/56) and The Australian National University Human Research Ethics Committee (Protocol 2015/177).

RESULTS

Model outcome and fit

Figure S2 shows the model fitted to RSV hospitalisations for children younger than two years by age group. Fitted parameter values are in Tables 1 and S1. We compared the model outputs with the proportion of infections in young children caused by an older sibling in this dataset, and therefore determined that the infectivity of individuals age ten years and older was 60% of that of younger children (Table S2). The base and maternal vaccination model outputs retain

the biennial seasonal infection pattern typically observed in metropolitan WA (Figure S1), therefore we present the avoided RSV hospitalisations over a two-year period to capture both a large and small RSV season.

Reduction in hospitalisations

The modelled introduction of a maternal RSV vaccine reduced the number of infections and hospitalisations in young children. The range of modelled scenarios showed a 6–51% reduction in RSV hospitalisations in children younger than two months, with a 6% reduction only if vaccine effectiveness was poor (Table 2). Figure 2 shows the base model output compared to the vaccination model for vaccine effectiveness levels in the range 60–90%. The percentage reduction in hospitalisations in children aged 3–5 months was higher than for children aged 0–2 months under most scenarios, except where vaccine protection was assumed to last only three or four months. The default scenario (80% vaccine effectiveness, 50% coverage and a maximum of six months' vaccine-induced immunity) resulted in a 26% reduction in hospitalisations in children younger than two months, and 40% in children aged 3–5 months (Table 2). For all modelled scenarios, the vaccine had a negligible impact on the number of RSV hospitalisations in children aged 6–11 months and 12–23 months, as demonstrated in Figure S3.

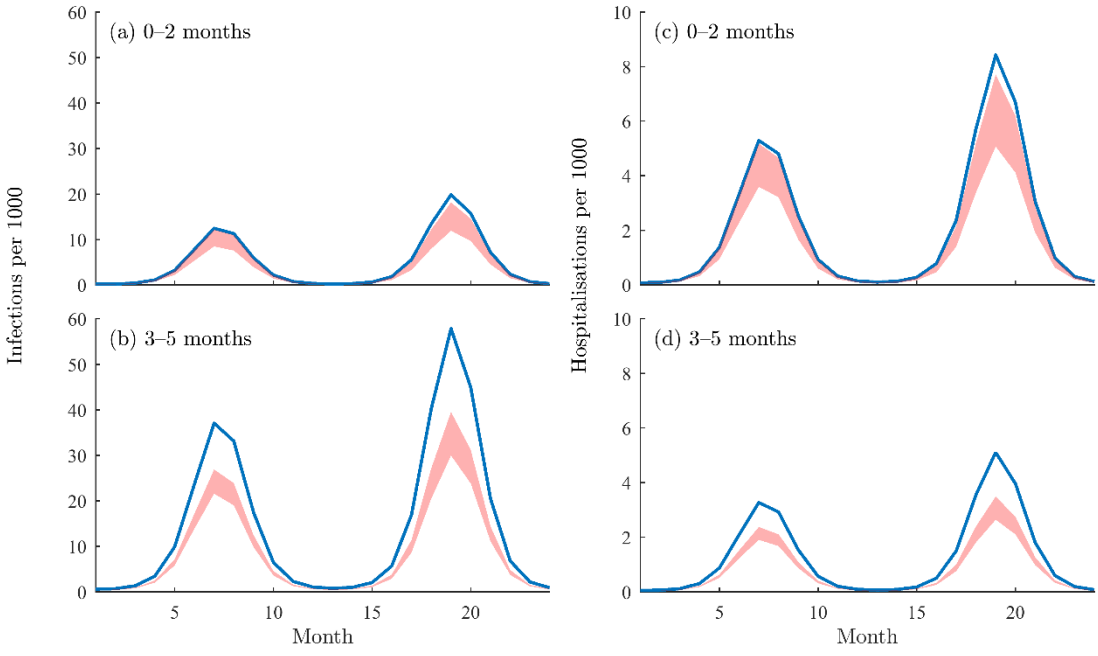

Figure 2. Comparison of the modelled number of RSV infections (panels (a) and (b)) and hospitalisations (panels (c) and (d)) per month in the age groups 0–2 months and 3–5 months, per 1000 children in that age group, over a time period of 24 months. The blue line represents the base model, and the red shaded area represents the range of outputs of the vaccination model for vaccine effectiveness levels between 60% and 90%.

Table 3. Sensitivity analysis for natural maternally-derived immunity parameters. This table shows the avoided hospitalisations over a 24 month period for the scenario with lower natural maternally-derived immunity, compared to the default scenario, represented as the number of avoided hospitalisations per 1,000 children in that age group, and as a percentage reduction.

Scenario	**0–2 month age group per 1000 (percentage reduction)**	**3–5 month age group per 1000 (percentage reduction)**
Default $\sigma_1 = 0.08, \sigma_2 = \sigma_3 = 0.45$	13 per 1000 (26%)	12 per 1000 (40%)
Reduced natural maternal immunity $\sigma_1 = 0.25, \sigma_2 = \sigma_3 = 0.65$	16 per 1000 (33%)	12 per 1000 (40%)
No natural maternal immunity $\sigma_1 = \sigma_2 = \sigma_3 = 1$	20 per 1000 (41%)	12 per 1000 (41%)

Sensitivity analysis

As the model parameters capturing maternal immunity in unvaccinated children were based on a single study, we tested alternative assumptions. With a lower level of natural maternally-derived protection, we found that the impact of vaccination in the 0–2 month old age group was larger, with 33% and 41% of hospitalisations avoided for the reduced and no maternal immunity scenarios respectively, compared to 26% for the default scenario (Table 3). The impact on older age groups was minimal. By reducing the natural maternally-derived protection, the hospitalisation scaling factor in the 0–2 month old age group decreased, but the fitted parameters did not greatly change (Table S5).

Model outcomes were insensitive to changes in the level of transmission from individuals aged over ten years (Table S3). We also conducted the analysis for the default parameter set using models with a non-uniform age distribution, but found that the proportions of hospitalisations avoided changed only slightly (Figure S4 and Table S4). Finally, we repeated our analysis with the default parameter set, using a more finely stratified contact structure in children younger than five years of age, but the results did not change.

DISCUSSION

The introduction of a maternal vaccine for RSV, with similar coverage to that for existing maternal vaccination programs in WA, is likely to reduce the RSV hospitalisation burden in children younger than three months of age by 6–37%, and by approximately 30–46% in children between three and five months of age, for vaccine effectiveness levels between 60% and 90%. If both vaccine effectiveness and coverage are high, hospitalisations may be reduced by up to 51% and 63% in these two age groups respectively. For children six months and older, maternal vaccination had a negligible impact, indicating the herd immunity impact may be small. In our analysis, the percentage of RSV hospitalisations avoided was lower in the younger age group, due to natural maternally-derived immunity in the first three months of life. We also found that a maternal vaccine would be unlikely to change the biennial RSV infection pattern observed in WA.

An RSV intervention that prevents infection in young children would reduce the health system burden and cost during the winter months. One Australian study estimated that the median length of stay for a RSV hospitalisation is three days, and the mean cost of each RSV hospitalisation episode for children younger than five years is AUD 6350 [45]. Our study was based on data from a total population birth cohort of children born in WA during 1996–2012, and restricted to hospital admissions for ALRI. As RSV has also been detected in admissions without a diagnosis for ALRI [19], these data likely underrepresent the number of RSV hospitalisations in young children in WA, meaning the findings from our study are a conservative estimate of the true impact. A maternal vaccine for RSV would also provide broader health benefits; there is evidence that if an infant's first RSV episode is delayed, the risk of later respiratory issues such as asthma and wheezing may be reduced [3]. Further, in our model we did not incorporate a reduction in susceptibility to RSV for women protected by the maternal vaccine, due to a lack of information on the likely duration or protection mechanism of the vaccine in adults. With pregnant women forming only a small proportion of the population spread over a large age range, this assumption is unlikely to have influenced our findings, but may provide an additional health benefit. In addition, as this study focussed on avoided hospitalisations, the findings reported here do not account for the public health and economic benefit of reduced community-level RSV in young children arising from a vaccine.

Previous RSV vaccine mathematical modelling studies have focussed on infant and childhood vaccines in order to evaluate cost-effectiveness [9–11]. Other studies have considered the possible impact of RSV vaccines in the low income country setting of Kenya [8,15]. Poletti and colleagues used a stochastic individual-based modelling approach to simulate vaccine implementation for several key population groups, including pregnant women [15]. Their study, based on the social structure of rural Kenya, found that maternal vaccination could reduce RSV infection in infants by 31.5%, assuming a four month duration of natural maternally-derived immunity and an additional four months of vaccine-derived protection, and that for this vaccine strategy, the reduction in RSV infections was not greatly affected by sub-optimal coverage. While in our study we found that vaccine coverage is important, our model was for a different setting and assumed a different duration of protection.

Maternal vaccination is a realistic public health strategy and has been successfully implemented for other diseases such as influenza and pertussis. Mathematical models are instrumental in assessing the health and economic benefits of such an intervention, and are needed to aid decision-making about the cost-effectiveness of immunisation policies for different jurisdictions. A key strength of this study is that the model was validated using population-level linked data from WA, allowing a more accurate assessment of the vaccine impact. However, our model structure is also flexible enough that it can be adapted to account for the demography, hospitalisation data and contact patterns in other regions, to allow assessment of the likely vaccine impact elsewhere. This model can also be readily updated to incorporate information about vaccine characteristics as clinical trials progress.

While the importance of transplacental transfer of protective antibodies from a pregnant woman to her unborn child is known, there is a gap in understanding how maternal antibodies interact with the infant immune system, and the factors that influence the transfer and decay of

these antibodies [44]. Our parameters for maternally-derived immunity were based on a single seropositivity study [30], however, our parameter choices are broadly aligned with the current understanding about the duration and protectiveness of RSV-specific antibodies in neonates. A recent study of children in Kenya found that RSV-specific antibody seroprevalence was high in the first three months of life, with 100% of children in the study seropositive in the 0–<1 month age group, and 75% seropositive in the 2–<3 month age group [33]. We found that our model was sensitive to assumptions about maternal antibody protection, so we tested two reduced maternal protection scenarios (Tables 3 and S5). We found that reducing the level of natural maternally-derived protection increased the vaccine impact in 0–2 month old children, but did not greatly change the impact in the older age groups. We also found that the hospitalisation scaling parameter h_{0-2} decreased to 0.140 with no maternally-derived protection, meaning a smaller percentage of the modelled 0–2 month old infections resulted in a hospitalisation, compared to the much higher value of 0.424 in the default scenario. In many settings, the highest number of RSV hospitalisations is observed in 0–2 month old children compared to any other age group, yet this is the age group in which RSV-specific antibody seroprevalence is typically highest. It is possible that the infants in this age group who do become infected are much more likely to be hospitalised, but understanding this interaction, and considering how best to incorporate maternal antibody dynamics in models for RSV vaccines, is an area for ongoing research.

Our model was fitted to data for children under two years of age, therefore we needed to use other data to accurately parameterise the force of infection for older children and adults. We scaled the infectiousness for older individuals such that the age of the infector was consistent with observations from this birth cohort [40]. As the herd immunity effect due to a maternal vaccine is small in our model, we observed little impact of the contact structure in young children on our findings. By fitting the model to RSV data in children younger than two years, we ensured that the force of infection acting on infants reflects the available data, and we do not expect this force of infection to change noticeably following the implementation of a vaccine.

It is understood that an individual's susceptibility to RSV is dependent on both age and the history of infection. In our model we focussed on age as the main determinant of susceptibility, and introduced a parameter to scale susceptibility to infection in older age groups, although others have incorporated additional disease states in the modelling framework to account for initial and subsequent infections [8,13]. There is evidence that increasing age is more important than previous exposure to infection in influencing reduced susceptibility to disease in older infants and children [46]. Further, our focus was on infant RSV infections. We fitted to linked data on early-life infections with RSV and demonstrated that the model effectively captures hospitalisation risk in children under two years of age.

Our modelling framework incorporated only a single type of RSV vaccine intervention, based on the current information about RSV vaccine development progress. However, with a maternal RSV vaccine unlikely to offer protection to infants older than six months, it may be infeasible for this type of vaccine to exist as a standalone preventative strategy for RSV [44]. With vaccine candidates for infants, older children, and the elderly also in various stages of the

clinical trials pipeline, there is scope for further development of mathematical models to estimate the reduction in disease burden in other target population groups, and to assess the likely public health impact of combined vaccine interventions.

Acknowledgements: We thank the Linkage and Client Services Teams at the WA Data Linkage Branch, including Alexandra Merchant and Mikhalina Dombrovskaya, as well as custodians of all datasets used. We thank Charmaine Tonkin and Brett Cawley from PathWest Laboratory Medicine for their support for this study. We also thank Timothy Kinyanjui for helpful advice on the model structure and fitting.

Funding: This work was supported by a National Health and Medical Research Council (NHMRC) Project Grant (APP1045668), ANU University Research Scholarship (to ABH), NHMRC Centre of Research Excellence (APP1058804 to PTC), NHMRC Career Development Fellowship (APP1111596 to CCB), University of Western Australia Postgraduate Award (to FJL), and NHMRC Fellowship (APP1034254 to HCM).

Conflict of interest statement: ABH, PTC, CCB, FJL, SD, PF and HCM have no interests to disclose. KG reports grants from BioIntellect, outside the submitted work.

REFERENCES

[1] Nair H, Nokes DJ, Gessner BD, Dherani M, Madhi SA, Singleton RJ, et al. Global burden of acute lower respiratory infections due to respiratory syncytial virus in young children: a systematic review and meta-analysis. Lancet 2010;375:1545–55. doi:10.1016/S0140-6736(10)60206-1.

[2] Brandenburg AH, Groen J, van Steensel-Moll HA, Claas EC, Rothbarth PH, Neijens HJ, et al. Respiratory syncytial virus specific serum antibodies in infants under six months of age: limited serological response upon infection. J Med Virol 1997;52:97–104.

[3] Saso A, Kampmann B. Vaccination against respiratory syncytial virus in pregnancy: a suitable tool to combat global infant morbidity and mortality? Lancet Infect Dis 2016;16:e153–63. doi:10.1016/S1473-3099(16)00119-5.

[4] Roberts JN, Graham BS, Karron RA, Munoz FM, Falsey AR, Anderson LJ, et al. Challenges and opportunities in RSV vaccine development: meeting report from FDA/NIH workshop. Vaccine 2016;34:4843–9. doi:10.1016/j.vaccine.2016.07.057.

[5] PATH. RSV Vaccine and mAb Snapshot 2017. http://www.path.org/publications/files/CVIA_rsv_snapshot_final.pdf (accessed June 6, 2017).

[6] ClinicalTrials.gov. A Study to Determine the Safety and Efficacy of the RSV F Vaccine to Protect Infants Via Maternal Immunization 2016.

[7] Jorquera PA, Anderson L, Tripp RA. Understanding respiratory syncytial virus (RSV) vaccine development and aspects of disease pathogenesis. Expert Rev Vaccines 2015;15:173–87. doi:10.1586/14760584.2016.1115353.

[8] Kinyanjui TM, House TA, Kiti MC, Cane PA, Nokes DJ, Medley GF. Vaccine induced herd immunity for control of respiratory syncytial virus disease in a low-income country setting. PLoS One 2015;10:e0138018. doi:10.1371/journal.pone.0138018.

[9] Acedo L, Moraño J-A, Díez-Domingo J. Cost analysis of a vaccination strategy for respiratory syncytial virus (RSV) in a network model. Math Comput Model 2010;52:1016–22. doi:10.1016/j.mcm.2010.02.041.

[10] Bos JM, Rietveld E, Moll HA, Steyerberg EW, Luytjes W, Wilschut JC, et al. The use of health economics to guide drug development decisions: Determining optimal values for an RSV-vaccine in a model-based scenario-analytic approach. Vaccine 2007;25:6922–9. doi:10.1016/j.vaccine.2007.07.006.

[11] Meijboom MJ, Rozenbaum MH, Benedictus A, Luytjes W, Kneyber MCJ, Wilschut JC, et al. Cost-effectiveness of potential infant vaccination against respiratory syncytial virus infection in The Netherlands. Vaccine 2012;30:4691–700. doi:10.1016/j.vaccine.2012.04.072.

[12] Acedo L, Díez-Domingo J, Moraño J-A, Villanueva R-J. Mathematical modelling of respiratory syncytial virus (RSV): vaccination strategies and budget applications. Epidemiol Infect 2010;138:853–60. doi:10.1017/S0950268809991373.

[13] Yamin D, Jones FK, DeVincenzo JP, Gertler S, Kobiler O, Townsend JP, et al. Vaccination strategies against respiratory syncytial virus. Proc Natl Acad Sci 2016:1–6. doi:10.1073/pnas.1522597113.

[14] Pan-Ngum W, Kinyanjui T, Kiti M, Taylor S, Toussaint J-F, Saralamba S, et al. Predicting the relative impacts of maternal and neonatal respiratory syncytial virus (RSV) vaccine target product profiles: A consensus modelling approach. Vaccine 2016;35:1–7. doi:10.1016/j.vaccine.2016.10.073.

[15] Poletti P, Merler S, Ajelli M, Manfredi P, Munywoki PK, Nokes JD, et al. Evaluating vaccination strategies for reducing infant respiratory syncytial virus infection in low-income settings. BMC Med 2015;13:1–11. doi:10.1186/s12916-015-0283-x.

[16] Hogan A, Anderssen R, Davis S, Moore H, Lim F, Fathima P, et al. Time series analysis of RSV and bronchiolitis seasonality in temperate and tropical Western Australia. Epidemics 2016;16:49–55. doi:10.1016/j.epidem.2016.05.001.

[17] Holman CDJ, Bass AJ, Rouse IL, Hobbs MST. Population-based linkage of health records in Western Australia: development of a health services research linked database. Aust N Z J Public Health 1999;23:453–9. doi:10.1111/j.1467-842X.1999.tb01297.x.

[18] Moore HC, de Klerk N, Keil AD, Smith DW, Blyth CC, Richmond P, et al. Use of data linkage to investigate the aetiology of acute lower respiratory infection hospitalisations in children. J Paediatr Child Health 2011;48:520–8. doi:10.1111/j.1440-1754.2011.02229.x.

[19] Lim FJ, Blyth CC, Keil AD, De Klerk N, Moore HC. Using record linkage to examine testing patterns for respiratory viruses among children born in Western Australia. Epidemiol Infect 2017:1–11. doi:10.1017/S0950268817000413.

[20] Australian Bureau of Statistics. 3235.0 - Population by Age and Sex, Regions of Australia 2014. http://www.abs.gov.au/AUSSTATS/abs@.nsf/allprimarymainfeatures/DAD34AA83C48279ACA25801200168437?opendocument (accessed September 12, 2016).

[21] Hogan AB, Glass K, Moore HC, Anderssen R. Exploring the dynamics of respiratory syncytial virus (RSV) transmission in children. Theor Popul Biol 2016;110:78–85. doi:10.1016/j.tpb.2016.04.003.

[22] Moore HC, Jacoby P, Hogan AB, Blyth CC, Mercer GN. Modelling the seasonal epidemics of

respiratory syncytial virus in young children. PLoS One 2014;9:e100422. doi:10.1371/journal.pone.0100422.

[23] Keeling MJ, Rohani P. Modeling Infectious Diseases in Humans and Animals. United States and United Kingdom: Princeton University Press; 2008.

[24] Brisson M, Melkonyan G, Drolet M, De Serres G, Thibeault R, De Wals P. Modelling the impact of one- and two-dose varicella vaccination on the epidemiology of varicella and zoster. Vaccine 2010;28:3385–97. doi:10.1016/j.vaccine.2010.02.079.

[25] Schenzle D. An Age-Structured Model of Pre- and Post-Vaccination Measles Transmission. IMA J Math Appl Med Biol 1984;1:169–91.

[26] Lessler J, Reich NG, Brookmeyer R, Perl TM, Nelson KE, Cummings DA. Incubation periods of acute respiratory viral infections: a systematic review. Lancet Infect Dis 2009;9:291–300. doi:10.1016/S1473-3099(09)70069-6.

[27] Weber A, Weber M, Milligan P. Modeling epidemics caused by respiratory syncytial virus (RSV). Math Biosci 2001;172:95–113.

[28] Leecaster M, Gesteland P, Greene T, Walton N, Gundlapalli A, Rolfs R, et al. Modeling the variations in pediatric respiratory syncytial virus seasonal epidemics. BMC Infect Dis 2011;11:105. doi:10.1186/1471-2334-11-105.

[29] Piedra PA, Munoz FM. The significance of transplacental antibody against respiratory syncytial virus. J Infect Dis 2014;210:1526–8. doi:10.1093/infdis/jiu323.

[30] Cox MJ, Azevedo RS, Cane PA, Massad E, Medley GF. Seroepidemiological study of respiratory syncytial virus in São Paulo state, Brazil. J Med Virol 1998;55:234–9.

[31] Ochola R, Sande C, Fegan G, Scott PD, Medley GF, Cane PA, et al. The level and duration of RSV-specific maternal IgG in infants in kilifi Kenya. PLoS One 2009;4:4–9. doi:10.1371/journal.pone.0008088.

[32] Hacimustafaoglu M, Celebi S, Aynaci E, Sinirtas M, Koksal N, Kucukerdogan A, et al. The progression of maternal RSV antibodies in the offspring. Arch Dis Child 2004;89:52–3. doi:10.1136/adc.2002.017780.

[33] Nyiro JU, Kombe IK, Sande CJ, Kipkoech J, Kiyuka K, Onyango CO, et al. Defining the vaccination window for respiratory syncytial virus (RSV) using age-seroprevalence data for children in Kilifi, Kenya. PLoS One 2017:1–14.

[34] Falsey AR, Walsh EE. Respiratory syncytial virus infection in adults. Clin Microbiol Rev 2000;13:371–84.

[35] Heikkinen T, Valkonen H, Waris M, Ruuskanen O. Transmission of respriatory syncytial virus within families. Open Forum Infect Dis 2015;2:1–6. doi:10.1093/ofid/ofu11.

[36] Munywoki PK, Koech DC, Agoti CN, Lewa C, Cane P a, Medley GF, et al. The source of respiratory syncytial virus infection in infants: a household cohort study in rural Kenya. J Infect Dis 2014;209:1685–92. doi:10.1093/infdis/jit828.

[37] Mossong J, Hens N, Jit M, Beutels P, Auranen K, Mikolajczyk R, et al. Social contacts and mixing patterns relevant to the spread of infectious diseases. PLoS Med 2008;5:e74. doi:10.1371/journal.pmed.0050074.

[38] Fumanelli L, Ajelli M, Manfredi P, Vespignani A, Merler S. Inferring the Structure of Social Contacts from Demographic Data in the Analysis of Infectious Diseases Spread. PLoS Comput Biol 2012;8:35–9. doi:10.1371/journal.pcbi.1002673.

[39] MATLAB and Statistics Toolbox Release 2012b n.d.

[40] Jacoby P, Glass K, Moore HC. Characterizing the risk of respiratory syncytial virus in infants with older siblings: a population-based birth cohort study. Epidemiol Infect 2016;145:266–71. doi:10.1017/S0950268816002545.

[41] Government of Western Australia Department of Health. Western Australian Immunisation Strategy 2016-2020. 2016.

[42] Openshaw PJM, Chiu C, Culley FJ, Johansson C. Protective and Harmful Immunity to RSV Infection. Annu Rev Immunol 2017;35:annurev-immunol-051116-052206. doi:10.1146/annurev-immunol-051116-052206.

[43] Modjarrad K, Giersing B, Kaslow DC, Smith PG, Moorthy VS. WHO consultation on Respiratory Syncytial Virus Vaccine Development Report from a World Health Organization Meeting held on 23-24 March 2015. Vaccine 2015;34:190–7. doi:10.1016/j.vaccine.2015.05.093.

[44] Heath PT, Culley FJ, Jones CE, Kampmann B, Le Doare K, Nunes MC, et al. Group B streptococcus and respiratory syncytial virus immunisation during pregnancy: A landscape analysis. Lancet Infect Dis 2017;3099:1–12. doi:10.1016/S1473-3099(17)30232-3.

[45] Homaira N, Oei J-L, Mallitt K-A, Abdel-Latif ME, Hilder L, Bajuk B, et al. High burden of RSV hospitalization in very young children: a data linkage study. Epidemiol Infect 2015;144:1612–21. doi:10.1017/S0950268815003015.

[46] Ohuma EO, Okiro EA, Ochola R, Sande CJ, Cane PA, Medley GF, et al. The natural history of respiratory syncytial virus in a birth cohort: the influence of age and previous infection on reinfection and disease. Am J Epidemiol 2012;176:794–802. doi:10.1093/aje/kws257.

Supplementary Material

Potential impact of a maternal vaccine for RSV: a mathematical modelling study

Alexandra B Hogan*, Patricia T Campbell, Christopher C Blyth, Faye J Lim, Parveen Fathima, Stephanie Davis, Hannah C Moore†, Kathryn Glass†

*Corresponding author, †Joint senior authors

S1. Model equations

The overall modelling approach was to fit the RSV transmission model (the 'base model') to data, introduce a maternal vaccine (the 'vaccination model'), and compare the outputs of these two models for a range of scenarios. The equations below describe the base and vaccination models respectively. In the equations, S_i represents the number of susceptible individuals in age class i, E_i represents the number of exposed individuals, I_i represents the number of infectious individuals, R_i represents the number of recovered and temporarily immune individuals, and V_i represents the number of vaccinated individuals. The parameters are defined in Table S1.

Cohort ageing was implemented such that at the end of each month, a proportion of each age group was instantaneously moved to the next age group [8, 15]. The models were implemented in MATLAB, using the inbuilt *ode45* equation solver [17]. Numerically, cohort ageing was implemented by updating the initial conditions at fixed time points.

Base model equations

The continuous time dynamics in the base model are represented by the following equations.

$$\begin{aligned}
\frac{dS_i}{dt} &= -\lambda_i \sigma_i S_i + \nu R_i \\
\frac{dE_i}{dt} &= \lambda_i \sigma_i S_i - \delta E_i \\
\frac{dI_i}{dt} &= \delta E_i - \gamma I_i \\
\frac{dR_i}{dt} &= \gamma I_i - \nu R_i \\
\lambda_i &= b_0(1 + b_1 \cos(\frac{2\pi t}{12} + \phi))\frac{1}{N_i}\sum_{j=1}^{75} M_{i,j}\omega_j I_j
\end{aligned}$$

The transmission function $\lambda_i(t)$ represents the force of infection on age group i over time t, where the indices i and j represent the 75 age cohorts; b_0 represents overall transmission; b_1 represents the amplitude of seasonal forcing; ϕ represents the phase shift; ω_j represents reduced infectiousness in age group j; and the mixing matrix $M_{i,j}$ represents the number of contacts the number of contacts that an individual in age class j has with individuals in age class i.

Ageing is not represented in the differential equations as it is a discontinuous event that takes place each month. Instead, ageing was implemented by updating the initial conditions of the ordinary differential equations (ODEs) each month as follows.

$$\begin{aligned}
&S_i = N/(80 \times 12), E_i = I_i = R_i = 0, && \text{if } i = 1 \\
&Q_i = Q_{i-1}, && \text{if } 2 \leq i \leq 60 \\
&Q_i = Q_i + Q_{i-1} - Q_i/60, && \text{if } i = 61 \\
&Q_i = Q_i + Q_{i-1}/60 - Q_i/60, && \text{if } 62 \leq i \leq 75 \\
&\text{where } Q_i \in \{S_i, E_i, I_i, R_i\}
\end{aligned}$$

The mixing matrix $M_{i,j}$ was created using data from the POLYMOD study, using all reported contacts (physical and non-physical) for Great Britain [13]. Let $K_{i,j}$ denote the POLYMOD matrix. The matrix $K_{i,j}$ was made symmetric by averaging the non-diagonal values of the matrix, so that

$$L_{i,j} = \frac{K_{i,j} + K_{j,i}}{2}$$

as in Brisson et al [3]. Since the age classes in the POLYMOD matrices are in groups of five years, we adapted the contact matrix to match the age structure in our model. The following equations describe this process.

$$\begin{aligned}
M_{i,j} &= L_{1,1}/60, && \text{if } 1 \le i \le 60,\ 1 \le j \le 60 \\
M_{i,j} &= L_{i-59,j-59}, && \text{if } 61 \le i \le 75,\ 61 \le j \le 75 \\
M_{i,j} &= L_{i-59,1}, && \text{if } 61 \le i \le 75,\ 1 \le j \le 60 \\
M_{i,j} &= L_{i-59,1}/60, && \text{if } 1 \le i \le 60,\ 61 \le j \le 75
\end{aligned}$$

Finally, the matrix was transposed and daily values were converted to monthly.

Vaccination model equations

The continuous time dynamics are represented by the following equations.

$$\begin{aligned}
\frac{dS_i}{dt} &= -\lambda_i \sigma_i S_i + \nu R_i \\
\frac{dE_i}{dt} &= \lambda_i \sigma_i S_i + \lambda_i (1-\rho_i) V_i - \delta E_i \\
\frac{dI_i}{dt} &= \delta E_i - \gamma I_i \\
\frac{dR_i}{dt} &= \gamma I_i - \nu R_i \\
\frac{dV_i}{dt} &= -\lambda_i (1-\rho_i) V_i \\
\lambda_i &= b_0 (1 + b_1 \cos(\frac{2\pi t}{12} + \phi)) \frac{1}{N_i} \sum_{j=1}^{75} M_{i,j} \omega_j I_j
\end{aligned}$$

Ageing was implemented according to the following routine.

$$\begin{aligned}
&S_i = (1-\kappa)N/(80 \times 12), \\
&E_i = I_i = R_i = 0, && \text{if } i = 1 \\
&V = \kappa N/(80 \times 12), \\
&Q_i = Q_{i-1}, && \text{if } 2 \le i \le p_{vacc} \\
&S_i = S_{i-1}/60 + S_i - S_i/60 + V_{i-1}, \\
&E_i = E_{i-1},\ I_i = I_{i-1}, && \text{if } i = p_{vacc+1} \\
&R_i = R_{i-1},\ V_i = 0, \\
&Q_i = Q_{i-1}, && \text{if } p_{vacc+2} \le i \le 60 \\
&Q_i = Q_i + Q_{i-1} - Q_i/60, && \text{if } i = 61 \\
&Q_i = Q_i + Q_{i-1}/60 - Q_i/60, && \text{if } 62 \le i \le 75
\end{aligned}$$

$$\text{where } Q_i \in \{S_i, E_i, I_i, R_i\}$$

In the first three one-month cohorts, susceptible individuals are either in the vaccinated class, with some vaccine protection, or in the non-vaccinated susceptible class, with some natural maternal antibody protection. It follows that a vaccinated individual cannot be less well protected than if they had not been vaccinated. Therefore, in the numerical model formulation, we included the condition that the maternal vaccine must be

at least as protective for infants as naturally-derived maternal antibodies.

Model outputs over a ten-year time period, showing the number of modelled infectious individuals in the 0–2 and 3–5 month age groups, are shown in Figure S1.

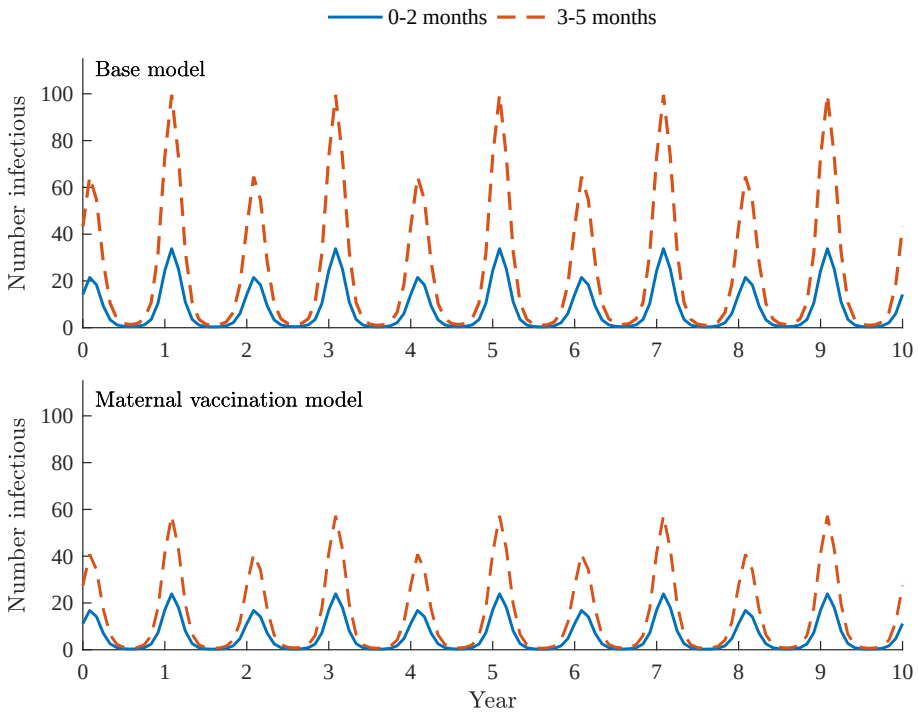

Figure S1: Model outputs for the number of infectious individuals in the 0–2 month and 3–5 month age classes, for the base and vaccination models, over a ten year time period for the default parameter set. Both the base and vaccination models display biennial dynamics. Note that this output shows the number of infectious individuals at each time point, rather than the modelled incidence.

S2. Model fitting and validation

We fitted three parameters b_0, b_1, and ϕ to the data using maximum likelihood estimation. To derive our fitting function, we assumed that the number of RSV-related hospitalisations each month followed a Poisson distribution. Using simplified notation, if we define the likelihood of observing x hospitalisations when our model generated y hospitalisations, the likelihood would be

$$L(x, y) = \frac{e^{-y} y^x}{x!}.$$

The likelihood of observing the entire set of hospitalisations data is the product of the likelihoods for each of the n data points:

$$L = L_1 L_2 ... L_n.$$

The log likelihood is then

$$\begin{aligned}
\log L &= \log L_1 + \log L_2 + ... + \log L_n \\
&= -y_1 + x_1 \log y_1 - \log(x_1!) - y_2 + x_2 \log y_2 - \log(x_2!) - ... - y_n + x_n \log y_n - \log(x_n!) \\
&= \sum_{i=1}^{n} (-y_i + x_i \log y_i - \log(x_i!)).
\end{aligned}$$

In practice, the $-\log(x_i!)$ term can be ignored as it is not dependent on the model output. Also, rather than maximising the log likelihood function, is can be numerically simpler to instead minimise the negative log likelihood function, which is the approach taken below.

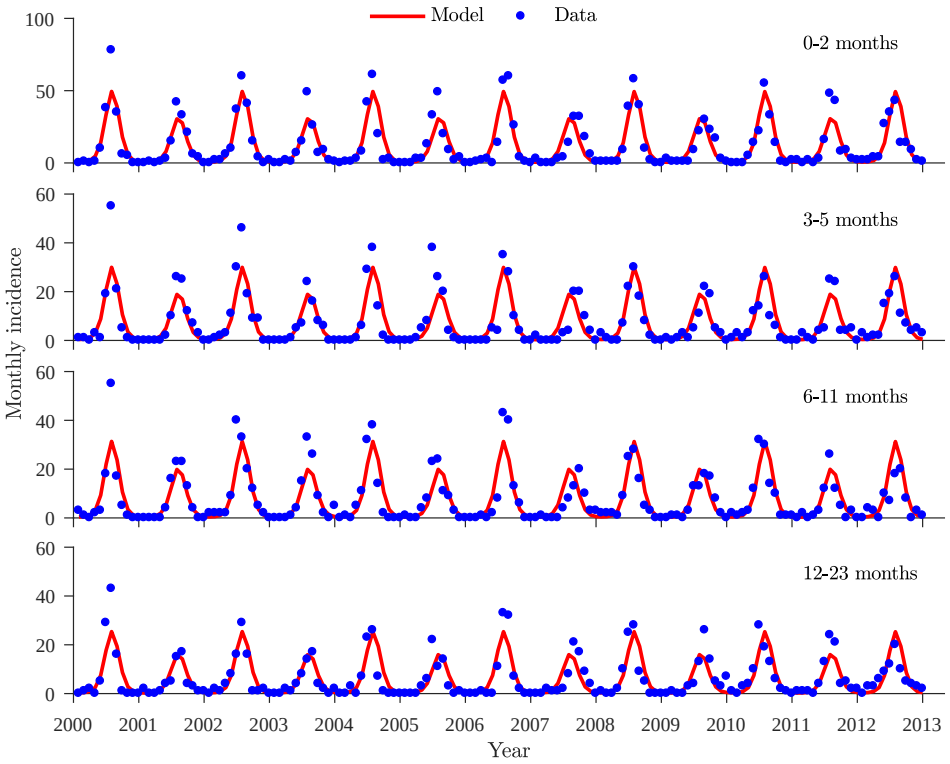

Figure S2: The model fitted to the RSV hospitalisation data for four age groups younger than 24 months of age with default parameters ($\omega = 0.6$). Data is shown with blue dots and model output with red lines.

Using the notation of our model, the negative log likelihood function is

$$F = -\sum_{k=1}^{4}\sum_{m=1}^{n}(\text{data}_{k,m} \times \log(\text{model}_{k,m}) - \text{model}_{k,m}).$$

In this function, $\text{data}_{k,m}$ is the number of RSV hospitalisations in children in group k at month m, and $\text{model}_{k,m}$ represents the model outcome, which is the modelled incidence for age group k at month m, multiplied by h_k, the sum of all cases in the data divided by the sum of the modelled incidence. The subscript k denotes the four age classes 0–2 months, 3–5 months, 6–11 months and 12–23 months. The parameter h_k therefore represents the proportion of infections that are hospitalised in that age group.

At first, we attempted to include the reduced infectiousness parameter as a fourth fitted parameter using the fitting routine described above. However, we found that the model would fit the data well for any of a range of plausible values of . Therefore, we used a different approach to estimate ω. In a study of subcohort data extracted the same birth cohort from which our RSV-related hospitalisation data was derived, it was estimated that 45% of the RSV detections in that subcohort were attributable to infection from an older sibling [8]. We ran the fitting routine with only three fitted parameters (b_0, b_1, and ϕ) for different fixed values of ω. We then compared the model output to estimates derived from our cohort of the proportion of infections that were due to an elder sibling as follows. For each fitted parameter set and for each of five age groups (0–23 months, 2–14 years, 15–24 years, 25–44 years, and 45–79 years), we calculated the proportion of infections arising from their own and the other four age groups. Considering the proportion of infected 0–23 month old children who were infected by an individual 2–14 years of age, we estimated that $\omega = 0.6$ most closely reflected the estimate of 45% (Figure S1). The susceptible/infectious tables are shown in Table S2.

Table S1:Parameter values for the 75 cohort model, for selected values of the reduced infectiousness parameter ω, with default values highlighted. Rates in the model are in months.

Parameter	Definition	Fixed/ Fitted	Value				Ref.
ω	Reduced infectiousness in older age groups	Fixed	0.5	0.6	0.7	0.8	
$1/\delta$	Latent period (days)	Fixed	4	4	4	4	[11, 16]
$1/\gamma$	Infectious period (days)	Fixed	9	9	9	9	[1, 10, 16]
$1/\nu$	Immunity period (days)	Fixed	230	230	230	230	[6]
σ_1	Reduced susceptibility due to natural maternal immunity first month	Fixed	0.08	0.08	0.08	0.08	[4]
σ_2, σ_3	Reduced susceptibility due to natural maternal immunity second and third months	Fixed	0.45	0.45	0.45	0.45	[4]
N	Total population of Greater Perth for ages 0–79 years	Fixed	1,861,923	1,861,923	1,861,923	1,861,923	[2]
κ	Vaccine coverage	Fixed	0.5	0.5	0.5	0.5	[5]
$1-\rho_i$, $i \leq p_{vacc}$	Reduced susceptibility due to vaccine	Fixed	0.2	0.2	0.2	0.2	
$1-\rho_i$, $i > p_{vacc}$	Reduced susceptibility due to vaccine	Fixed	1	1	1	1	
p_{vacc}	Maximum duration of vaccine-induced protection in months	Fixed	6	6	6	6	[9, 14]
b_0	Transmission rate	Fitted	0.017	0.015	0.014	0.013	
b_1	Amplitude of seasonal forcing	Fitted	0.389	0.397	0.398	0.407	
ϕ	Phase of seasonal forcing function	Fitted	0.977	0.985	0.981	0.984	
h_{0-2}	Proportion of modelled infections leading to hospitalisation in the 0–2 month age group		0.459	0.424	0.412	0.413	
h_{3-5}	Proportion of modelled infections leading to hospitalisation in the 3–5 month age group		0.095	0.088	0.086	0.086	
h_{6-11}	Proportion of modelled infections leading to hospitalisation in the 6–11 month age group		0.051	0.047	0.046	0.046	
h_{12-23}	Proportion of modelled infections leading to hospitalisation in the 12–23 month age group		0021	0.020	0.019	0.019	

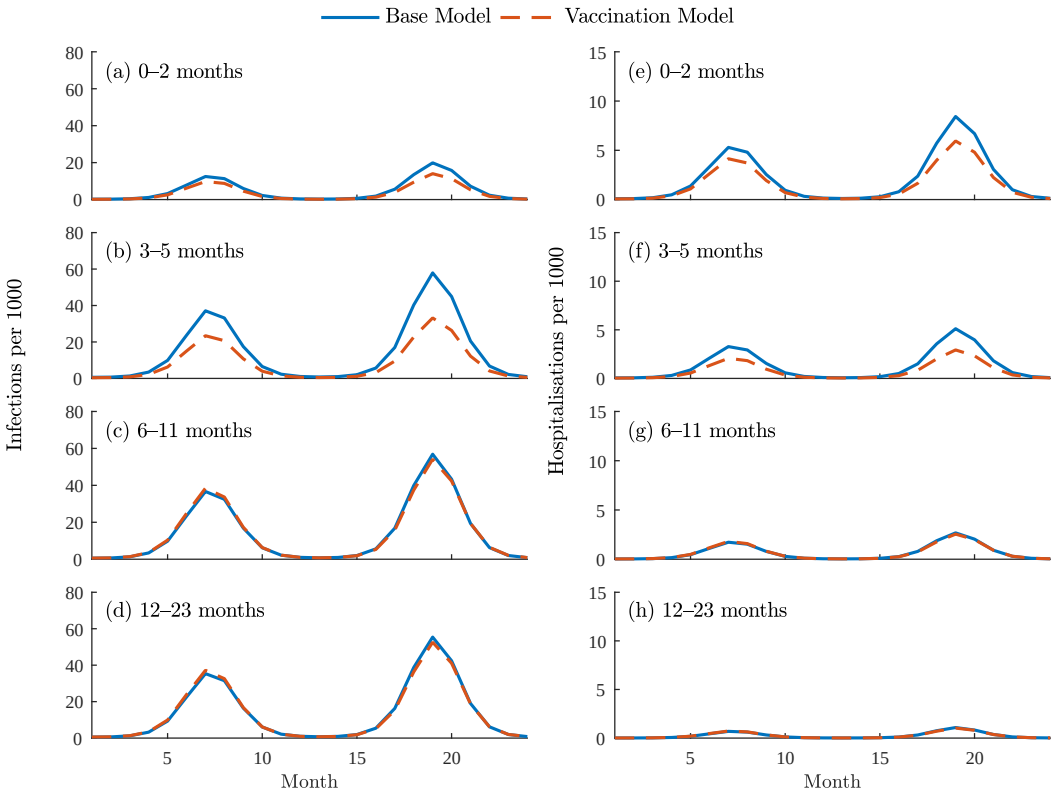

Figure S3: Comparison of the modelled number of RSV infections (panels (a) to (d)) and hospitalisations (panels (e) to (h)) per month in key age groups, per 1000 children in that age group, over a time period of 24 months, in the base model (the blue line) and the vaccination model (the red dashed line), for the default parameter set.

Table S2: Percentage of the total number of infections within each susceptible age group, arising from each infectious age group, for the parameter sets for different values of the reduced infectiousness parameter ω. The parameter set with $\omega = 0.6$ was chosen as most closely reflecting the data, based on the proportion of susceptible 0–23 month individuals infected by a 2–14 year individual (45%).

		Infectious				
		0–23m	2–14y	15–24y	25–44y	45–79y
Susceptible	$\omega = 0.5$					
	0–23m	10%	51%	6%	25%	8%
	2–14y	2%	74%	5%	14%	5%
	15–24y	1%	23%	41%	22%	13%
	25–44y	3%	38%	11%	31%	17%
	45–79y	2%	22%	11%	30%	35%
	$\omega = 0.6$					
	0–23m	9%	45%	7%	29%	10%
	2–14y	2%	69%	6%	16%	6%
	15–24y	1%	19%	44%	22%	14%
	25–44y	3%	32%	12%	33%	20%
	45–79y	1%	18%	12%	30%	38%
	$\omega = 0.7$					
	0–23m	8%	40%	9%	32%	11%
	2–14y	8%	66%	7%	18%	7%
	15–24y	1%	16%	46%	22%	15%
	25–44y	2%	28%	13%	35%	21%
	45–79y	1%	16%	13%	31%	40%
	$\omega = 0.8$					
	0–23m	8%	37%	9%	34%	12%
	2–14y	2%	63%	8%	20%	8%
	15–24y	1%	14%	47%	22%	15%
	25–44y	2%	25%	14%	36%	23%
	45–79y	1%	14%	13%	31%	42%

S3. Sensitivity analysis

Reduced infectiousness of older children

We tested the sensitivity of the model outcome to changes in the reduced infectiousness of children ten years and older (Table S3). The analysis showed that the model outcome was not very sensitive to changes in this parameter, producing a reduction in hospitalisations approximately equivalent to that in the default parameter scenario.

Table S3: Results of the sensitivity analysis for the reduced infectiousness parameter ω compared to the default parameter scenario. The model outcome is the avoided hospitalisations over a 24 month represented as the number of avoided hospitalisations per 1,000 children in that age group, and as a percentage reduction.

Scenario	0–2 month age group per 1000 (percentage reduction)	3–5 month age group per 1000 (percentage reduction)
Default ($\omega = 0.6$)	13 per 1000 (26%)	12 per 1000 (40%)
$\omega = 0.4$	13 per 1000 (27%)	12 per 1000 (41%)
$\omega = 0.5$	13 per 1000 (27%)	12 per 1000 (40%)
$\omega = 0.7$	13 per 1000 (26%)	12 per 1000 (40%)
$\omega = 0.8$	13 per 1000 (26%)	12 per 1000 (40%)

Age distribution

We assumed a uniform age distribution for the main model simulations. Therefore, we also ran the simulations for the default parameter set with a non-uniform distribution, based on data for the population of Greater Perth in 2014 [14]. The different distributions are shown in Figure S4. While the number of people in each cohort varied according to the population distribution data, a fixed number of people moved each month in the cohort ageing process, so that the total population did not change. We found that there was almost no change in the model outcome for the non-uniformly distributed population (Table S4), therefore we retained a uniform distribution for the main analysis for simplicity.

Table S4: Avoided hospitalisations over a 24 month period for the model with a non-uniform population age distribution, compared to the model with a uniformly distributed population. Both scenarios are based on the default parameter set.

Scenario	0–2 month age group per 1000 (percentage reduction)	3–5 month age group per 1000 (percentage reduction)
Uniform population distribution	13 per 1000 (26%)	12 per 1000 (40%)
Non-uniform population distribution	12 per 1000 (26%)	11 per 1000 (40%)

Maternally-derived immunity

The parameters representing reduced susceptibility to infection due to natural maternally-derived immunity were based on a single study. We therefore tested perfect maternally-derived immunity (with $\sigma_1 = \sigma_2 = \sigma_3 = 0$), but were unable to fit this model to our data, which includes RSV infections in children younger than three months. We also ran the model assuming a lower level of natural maternally-derived protection, and for a scenario with no naturally-derived maternal immunity. We found that the fitted hospitalisation scaling parameter h_{0-2} decreased in accordance with the higher susceptibility to infection in children younger than three months, and that with a lower level of naturally-derived maternal immunity, there was an increased vaccine impact in the youngest age cohort. The impact on children in the 3–5 month cohort did not change (Tables 3 and S5).

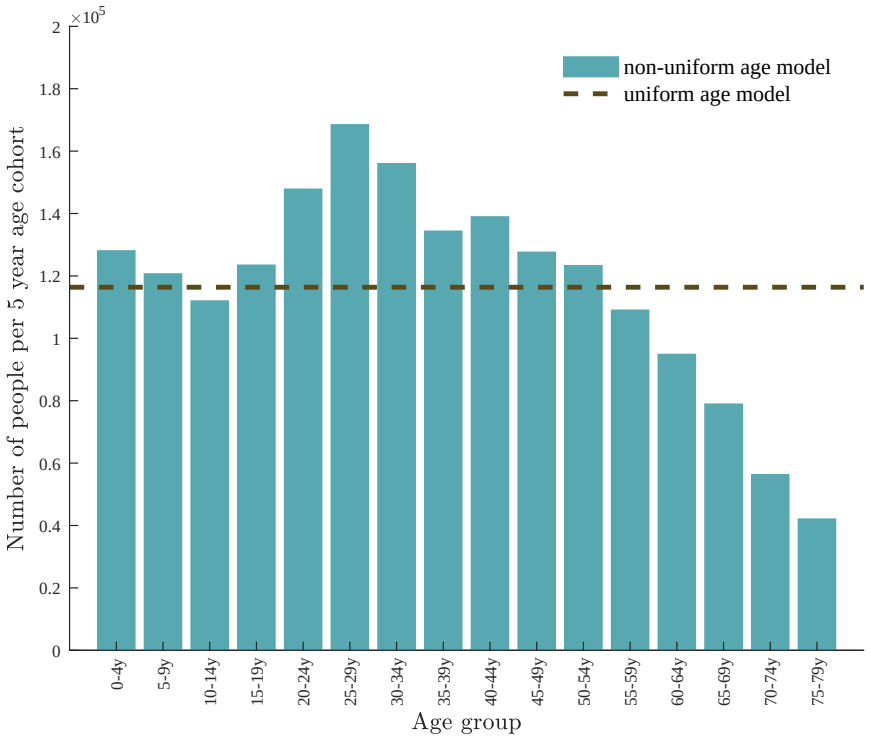

Figure S4: Number of individuals per five year age cohort in the uniform age model (the dashed line) compared to the non-uniform age model (the blue bars).

Table S5: Parameter values for the 75 cohort model with maternal vaccination, for the scenarios with lower natural maternally-derived immunity. Fixed parameters not described here have the values listed in Table S1.

Parameter	Definition	Fixed/ Fitted	Value		
			Default	Reduced maternal immunity	No maternal immunity
σ_1	Reduced susceptibility due to natural maternal immunity first month	Fixed	0.08	0.25	1
σ_2	Reduced susceptibility due to natural maternal immunity second month	Fixed	0.45	0.65	1
σ_3	Reduced susceptibility due to natural maternal immunity third month	Fixed	0.45	0.65	1
ω	Reduced infectiousness	Fixed	0.6	0.6	0.6
b_0	Transmission rate	Fitted	0.015	0.015	0.015
b_1	Amplitude of seasonal forcing	Fitted	0.397	0.393	0.393
ϕ	Phase of seasonal forcing function	Fitted	0.985	0.978	0.974
h_{0-2}	Proportion of modelled infections leading to hospitalisation in the 0–2 month age group		0.424	0.252	0.140
h_{3-5}	Proportion of modelled infections leading to hospitalisation in the 3–5 month age group		0.088	0.088	0.089
h_{6-11}	Proportion of modelled infections leading to hospitalisation in the 6–11 month age group		0.047	0.047	0.047
h_{12-23}	Proportion of modelled infections leading to hospitalisation in the 12–23 month age group		0.020	0.019	0.019

References

[1] Acedo L, Morao J-A, Dez-Domingo J. Cost analysis of a vaccination strategy for respiratory syncytial virus (RSV) in a network model. *Math Comput Model* 2010;52:101622. doi:10.1016/j.mcm.2010.02.041.

[2] Australian Bureau of Statistics. 3235.0 - Population by Age and Sex, Regions of Australia 2014. http://www.abs.gov.au/AUSSTATS/abs@.nsf/allprimarymainfeatures/DAD34AA83C48279ACA25801200168437?opendocument (accessed September 12, 2016).

[3] Brisson M, Melkonyan G, Drolet M, De Serres G, Thibeault R, De Wals P. Modelling the impact of one- and two-dose varicella vaccination on the epidemiology of varicella and zoster. *Vaccine* 2010;28:338597. doi:10.1016/j.vaccine.2010.02.079.

[4] Cox MJ, Azevedo RS, Cane PA, Massad E, Medley GF. Seroepidemiological study of respiratory syncytial virus in So Paulo state, Brazil. *J Med Virol* 1998;55:2349.

[5] Government of Western Australia Department of Health. *Western Australian Immunisation Strategy 2016-2020*. 2016.

[6] Hogan AB, Glass K, Moore HC, Anderssen R. Exploring the dynamics of respiratory syncytial virus (RSV) transmission in children. *Theor Popul Biol* 2016;110:7885. doi:10.1016/j.tpb.2016.04.003.

[7] Jacoby P, Glass K, Moore HC. Characterizing the risk of respiratory syncytial virus in infants with older siblings: a population-based birth cohort study. Epidemiol Infect 2016;145:26671. doi:10.1017/S0950268816002545.

[8] Keeling MJ, Rohani P. *Modeling Infectious Diseases in Humans and Animals*. United States and United Kingdom: Princeton University Press; 2008.

[9] Kinyanjui TM, House TA, Kiti MC, Cane PA, Nokes DJ, Medley GF. Vaccine induced herd immunity for control of respiratory syncytial virus disease in a low-income country setting. *PLoS ONE* 2015;10:e0138018. doi:10.1371/journal.pone.0138018.

[10] Leecaster M, Gesteland P, Greene T, Walton N, Gundlapalli A, Rolfs R, et al. Modeling the variations in pediatric respiratory syncytial virus seasonal epidemics. *BMC Infect Dis* 2011;11:105. doi:10.1186/1471-2334-11-105.

[11] Lessler J, Reich NG, Brookmeyer R, Perl TM, Nelson KE, Cummings DA. Incubation periods of acute respiratory viral infections: a systematic review. *Lancet Infect Dis* 2009;9:291300. doi:10.1016/S1473-3099(09)70069-6.

[12] Moore HC, Jacoby P, Hogan AB, Blyth CC, Mercer GN. Modelling the seasonal epidemics of respiratory syncytial virus in young children. *PLoS ONE* 2014;9:e100422. doi:10.1371/journal.pone.0100422.

[13] Mossong J, Hens N, Jit M, Beutels P, Auranen K, Mikolajczyk R, et al. Social contacts and mixing patterns relevant to the spread of infectious diseases. *PLoS Med* 2008;5:e74. doi:10.1371/journal.pmed.0050074.

[14] Poletti P, Merler S, Ajelli M, Manfredi P, Munywoki PK, Nokes JD, et al. Evaluating vaccination strategies for reducing infant respiratory syncytial virus infection in low-income settings. *BMC Med* 2015;13:111. doi:10.1186/s12916-015-0283-x.

[15] Schenzle D. An Age-Structured Model of Pre- and Post-Vaccination Measles Transmission. *IMA J Math Appl Med Biol* 1984;1:16991.

[16] Weber A, Weber M, Milligan P. Modeling epidemics caused by respiratory syncytial virus (RSV). *Math Biosci* 2001;172:95113.

[17] The Mathworks, Inc. MATLAB and Statistics Toolbox Release 2012b.

8

Discussion and conclusion

The objective of this research was to use mathematical models to investigate the seasonal patterns of respiratory syncytial virus (RSV) in Western Australia. In the first stages of this project, I developed simple age-structured compartmental models and fitted these models to data (Chapter 4). I performed numerical analyses to quantify and visualise the broad range of model dynamics, and related these outputs to observed patterns in different regions (Chapter 5). I then conducted a time series analysis of data for Western Australia to identify seasonal patterns in tropical and temperate regions. I also captured changes in the yearly epidemics of respiratory illness in children from year to year in terms of the timing and magnitude of the epidemic peak (Chapter 6). Finally, I extended these models to incorporate a finer age structure and maternally-derived immunity, to evaluate the possible impact of a maternal RSV vaccine program on the number of hospitalised RSV cases in young children (Chapter 7).

In this chapter I first provide an overview of the key findings relating to each of the three research themes, and discuss the implications of these findings and their relationship to the existing literature. I then address the strengths and limitations of this research, and suggest directions for future work.

8.1 Findings for each research theme

This thesis is largely based on mathematical compartmental ordinary differential equation (ODE) models, as described in Chapter 2. I began the research with simple compartmental

models, and explored the dynamics of these models before adding complexities, such as additional age classes, age-dependent scaling of infectiousness and susceptibility, a contact structure, and maternally-derived immunity. Here I discuss the main findings for each of the three themes.

Research theme 1: Age structure and immunity

RSV detections demonstrate a clear age structure, with infections mainly identified in children younger than two years and the largest burden in children under six months of age. The duration of immunity following an RSV infection is not well understood, although it is described as being partial and short-lived (Ohuma et al., 2012), and some modelling studies have applied an immunity period of about 200 days (Weber et al., 2001). In order to capture the known age structure of RSV, as well as waning immunity and seasonality, I developed models for RSV transmission with one, two and three age classes. I then fitted the two age class model to data for Western Australia to validate these models and obtain parameter values for subsequent analysis and model development, as described in Chapter 4. I found that the parameter corresponding to the duration of immunity aligned with estimates used elsewhere, with a fitted value of 230 days for the two age class model.

In this thesis I implemented a range of methods to build a complete picture of expected model behaviour, applying analytic, brute-force and numerical algorithm methods to document the different types of model outputs for parameter ranges of interest. The bifurcation analysis and the systematic parameter space mapping presented in Chapter 5 showed that the model could reproduce patterns observed in different parts of the world, and identified the parameters to which the model was most sensitive. A particularly interesting feature was the bifurcation structure. As it was not possible to examine the bifurcation points analytically, I used specialised numerical integration software XPP-AUTO to track the bifurcation points. The period doubling and halving feature allowed the model to produce annual and biennial dynamics for different ranges of the transmission and seasonality parameters, and was a robust feature of the model. It confirmed the brute-force bifurcation analysis presented in Chapter 4, and provided an example of the doubling and period halving phenomenon previously identified in other models (Stone, 1993). This may help explain why strong biennial patterns are often observed in temperate regions, such as in Switzerland (Duppenthaler et al., 2003).

The model also reproduced the 'delayed biennial' pattern observed in Finland and Germany (Terletskaia-Ladwig et al., 2005; Waris, 1991), for a range of plausible parameter values, and the shallow epidemic fluctuations that are more typical of RSV patterns in the tropics. I used the Next Generation Matrix method to calculate the basic reproduction number analytically, and found that the value of R_0 in the absence of seasonal forcing was similar to values documented elsewhere (Weber et al., 2001). Overall, my findings show that relatively simple model structures capture the known biology and epidemiology of RSV, and that these models could be adapted for use in a range of real world settings.

The duration of immunity and birth rate were key parameters in the model, and I found that these factors likely play an important role in RSV infection dynamics. These parameters could be varied within reasonable ranges to produce either annual, biennial or delayed biennial patterns in the models, as discussed in Chapter 5. This result helps clarify why latitude, climatic variation and weather variables do not fully explain why some countries exhibit annual RSV epidemics, and other countries experience biennial epidemic patterns. This finding also provides evidence that a shifting birth rate may cause RSV epidemics to change in character from annual to biennial, or vice versa, over time. Indeed, this has been proposed as an explanation for the transition from biennial to annual RSV dynamics in California between the 1990s and 2000s (Pitzer et al., 2015).

A key component of this thesis was the use of population-level linked data to parametrise the models. In Chapters 4 and 5, I used a modified least squares fitting routine to fit models with two age cohorts to RSV detection data for children younger than 24 months of age. In the model fitting process, a function calculating the distance between the modelled incidence and the data was numerically minimised. A limitation is the inherent assumption underpinning the least squares method that the errors are independent and identically normally distributed. I considered the method appropriate given that the data was very regular and involved many cases, however, this fitting method may not be suitable to fit such models to data for other regions. In Chapter 7, I instead used the method of maximum likelihood estimation to perform the model fitting, by assuming a Poisson distribution for the probability of observing k hospitalisations in a given time interval. The benefit of maximum likelihood estimation is that it assumes that the absolute error in the predicted incidence at each point is proportional to the observed data, whereas the least squares method assumes constant absolute expected error at each point. As a separate exercise, I

refitted the 75 age cohort model to the data using a least squares fit statistic, but found that the fitted parameters did not greatly change, justifying the use of the simpler fitting technique in the earlier chapters.

Given the renewed interest in RSV interventions, and with few mathematical models for RSV published to date, the results in Chapters 4 and 5 provide a starting point for future RSV model development, as explored in the following two research themes. This research also sheds light on why different RSV epidemic patterns occur in different regions. This may aid health practitioners in anticipating the characteristics of future epidemics, which has implications for health service planning.

Research theme 2: Seasonality and climate

As discussed in Chapter 2, RSV displays different epidemic patterns in temperate versus tropical regions. Western Australia is a particularly interesting region for the study of RSV dynamics because the state spans a range of climatic zones, from temperate in the south, to tropical in the far north. This study was enabled by the availability of RSV testing data across the state, through a centralised public pathology provider. For this research theme I adopted both dynamic modelling and time series analysis approaches: one aspect of this theme was to explore the model dynamics in relation to the seasonality parameter, and the other was to conduct analysis of the Western Australian data.

In the compartmental models for RSV, a sinusoidal forcing term was incorporated to allow RSV transmission to fluctuate. This forcing term was a proxy for a range of climatic or weather-related factors that are assumed to influence RSV transmission at different times of the year in temperate regions – increasing transmission in winter and reducing it in the summer months. In the seasonal forcing function, the parameter b_1 represented the amplitude of seasonal forcing, as described in Chapter 2. As this parameter does not have a clear physical interpretation, I estimated its value in the model fitting exercise and subsequently explored the range of values that produce different model outputs. The sensitivity analyses presented in Chapter 5 showed that the model was not particularly sensitive to the strength of seasonal forcing, however, the variation in epidemic patterns for different countries is well known, as discussed in Chapter 2, therefore this parameter may vary by region and is important to consider in the model analysis. The bifurcation analysis in Chapter 5 showed that the seasonality parameter must exceed a minimum threshold for

the model to produce biennial dynamics, which aligns with biennial dynamics generally only being documented in temperate regions, and delayed biennial dynamics being observed in high latitude locations that experience strong seasonal change between summer and winter, such as Switzerland and Finland.

In this thesis, I found that using both dynamic modelling and data analysis approaches can enrich the overall findings and provide information to inform future interventions. As established in Chapter 5, the RSV transmission models presented in this thesis capture RSV dynamics observed in both temperate and tropical regions, which means that these models could be fitted to data for a range of locations with different seasonal characteristics, and used to inform region-specific interventions. This finding is complemented by the data analysis in Chapter 6, which showed that in Western Australia, the epidemic peak timing in the northern region is earlier than that in the south, which indicates that prophylaxis and vaccination strategies may need to be timed differently across the state.

Complex demodulation is a mathematical time series analysis method for extracting the amplitude and phase from data with a strong regular periodicity. It has previously been applied in the context of sleep pattern, heart rhythm and geomagnetic storm data (Hayano et al., 1993; Kingan et al., 1980; Kondo et al., 2014), but to my knowledge, it has not previously been applied in the infectious disease setting. In Chapter 6 I explored how complex demodulation could be used to analyse seasonal infectious disease data. I created synthetic time series that displayed the key features of different epidemic patterns, and applied complex demodulation to these synthetic data. I extracted the changing amplitudes and phases with respect to the dominant underlying periodicity, and conveyed how to relate these outputs to the size and timing of epidemic data. I also illustrated the application of complex demodulation using national influenza notifications. This analysis establishes a role for complex demodulation in the analysis of seasonal infectious disease data. I showed that complex demodulation is applicable where the dominant frequency in the data is unchanging, that the method is straightforward to apply, and the outputs are readily interpretable.

Studies show that approximately 70% of bronchiolitis hospitalisations in young children are attributable to an RSV infection (Haynes, 2013; Mansbach et al., 2012). RSV is identified via a laboratory test of a respiratory specimen and bronchiolitis is a clinical diagnosis. As

RSV is not a notifiable disease, and laboratory tests for RSV are not routinely conducted, clinical diagnosis data from hospital discharge records (the source of bronchiolitis data) are more readily available than laboratory data for detected pathogens (the source of RSV data). Therefore, I used complex demodulation to determine the extent to which bronchiolitis data represent RSV diagnoses over time in metropolitan Western Australia. As there were fewer cases outside the metropolitan region, due to smaller populations, I could not apply complex demodulation to the data for the Kimberley and Pilbara regions. The results demonstrated that bronchiolitis hospitalisation data are representative of RSV detection data in terms of timing, although RSV data show a more marked change in epidemic size from year to year. With RSV vaccines in clinical trials, locally-relevant data are required to plan for vaccine rollout strategies. My finding that bronchiolitis is a reasonable proxy for RSV therefore illustrates that bronchiolitis hospitalisation data may be used in areas where RSV laboratory data are not readily available.

The complex demodulation analysis in Chapter 6 showed small 'blips', or deviations, in the phase outputs for some of the synthetic and real datasets. In complex demodulation, a demodulator and filter must be chosen with a frequency corresponding to the dominant frequency in the data, however, some datasets may have both strong annual and biennial signals. I concluded that these deviations arise when an annual demodulator and filter is applied to data with a strong biennial frequency. This suggests that complex demodulation may not be appropriate to use for prediction, but as demonstrated in Chapter 6, has utility in extracting information from data that is not immediately visually apparent, and in comparing datasets for different pathogens or regions.

Research theme 3: Vaccination

Maternal immunisation for RSV has been proposed as a possible strategy for preventing RSV infection in very young children, and a vaccine candidate for pregnant women is now in phase 3 trials (ClinicalTrials.gov, 2016). The final theme extended the models and findings from the first parts of the research to assess the likely impact of a RSV maternal vaccine on RSV hospitalisations in young children.

I expanded the simple age structured model presented in Chapters 4 and 5 to simulate RSV transmission in 75 age cohorts, and validated the model using RSV hospitalisation data. I incorporated an additional compartment to account for infants with reduced susceptibility

to infection arising from maternal vaccination, and compared the vaccine and non-vaccine models to estimate the intervention impact. I found that a maternal RSV vaccine is likely to reduce infant hospitalisations for respiratory infection, primarily in children younger than six months of age. Such a vaccine may reduce RSV-related hospitalisations by around 6–37% in 0–2 month old children, and 30–46% in 3–5 month old children, for a range of vaccine effectiveness levels, and similar maternal vaccine uptake to that for pertussis and influenza vaccines in Western Australia. Assuming that a vaccine would afford a similar duration of immunity to that derived from a natural RSV infection (about six months), the modelled maternal vaccination had a negligible impact on children six months of age and older. This finding is in line with the objective of a maternal RSV vaccine to delay the onset of a child's first RSV infection beyond their first few months of life, when illness is generally more severe.

One of the uncertain aspects of the development of a maternal vaccine for RSV relates to the existing RSV-specific antibodies in pregnant women that are transferred transplacentally to the unborn infant. While the importance of these antibodies is accepted, it is not well known how the infant antibody level at birth correlates with protection from disease. Also, it is not clear why seroprevalence surveys measure the highest levels of RSV-specific antibody titres in newborn infants compared to older children, when this is also the age group in which the highest numbers of RSV hospitalisations are observed (Cox et al., 1998; Nyiro et al., 2017). To reflect existing naturally-derived protection in the maternal vaccination model, I scaled susceptibility to infection in the first three one-month age groups, and ran the analysis for a range of protection scenarios. I found that the model outcome was sensitivity to the assumptions about maternally-derived immunity in the first three months of life, therefore it will be important to consider how to more accurately capture this type of immunity in ongoing model development for RSV vaccine interventions.

Modelling studies that evaluate the public health impact of a new vaccine are valuable for health policy decision-makers. In Australia, the vast majority of vaccines are funded under the Immunise Australia Program, which administers the National Immunisation Program (NIP) Schedule. The decision to include a vaccine on the NIP is largely dependent on recommendations from the Pharmaceutical Benefits Advisory Committee, which takes into account information on a vaccine's clinical efficacy as well as its cost effectiveness. Depending on the outcomes of the RSV vaccine clinical trials currently underway, the

findings in this thesis could be useful in decision-making about funding a maternal RSV vaccine in Australia. A strength of this model is that is flexible and so can be adapted to account for the particular birth rates, contact patterns and hospitalisations in different regions, and could therefore be used in assessing vaccine strategies for other jurisdictions.

8.2 Strengths and limitations

To my knowledge, this is the first mathematical modelling study of RSV conducted in the Australian setting. A key strength of this research is that the models were validated using RSV laboratory detections accessed through a population-level linked data project. Further, the residential postcode was available on the linked dataset to allow RSV detections and bronchiolitis hospitalisations to be examined in different geographic regions of Western Australia, where consistent data collection and testing protocols were applied between regions. However, as as the majority of RSV detections were associated with hospitalised children, the data likely only represent the severe end of the disease spectrum, and RSV prevalence in the community is not well known. With this in mind, my research focussed on the broad, seasonal patterns in the data, assuming that dynamics observed in laboratory confirmed cases are representative of community dynamics. Finally, the data relate to a birth cohort of children born in Western Australia and do not capture cases in individuals born outside the state. This again means that the data likely under-represent the true respiratory illness burden in Western Australia.

A strength of this thesis is that the model used to simulate vaccine impact was based on simpler models that had been analysed extensively. I applied a range of analytic and numeric techniques to understand the behaviour of the simpler models, including sensitivity analyses to determine the parameters that most influenced the model output. I then used this information in determining the most appropriate structure and parameter choices for the more realistic maternal vaccine model. This model development process demonstrates the value in having an understanding of the impact of different parameters on the model output. This understanding can help determine the most appropriate structure for a model that is intended to help answer public health questions, and can allow models to be developed that are only as complex as necessary, and readily interpretable. This is important if mathematical epidemiology is to have a tangible impact on public health policy.

In this thesis, I examined the dynamics of RSV specifically in relation to children, due to the age range of infection episodes captured in the available data. While the disease burden of RSV is often described in the context of young children, RSV is increasingly recognised as causing serious illness in elderly persons and has been identified as playing a significant role in elderly mortality, alongside influenza A (van Asten et al., 2012). RSV outbreaks have been documented in aged care facilities, and RSV is identified as an important respiratory pathogen in older persons living in the community (Falsey et al., 2005; Falsey, 1998). However, there are significant gaps in our understanding of RSV in older persons (Falsey and Walsh, 2000). The transmission characteristics of RSV in older people are not well documented, and representative mathematical models that focus specifically on RSV in the elderly have yet to be developed. This area will likely become increasingly important for research, as vaccine candidates specifically targeting the elderly are currently in the clinical trials pipeline (PATH, 2017).

Compartmental ODE models have been widely used in the study of infectious disease dynamics. Advantages of these models are that they are generally analytically tractable, computationally efficient, and lend themselves to the inclusion of a vaccination strategy. However, as discussed in Chapter 2, these types of ODE models may be criticised for being overly simplistic, and for assuming a homogeneous population. The research in Chapters 4 and 5 showed that while the models shown here are relatively simple, they model RSV transmission well and produce reasonable fitted parameters and alignment with the data. I also introduced specific heterogeneities, such as age structures and contact patterns, where applicable, while ensuring that the models remained computationally efficient.

In this thesis I used two types of fitting methods to parametrise the models – least squares and maximum likelihood estimation. A limitation of both fitting methods is that there is no simple way to adjust for deviations in the timing of peaks from year to year. As noted in Chapter 4, the model did not fit as well in the year 2005, compared to the earlier years, due to the RSV season starting earlier that year. However, I did not consider this a major limitation given the overall regularity in the data. Another limitation of these fitting methods is that they did not capture the sharp peaks in the data at the height of each epidemic. This was likely due to the choice of the sine and cosine forcing functions that were used to represent seasonality. It would be possible to consider other seasonal forcing functions that more accurately capture the high-incidence peaks, however, sine and

cosine forcing functions are well accepted in the literature, straightforward to implement, and overall, the fitted model captured the epidemic characteristics well.

Age is an important determinant of RSV infection and a key aspect of RSV epidemiology (Nyiro et al., 2017). In my thesis I used models with a variety of age structures to answer different research questions. In Chapters 4 and 5, I developed models with one, two and three age classes, with continuous ageing between classes, as the continuous ageing structure lends itself to the types of analytical and numerical methods I used to explore the parameter space. However, there are limitations associated with continuous ageing, as the rate at which individuals age from one class to the next is exponentially distributed. The bifurcation analysis for models of one, two and three age classes, presented in Chapter 5, showed that the annual-biennial-annual bifurcation structure was common to all three models, therefore I considered that continuous ageing was acceptable when analysing the simpler models, where only the broad dynamics were of interest. I then addressed the exponential distribution limitation when considering models for vaccination in Chapter 7, by using smaller age classes and cohort ageing, to reflect a more realistic ageing process. Partial differential equation models can also be used to capture a more realistic ageing process, however these models are more difficult to analyse and solve numerically, therefore I did not consider them for this thesis.

With vaccines for RSV still in clinical trials, there was limited information available to inform the choice of the vaccine-related parameters in the model for maternal vaccination – particularly the parameters relating to vaccine efficacy, duration of vaccine-induced immunity, and anticipated vaccine coverage. I made an effort to overcome this uncertainty by using the existing vaccine literature and current estimates of pertussis vaccine coverage in Western Australia. I also conducted a sensitivity analysis across a broad range of parameters. These models can be applied to specific vaccination scenarios as more information about vaccine characteristics becomes available.

8.3 Future work

There are several avenues for future research arising from the findings in this thesis. Here I identify three target areas: incorporating real weather variables to simulate seasonality;

modelling multiple strains and interaction with other respiratory viruses; and further investigation of vaccine programs as vaccine candidates progress through clinical trials.

Although I identified that the birth rate and duration of immunity play a key role in influencing RSV epidemic patterns, there remains a question about the weather variables that influence seasonal transmission. Some studies have used time series methods to investigate the link between meteorological factors and RSV hospitalisations. Humidity, temperature and rainfall have each been identified as possible factors, although findings vary between different studies, particularly in tropical regions (du Prel et al., 2009; Noyola and Mandeville, 2008; Paynter et al., 2014a; Tang and Loh, 2014; Welliver, 2009). In this thesis, I focussed on dynamic models, with a sinusoidal forcing term as a proxy for a range of possible climatic influences (discussed in Chapter 5). However, there is also scope to develop mathematical models that combine dynamic and time series methods, as Finkenstädt and Grenfell (2000) applied to the study of measles dynamics in England and Wales. Such an approach could be used to better understand the relative impacts of weather factors such as rainfall, temperature, humidity, and solar exposure on RSV transmission.

There are two serotypes of RSV: RSV-A and RSV-B, yet there is limited information on how the epidemiology of the two strains differs, and a lack of published RSV data that differentiates between the two strains. As much of the modelling work to date does not distinguish between the different strains, there is a role for mathematical models that include strain-specific dynamics. Further, given the lack of understanding about patterns and mechanisms of interference between RSV and other respiratory viruses such as influenza, rhinovirus and parainfluenza (Roche et al., 2003), mathematical models have a role in simulating and quantifying the interaction between different pathogens. In this thesis I proposed a role for the mathematical time series analysis method of complex demodulation in the future analysis of seasonal infectious disease data. Such approaches could be used to compare the timing and magnitude of epidemics for different respiratory illnesses such as influenza and RSV, for different strains of a single virus, or for comparing seasonal dynamics for different regions.

Finally, there will likely be increasing interest in population-level models for RSV as clinical trials for RSV vaccine candidates progress. The model for a maternal vaccine presented in this thesis is a starting point for investigating the potential impact of a vaccine, and

can be refined as more information about a vaccine becomes available, particularly relating to vaccine duration and efficacy. Further, there are vaccines for other target groups in clinical development, prompting the need for models that estimate the impact of a vaccine for infants, children and the elderly, and studies that estimate the herd immunity effects arising from these vaccines. Individual-based models that incorporate household structures have only been recently applied in the context of RSV, in the low-income setting (Poletti et al., 2015), therefore there is a role for further development of these types of models to assess vaccine strategies to protect newborn children. Our model considered only a single type of vaccine, however, with a maternal RSV vaccine unlikely to protect infants older than six months, it is likely that the public health impact of a maternal vaccine will need to be considered in conjunction with other vaccine interventions (Heath et al., 2017), and mathematical models that reflect these intervention combinations will be required.

8.4 Conclusion

RSV is recognised as a major health burden, particularly in young children, and causes a significant health system and economic impact. As the vaccine landscape for RSV is rapidly changing, with a number of candidates in the clinical trials pipeline, understanding the transmission characteristics of RSV is critical for assessing interventions. In this thesis I used mathematical modelling and data analysis approaches to explore RSV transmission, focussing on age structure and immunity, seasonality and climate, and vaccination strategies, in the context of Western Australia. The models presented here could be adapted to incorporate local transmission patterns, demography and hospitalisation data, and can therefore be readily applied to other jurisdictions. This thesis has made a unique contribution to the epidemiological knowledge of RSV and provides an avenue for future work in this area.

References

Acedo, L., Díez-Domingo, J., Moraño, J.-A., and Villanueva, R.-J. (2010a). Mathematical modelling of respiratory syncytial virus (RSV): vaccination strategies and budget applications. *Epidemiology and Infection*, 138(6):853–860.

Acedo, L., Moraño, J.-A., and Díez-Domingo, J. (2010b). Cost analysis of a vaccination strategy for respiratory syncytial virus (RSV) in a network model. *Mathematical and Computer Modelling*, 52(7-8):1016–1022.

Acedo, L., Moraño, J.-A., Villanueva, R.-J., Villanueva-Oller, J., and Díez-Domingo, J. (2011). Using random networks to study the dynamics of respiratory syncytial virus (RSV) in the Spanish region of Valencia. *Mathematical and Computer Modelling*, 54(7-8):1650–1654.

Alexander, P. M., Eastaugh, L., Royle, J., Daley, A. J., Shekerdemian, L. S., and Penny, D. J. (2012). Respiratory syncytial virus immunoprophylaxis in high-risk infants with heart disease. *Journal of Paediatrics and Child Health*, 48(5):395–401.

Altizer, S., Dobson, A., Hosseini, P., Hudson, P., Pascual, M., and Rohani, P. (2006). Seasonality and the dynamics of infectious diseases. *Ecology Letters*, 9(4):467–484.

Anderson, L. J., Dormitzer, P. R., Nokes, D. J., Rappuoli, R., Roca, A., and Graham, B. S. (2013). Strategic priorities for respiratory syncytial virus (RSV) vaccine development. *Vaccine*, 31S:B209–B215.

Anderson, R. M. and May, R. M. (1991). *Infectious Diseases of Humans: Dynamics and Control*. Oxford University Press, New York, United States.

Australian Technical Advisory Group on Immunisation (2013). *The Australian Immunisation Handbook*, 10th edition. Retrieved from http://www.immunise.health.gov.au/internet/immunise/publishing.nsf/Content/Handbook10-home.

Avendaño, L. F., Palomino, M. A., and Larrañaga, C. (2003). Surveillance for respiratory syncytial virus in infants hospitalized for acute lower respiratory infection in Chile (1989 to 2000). *Journal of Clinical Microbiology*, 41(10):4879–4882.

Bansal, S., Grenfell, B. T., and Meyers, L. A. (2007). When individual behaviour matters: homogeneous and network models in epidemiology. *Journal of The Royal Society Interface*, 4(16):879–891.

Beigelman, A., Castro, M., Schweiger, T. L., Wilson, B. S., Zheng, J., Yin-DeClue, H., Sajol, G., Giri, T., Sierra, O. L., Isaacson-Schmid, M., Sumino, K., Schechtman, K. B., and Bacharier, L. B. (2015). Vitamin D levels are unrelated to the severity of respiratory syncytial virus bronchiolitis among hospitalized infants. *Journal of the Pediatric Infectious Diseases Society*, 4(3):182–188.

Belderbos, M. E., Houben, M. L., Wilbrink, B., Lentjes, E., Bloemen, E. M., Kimpen, J. L. L., Rovers, M., and Bont, L. (2011). Cord blood vitamin D deficiency is associated with respiratory syncytial virus bronchiolitis. *Pediatrics*, 127(6):e1513–e1520.

Bolisetty, S., Wheaton, G., and Chang, A. B. (2005). Respiratory syncytial virus infection and immunoprophylaxis for selected high-risk children in Central Australia. *Australian Journal of Rural Health*, 13(5):265–270.

Borchers, A. T., Chang, C., Gershwin, M. E., and Gershwin, L. J. (2013). Respiratory syncytial virus—a comprehensive review. *Clinical Reviews in Allergy & Immunology*, 45:331–379.

Bos, J. M., Rietveld, E., Moll, H. A., Steyerberg, E. W., Luytjes, W., Wilschut, J. C., de Groot, R., and Postma, M. J. (2007). The use of health economics to guide drug development decisions: Determining optimal values for an RSV-vaccine in a model-based scenario-analytic approach. *Vaccine*, 25(39-40):6922–6929.

Bourgeois, F. T., Valim, C., McAdam, A. J., and Mandl, K. D. (2009). Relative impact of influenza and respiratory syncytial virus in young children. *Pediatrics*, 124(6):e1072–1080.

Brandenburg, A. H., Groen, J., van Steensel-Moll, H. A., Claas, E. C., Rothbarth, P. H., Neijens, H. J., and Osterhaus, A. D. (1997). Respiratory syncytial virus specific serum antibodies in infants under six months of age: limited serological response upon infection. *Journal of Medical Virology*, 52(1):97–104.

Broadbent, L., Groves, H., Shields, M. D., and Power, U. F. (2015). RSV, an ongoing medical dilemma: an expert commentary on RSV prophylactic and therapeutic pharmaceuticals currently in clinical trials. *Influenza and Other Respiratory Viruses*, 9(4):169–178.

Burr, T. L. and Chowell, G. (2008). Signatures of non-homogeneous mixing in disease outbreaks. *Mathematical and Computer Modelling*, 48(1-2):122–140.

Cane, P., Matthews, D., and Pringle, C. (1994). Analysis of respiratory syncytial virus strain variation in successive epidemics in one city. *Journal of Clinical Microbiology*, 32(1):1–5.

Cane, P. A. (2001). Molecular epidemiology of respiratory syncytial virus. *Reviews in Medical Virology*, 11(2):103–116.

Capistrán, M., Moreles, M., and Lara, B. (2009). Parameter estimation of some epidemic models. The case of recurrent epidemics caused by respiratory syncytial virus. *Bulletin of Mathematical Biology*, 71:1890–1901.

Chan, P. W. K., Chew, F. T., Tan, T. N., Chua, K. B., and Hooi, P. S. (2002). Seasonal variation in respiratory syncytial virus chest infection in the tropics. *Pediatric Pulmonology*, 34(1):47–51.

Cheon, I. S., Shim, B.-S., Park, S.-M., Choi, Y., Jang, J. E., Jung, D. I., Kim, J.-O., Chang, J., Yun, C.-H., and Song, M. K. (2014). Development of safe and effective RSV vaccine by modified CD4 epitope in G protein core fragment (Gcf). *PLoS ONE*, 9(4):e94269.

Chew, F. T., Doraisingham, S., Ling, A. E., Kumarasinghe, G., and Lee, B. W. (1998). Seasonal trends of viral respiratory tract infections in the tropics. *Epidemiology and Infection*, 121(1):121–128.

Chi, H., Chang, I.-S., Tsai, F.-Y., Huang, L.-M., Shao, P.-L., Chiu, N.-C., Chang, L.-Y., and Huang, F.-Y. (2011). Epidemiological study of hospitalization associated with respiratory syncytial virus infection in Taiwanese children between 2004 and 2007. *Journal of the Formosan Medical Association*, 110(6):388–396.

ClinicalTrials.gov (2016). A Study to Determine the Safety and Efficacy of the RSV F Vaccine to Protect Infants Via Maternal Immunization. Retrieved from https://clinicaltrials.gov/ct2/show/NCT02624947?term=RSV&rank=6.

Corberán-Vallet, A. and Santonja, F. J. (2014). A Bayesian SIRS model for the analysis of respiratory syncytial virus in the region of Valencia, Spain. *Biometrical Journal*, 56(5):808–818.

Cox, M. J., Azevedo, R. S., Cane, P. A., Massad, E., and Medley, G. F. (1998). Seroepidemiological study of respiratory syncytial virus in São Paulo state, Brazil. *Journal of Medical Virology*, 55(3):234–9.

de Silva, L. M. and Hanlon, M. G. (1986). Respiratory syncytial virus: a report of a 5-year study at a children's hospital. *Journal of Medical Virology*, 19(4):299–305.

Diekmann, O., Heesterbeek, H., and Britton, T. (2013). *Mathematical Tools for Understanding Infectious Disease Dynamics*. Princeton University Press, Princeton and Oxford.

Doedel, E. J. (1981). AUTO: A program for the automatic bifurcation analysis of autonomous systems. *Congressus Numerantium*, 30:265–284.

Domachowske, J. B. and Rosenberg, H. F. (1999). Respiratory syncytial virus infection: immune response, immunopathogenesis, and treatment. *Clinical Microbiology Reviews*, 12(2):298–309.

Dowell, S. F. (2001). Seasonal variation in host susceptibility and cycles of certain infectious diseases. *Emerging Infectious Diseases*, 7(3):369–374.

du Prel, J.-B., Puppe, W., Gröndahl, B., Knuf, M., Weigl, J. A. I., Schaaff, F., and Schmitt, H.-J. (2009). Are meteorological parameters associated with acute respiratory tract infections? *Clinical Infectious Diseases*, 49(6):861–868.

Duppenthaler, A., Gorgievski-Hrisoho, M., and Aebi, C. (2001). Regional impact of prophylaxis with the monoclonal antibody palivizumab on hospitalisations for respiratory syncytial virus in infants. *Swiss Medical Weekly*, 131(11-12):146–151.

Duppenthaler, A., Gorgievski-Hrisoho, M., Frey, U., and Aebi, C. (2003). Two-year periodicity of respiratory syncytial virus epidemics in Switzerland. *Infection*, 31(2):75–80.

Ermentrout, B. (2002). *Simulating, analyzing, and animating dynamical systems: a guide to XPPAUT for researchers and students*. SIAM.

Ermentrout, B. (2016). XPPAUT 8.0 January 2016. Retrieved from http://www.math.pitt.edu/ bard/xpp/xpp.html.

Esposito, S., Piralla, A., Zampiero, A., Bianchini, S., Di Pietro, G., Scala, A., Pinzani, R., Fossali, E., Baldanti, F., and Principi, N. (2015). Characteristics and their clinical relevance of respiratory syncytial virus types and genotypes circulating in northern Italy in five consecutive winter seasons. *PLoS ONE*, 10(6):e0129369.

Falsey, A., Hennessey, P., Formica, M., Cox, C., and Walsh, E. (2005). Respiratory syncytial virus infection in elderly and high-risk adults. *New England Journal of Medicine*, 352(17):1749–1760.

Falsey, A. R. (1998). Respiratory syncytial virus infection in older persons. *Vaccine*, 16(18):1775–1778.

Falsey, A. R. and Walsh, E. E. (2000). Respiratory syncytial virus infection in adults. *Clinical Microbiology Reviews*, 13(3):371–384.

Fields, B. S., House, B. L., Klena, J., Waboci, L. W., Whistler, T., and Farnon, E. C. (2013). Role of global disease detection laboratories in investigations of acute respiratory illness. *The Journal of Infectious Diseases*, 208 Suppl(Suppl 3):S173–176.

Finkenstädt, B. F. and Grenfell, B. T. (2000). Time series modelling of childhood diseases: a dynamical systems approach. *Journal of the Royal Statistical Society: Series C (Applied Statistics)*, 49(2):187–205.

Fitzgerald, D. A., Isaacs, D., and Tobin, B. (2012). Palivizumab: a debate about funding. *Journal of Paediatrics and Child Health*, 48(5):373–377.

González, P. A., Bueno, S. M., Carreño, L. J., Riedel, C. A., and Kalergis, A. M. (2012). Respiratory syncytial virus infection and immunity. *Reviews in Medical Virology*, 22:230–244.

Graham, B. S. (2014). Protecting the family to protect the child: vaccination strategy guided by RSV transmission dynamics. *Journal of Infectious Diseases*, 209(11):1679–1681.

Grassly, N. C. and Fraser, C. (2006). Seasonal infectious disease epidemiology. *Proceedings of the Royal Society B: Biological Sciences*, 273(1600):2541–2550.

Hall, C. B. (1981). Respiratory syncytial virus. In: Feigin R.D., Cherry J.D., Textbook of Paediatric Infectious Diseases, 1st edn. In Feigin, R. D. and Cherry, J. D., editors, *Textbook of Paediatric Infectious Diseases,* (Volume II), 1247–1267. W. B. Saunders Company, Philadelphia and London.

Hall, C. B. (2001). Respiratory syncytial virus and parainfluenza virus. *New England Journal of Medicine*, 344(25):1917–1928.

Hall, C. B. (2010). Respiratory syncytial virus in young children. *The Lancet*, 375(9725):1500–1502.

Hall, C. B. and Douglas, R. G. (1981). Modes of transmission of respiratory syncytial virus. *The Journal of Pediatrics*, 99(1):100–103.

Hall, C. B., Douglas, R. G., and Geiman, J. M. (1976a). Respiratory syncytial virus infections in infants: quantitation and duration of shedding. *The Journal of Pediatrics*, 89(1):11–15.

Hall, C. B., Geiman, J. M., Biggar, R., Kotok, D. I., Hogan, P. M., and Douglas Jr, R. G. (1976b). Respiratory syncytial virus infections within families. *New England Journal of Medicine*, 294(8):414–419.

Hall, C. B., Walsh, E. E., Long, C. E., and Schnabel, K. C. (1991). Immunity to and frequency of reinfection with respiratory syncytial virus. *The Journal of Infectious Diseases*, 163(4):693–698.

Hall, C. B., Walsh, E. E., Schnabel, K. C., Long, C. E., McConnochie, K. M., Hildreth, S. W., and Anderson, L. J. (1990). Occurrence of groups A and B of respiratory syncytial virus over 15 years: associated epidemiologic and clinical characteristics in hospitalized and ambulatory children. *The Journal of Infectious Diseases*, 162(6):1283–1290.

Hall, C. B., Weinberg, G. A., Blumkin, A. K., Edwards, K. M., Staat, M. A., Schultz, A. F., Poehling, K. A., Szilagyi, P. G., Griffin, M. R., Williams, J. V., Zhu, Y., Grijalva, C. G., Prill, M. M., and Iwane, M. K. (2013). Respiratory syncytial virus-associated hospitalizations among children less than 24 months of age. *Pediatrics*, 132(2):e341–348.

Han, L. L., Alexander, J. P., and Anderson, L. J. (1999). Respiratory syncytial virus pneumonia among the elderly: an assessment of disease burden. *The Journal of Infectious Diseases*, 179(1):25–30.

Hardelid, P., Pebody, R., and Andrews, N. (2013). Mortality caused by influenza and respiratory syncytial virus by age group in England and Wales 1999-2010. *Influenza and Other Respiratory Viruses*, 7(1):35–45.

Hayano, J., Taylor, J. A., Yamada, A., Mukai, S., Hori, R., Asakawa, T., Yokoyama, K., Watanabe, Y., Takata, K., and Fujinami, T. (1993). Continuous assessment of hemodynamic control by complex demodulation of cardiovascular variability. *The American Journal of Physiology*, 264(4 Pt 2):H1229–H1238.

Haynes, L. M. (2013). Progress and challenges in RSV prophylaxis and vaccine development. *The Journal of Infectious Diseases*, 208(Suppl 3):S177–183.

Heath, P. T., Culley, F. J., Jones, C. E., Kampmann, B., Le Doare, K., Nunes, M. C., Sadarangani, M., Chaudhry, Z., Baker, C. J., and Openshaw, P. J. (2017). Group B streptococcus and respiratory syncytial virus immunisation during pregnancy: A landscape analysis. *The Lancet Infectious Diseases*, 3099(17):1–12.

Henderson, F. W., Collier, A. M., Clyde Jr, W. A., and Denny, F. W. (1979). Respiratory-syncytial-virus infections, reinfection and immunity: a prospective, longitudinal study in young children. *New England Journal of Medicine*, 300(10):530–534.

Hethcote, H. W. (2007). The mathematics of infectious diseases. *SIAM Review*, 42(4):599–653.

Hirsh, S., Hindiyeh, M., Kolet, L., Regev, L., Sherbany, H., Yaary, K., Mendelson, E., and Mandelboim, M. (2014). Epidemiological changes of respiratory syncytial virus (RSV) infections in Israel. *PLoS ONE*, 9(3):e90515.

Hogan, A. B., Mercer, G. N., Glass, K., and Moore, H. C. (2013). Modelling the seasonality of respiratory syncytial virus in young children. In *Proceedings of the 20th International Congress on Modelling and Simulation,* 338–344.

Holman, C. D. J., Bass, A. J., Rouse, I. L., and Hobbs, M. S. T. (1999). Population-based linkage of health records in Western Australia: development of a health services research linked database. *Australian and New Zealand Journal of Public Health*, 23(5):453–459.

Homaira, N., Oei, J.-L., Mallitt, K.-A., Abdel-Latif, M. E., Hilder, L., Bajuk, B., Lui, K., Ferson, M., Nurik, A., Chambers, G. M., Rawlinson, W., Snelling, T., and Jaffe, A. (2015). High burden of RSV hospitalization in very young children: a data linkage study. *Epidemiology and Infection*, 144(8):1612–1621.

Ismail, N. and Reisner, B. (2001). Update on human respiratory syncytial virus. *Clinical Micobiology Newsletter*, 23(12):91–97.

Keeling, M. J. and Rohani, P. (2008). *Modeling Infectious Diseases in Humans and Animals*. Princeton University Press, United States and United Kingdom.

Keener, A. B. (2014). Efficacy studies build up the case for prenatal immunization. *Nature Medicine*, 20(9):970–972.

Kelman, C. W., Bass, A. J., and Holman, C. D. J. (2002). Research use of linked health data – a best practice protocol. *Australian and New Zealand Journal of Public Health*, 26(3):251–255.

Kermack, W. O. and McKendrick, A. G. (1927). A contribution to the mathematical theory of epidemics. *Proceedings of the Royal Society A: Mathematical, Physical and Engineering Sciences*, 115:700–721.

Kim, H. W., Arrobio, J. O., Brandt, C. D., Jeffries, B. C., Pyles, G., Reid, J. L., Chanock, R. M., and Parrott, R. H. (1973). Epidemiology of respiratory syncytial virus infection in Washington, D.C. I: Importance of the virus in different respiratory tract disease syndromes and temporal distribution of infection. *American Journal of Epidemiology*, 98:216–225.

Kingan, P. A., Bloomfield, P., and Anderssen, R. S. (1980). Phase drift and coherence in geomagnetic data during a magnetic storm (Dst). *Journal of Geomagnetism and Geoelectricity*, 32(1):57–65.

Kinyanjui, T. M., House, T. A., Kiti, M. C., Cane, P. A., Nokes, D. J., and Medley, G. F. (2015). Vaccine induced herd immunity for control of respiratory syncytial virus disease in a low-income country setting. *PLoS ONE*, 10(9):e0138018.

Kondo, H., Ozone, M., Ohki, N., Sagawa, Y., Yamamichi, K., Fukuju, M., Yoshida, T., Nishi, C., Kawasaki, A., Mori, K., Kanbayashi, T., Izumi, M., Hishikawa, Y., Nishino, S., and Shimizu, T. (2014). Association between heart rate variability, blood pressure and autonomic activity in cyclic alternating pattern during sleep. *Sleep*, 37(1):187–94.

Krylova, O. and Earn, D. J. D. (2013). Effects of the infectious period distribution on predicted transitions in childhood disease dynamics. *Journal of The Royal Society Interface*, 10(84).

Leader, S. and Kohlhase, K. (2003). Recent trends in severe respiratory syncytial virus (RSV) among US infants, 1997 to 2000. *The Journal of Pediatrics*, 143(5 Suppl):S127–132.

Leecaster, M., Gesteland, P., Greene, T., Walton, N., Gundlapalli, A., Rolfs, R., Byington, C., and Samore, M. (2011). Modeling the variations in pediatric respiratory syncytial virus seasonal epidemics. *BMC Infectious Diseases*, 11(1):105.

Lessler, J., Reich, N. G., Brookmeyer, R., Perl, T. M., Nelson, K. E., and Cummings, D. A. T. (2009). Incubation periods of acute respiratory viral infections: a systematic review. *The Lancet Infectious Diseases*, 9(5):291–300.

Lyon, J. L., Stoddard, G., Ferguson, D., Caravati, M., Kaczmarek, A., Thompson, G., Hegmann, K., and Hegmann, C. (1996). An every other year cyclic epidemic of infants hospitalized with respiratory syncytial virus. *Pediatrics*, 97(1):152–153.

Mansbach, J. M., Piedra, P. A., Teach, S. J., Sullivan, A. F., Forgey, T., Clark, S., Espinola, J. A., and Camargo, C. A. (2012). Prospective multicenter study of viral etiology and hospital length of stay in children with severe bronchiolitis. *Archives of Pediatrics & Adolescent Medicine*, 166(8):700–706.

McLennan-Smith, T. (2012). *Analysis of a seasonal, multi-subclass dengue model*. Master of Mathematical Sciences Thesis, The Australian National University.

McNamara, P. S. and Smyth, R. L. (2002). The pathogenesis of respiratory syncytial virus disease in childhood. *British Medical Bulletin*, 61:13–28.

Meijboom, M. J., Rozenbaum, M. H., Benedictus, A., Luytjes, W., Kneyber, M. C. J., Wilschut, J. C., Hak, E., and Postma, M. J. (2012). Cost-effectiveness of potential infant vaccination against respiratory syncytial virus infection in The Netherlands. *Vaccine*, 30(31):4691–700.

Mercer, G. N. and Siddiqui, M. R. (2011). Application of a hepatitis E transmission model to assess intervention strategies in a displaced persons camp in Uganda. In *Proceedings of the 19th International Congress on Modelling and Simulation*, 940–946.

Mlinaric-Galinovic, G., Vojnovic, G., Cepin-Bogovic, J., Bace, A., Bozikov, J., Welliver, R. C., Wahn, U., and Cebalo, L. (2009). Does the viral subtype influence the biennial cycle of respiratory syncytial virus? *Virology Journal*, 6(133).

Mlinaric-Galinovic, G., Welliver, R. C., Vilibic-Cavlek, T., Ljubin-Sternak, S., Drazenovic, V., Galinovic, I., and Tomic, V. (2008). The biennial cycle of respiratory syncytial virus outbreaks in Croatia. *Virology Journal*, 5(18).

Moore, H. C. (2011). *Epidemiological perspectives of Acute Lower Respiratory Infections in young Western Australian Aboriginal and non-Aboriginal children*. PhD Thesis, The University of Western Australia.

Moore, H. C., de Klerk, N., Keil, A. D., Smith, D. W., Blyth, C. C., Richmond, P., and Lehmann, D. (2011). Use of data linkage to investigate the aetiology of acute lower respiratory infection hospitalisations in children. *Journal of Paediatrics and Child Health*, 48(6):520–528.

Moore, H. C., de Klerk, N., Richmond, P., Keil, A. D., Lindsay, K., Plant, A., and Lehmann, D. (2009a). Seasonality of respiratory viral identification varies with age and Aboriginality in metropolitan Western Australia. *The Pediatric Infectious Disease Journal*, 28(7):598–603.

Moore, H. C., Hall, G. L., and De Klerk, N. (2015). Infant respiratory infections and later respiratory hospitalisation in childhood. *European Respiratory Journal*, 46(5):1334–1341.

Moore, H. C., Jacoby, P., Hogan, A. B., Blyth, C. C., and Mercer, G. N. (2014). Modelling the seasonal epidemics of respiratory syncytial virus in young children. *PLoS ONE*, 9(6):e100422.

Moore, H. C., Keil, A. D., Richmond, P. C., and Lehmann, D. (2009b). Timing of bronchiolitis hospitalisations and respiratory syncytial virus immunoprophylaxis in non-metropolitan Western Australia. *The Medical Journal of Australia*, 191(10):574.

Munywoki, P. K., Koech, D. C., Agoti, C. N., Lewa, C., Cane, P. a., Medley, G. F., and Nokes, D. J. (2014). The source of respiratory syncytial virus infection in infants: a household cohort study in rural Kenya. *The Journal of Infectious Diseases*, 209:1685–1692.

Nair, H., Nokes, D. J., Gessner, B. D., Dherani, M., Madhi, S. A., Singleton, R. J., O'Brien, K. L., Roca, A., Wright, P. F., Bruce, N., Chandran, A., Theodoratou, E., Sutanto, A., Sedyaningsih, E. R., Ngama, M., Munywoki, P. K., Kartasasmita, C., Simões, E. A. F., Rudan, I., Weber, M. W., and Campbell, H. (2010). Global burden of acute lower respiratory infections due to respiratory syncytial virus in young children: a systematic review and meta-analysis. *The Lancet*, 375(9725):1545–1555.

Noyola, D. E. and Mandeville, P. B. (2008). Effect of climatological factors on respiratory syncytial virus epidemics. *Epidemiology and Infection*, 136(10):1328–1332.

Nyiro, J. U., Kombe, I. K., Sande, C. J., Kipkoech, J., Kiyuka, K., Onyango, C. O., Munywoki, P. K., Kinyanjui, T. M., and Nokes, J. (2017). Defining the vaccination window for respiratory syncytial virus (RSV) using age-seroprevalence data for children in Kilifi, Kenya. *PLoS ONE*, pages 1–14.

Nyiro, J. U., Sande, C., Mutunga, M., Kiyuka, P., Munywoki, P., Scott, J. A., and Nokes, D. J. (2015). Quantifying maternally derived respiratory syncytial virus specific neutralising antibodies in a birth cohort from coastal Kenya. *Vaccine*, 33(15):1797–1801.

Ohuma, E. O., Okiro, E. A., Ochola, R., Sande, C. J., Cane, P. A., Medley, G. F., Bottomley, C., and Nokes, D. J. (2012). The natural history of respiratory syncytial virus in a birth cohort: the influence of age and previous infection on reinfection and disease. *American Journal of Epidemiology*, 176(9):794–802.

Okiro, E. A., White, L. J., Ngama, M., Cane, P. A., Medley, G. F., and Nokes, D. J. (2010). Duration of shedding of respiratory syncytial virus in a community study of Kenyan children. *BMC Infectious Diseases*, 10(15).

Onozuka, D. (2015). The influence of diurnal temperature range on the incidence of respiratory syncytial virus in Japan. *Epidemiology and Infection*, 143(4):813–820.

Paes, B. A. (2003). Current strategies in the prevention of respiratory syncytial virus disease. *Paediatric Respiratory Reviews*, 4:21–27.

Panozzo, C. A., Fowlkes, A. L., and Anderson, L. J. (2007). Variation in timing of respiratory syncytial virus outbreaks: lessons from national surveillance. *The Pediatric Infectious Disease Journal*, 26(11 Suppl):S41–45.

Paramore, L., Ciuryla, V., Ciesla, G., and Liu, L. (2004). Economic impact of respiratory syncytial virus-related illness in the US. *PharmacoEconomics*, 22(5):275–284.

Parrott, R. H., Kim, H. W. H. A., Brandt, C. D., and Chanock, R. M. (1974). Respiratory syncytial virus in infants and children. *Preventive Medicine*, 3:473–480.

PATH (2017). RSV Vaccine and mAb Snapshot. Available at http://www.path.org/vaccineresources/details.php?i=1562 [updated 3 March].

Paynter, S., Sly, P. D., Ware, R. S., Williams, G., and Weinstein, P. (2014a). The importance of the local environment in the transmission of respiratory syncytial virus. *The Science of the Total Environment*, 493C:521–525.

Paynter, S., Ware, R. S., Sly, P. D., Weinstein, P., and Williams, G. (2015). Respiratory syncytial virus seasonality in tropical Australia. *Australian and New Zealand Journal of Public Health*, 39(1):8–10.

Paynter, S., Yakob, L., Simões, E. A. F., Lucero, M. G., Tallo, V., Nohynek, H., Ware, R. S., Weinstein, P., Williams, G., and Sly, P. D. (2014b). Using mathematical transmission modelling to investigate drivers of respiratory syncytial virus seasonality in children in the Philippines. *PLoS ONE*, 9(2):e90094.

Pitzer, V. E., Viboud, C., Alonso, W. J., Wilcox, T., Metcalf, C. J., Steiner, C. A., Haynes, A. K., and Grenfell, B. T. (2015). Environmental drivers of the spatiotemporal dynamics of respiratory syncytial virus in the United States. *PLoS Pathogens*, 11(1):e1004591.

Polack, F. P. (2015). The changing landscape of respiratory syncytial virus. *Vaccine*, 33:6473–6478.

Poletti, P., Merler, S., Ajelli, M., Manfredi, P., Munywoki, P. K., Nokes, J. D., and Melegaro, A. (2015). Evaluating vaccination strategies for reducing infant respiratory syncytial virus infection in low-income settings. *BMC Medicine*, 13(1):1–11.

Ranmuthugala, G., Brown, L., and Lidbury, B. A. (2011). Respiratory syncytial virus the unrecognised cause of health and economic burden among young children in Australia. *Clinical Infectious Diseases*, 35(2):177–184.

Reese, P. E. and Marchette, N. J. (1991). Respiratory syncytial virus infection and prevalence of subgroups A and B in Hawaii. *Journal of Clinical Microbiology*, 29(11):2614–2615.

Ren, L., Xia, Q., Xiao, Q., Zhou, L., Zang, N., Long, X., Xie, X., Deng, Y., Wang, L., Fu, Z., Tian, D., Zhao, Y., Zhao, X., Li, T., Huang, A., and Liu, E. (2014). The genetic variability of glycoproteins among respiratory syncytial virus subtype A in China between 2009 and 2013. *Infection, Genetics and Evolution*, 27:339–347.

Resch, B. (2014). Respiratory syncytial virus infection in high-risk infants an update on palivizumab prophylaxis. *The Open Microbiology Journal*, 8:71–77.

Reyes, M., Eriksson, M., Bennet, R., Hedlund, K.-O., and Ehrnst, A. (1997). Regular pattern of respiratory syncytial virus and rotavirus infections and relation to weather in Stockholm, 1984–1993. *Clinical Microbiology and Infection*, 3(6):640–646.

Roberts, J. N., Graham, B. S., Karron, R. A., Munoz, F. M., Falsey, A. R., Anderson, L. J., Marshall, V., Kim, S., and Beeler, J. A. (2016). Challenges and opportunities in RSV vaccine development: meeting report from FDA/NIH workshop. *Vaccine*, 34(41):4843–4849.

Roberts, M. G. and Tobias, M. I. (2000). Predicting and preventing measles epidemics in New Zealand: application of a mathematical model. *Epidemiology and Infection*, 124(2):279–287.

Roche, P., Lambert, S., and Spencer, J. (2003). Surveillance of viral pathogens in Australia: respiratory syncytial virus. *Communicable Diseases Intelligence*, 27(1):117–122.

Ruckwardt, T. J., Morabito, K. M., and Graham, B. S. (2016). Determinants of early life immune responses to RSV infection. *Current Opinion in Virology*, 16:151–157.

Saso, A. and Kampmann, B. (2016). Vaccination against respiratory syncytial virus in pregnancy: a suitable tool to combat global infant morbidity and mortality? *The Lancet Infectious Diseases*, 16(8):e153–e163.

Sigurs, N., Bjarnason, R., Sigurbergsson, F., and Kjellman, B. (2000). Respiratory syncytial virus bronchiolitis in infancy is an important risk factor for asthma and allergy at age 7. *American Journal of Respiratory and Critical Care Medicine*, 161(5):1501–1507.

Simoes, E. A. F. (2003). Environmental and demographic risk factors for respiratory syncytial virus lower respiratory tract disease. *The Journal of Pediatrics*, 143(5 Suppl):S118–S126.

Smyth, R. L. and Openshaw, P. J. M. (2006). Bronchiolitis. *The Lancet*, 368(9532):312–322.

Sorce, L. R. (2009). Respiratory syncytial virus: from primary care to critical care. *Journal of Pediatric Health Care*, 23(2):101–108.

Spaeder, M. C. and Fackler, J. C. (2012). A multi-tiered time-series modelling approach to forecasting respiratory syncytial virus incidence at the local level. *Epidemiology and Infection*, 140(4):602–607.

Stensballe, L. G., Devasundaram, J. K., and Simoes, E. A. F. (2003). Respiratory syncytial virus epidemics: the ups and downs of a seasonal virus. *The Pediatric Infectious Disease Journal*, 22(2):S21–S32.

Stone, L. (1993). Period-doubling reversals and chaos in simple ecological models. *Nature*, 365(6447):617.

Sullender, W. M. (2000). Respiratory syncytial virus genetic and antigenic diversity. *Clinical Microbiology Reviews*, 13(1):1–15.

Tang, J. W. and Loh, T. P. (2014). Correlations between climate factors and incidence a contributor to RSV seasonality. *Reviews in Medical Virology*, 24:15–34.

Terletskaia-Ladwig, E., Enders, G., Schalasta, G., and Enders, M. (2005). Defining the timing of respiratory syncytial virus (RSV) outbreaks: an epidemiological study. *BMC Infectious Diseases*, 5(20).

The IMpact-RSV Study Group (1998). Palivizumab, a humanized respiratory syncytial virus monoclonal antibody, reduces hospitalization from respiratory syncytial virus infection in high-risk infants. *Pediatrics*, 102(3):531–537.

Tregoning, J. S. and Schwarze, J. (2010). Respiratory viral infections in infants: causes, clinical symptoms, virology, and immunology. *Clinical Microbiology Reviews*, 23(1):74–98.

Tsutsumi, H., Onuma, M., Suga, K., Honjo, T., Chiba, Y., Chiba, S., and Ogra, L. (1988). Occurrence of respiratory syncytial virus subgroup A and B strains in Japan, 1980 to 1987. *Journal of Clinical Microbiology*, 26(6):1171–1174.

van Asten, L., van den Wijngaard, C., van Pelt, W., van de Kassteele, J., Meijer, A., van der Hoek, W., Kretzschmar, M., and Koopmans, M. (2012). Mortality attributable to 9 common infections: significant effect of influenza A, respiratory syncytial virus, influenza B, norovirus, and parainfluenza in elderly persons. *The Journal of Infectious Diseases*, 206(5):628–639.

van der Sande, M. A. B., Goetghebuer, T., Sanneh, M., Whittle, H. C., and Weber, M. W. (2004). Seasonal variation in respiratory syncytial virus epidemics in The Gambia, West Africa. *The Pediatric Infectious Disease Journal*, 23(1):73–74.

Vandini, S., Corvaglia, L., Alessandroni, R., Aquilano, G., Marsico, C., Spinelli, M., Lanari, M., and Faldella, G. (2013). Respiratory syncytial virus infection in infants and correlation with meteorological factors and air pollutants. *Italian Journal of Pediatrics*, 39(1):1.

Ventre, K. and Randolph, A. (2007). Ribavirin for respiratory syncytial virus infection of the lower respiratory tract in infants and young children. *Cochrane Database of Systematic Reviews*, (1):i–19.

Walton, N. A., Poynton, M. R., Gesteland, P. H., Maloney, C., Staes, C., and Facelli, J. C. (2010). Predicting the start week of respiratory syncytial virus outbreaks using real time weather variables. *BMC Medical Informatics and Decision Making*, 10(1):68.

Wang, E. E. and Law, B. J. (1998). Respiratory syncytial virus infection in pediatric patients. *Seminars in Pediatric Infectious Diseases*, 9(2):146–153.

Waris, M. (1991). Pattern of respiratory syncytial virus epidemics in Finland: two-year cycles with alternating prevalence of groups A and B. *The Journal of Infectious Diseases*, 163(3):464–469.

Weber, A., Weber, M., and Milligan, P. (2001). Modeling epidemics caused by respiratory syncytial virus (RSV). *Mathematical Biosciences*, 172(2):95–113.

Weber, M. W., Mulholland, E. K., and Greenwood, B. M. (1998). Respiratory syncytial virus infection in tropical and developing countries. *Tropical Medicine and International Health*, 3(4):268–280.

Weigl, J., Puppe, W., and Schmitt, H.-J. (2002). Seasonality of respiratory syncytial virus-positive hospitalizations in children in Kiel, Germany, over a 7-year period. *Infection*, 30(4):186–192.

Welliver, R. (2009). The relationship of meteorological conditions to the epidemic activity of respiratory syncytial virus. *Paediatric Respiratory Reviews*, 10 Suppl 1:6–8.

White, L. J., Mandl, J. N., Gomes, M. G. M., Bodley-Tickell, A. T., Cane, P. A., Perez-Brena, P., Aguilar, J. C., Siqueira, M. M., Portes, S. A., Straliotto, S. M., Waris, M., Nokes, D. J., and Medley, G. F. (2007). Understanding the transmission dynamics of respiratory syncytial virus using multiple time series and nested models. *Mathematical Biosciences*, 209(1):222–239.

White, L. J., Waris, M., Cane, P. A., Nokes, D. J., and Medley, G. F. (2005). The transmission dynamics of groups A and B human respiratory syncytial virus (hRSV) in England & Wales and Finland: seasonality and cross-protection. *Epidemiology and Infection*, 133(2):279–289.

Yorita, K. L., Holman, R. C., Steiner, C. a., Effler, P. V., Miyamura, J., Forbes, S., Anderson, L. J., and Balaraman, V. (2007). Severe bronchiolitis and respiratory syncytial virus among young children in Hawaii. *The Pediatric Infectious Disease Journal*, 26(12):1081–1088.

Yusuf, S., Piedimonte, G., Auais, A., Demmler, G., Krishnan, S., Van Caeseele, P., Singleton, R., Broor, S., Parveen, S., Avendano, L., Parra, J., Chaves-Bueno, S., Murguia de Sierra, T., Simoes, E. A. F., Shaha, S., and Welliver, R. (2007). The relationship of meteorological conditions to the epidemic activity of respiratory syncytial virus. *Epidemiology and Infection*, 135(7):1077–1090.

Zachariah, P. and Shah, S. (2009). Predictors of the duration of the respiratory syncytial virus season. *The Pediatric Infectious Disease Journal*, 28:772–776.

Zlateva, K. T., Vijgen, L., Dekeersmaeker, N., Naranjo, C., and Van Ranst, M. (2007). Subgroup prevalence and genotype circulation patterns of human respiratory syncytial virus in Belgium during ten successive epidemic seasons. *Journal of Clinical Microbiology*, 45(9):3022–3030.

Ørstavik, I., Carlsen, K.-H., and Halvorsen, K. (1980). Repiratory syncytial virus infections in Oslo 1972-1978. 1. Virological and Epidemiological Studies. *Acta Paediatrica Scandinavica*, 69:717–722.

Appendix A

Additional publication

The Formation and Launch of the Asia Pacific Consortium of Mathematics for Industry (APCMfI)

Masato Wakayama, Alexandra B. Hogan and Robert S. Anderssen

The evolving dynamics of the interaction between society and industry is recorded in the language of mathematics.

Abstract The Forum "Math-for-Industry" 2014 (FMfI 2014) represented the first opportunity to formally showcase the concept and formation of the Asia Pacific Consortium of Mathematics for Industry (APCMfI). This new initiative is intended to support the development of mathematics and its applications, and to enhance innovation and technology, in order to explore new research fields and improve the quality of life. A primary goal is to develop industrial mathematical research in the common Asia Pacific time zone of the East Asia and Oceania countries and to stimulate the two-way interaction between mathematics in academia and industry.

Keywords Mathematics-for-industry · Industrial problems · Two-way interaction

1 The Formation of APCMfI

The initial meetings for the planning of the Asia Pacific Consortium of Mathematics for Industry (APCMfI) took place in Canberra, Australia, from 31 March

M. Wakayama ( )
Kyushu University, Fukuoka, Japan
e-mail: wakayama@imi.kyushu-u.ac.jp

A.B. Hogan
The Australian National University, Canberra, Australia
e-mail: alexandra.hogan@anu.edu.au

R.S. Anderssen
The Commonwealth Scientific and Industrial Research Organisation, Acton, Australia
e-mail: bob.anderssen@csiro.au

R.S. Anderssen et al. (eds.), *Applications + Practical Conceptualization + Mathematics = fruitful Innovation*, Mathematics for Industry 11,
DOI 10.1007/978-4-431-55342-7_13

to 2 April, 2014. Those present were a small group of colleagues from Japan, Malaysia, New Zealand and Australia, in order to provide representation across the Asia Pacific region. The meetings formalized a planning structure for the formation of APCMfI: formulated a management structure; discussed opportunities for seed funding; planned a membership base; and considered future activities that would benefit APCMfI members.

A central idea that emerged from the meetings was the need to emphasis the 'for' in Mathematics ***for*** Industry, so as to reflect how, in the solution of industrial problems, one must turn to the utilization of mathematics in the answering of the questions under consideration. It is of crucial importance to recognize the impact that industrial applications are having and can have on the development of fundamental mathematical concepts, and how solving practical complex problems can stimulate ideas for new mathematics.

2 Earlier History

Before the Canberra meeting, there were various discussions about the need to have an Asia Mathematics-for-Industry (MfI) consortium similar to the European Consortium for Mathematics in Industry (ECMI). The first meeting to test the water about the merits of such a collaboration occurred in Fukuoka prior to the Forum "Math-for-Industry" (FMfI) 2009. There was strong support for the idea with different colleagues agreeing to assist. The possibility of having such a consortium was again discussed and supported among the participants at the FMfI 2010 Forum in Hawaii. The next discussion occurred at Joint Workshop of the Institute for Mathematical Sciences (IMS) in the National University of Singapore and Institute of Mathematics for Industry (IMI) in Kyushu University on Mathematics for Industry "Biological and Climatic Prospects", held at the IMS meeting in 2012. It was on this occasion that it was agreed that the consortium, when formalized, should be called the Asia Pacific Consortium of Mathematics *for* Industry (APCMfI). During these various discussions, there was always strong support for the concept from colleagues across the Asia Pacific region including Australia, China, Indonesia, Japan, New Zealand, Singapore, South Korea and Vietnam.

Even though the support was strong that such a consortium should be formed, it was not until March of 2014 that the first formal organizational meeting occurred. The subsequent announcement about the decisions made at that meeting to have an APCMfI has since been circulated [1].

3 Management Structure and Membership

An interim management committee will provide direction for APCMfI for a two year establishment phase (starting April 2014). Following this phase, APCMfI manage-

ment will consist of an elected board, as well as a council of representatives made up from APCMfI members. The operations of APCMfI will be in accordance with our constitution, which is currently being developed.

Current planning is that there will be three membership categories: full members (which include university departments or centers, and learned societies); industry and agency members; and individual members.

4 Planned Activities

A feature of APCMfI will be the practical activities undertaken to benefit its members. These planned activities include the following: participation in FMfI; student participation in the student poster session at FMfI; APCMfI prizes at the student poster session; internships for graduate students; regular Mathematics-for-Industry Study Groups (MISG), Math-for-Industry workshops and forums; the exchange of information and new research via a regular newsletter; and the organization of joint lectures and programs. Annual meetings will be held at a different Asia Pacific location.

The overall aim is to foster a fruitful two-way interaction between mathematical and statistical individuals and institutions on one side, and the needs of industry on the other. A special focus will be on encouraging and supporting students involvement in MfI activities, such as the FMfI students' poster session and internships.

Announcements about the establishment of APCMfI have recently been published in several international mathematical bulletins and we are pleased with the strong support and encouragement from our colleagues in China, Hawaii, South Korea, Malaysia and Singapore as well as Australia, New Zealand and Japan.

An official website for APCMfI has also been launched [2]. Here, interested parties can find information about the Consortium including information about how to become an industry, academic, or individual member. In addition, the plan is to make the Website available to colleagues throughout the Asia Pacific region to circulate information about industrial mathematics opportunities. This can be done by submitting information to the APCMfI website administrator.

5 The Importance of APCMfI

A key goal for APCMfI is to become a central body in the Asia Pacific region that not only connects people, but strengthens and highlights the excellent research being done in mathematics for industry in this region. There are many benefits in taking an international approach in building this new network. There are opportunities in sharing international experiences and benefits in linking junior and senior mathematicians. The broader geographical focus that APCMfI will stimulate will enhance industrial mathematics innovation in the Asia Pacific region (Fig. 1)

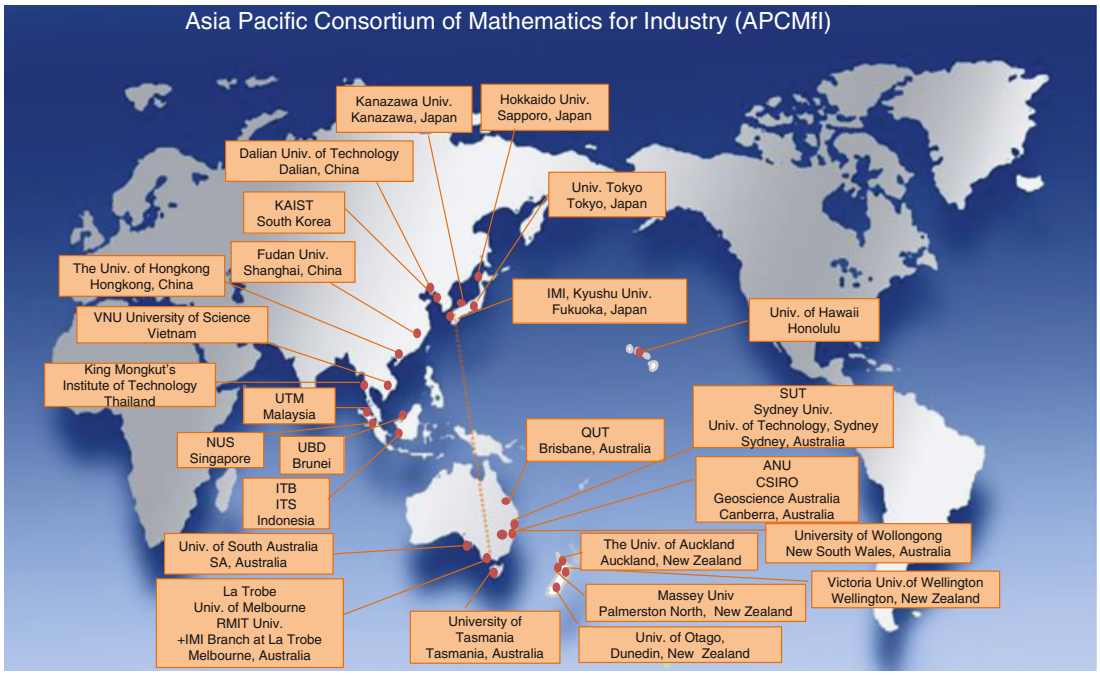

Fig. 1 The map shows the geographical region envisaged for APCMfI members, and highlights the opportunity provided by adjacent time zones

One way of stressing the future importance of APCMfI is to look at reinterpretations of the APCMfI acronym from various mathematical perspectives. The theme for FMfI 2014 was:

$$Applications + Perceptive\,Conceptualizations + Mathematics = fruitful\,Innovation.$$

As motivation for the study of mathematics, one possibility is:

$$Active\,Participation\,(in)\,Challenging\,Mathematics = future\,Intelligence.$$

6 APCMfI and Industrial Mathematics

The annual FMfI events have illustrated the growing importance of industrial mathematics for mathematics and innovation, and has fostered strong Asia Pacific collaboration and involvement, as well as international. The annual FMfI events started in Fukuoka in Japan, attracting guests from many countries. In order to support the APCMfI initiative, the plan is to extend this event throughout the Asia Pacific region, with plans for FMfI to be held in Brisbane, Australia, in 2016 and in Hawaii in 2017.

The different ways in which industrial mathematics performs a fundamental linking of the two way interaction between applications and mathematics have been the themes for the Forums in recent years. The details can be found using the links on the APCMfI website.

Acknowledgments The authors wish to thank the individuals who contributed to the first APCMfI planning meeting: Yasuhide Fukumoto (Japan), Graeme Wake (New Zealand), Zainal Aziz (Malaysia), Frank de Hoog (Australia) and the late Geoff Mercer (Australia). The authors also thank a secretary of the Institute of Mathematics for Industry at Kyushu University, Kazuko Ito, for her efficient assistance to APCMfI.

References

1. Announcement—Motivation and Planning for the Formation and Launch of APCMfI (2014). http://www.apcmfi.org/about/outline.html
2. APCMfI website. http://www.apcmfi.org/

Appendix B

Code for the vaccination model

An example of the script used to run the 75 age class RSV transmission model, with cohort ageing and a maternal vaccine, is shown below.

Main routine

```
global nAges

% Read in fitted parameters from file
A=csvread('paramfitted_omega06.csv');
b0=A(1); b1=A(2); phi=A(3); h1=A(4);
h2=A(5); h3=A(6); h4=A(7); omega=A(8);

% Vaccine parameters
rho=0.8;        % vaccine-induced protection
kappa=0.5;      % vaccine coverage
p_vacc=6;       % duration of vaccine-conferred immunity (in months)

% Ageing and mixing parameters
perth_pop=1861923; % 2014 greater perth pop, 0-79 years, ABS
age_vect_years=[0:1/12:5-1/12 5:5:75];
nAges=length(age_vect_years); % number of age cohorts
final_age=80;
```

```
age_vect_months=age_vect_years*12;
size_cohorts_months=[diff(age_vect_months) ...
    final_age*12-age_vect_months(end)];
trans_rate=1./size_cohorts_months;
rel_sizes=size_cohorts_months./sum(size_cohorts_months);
mixing=csvread('mixing_75_symmetrical.csv',0,0);
mixing=mixing*365/12; % convert to monthly matrix

% Transmission and timing parameters
delta=7.623;      % latent parameter
gamma=3.342;      % infectious rate
MaxTime=200*12;
dT=0.25;          % timestep for reporting
nu=0.132;         % immunity

% Reduced infectiousness vector
omega_vect=ones(1,nAges);
red_inf_age=10;  % age in years at which individuals begin to have ...
    reduced infectiousness
A=(age_vect_years<red_inf_age);
omega_vect(~A)=omega;

% Reduced susceptibility in youngest cohorts to reflect natural
% maternally-derived immunity
sigma_vect=ones(1,nAges);
sigma_vect(1)=0.08; sigma_vect(2)=0.45; sigma_vect(3)=0.45;

% Waning immunity vector
nu_vect=ones(1,nAges);
nu_vect=nu_vect*nu;

% Vaccine protection vector
rho_vect=zeros(1,nAges);
C=(age_vect_months>=p_vacc);
rho_vect(~C)=rho;

```

```
52 % Define xi=1-rho to scale susceptibility to infection in the vaccinated
53 % class
54 xi_vect=1-rho_vect;
55
56 % Vaccine must be at least as protective as natural maternal immunity
57 for i=1:3
58 if sigma_vect(i)<(xi_vect(i))
59 xi_vect(i)=sigma_vect(i);
60 end
61 end
62
63 % Initial conditions
64 I0=rel_sizes*perth_pop*0.001;
65 S0=rel_sizes*perth_pop*0.999;
66 E0=zeros(1,nAges);
67 R0=zeros(1,nAges);
68 V0=zeros(1,nAges);
69 cum_Inc0=zeros(1,nAges);
70 cum_lambda0=zeros(1,nAges);
71 force_inf0=zeros(1,nAges^2);
72 H0=[0 0 0 0];
73
74 % The main iteration
75 options = odeset('RelTol', 1e-4,'AbsTol', 1e-4);
76 T0=0; S=[]; E=[]; I=[]; R=[]; V=[]; T=[]; H=[]; cum_Inc=[]; ...
       cum_lambda=[]; force_inf=[];
77 params = [delta gamma b0 b1 phi h1 h2 h3 h4 reshape(mixing,1,nAges^2) ...
       omega_vect sigma_vect nu_vect xi_vect];
78 while T0<MaxTime
79 [t, pop]=ode45(@RSV_ODEs_75cohorts_vaccine,[T0:dT:T0+1],[S0 E0 I0 R0 V0 ...
       cum_Inc0 cum_lambda0 force_inf0 H0],options,params);
80
81 T=[T(1:end); t(end)]; S=[S(1:end,:); pop(end,1:nAges)]; E=[E(1:end,:); ...
       pop(end,nAges+1:2*nAges)]; I=[I(1:end,:); pop(end,2*nAges+1:3*nAges)];
82 R=[R(1:end,:); pop(end,3*nAges+1:4*nAges)]; V=[V(1:end,:); ...
       pop(end,4*nAges+1:5*nAges)];
```

```
cum_Inc=[cum_Inc(1:end,:); pop(end,5*nAges+1:6*nAges)];
cum_lambda=[cum_lambda(1:end,:); pop(end,6*nAges+1:7*nAges)];
force_inf=[force_inf(1:end,:); pop(end,7*nAges+1:82*nAges)];
H=[H(1:end,:); pop(end,82*nAges+1:82*nAges+4)];

% Cohort ageing

S0(1)=perth_pop*rel_sizes(1)*(1-kappa);  E0(1)=0; I0(1)=0; R0(1)=0; ...
    V0(1)=perth_pop*rel_sizes(1)*kappa;

for i=2:p_vacc
S0(i)=S(end,i-1)*trans_rate(i-1)+S(end,i)-S(end,i)*trans_rate(i);
E0(i)=E(end,i-1)*trans_rate(i-1)+E(end,i)-E(end,i)*trans_rate(i);
I0(i)=I(end,i-1)*trans_rate(i-1)+I(end,i)-I(end,i)*trans_rate(i);
R0(i)=R(end,i-1)*trans_rate(i-1)+R(end,i)-R(end,i)*trans_rate(i);
V0(i)=V(end,i-1)*trans_rate(i-1)+V(end,i)-V(end,i)*trans_rate(i);
end

for i=p_vacc+1
S0(i)=S(end,i-1)*trans_rate(i-1)+S(end,i)-S(end,i)*trans_rate(i)...
    +V(end,i-1);
E0(i)=E(end,i-1)*trans_rate(i-1)+E(end,i)-E(end,i)*trans_rate(i);
I0(i)=I(end,i-1)*trans_rate(i-1)+I(end,i)-I(end,i)*trans_rate(i);
R0(i)=R(end,i-1)*trans_rate(i-1)+R(end,i)-R(end,i)*trans_rate(i);
V0(i)=0;
end

for i=p_vacc+2:nAges
S0(i)=S(end,i-1)*trans_rate(i-1)+S(end,i)-S(end,i)*trans_rate(i);
E0(i)=E(end,i-1)*trans_rate(i-1)+E(end,i)-E(end,i)*trans_rate(i);
I0(i)=I(end,i-1)*trans_rate(i-1)+I(end,i)-I(end,i)*trans_rate(i);
R0(i)=R(end,i-1)*trans_rate(i-1)+R(end,i)-R(end,i)*trans_rate(i);
V0(i)=0;
end

T0=T(end);
```

```
118
119 % Reset ICs to equal final value from previous month
120 cum_Inc0=cum_Inc(end,:);
121 cum_lambda0=cum_lambda(end,:);
122 force_inf0=force_inf(end,:);
123 H0=H(end,:);
124 end
```

ODE file

```
1  function dPop=RSV_ODEs_75cohorts_vaccine(t, pop, parameter)
2  global nAges
3  delta=parameter(1); gamma=parameter(2); b0=parameter(3);
4  b1=parameter(4); phi=parameter(5); h1=parameter(6);
5  h2=parameter(7); h3=parameter(8); h4=parameter(9);
6  mixing=reshape(parameter(10:nAges^2+9),nAges,nAges);
7  omega_vect=parameter(nAges^2+10:nAges^2+9+nAges)';
8  sigma_vect=parameter(nAges^2+10+nAges:nAges^2+9+2*nAges)';
9  nu_vect=parameter(nAges^2+10+2*nAges:nAges^2+9+3*nAges)';
10 xi_vect=parameter(nAges^2+9+3*nAges+1:nAges^2+9+4*nAges)';
11
12 S=pop(1:nAges); E=pop(nAges+1:2*nAges); I=pop(2*nAges+1:3*nAges);
13 R=pop(3*nAges+1:4*nAges); V=pop(4*nAges+1:5*nAges);
14 dPop=zeros(8*nAges+4,1);
15
16 N=S+E+I+R+V;
17 beta=b0*(1+b1*cos(2*pi*t/12+phi))
18
19 lambda=beta*(mixing*((omega_vect.*I)./N));
20 Inf=lambda.*sigma_vect.*S;
21 Inf_V=lambda.*xi_vect.*V;
22
23 % calculate force of infection arising from each cohort, onto each cohort
24 force=ones(75,75);
```

```
for i=1:nAges
infect=(omega_vect(i).*I(i))./N(i)
force(:,i)=beta.*mixing(:,i).*infect.*sigma_vect.*S;
end

dPop(1:nAges)= - Inf + nu_vect.*R;
dPop(nAges+1:2*nAges)= Inf - delta*E + Inf_V;
dPop(2*nAges+1:3*nAges)= delta*E- gamma*I;
dPop(3*nAges+1:4*nAges)= gamma*I - nu_vect.*R;
dPop(4*nAges+1:5*nAges)=-Inf_V;
dPop(5*nAges+1:6*nAges)=Inf+Inf_V;
dPop(6*nAges+1:7*nAges)=lambda;
dPop(7*nAges+1:82*nAges)=reshape(force,1,nAges^2);
dPop(82*nAges+1)=h1*sum(Inf(1:3))+h1*sum(Inf_V(1:3));
dPop(82*nAges+2)=h2*sum(Inf(4:6))+h2*sum(Inf_V(4:6));
dPop(82*nAges+3)=h3*sum(Inf(7:12))+h3*sum(Inf_V(7:12));
dPop(82*nAges+4)=h4*sum(Inf(13:24))+h4*sum(Inf_V(13:24));

end
```